CATALYTIC OXIDATIVE COUPLING OF METHANE TO C_2 HYDROCARBON

Mohd Ridzuan Nordin

B.Sc. (Hons.), Tasmania

A thesis submitted in fulfilment of the requirement for the degree of

DOCTOR OF PHILOSOPHY

at

University of Tasmania

August 1989

DECLARATION

To the best of my knowledge this thesis contains no material which has been accepted fo the award of any other degree or diploma in any university, and contains no material previously published or written by another person except where due reference is made.

Mohd Ridzuan Nordin
Department of Chemistry
University of Tasmania
August 1989

ACKNOWLEDGEMENT

I wish to express my sincere appreciation to those who help me in making the work possible:

Professor Frank P. Larkins, for his supervision, guidance and patience.

Dr. Barry O.V. Grady, for his help in the azomethane experiments.

Messrs. Marshall Hughes, Peter Dove, and John Davis, for their technical assistance.

Drs. Ashraf Khan and Brad Armen, for their helpful advices on the manuscript.

Mr Supachai Supaluknari, Ms. Elzbieta Chelkowska, Mr Gerard Roe and Dr Jon Youing, for their company and useful discussions.

My parents, Nordin Hj. Thambychik and Maimon Hj. Dol, for their perseverence in having me away since 1980.

My wife, Norainin Abd. Latif, for her patience and understanding.

ABSTRACT

In this work the direct conversion of methane to C_2 hydrocarbons through the catalytic oxidative coupling reaction ($nCH_4 + y/2\ O_2 \Rightarrow C_nH_{4n-2y} + y\ H_2O$) is investigated.

The catalytic materials studied can be categorised as single chemical compounds, different loading of Li_2CO_3 on MgO, various lithium salts on MgO, Li_2CO_3 on various metal oxides, transition metal oxides on MgO and transition metal oxides on Li_2CO_3/MgO systems. Most of these materials were prepared by wet aggregation or impregnation methods and precalcined at 900°C for 10 hours.

Atomic absorption spectroscopy was used to determine the metal composition of these materials. Their nature after calcination was studied by SEM and X-ray Micro-Probe Analysis. Surface area measurements and XRD analysis were also performed on most of the catalytic materials. The nature of selected materials under conditions similar to the catalytic studies were monitored by FTIR, ESCA and TGA. Changes occurring on the material during the reaction were simulated and studied *in situ* by FTIR techniques. A conventional flow reactor operating under atmospheric pressure was used in the activity determinations. The effects of reaction temperature, reactant composition, CO partial pressure in reactant flow and time-on-stream were investigated. The decomposition of azomethane under the conditions of the catalytic studies was also performed in order to determine if similar product distributions can be achieved.

The precalcination was found to cause large physical and chemical changes on some materials. Segregation of Li_2CO_3 on the Li_2CO_3/MgO based catalysts occurred resulting in the enrichment of this component on the surface. Considerable transformation also occurred on these catalysts during the catalytic reaction. Various materials were found to be active for the oxidation of methane and generally a chemically basic material formed a better oxidative coupling catalyst. The surface area of these materials did not determine whether they were active for the oxidative reaction

but for an active material, good oxidative coupling behaviour was associated with small surface area. It was noted that materials with a reducible oxidation state favoured the exhaustive oxidation reaction while the addition of Li_2CO_3 increased the oxidative coupling properties accompanied by the reduction in available redox sites. An "intrinsic limit" for the C_2 hydrocarbon yield was also observed, while the results of azomethane experiments agreed with the proposal of the occurrence of methyl radicals coupling reactions in the gaseous phase.

TABLE OF CONTENTS

			page
CHAPTER 1	**INTRODUCTION**		
1.1	Oil and Natural Gas		1
1.2	Routes for Upgrading Methane		1
1.3	Thermodynamic and Kinetic Factors		3
1.4	Project Objectives		6
CHAPTER 2	**LITERATURE REVIEW**		
2.1	Activation of Methane		7
2.2	Oxygen Species		8
2.3	Non-reducible Catalytic Materials		9
2.4	Catalytic Material with Variable Oxidation States		10
2.5	Rare Earth Oxide Catalysts		12
2.6	Chloride Containing Catalysts		14
2.7	Partial Oxidation Route		15
2.8	The Gas Phase Reaction		17
2.9	The Effect of Process Condition		19
	2.9.1	Reactant Gas Type	19
	2.9.2	The composition and total pressure of reactant gas	21
	2.9.3	Temperature and flow condition	24
	2.9.4	Role of additive gas	26
2.10	Active Site for Catalytic Reaction		27
	2.10.1	Reducible materials	27
	2.10.2	Catalysts with fixed oxidation state	27
	2.10.3	Reducible metal oxide doped with alkali metal compounds	29
	2.10.4	Implication for catalytic activity	29
2.11	Mechanism for Oxidative Coupling Reaction		30
2.12	Comparing the Catalytic Performances		33
CHAPTER 3	**EXPERIMENTAL**		
3.1	Catalytic Activity		38
3.2	Catalysts Preparation		39
3.3	Activity Determination		40
	3.3.1	The reactor system	40

	3.3.2	Products Determination	41
3.4	Catalysts Characterization		42
	3.4.1	Composition of catalysts by AAS	42
	3.4.2	Surface area Determination	42
	3.4.3	X-Ray powder Diffraction pattern	43
	3.4.4	Temperature Programmed Reduction	43
	3.4.5	Thermogravimetric Analysis	44
	3.4.6	SEM, microprobe, and XPS	45
	3.5.7	Infra Red Spectroscopy	47
	3.4.7.1	Cell Design	47
	3.4.7.2	Cell Testing	49

CHAPTER 4 ACTIVITY OF Li_2CO_3/MgO TYPE CATALYTIC MATERIAL AND FRESH CHEMICAL COMPOUNDS; RESULTS AND DISCUSSION

4.1	Homogeneous Oxidative Reaction of Methane		51
4.2	Activity of calcined 7.8wt.%Li_2CO_3/MgO Catalysts		53
	4.2.1	The effect of reaction temperature	53
	4.2.2	The effect of changing the P_{O_2}/P_{CH_4} ratio	54
4.3	Effect of lithium loading on the ctivity of Li_2CO_3/MgO Catalysts		56
	4.3.1	Activity of calcined catalysts at 800°C	56
	4.3.2	Activity of uncalcined catalysts at 800°C	58
	4.3.3	Effect of time-on-stream on the activity calcined MgO and 7.8wt.% Li_2CO_3/MgO at 800°C	60
	4.3.4	Effect of time-on-stream on the activity on the activity of calcined 7.8wt.%Li_2CO_3/MgO catalysts with P_{O_2}/P_{CH_4} of about 1	61
	4.3.5	Effect of time on stream on the activity of fresh 1.3wt.% and 8.4wt.% Li_2CO_3/MgO catalysts	63
4.4	Further Activity Determination of MgO		67
	4.4.1	The activity of MgO obtained from different from different sources	67
	4.4.2	The activity of Strem MgO with time on stream at 800°C	67
	4.4.3	The effect of the amount of MgO used	68
	4.4.4	Activity of prepared MgO which were precalcined at different temperature	69
	4.4.5	Effect of length of *in-situ* calcination time	

at 800°C on the activity of fresh MgO 71

4.5 Activity Determination of Fresh Chemicals 73

4.5.1 The activity of chemical used for supporting Li_2CO_3 73

4.5.1.1 Activity of $Mg(OH)_2$, $Ca(OH)_2$ and CaO 73

4.5.1.2 Activity of γ-Al_2O_3, SiO_2 and TiO_2 75

4.5.2 Activity of $AlPO_4$-5 and Al_2O_3/SiO_2 76

4.5.3 Activity of Sm_2O_3 77

4.5.3.1 Effect of temperature on the activity of Sm_2O_3 77

4.5.3.2 The influence of P_{O_2}/P_{CH_4} in reactant stream on the activity of Sm_2O_3 78

4.5.3.3 Time stability at 800°C 79

4.5.4 The activity of various carbonates 80

4.5.4.1 The activity of the first row carbonates at 800°C 80

4.5.4.1 The activity of the second row carbonates at 800°C 82

4.6 Activity of Various Lithium Salts on MgO 83

4.6.1 Activity of calcined samples at 800°C 83

4.6.2 Activity of uncalcined samples at 800°C 85

4.6.3 Further studies on calcined LiCl/MgO catalysts 87

4.6.3.1 Effect of P_{O_2}/P_{CH_4} ratio on the activity at 800°C 87

4.6.3.2 The effect of time-on-stream on the activity of LiCl/MgO 88

4.6.3.3 Physical and chemical changes on LiCl/MgO after 25 hours on-stream 88

4.7 Activity of Li_2CO_3 supported on various oxide 91

4.7.1 Activity of calcined catalysts at 800°C 91

4.7.2 Activity of uncalcined catalysts at 800°C 92

4.7.3 Further studies on the Li_2CO_3/CaO system 94

4.7.3.1 Effect of reaction temperature 94

4.7.3.2 Effect of P_{O_2}/P_{CH_4} ratio 94

4.7.3.3 Effect of time-on-stream 95

4.7.3.4 physical and chemical nature of various Li_2CO_3/CaO catalysts 96

4.8 Summary of findings 99

CHAPTER 5 CHEMICAL AND PHYSICAL PROPERTIES OF OXIDATIVE COUPLING CATALYSTS; RESULTS AND DISCUSSION

5.1 Introduction 101

5.2 Li_2CO_3/MgO catalysts 101

5.2.1 Effect of calcination on the physical nature of Li_2CO_3/MgO 101

5.2.2 Effect of precalcination on the bulk composition of Li_2CO_3/MgO catalysts 107

5.2.3 The nature of calcined 7.8wt.%Li_2CO_3/MgO catalysts at high temperature 108

5.2.4 Further studies on the stability of Li_2CO_3/MgO at high temperature 119

5.3 The nature of MgO doped with different lithium salts 124

5.3.1 SEM studies on calcined samples 124

5.3.2 The composition of lithium salt doped MgO 127

5.3.3 FTIR study on calcined catalysts 129

5.3.4 XPS experiment on Li_2SO_4/MgO catalysts 131

5.4 The nature of Li_2CO_3/MO system 133

5.4.1 SEM studies of calcined samples 133

5.4.2 AAS and XRD studies 135

5.5 Further FTIR studies on catalytic materials 138

5.6 The influence of Physical and Chemical Properties on Catalytic activity 143

5.6.1 Surface area and activity 143

5.6.2 Basicity and activity 147

5.6.3 The effect of catalysts stability on its activity 148

5.7 Summary of findings 150

CHAPTER 6 TRANSITION METAL OXIDE DOPED MgO AND Li_2CO_3/MGO CATALYSTS; RESULTS AND DISCUSSION

6.1 Introduction 152

6.2 Activity Studies

6.2.1 Preliminary studies on the activity of fresh and calcined Li_2CO_3/MgO doped with different transition metal oxide 152

6.2.1.1 Composition and activity of catalysts 152
6.2.1.2 Effect of reaction temperature on activity 157
6.2.2 Different loading of iron oxide on Li_2CO_3/MgO and MgO 159
6.2.2.1 Catalysts composition 159
6.2.2.2 Catalysts activity 160
6.2.3 Different loading of zinc oxide on Li_2CO_3/MgO and MgO 163
6.2.3.1 Catalysts composition 163
6.2.3.2 Catalysts activity 164
6.2.4 Different loading of manganese oxide on Li_2CO_3/MgO and MgO 167
6.2.4.1 Catalysts composition 167
6.2.4.2 Catalysts activity 168
6.2.5 Different loading of chromium oxide on Li_2CO_3/MgO and MgO 171
6.2.5.1 Catalysts composition 171
6.2.5.2 Catalysts activity 172
6.3 Further studies on the activity 0.6wt.% manganese oxide doped Li_2CO_3/MgO catalysts 174
6.3.1 The effect of reactant composition on the activity 174
6.3.2 The activity at 805°C with time-on-stream 175
6.4 Physical and Chemical nature of the catalysts 180
6.4.1 Introduction 180
6.4.2 Iron oxide doped system 181
6.4.3 Zinc oxide doped system 194
6.4.4 Manganese oxide doped system 206
6.4.5 Chromium oxide doped syestem 217
6.5 The effect of ionic radii factor on the physical and chemical properties and on catalytic activity 225
6.6 Summary of findings 230

CHAPTER 7 CATALYSTS NATURE UNDER REACTION CONDITIONS AND THE EXTENT OF CATALYTIC REACTION; RESULTS AND DISCUSSION

7.1 Introduction 232
7.2 *In-situ* FTIR experiments 233
7.2.1 Probing the reaction intermediates 233

7.2.2 Changes to metal oxide catalysts during the oxidative reaction of methane at 750°C 234

7.2.3 Changes to various lithium salts supported on MgO catalysts during the oxidative reaction of methane 242

7.2.4 Changes to Li_2CO_3/SiO_2, Li_2CO_3/γ-Al_2O_3 and Li_2CO_3/CaO catalysts 245

7.2.5 Probing the hydroxyl species formation on Li_2CO_3/MgO catalysts 249

7.3 Probing the extent of gaseous phase and surface reactions 254

7.3.1 Gaseous phase and catalysed oxidative reaction of hydrocarbon mixture 254

7.3.2 Effect of CO partial pressure on the oxidative reaction of methane over various catalysts 257

7.4 Overall Analysis of Activity Results 262

7.5 Using Azomethane to Model the Catalytic Oxidative Reaction of Methane 265

7.5.1 Decomposition of azomethane at different temperature 267

7.5.2 Effect of azomethane partial pressure on the product distribution at 800°C 269

7.5.3 The reaction of azomethane in different partial pressure of oxygen 270

7.5.4 The oxidative reaction of azomethane under various condition 271

7.6 Contribution of this work towards understanding the mechanism of the catalytic oxidative reaction of methane 274

CHAPTER 8 CONCLUSION AND FUTURE WORK

8.1 Conclusion 276

8.1.1 Catalyst screening 276

8.1.2 Physico-chemical properties and catalytic activity 278

8.1.3 Active sites 281

8.1.4 Reaction mechanism 282

8.2 Future Work 282

REFERENCES 284

CHAPTER 1

INTRODUCTION

1.1 Oil and Natural Gas

The current global oil reserves stand at about 997 G bbl. and using the estimated 1987 production rate (56 M bbl/d) this reserve will last for about 45 years (Petroleum Gazette 1988). In the case of natural gas, the situation is only slightly better. Existing reserves are estimated to be about 107 T m^3 and will last for about 56 years. Large deposits of natural gas are found throughout the world. Depending on its location, between 50-98% of natural gas is made up of methane (Kirk Othmer, 1980). In most cases this gas is transported to the consumers' market by gas pipelines and shipping. However, not all of the natural gases found have been utilised. Some, which are located in remote areas have been left unused due to the expensive transportation cost. When found in remote areas together with oil, they are normally flared.

Currently, oil serves as a major feed stock for the petroleum and petrochemical industries. On the other hand, only a relatively small fraction of natural gas is used in this respect, but is normally used as a source of heat energy. With the continual depletion of natural oil, the demand for this resource will certainly increase. There will be some need for technologies which can utilise methane from natural gas more efficiently. An area where these technologies can contribute significantly is in converting methane from natural gas into a better feed stock for the petroleum and petrochemical industries.

1.2 Routes for Upgrading Methane

The largest chemical application of methane is in the production of synthesis gas for the manufacture of ammonia, methanol, and oxoaldehydes. Methane is also used in the production of hydrogen cyanide, halogenated methane and carbon disulphide.

Acetylene, once a primary feedstock for the polymer industry, can be produced from methane via two routes (Waddams, 1978). The first route is through a thermal cracking process at temperatures in excess of 1200°C followed by the quick quenching of the products as performed in the Hull and Wulf process. The second route, the Sachsce or BASF process, employs a partial oxidation reaction as a means of providing the energy for the main reaction. Up to an 8% yield of acetylene can be achieved by the latter route while the by-products H_2 and CO may be integrated into a synthesis gas system.

Recently there has been significant interest in the production of ethylene and higher hydrocarbons, especially aromatics, in the context of producing liquid fuels from methane. Table 1.2.a lists the various routes for producing higher hydrocarbons from methane. The current technology for producing higher hydrocarbons from methane, the Mobil GTG process, has been implemented in New Zealand (Maiden,1988). A modification of this process, the TIGAS process (Top-Jorgensen, 1988) claims to result in lower capital investment due to the integration of the synthesis gas and MTG processes. An alternative technology is Shell's middle distillate process where partial oxidation is used to produce CO and H_2 followed by the Fischer-Thropsch reaction to produce the higher hydrocarbons (Burgt. 1988). All of the above processes involve the highly endothermic synthesis gas production. Superficially it would seem energetically more attractive to convert methane directly to methanol or higher hydrocarbons in a single step. From methanol, production of higher hydrocarbons can be achieved through the Mobil MTG technology while the light unsaturated hydrocarbons can be upgraded by the oligomerization reactions.

Other potential routes are the direct formation of methanol from methane through the partial oxidation reaction, and the formation of higher hydrocarbons from high temperature pyrolysis of methane, either homogeneous or catalysed. Higher hydrocarbons can also be achieved through the chloro hydrocarbon routes. A route which might have the greatest potential is the oxidative coupling route where C_2 hydrocarbons can be produced at high yield through reaction of methane and oxidant

over a catalyst at moderately high temperature. Reviews on recent efforts in this area can be found in Jones et al.,1987a, Scurrell, 1987, Lunsford, 1988, Bhasin, 1988, Haggin, 1988a, 1988b, Smith, 1988 and Anderson, 1989.

Table 1.2.a Routes for the production of higher hydrocarbons from methane.

Established Route

1. **Synthesis gas, methanol formation and Mobil process**

   Implemented in Synfuel plant of New Zealand

   [$H_2O + CH_4 <=> 3H_2 + CO$] [$CO_2 + 3H_2 <=> CH_3OH + H_2O$]

   [CH_3OH <=> synthetic fuels]

2. **Partial Oxidation to CO and Fischer-Tropsch reaction**

   Shell Middle distillate, yet to be commercialised

   [$CH_4 + 0.5\ O_2 <=> CO + 2H_2$] [$CO + 2H_2 <=> (-CH_2-) + H_2O$]

Alternative route

1. **Pyrolysis and Oligomerization**

   Still in development.

   [$2CH_4 <=> C_2H_2 + 3H_2$] [C_2H_2 <=>synthetic fuels]

2. **Partial oxidation and Oligomerization**

   Still in development

   [$O_2 + 2CH_4 <=> C_2H_4 + 2H_20$] [$C_2H_4$<=>synthetic fuels]

1.3 Thermodynamic and kinetic factors

Methane is the smallest and most stable molecule among the hydrocarbons. Any reaction of methane would involve breaking the strong C-H bonds, and for this to happen a severe reaction condition is required. Due to the extreme condition required to react methane it is normally difficult to control the extent of reaction and hence the

reaction products. Moreover, in most cases the reaction products are less stable than methane and are likely to react further.

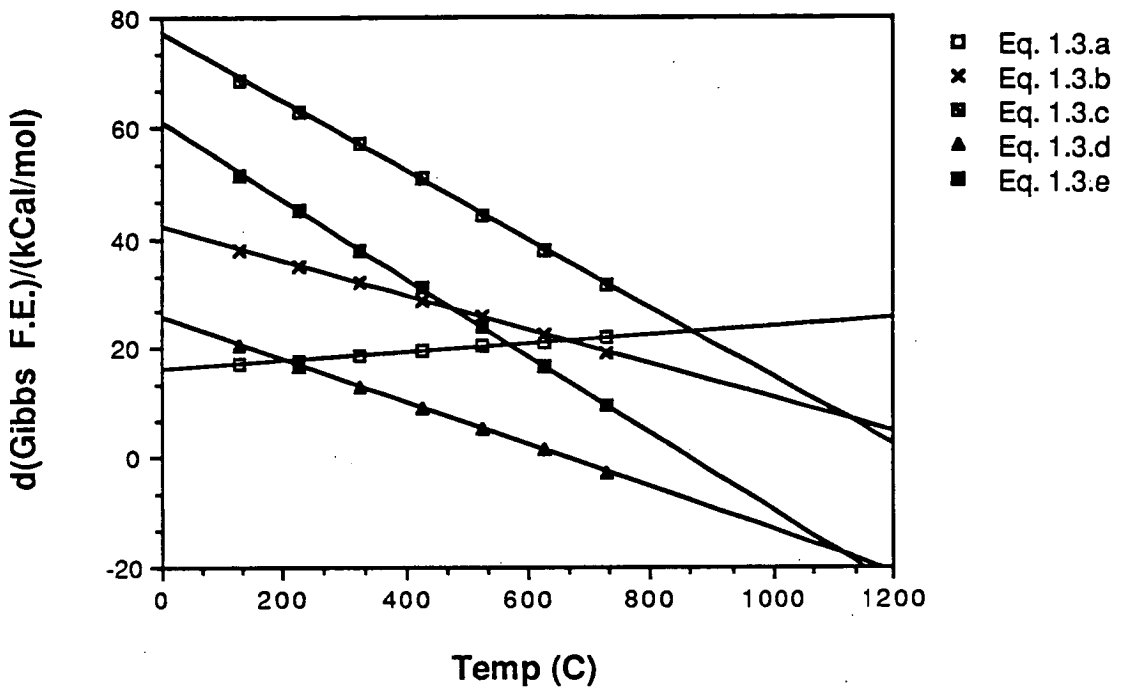

Figure 1.3.a Free energy changes (dG^o) for the gas-phase reaction of pure CH_4 and C_2 as a function of temperature.

Eq. 1.3.a.	$2CH_4$	--->	$C_2H_6 + H_2$
Eq. 1.3.b.	$2CH_4$	--->	$C_2H_4 + 2H_2$
Eq..1.3.c	$2CH_4$	--->	$C_2H_2 + 3H_2$
Eq. 1.3.d	C_2H_6	--->	$C_2H_4 + H_2$
Eq. 1.3.e	C_2H_4	--->	$C_2H_2 + H_2$

The thermal reactions of pure methane are not thermodynamically feasible until a very high reaction temperature is reached (Pitchai and Klier,1986). The formation of C_2 hydrocarbons from methane does not occur until the reaction temperature is above 1200°C and acetylene is the favoured product (figure 1.3.a). A thermodynamic barrier also exists for the thermal reaction of pure C_2 hydrocarbons. Formation of ethene from ethane only becomes thermodynamically feasible above 600°C while the

formation of acetylene cannot occur until above 850°C. For the formation of acetylene from ethene, a reaction temperature of 1080°C, is required.

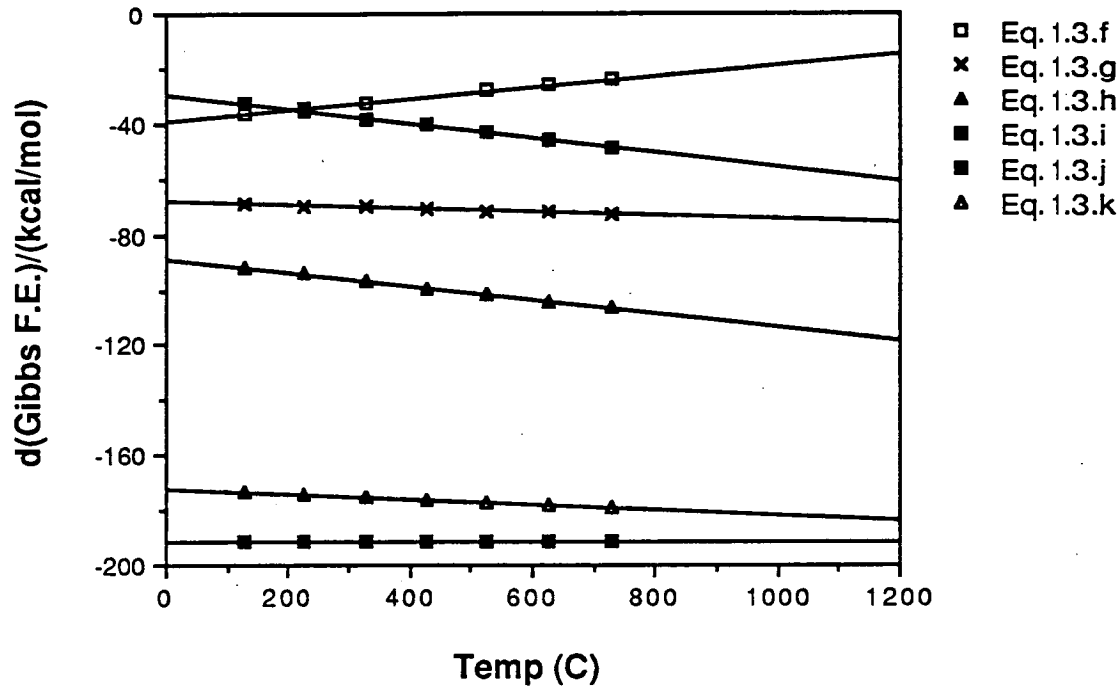

Figure 1.3.b Free energy changes (dG^o) for the gas-phase oxidative conversion of CH_4 and C_2 as a function of temperature.

Eq. 1.3.f	$2CH_4 + 1/2\ O_2$	--->	$C_2H_6 + H_2O$
Eq. 1.3.g	$2CH_4 + O_2$	--->	$C_2H_4 + 2H_2O$
Eq. 1.3.h	$2CH_4 + 3/2\ O_2$	--->	$C_2H_2 + 3H_2O$
Eq. 1.3.i	$CH_4 + 2\ O_2$	--->	$CO_2 + 2H_2O$
Eq. 1.3.j	$C_2H_6 + 1/2\ O_2$	--->	$C_2H_4 + H_2O$
Eq. 1.3.k	$C_2H_6 + 7/2\ O_2$	--->	$2CO_2 + 3H_2O$

When oxygen is present with methane, the thermodynamic barrier for the thermal reaction of methane and C_2 hydrocarbons is reduced (figure 1.3.b). The exhaustive oxidation of these hydrocarbons to carbon oxides are thermodynamically more favoured. Therefore significant conversion of methane to higher hydrocarbons can be achieved through kinetic means. In the production of C_2 from methane,

ethane is normally obtained as a major product and can be readily converted to ethylene. Since the homolytic bond dissociation energy of ethylene (109.9kCal/mol) is higher than that for methane (104.9kCal/mol) a higher selectivity to ethylene can be achieve if the reaction involving the carbon to carbon double bond can be minimised. Besides O_2, other oxidants like N_2O, H_2O and Cl_2 also facilitate the reaction of methane to higher hydrocarbons.

The partial oxidation of methane to C_2 hydrocarbons is certainly a challenging kinetic problem. Theoretically it should be possible to find a catalyst which has a high activity for methane conversion and also a high selectivity to C_2 hydrocarbons, especially to ethylene.

1.4 Project Objectives

The central objective of this work is to evaluate the potential of direct conversion of methane to C_2 hydrocarbons through the catalytic oxidative coupling $nCH_4 + y/2\ O_2$ ----> $C_nH_{4n-2y} + yH_2O$ route. Among the questions addressed are:

Q1. Where do the various chemical systems which were reported to be catalytically active stand when compared under similar reaction conditions ?

Q2. What correlations exist between catalytic activity of fresh chemicals and their physical and chemical properties ?

Q3. Since Li_2CO_3 melts at 618°C (Aylward and Findlay, 1974), what is the nature of Li_2CO_3/MgO catalyst under reaction conditions ?

Q4. Can modifications be made to a catalyst to improve its catalytic activity ?

Q5. How sensitive are the catalytic reactions towards a range of reaction variables ?

Q6. To what extent do the gaseous phase reactions occur ?

Q7. What is happening on the catalyst during the reaction ?

CHAPTER 2

LITERATURE REVIEW

2.1 Activation of Methane

Most of the earlier works on the reactions of methane are related to fundamental kinetics experiments and to combustion chemistry. Reviews on this research have been presented by Gardiner and Olson, 1980 and Warnatz, 1983.

The reaction of methane and other alkanes in the gaseous phase with O^- have been studied by Bohme and Fehsenfeld, 1969. O^- species were produced by the dissociative ionization reaction $e + O_2 \rightarrow O^- + O^+ + e$ and to a lesser extent the $O_2 + e \rightarrow O^- + O$ process. It was found that the reaction probability increases with higher carbon number. Even for methane (Equation 2.1.a.), the probability of 0.08 was observed, indicating significant activity of the oxygen species towards methane.

Equation 2.1.a $\quad O^- + CH_4 \rightarrow CH_3 + OH^-$

However under the combustion condition, as in flame or shock tube experiments (Skinner and Ruehrwein, 1959), other oxygen species can also be responsible for activating the C-H bond of methane.

The activation of methane on a solid surface has also been studied under various conditions. On metallic surfaces and in the absence of oxidants, low temperature reactions normally result in complete dissociation of methane into surface carbide and adsorbed hydrogen (Kuijpers et al.,1981, and references therein). In this case metal species serve as the active site. Under oxidising conditions the surface is normally in the oxidised form. The active site for activating methane is normally an oxygen species and the activity of the surface would strongly depends on the treatment it has undergone. As an example, the activity of NiO/Al_2O_3 for methane oxidation at 710°C was much higher when the catalyst was reduced and oxidised prior to reaction (Gavalas et al.,1984). However the activity decreased with time to a stable value.

This variation of activity was suggested to be due to corresponding changes in the concentration of Ni^{3+}, and hence excess oxygen on the surfaces. The efficiency of the methane oxidation reaction is related to the ease of surface site oxidation and reduction. For example the Pt/Al_2O_3 system is less efficient than Pd/Al_2O_3 system (Cullis and Willat,1983) since palladium, but not platinum, can absorb oxygen into its bulk and provide a reservoir of oxygen which may prevent methane pyrolysis on the solid surface.

2.2 Oxygen Species

Che and Tench,1982, have reviewed research on the role of adsorbed oxygen species, their nature and chemical reactivity, and the chemical systems which contain them. Studies on MgO identified at least three types of oxygen species generated when MgO was exposed to different treatment. These oxygen species O^-, O_2^- and O_3^- are paramagnetic and can be studied by EPR. Pretreatment by neutron bombardment, U.V. irradiation and high temperature exposure could give rise to an electron donating centre in the forms of surface defects or hydroxyl species or low co-ordinated lattice oxygen (O^{2-}_{LC}) . These sites can react with an oxidant to form adsorbed oxygen species through the various reactions as given below:

$$e + N_2O \rightarrow O^- + N_2$$

$$O^- + O_2 \rightarrow O_3^-$$

$$e + O_2 \rightarrow O_2^-$$

$$OH^- + OH^- \rightarrow 2O^- + H_2$$

$$O^{2-}_{LC} + O_2 \rightarrow O_2^- + O^-_{LC}$$

The roles of these oxygen species in the partial oxidation of hydrocarbons have been reviewed by Lunsford, 1984. Even at low temperature, these oxygen species reacted with hydrocarbons, mainly via oxidative dehydrogenation. The order of their reactivity was $O^- >> O_3^- >> O_2^-$. Generally, it was found that these oxygen species are not stable at temperatures greater than -50°C However it was also found that variations of the O^- type oxygen species on the metal oxide system are stable at

higher temperature. These oxygen species were proposed to be the active sites for methane activation over the Mo/SiO_2 (Liu et al.,1984) and Li_2CO_3/MgO (Driscoll et al.,1985a) catalytic systems.

2.3 Non-reducible Catalytic Material

Driscoll and Lunsford, 1985 discovered that the reaction of methane over MgO and Li_2CO_3/MgO at 500°C resulted in the formation of methyl radicals. The methyl radical was trapped by the matrix isolation technique from the reactant stream, and this radical was proposed as the primary intermediate for the reaction of methane with the solid surface to form the various products. The presence of Li_2CO_3 on MgO was seen to increase the production of methyl radicals.

Under the catalyst screening condition (4gm of catalyst, P_{O_2} 117 torr, P_{CH_4} 218 torr and total flow rate of 50 ml/min), Ito and Lunsford, 1985, reported that a methane conversion of 37.5% with C_2 selectivity of 46.5% could be achieved at 770°C. Kimble and Kolts, 1987 and others have basically confirmed the effectiveness of the Li_2CO_3/MgO system. Kimble and Kolts, 1987 also show that Na/CaO, Li/CaO, Na/MgO and, to a lesser degree K/MgO systems are also active for the oxidative coupling of methane. The oxides MgO and CaO exhibit significant activity but a lower selectivity to C_2 hydrocarbons. At 780°C they observed a methane conversion of 18% and C_2 selectivity of 57% on Li/MgO catalyst at a CH_4/O_2 ratio of 8:1 and GHSV of 1000 $hour^{-1}$. Lin et al.,1988 has confirmed the effectiveness of Na/CaO as a catalytic material. With 2 gm of 6% Na/CaO catalysts and P_{O_2} of 115 torr, P_{CH_4} of 203 torr, total flow rates of 55 ml/min at 725°C, they observed 32.1% methane conversion and 40.6% selectively to C_2 hydrocarbons. Iwamatsu et al.,1988a, reported that for the Na/CaO system, a maximum of19% C_2 yield occurred for Na loading of 15 mole %. These workers also reported that Rb/MgO also formed an effective catalyst.

In an earlier work Moriyama et al.,1986, showed that doping of MgO with alkali metal always resulted in a more effective material for the oxidative coupling reaction compared to MgO itself or MgO doped with variable metal oxide. Iwamatsu,

et al.,1987,1988b, demonstrated that the alkali doped MgO had a low surface area which resulted in a high C_2 yield while other metal oxides supported on MgO having higher surface area resulted in lower C_2 yield. In addition the alkaline earth metal oxides and carbonates were shown by Aika, et al.,1986a, 1987, to be active for the oxidative coupling reaction. The highest yield of C_2 in this study was 20.2% for $BaCO_3$ promoted by 2% K (48% con., 42% sel.) at 800°C. Yamagata, et al.,1987, showed that alkaline earth metal oxides resulted in higher C_2 yield than other oxides. They also showed that the low surface area MgO and CaO resulted in higher C_2 yield than their high surface area counterpart. Lane and Wolf,1988a; Larkins and Nordin, 1988; Edwards and Tyler, 1988; Kasteren et al., 1988; Roos et al.,1987a; and Hutchings, et al.,1987, all confirmed the effective use of Li/MgO catalyst.

Other catalytic materials studied were Li/ZnO (Matsuura, et al.,1986 and Zhang et al.,1988), Li/BeO (Matsuura et al.,1987, and Doi, et al.,1988), sulphate treated zirconia (Scurrell and Cooks, 1988), synthetic kentrolite (Thomas et al.,1988), modernite (Kowalak and Moffat, 1988), Na_2O_3 (Otsuka et al.,1987), and silicic acid (Kastanas et al.,1988a).

2.4 Catalyts with variable oxidation states

The activity of 26 materials for catalytic oxidative coupling of methane have been determined by Keller and Bhasin, 1982. They observed that the reactant sequential feed mode resulted in 10 fold increased selectivity to hydrocarbon products than the co-feeding mode. The highest hydrocarbon yield in this work was 5%. These workers noted that the active material exhibiting high activity are those which have multiple oxidation states.

Shepelev and Ione,1984, studied the activity of Mo, Cu, Co and Fe oxides supported on zeolite using different oxidants in the 350°C - 500°C temperature range. Up to 30% methane conversion and 23% selectivity to hydrocarbon products were achieved over Fe and Mo oxide catalysts at 400°C with N_2O as oxidant.

Among the supported Pb, Sb, Sn and Mn oxide materials studied by Hinsen et al.,1984, PbO/Al_2O_3 was found to be the best catalyst. However for this material it was observed that prolonged time on stream resulted in the loss of hydrocarbon selectivity. The loss in selectivity was found to be due to PbO losses from the surface. The presence of Na_2O was found to promote the catalytic activity of PbO/Al_2O_3.

Asami et al.,1987a,1987b,1988a, have further studied the catalytic nature of PbO systems. These workers observed that generally higher C_2 yields could be achieved with PbO on a basic support. The highest C_2 yield achieved on these systems was 6%.

The activity of Pb/Al_2O_3, $Na/Pb/Al_2O_3$ have been compared with that of Li/MgO under similar reaction conditions by Roos et al.,1987. These workers found that Pb/Al_2O_3 resulted in lower C_2 yield than Li/MgO, but by doping Na on Pb/Al_2O_3 a similar hydrocarbon yield to Li/MgO was achieved. It was also noted that Pb/Al_2O_3 exhibited higher activity than $Na/Pb/Al_2O_3$ and Li/MgO at low reaction temperatures. The maximum activity for Pb/Al_2O_3 was achieved with only a slight increase in reaction temperature. However, the activity of $Na/Pb/Al_2O_3$ and Li/MgO systems were observed to increase gradually with the increase in reaction temperature.

Carreiro et al.,1988 have observed that for lead compounds, those having mobile lattice oxygen resulted in low selectivity to C_2 hydrocarbons and a relatively higher oxygenate formation. By supporting PbO on zeolite, Meng and Sanger,1987, observed that higher C_2 yield could be attained relative to PbO/Al_2O_3 when N_2O was used as the oxidant. The relative time stability between $PbO/\gamma\text{-}Al_2O_3$ and Na_2O/CaO catalysts has been studied by Follmer et al., 1988. The Na_2O/CaO catalysts was observed to be more stable and to give higher selectivity to C_2 hydrocarbons than the $PbO/\gamma\text{-}Al_2O_3$ catalyst.

Sofranko et al.,1987, and Jones et al.,1987a, 1987b, have studied the oxidative coupling reaction under reactant sequential feed and co-feed conditions in the 930-1270°C temperature range. Most of the materials studied were variable oxidation state compounds supported on silica. As in the work of Keller and Bhasin, 1981, it

was found that sequential feed mode was more suitable for these material. The 5% Mn/SiO_2 was found to be a good catalyst and its activity can further be promoted by the presence of alkali. The best activity measured was approximately 30% methane conversion with 65% selectivity to hydrocarbon products.

The activity of supported groups 3A, 4A and 5A oxides were studied by Amesh and Amenomiya, 1986. Bi_2O_3 was found to be active and selective for oxidative coupling reaction but Ga_2O_3, In_2O_3, Tl_2O_3, SeO_2 and Sb_2O_4 gave practically no C_2 hydrocarbons. The catalytic activity of $AlPO_4$-5 and metal doped $AlPO_4$-5 were studied by Garnet et al.,1988. Generally these materials resulted in exhaustive oxidation of methane. Ungar et al.,1988 studied the activity of complex oxide with rock salt structure. In their studies of perovskite type oxide, France et al.,1988 have found that for a series of alkali doped La/Mn/O compounds, higher binding energy of surface oxygen resulted in higher selectivity to C_2 hydrocarbons.

In this work we have compared the activity of transition metal oxide on MgO against that on Li_2CO_3/MgO systems. In line with other researchers we found that the doped Li_2CO_3/MgO systems resulted in higher C_2 yield than the doped MgO systems.

2.5 Rare Earth Oxide Catalysts

Fang and Yeh, 1981, found that the thermal reaction of pure methane over ThO_2/SiO_2 at 800°C occurs 300 times faster than the homogeneous gaseous phase reaction. The promotion effect by rare earth oxide compounds on the reaction of methane in an oxidative environment also occurs. Otsuka et al.,1985a, 1986a, 1986b, and Nakajima et al.,1986, 1987, found that Sm_2O_3 had the highest activity for the formation of C_2 hydrocarbons when N_2O was used as oxidant. If oxygen was used, the formation of carbon oxide was observed to be more significant. Doping alkali metal on Sm_2O_3 generally resulted in higher C_2 hydrocarbon yield. The best catalytic activity of 38% methane conversion and 57% selectivity to C_2 hydrocarbon was observed for Li/Sm_2O_3 system.

Lin et al.,1986 reported that under the same reaction condition La_2O_3 generated more methyl radicals than Li/MgO but resulted in lower selectivity and yield of C_2 hydrocarbons. It was suggested that the lower C_2 yield on La_2O_3 is due to its higher activity for oxidative reaction of methane. Campbell et al.,1988 have studied the activity of lanthanide oxides for the oxidative coupling reaction. Using their MIESR technique these workers found that Nd_2O_3 and La_2O_3 are more active per unit surface area than Sm_2O_3. However under this condition the maximum conversion occurring was less than 5%.

Imai and Tagawa, 1986 and Imai et al.,1987, 1988 reported that an unsupported $LaAl_2O_3$ prepared by mist decomposition gave higher activity per unit surface area than La_2O_3, Sm_2O_3 and $PbO/Na_2O/Al_2O_3$. On a weight basis $LaAlO_3$ has a similar activity to La_2O_3. The selectivity to C_2 on $LaAl_2O_3$ was always less than 50% (Imai et al, 1988). DeBoy and Hicks,1988a compared the activity of La_2O_3 system against that of Li/MgO and Pb/SiO_2. It was observed that doping alkali on La_2O_3 also resulted in higher C_2 yield, with Li having the greatest effect (21.6% conversion, 76% selectivity). The activity of Li/La_2O_3 is comparable to that of Li/MgO, Sn/La_2O_3 and better than that of Sm_2O_3 and Pb/SiO_2. These workers (De Boy and Hicks, 1988b) also noted that most of the rare earth oxides give good C_2 yields (~ 10%) under the screening conditions except CeO_2 and Pr_6O_{11}.

Michida and Enyo, 1987, have studied the oxidative coupling reaction over cerium mixed oxides and its relationship with their ion-conducting characteristics. It was found that $Ce_{0.95}Yb_{0.1}O_{1.95}$, and $Zr_{0.9}Yb_{0.1}O_{1.95}$ which were good O^{2-} conductors resulted in mainly the exhaustive oxidation of methane. The good conductor of H^+, $SrCe_{0.9}Yb_{0.1}O_{2.95}$ results in C_2 hydrocarbon yield of 31.6%.

Gaffney et al.,1988a, 1988b, reported that the presence of sodium on Pr_6O_{11} and Tb_4O_7 increased the selectivity to C_2 hydrocarbons significantly. Under reactant co-feeding conditions on 4% Na/Pr_6O_{11} 8.6% C_2 yield was achieved at 775°C. A much higher yield was achievable under reactant sequential feed mode. This activity result is similar to that of Sm_2O_3 as observed by Otsuka et al.,1986a. Korf et al.,1988

have further studied the effect of promoters on Sm_2O_3 while Yingli et al.,1988 reported a C_2 yield of around 20% for La_2O_3, Ce_2O_3, Pr_6O_{11}, Nd_2O_3, Sm_2O_3 supported on MgO at 700°C. These material show higher activity than Li/MgO under their reaction condition.

2.6 Chloride Containing Catalysts

Otsuka and co-workers have studied the partial oxidation reaction over many catalysts containing alkali halide compounds. $LiCl/Sm_2O_3$ was found to give C_2 hydrocarbon yield around 7.2-20% at 750°C with a high C_2H_4:C_2H_6 ratio. The presence of LiCl increases the hydrocarbon selectivity as well as that of C_2H_4 (Otsuka et al.,1986a). When LiCl was supported over various transition metal oxides (Otsuka et al., 1986a-e; Otsuka and Komatsu, 1986, 1987), it was observed that (Otsuka et al.,1986b) $LiCl/Mn_2O_3$ gives the highest C_2 yield of 31% followed by LiCl/NiO at 19%. LiCl on Cr and Fe oxide does not give significant hydrocarbon products. It was observed that the reduction of some metal oxides also occurs. In a following study, Otsuka and Komatsu,1986, found that LiCl/NiO have similar activity to $NaCl/Mn_2O_3$ indicating that the NaCl can also serve as a significant promoter on the transition metal oxides.

The effects of various alkali compounds have been reported in Otsuka et al.,1988a. These alkali compounds generally increase the hydrocarbon yield. The LiBr/NiO was observed to have similar activity, if not better, than LiCl/NiO (~15% yield). LiOH, $LiNO_3$ and Li_2CO_3 on NiO all resulted in about 6% hydrocarbon yield with the ratio of C_2H_4/C_2H_6 about 1. LiF on NiO seem to result in the lowest C_2 yield (2.6%). It was also shown that $NaCl/Mn_2O_3$ (Otsuka and Komatsu, 1987) have a higher catalytic activity than any previously reported catalyst, with yields of 30% to C_2 hydrocarbon at 750°C , 26% of of this yield resulting in C_2H_4 production. However it was also reported that for all these material the deactivation is very rapid (Otsuka et al.,1988a).

Another kind of catalytic material that has been studied in the context of oxidative coupling of methane is the layered Bismuth oxyhalide compound. Ueda and Thomas, 1988 found that among the layered Bismuth oxyhalide compounds, the oxychloride was the best catalyst. Even though oxybromide showed high activity it resulted in lower product selectivity while oxyflouride have much lower activity. The best activity data shows hydrocarbon yield of about 20% with a ratio of ethene to ethane in the product of about 3.5. However, as in the case of alkali halide containing catalysts, this family of compounds is also unstable under reaction conditions.

Another development in the direct conversion of methane to higher hydrocarbons is through the chloro-hydrocarbon route. Methane, oxygen and hydrogen chloride were reacted over an oxyhydrochlorination catalyst in the first stage to produce predominantly chlorocarbon (CH_3Cl, CH_2Cl_2) and water. In the second stage the chlorinated hydrocarbons were catalytically converted to higher hydrocarbon by alumino sulphate zeolite catalyst (Taylor and Noceti,1988 and Taylor et al.,1988). The condensation of the chlorocarbon compounds to higher hydrocarbons can generally be catalysed over acidic catalysts (Jens et al, 1988). Using methyl chloride as the reactant feed, up to 60% conversion at 400°C can be achieved over H^+ modernite impregnated with Zr^{4+} catalyst with 92% selectivity to C_2 and higher hydrocarbons. An alternative to the catalytic conversion of the chlorocarbon is through oxidative pyrolysis of the chlorocarbon at temperatures in excess of 900°C (Senkan 1987a,1987b; and Senkan et al., 1988a, 1988b).

2.7 Partial Oxidation Route

The literature on partial oxidation of methane to methanol and formaldehyde is quite extensive. Excellent reviews in this area can be found in Gesser et al, 1985, Foster, 1985, and Pitchai and Klier, 1986. An interesting development in the area was the work of Lunsford and co-workers. Since then there has been a significant increase of interest in this area. For the purpose of this thesis, only some of the current literature, 1985 onwards, plus the work of Lunsford et al will be reviewed.

The initial report by Liu et al.,1982 shows 16% conversion of methane and combined selectivity of 60% to methanol and formaldehyde over Mo/SiO_2 catalyst using N_2O as oxidant. Later works (Liu et al, 1984) could not reproduce the activity, however, 6% conversion with 58% selectivity was achievable. It was also observed that small amounts of water had a strong positive influence on formaldehyde selectivity. A mechanism for the reaction has also been proposed. Khan and Somarjai, 1985 have broadly reproduced the activity of Mo/SiO_2 and also performed the kinetic experiment on the reaction. It was also found that V_2O_5/SiO_2 is also active for the partial oxidation reaction (Zhen et al., 1985). Spencer 1988 has also studied the partial oxidation of methane on MoO_3/SiO_2 using O_2 as an oxidant. A best yield of 2% for formaldehyde was observed at 650°C. It was also observed that the presence of alkali on the catalyst decreases the yield of products. In their studies on the catalytic activity of molybdenum and vanadium based catalyst on silica, silica-titania and titania support, Lee and Ng, 1988 observed that a yield of 15% CH_3OH can be achieved over V_2O_5/SiO_2 catalyst at 600°C by using N_2O as oxidant. Currently this must be the highest yield reported in the literature.

Solymosi et al.,1985 studied the partial oxidation of methane by nitrous oxide over Bi_2O_3/SnO and found that at 550°C, 1.7-2.7% conversion and 95-84% selectivity can be achieved. Otsuka and Hatano, 1987 have studied the activity of various materials supported on silica, and generally, a formaldehyde yield of about 1% was observed. It was also found that the nature of the reaction occurring is sensitive to the electronegativity of the metal cation of the oxide. In the case of mixed Fe, Nb, and B oxides, Otsuka et al, 1988 found that a 38% yield of CH_3OH can be achieved over FeNbB-O catalyst at 810°C when O_2 was used as the oxidant. Kastanas et al.,1988a, 1988b have studied the activity of various silica based catalysts, metal oxide and silica acid. The best activity observed yielded about 3% formaldehyde.

Kasztelan and Moffat 1987a, have studied the partial oxidation on silica using O_2 and N_2O as oxidant at temperatures up to 600°C. In all cases low formadehyde yield was observed and O_2 results in higher methane conversion, than N_2O. The

activity of various heteropoly oxometallate was also studied using N_2O as oxidant (Kaztelan and Moffat, 1987b, 1988a and Ahmet et. al.,1988). Conversion of up to 5% was reported but still the total yield to oxygenated products is low. It was also observed that these compounds are not thermally stable at reaction temperatures (Kaztelan and Moffat, 1988b).

Yarlagadda et al.,1987 have determined the partial oxidation reaction at high pressure on ZSM5 catalyst at 380°C. About 1.3% hydrocarbon products were observed. They proposed that methanol was the intermediate product from homogeneous partial oxidation of methane and the hydrocarbons were produced from methanol over the catalyst by the MTG type process. Gesser et al, 1987a also found that methanol selectivity of 75%-80% at 8-10% conversion can be obtained from the homogeneous reaction at 65 atmospheres and 450°C and a residence time of about 4 min. These workers also observed that the reaction material also influence the reaction significantly. No significant increase of product yield was observed in the catalysed reactions.

2.8 The Gas Phase Reaction

As mentioned earlier in the introduction (section 1.2), the homogeneous pyrolytic reaction of methane has been used industrially to produce acetylene. This reaction can also be promoted over catalytic materials. Currently a lot of research activity is going on in the areas of catalytic pyrolysis of methane to higher hydrocarbons. A review on the homogeneous pyrolysis can be found in Khan and Crynes, 1980.

The gaseous phase reaction of methane with chlorine can also results in the formation of higher hydrocarbons. The activation of methane by chlorine was suggested by Baghal et al.,1978, 1979 and Benson, 1980 for the conversion of methane to ethylene and ethane at approximately 1000°C.

The gas phase oxidative reaction of methane has been extensively studied in the context of combustion chemistry and chemical kinetics and also for the production of

oxygenates. However under flame conditions, the oxygenates and higher hydrocarbons are minor products compared to carbon monoxide and carbon dioxide. The effort of producing oxygenates from partial oxidation of methane by O_2 or N_2O have shown that 3-7% yield of methanol can be achieved. The direct conversion of methane to methanol by controlled oxidation have been reviewed by Gesser et al.,1985. Recently, Gesser et al.,1987a, 1987b have observed that homogeneous reaction of methane and oxygen at 30 atmospheres and about 450°C can produce up to 7% yield of methanol. The effect of reaction sensitiser on the reaction has also been studied and found that they do not increase the products significantly.

Skinner et al.,1959 have studied the gaseous phase oxidation of methane using shock tube experiments. Under moderate conditons (residence time=1.5msec.; CH_4:O_2:Ar=12:2:8.6) ethane was the major hydrocarbon product and as the reaction conditions became more severe (higher temperature, longer residence times and higher CH_4/O_2 ratio) the selectivity to ethene increased The total hydrocarbon selectivity decreased as the methane conversion increased. The effect of pressure on homogeneous gas phase oxidative reaction of methane with O_2 has been studied by Asami et al.,1987c and 1988b. At 750°C, low total pressure does not result in any significant reaction and methane conversion increases at higher reactant total pressure. CO and ethane seems to be the primary reaction product and was followed by carbon dioxide, ethene and higher hydrocarbons. At high reactant total pressure (~15 atm.) CO was the main carbon oxide product while among the hydrocarbons, ethene was favoured. About 4% C_2 yield was observed, and it was proposed that the reaction involved the formation of methyl radicals.

Hutchings et al.,1988a, have compared the homogeneous reaction against the catalytic reaction at ~600°C and high total pressure. These workers demonstrated that the product distribution from high pressure homogeneous and catalytic reactions at ambient pressure are very similar. When the catalysed reaction was conducted at 5.9 atm., it was found that the product distribution are not sensitive at all to the nature of catalytic materials. Since the reaction at high pressure is similar to the catalysed

reaction at ambient pressure, these workers argue that the discovery of materials which are efficient oxidative coupling catalysts are of little significance. What is important is to achieve a material which can control the selectivity to the favoured hydrocarbon products.

Lane and Wolf, 1988b, 1988c, have also studied the homogeneous gas phase reaction of methane and oxygen at 600-850°C and 1 atmosphere total pressure. At a methane conversion of 2%, the hydrocarbon product selectivity was observed to be around 65% but at 32% conversion the selectivity decreases to around 29%. Comparing the catalysed reaction (over Li/TiO_2) against the homogeneous, in agreement with other workers, it was found that for the hydrocarbon product, ethane is the primary product while ethene is produced from a secondary reaction in both the homogeneous and catalysed reaction. In the case of carbon oxide products, as in other works, carbon monoxide is the dominant product of the homogeneous reaction while carbon dioxide is the dominant product for the catalysed reaction.

2.9 The Effect of Process Condition

2.9.1 Reactant Gas Type

Yang and Lunsford, 1980 demonstrated that by using N_2O as the oxidant, oxidative dehydrogenation of ethane over supported molybdenum oxide occurred. The reaction of methane with N_2O over the catalyst at about 600°C was reported (Liu et al, 1982, 1984) to give high selectivity to formaldehyde and methanol. At 594°C, 6% conversion occurs with 49.5% and 7.7% selectivity to formaldehyde and methanol respectively. It was also observed that the selectivity to oxygenates dropped considerably as the temperature was raised. N_2O was known to generate O^- sites which activates methane to form a methyl radical as intermediate. This site was also known to be present on MgO which was thermally pretreated and exposed to N_2O. Driscoll et al, 1985a, have studied the partial oxidation of methane over MgO and lithium doped MgO using O_2 and N_2O as the oxidant in the 450-500°C temperature regime. When N_2O was used as oxidant, the production of methyl radical was

observed to decrease continuously with time. It was proposed that the decrease in activity was due to a decrease in the availability of free electrons on the material necessary for the decomposition of N_2O. By using O_2, however, the production of methyl radicals remained fairly stable with time. The O^- type sites were also proposed to be the active centres over these materials. Khan and Somarjai,1985, have broadly reproduced the activity studies with a Mo/SiO_2 catalyst and N_2O as oxidant. A similar catalytic activity was observed for the V_2O_5/SiO_2 catalysts by Zhen et al.,1985.

N_2O was found by Shepelev and Ione, 1984 to be the most suitable oxidant with methane for generating hydrocarbons over transition metal oxides supported on zeolite catalysts in the 600-650°C temperature regime. Reaction of H_2O_2, NO and NO_2 with CH_4 were found to result in a product which was predominantly carbon oxide. Anderson and Tsai, 1985 also found that the oxidative reaction of methane with O_2 as an oxidant results in the formation of carbon oxides, but with N_2O some oxygenates and higher hydrocarbon products were observed on a ZSM5 catalyst. Kowalak and Moffat, 1988 also observed that significant selectivity to hydrocarbons can be achieved at 400°C when N_2O and methane were reacted over H-Mordernite and Fluorinated Mordernite. Such observations were also made by Meng and Sanger, 1987, but for Pb supported on Al_2O_3 or NaY zeolite at round 600°C.

In their earlier works Otsuka and Nakajima, 1986 observed that oxidative coupling of methane using N_2O as an oxidant proceeded with good selectivity to hydrocarbons over La_2O_3, Sm_2O_3 and Dy_2O_3 especially at temperatures lower than 650°C. However at higher temperature O_2 was found to be a better oxidant for the production of higher hydrocarbons (Otsuka and Nakajima, 1987). The production of oxygenate was, however, observed over various metal oxides supported on silica gel at 700°C from the reaction of methane with N_2O (Otsuka, and Hatano, 1987) and over mixed oxides of Fe, Nb and B oxides (Otsuka et al., 1988b). Lee and Ng, 1988 observed that a higher methane conversion to formaldehyde resulted when using N_2O rather than O_2 over V_2O_5-SiO_2 catalyst. Solymosi et al, 1985 also made similar observations using a Bi_2O_5 catalyst at 850°C. Katsztelan and Moffat, 1987a, 1987b,

1988a and 1988b, observed that over heteropolyoxometalates, the use of N_2O resulted in production of oxygenates while the use of O_2 caused full oxidation.

For the production of oxygenates over silica, Kasztelan and Moffat, 1987a found that O_2 produced a partial oxidation product under rather mild condition while nitrous oxide resulted in complete oxidation. Methane conversion over Mo/SiO_2 using O_2 also produce oxygenate (Spencer et al.,1988). The high pressure homogeneous reaction study by Gesser et al.,1987a, 1987b, showed that the reaction of O_2 with methane can produce oxygenates as products. However, under more severe conditions the hydrocarbon products were generally observed to be more favoured than the oxygenates. When O_2 was used as oxidant, conversion and selectivity to higher hydrocarbons increased at higher temperature, but N_2O favoured the exhaustive reaction. Hutchings et. al., 1988b, 1988c, and 1988d, have also studied the effect of different oxidants on the oxidative reaction of methane. Generally O_3 and N_2O are more reactive at lower temperature than O_2.

2.9.2 The Composition and Total Pressure of Reactant Gas

In flame chemistry, it is known that the ratio of fuel to oxidant influences the nature of the flame whereby different chemical species are produced. Similar phenomena also exist in the catalytic oxidative reaction.

Keller and Bhasin, 1982, have observed that the concurrent feeding mode gave low selectivities (20%) to hydrocarbon products while feed programming gave 50% selectivity. This was explained as being due to the elimination of the competing gas phase oxidation reaction. In this work and that of Sofranko et al.,1987, the catalytic material used possesses variable oxidation states and hence, reactions occur between methane and surface oxides resulting in the reduction of the surfaces. It was necessary to regenerate the surface by treating the catalyst in an oxygen flow.

The co-feeding mode has been found, however, to result in high selectivity to C_2 hydrocarbon, especially over a single oxidation state catalyst. The effect of the reactant composition on product distribution has been observed in nearly all research.

Shepelev and Ione, 1984, found that, with a constant concentration of nitrous oxide, as the concentration of methane was increased, conversion and selectivity to exhaustive oxidation decreased while the selectivity with respect to hydrocarbon increased. Hinsen et al.,1984, proposed that the selective and nonselective reaction steps of the oxidative coupling of methane depended differently on P_{O_2} and P_{CH_4} respectively. They noted that to maximise hydrocarbon selectivity, the partial pressure of oxygen should be low while that of methane should be maximised.

Matsuura et al.,1986 found that on Li/ZnO the amount of CH_4 converted increased smoothly with the increase in O_2 partial pressure below 100 torr but at a higher O_2 partial pressure the exhaustive oxidation was accelerated. The selectivity to C_2 increased with the lowering of the partial pressure of O_2 while, on the other hand, the selectivity to C_2 compounds became high with an increase in CH_4 pressure. Similar observations have also been made by Zhang et al., 1988. Meng and Sanger, 1987, observed that the yield of hydrocarbon products peaks at a ratio of CH_4/N_2O close to four. Roos et al.,1987 found that on Pb/Al_2O_3 and Li/MgO systems, methane conversion decreases when the CH_4/O_2 ratio is increased resulting in a net loss of C_2 yields. Kowalak and Moffat, 1988, also observed similar effects over their H-Mordenite catalyst.

In their studies on Li/BeO catalyst, Matsuura et al.,1987 observed that the selectivity of C_2 compounds was as high as 84% under a low partial pressure of O_2 with the value dropping with increases in O_2 pressure. In this work the optimum yield of C_2 compounds was obtained with the ratio of $P_{O_2}/(P_{O_2} + P_{CH_4})$ being in the range 0.2 and 0.3. Lin et al., 1988 have reported that the effect of varying the CH_4/O_2 ratio over Na/CaO was similar to that reported for Li/MgO and the amount of C_2 produced over both catalysts was comparable.

In all of these works, under low oxidant partial pressure, high selectivity to C_2 products is generally observed. This is highlighted by the feed programming mode where higher hydrocarbon selectivity is observed when CH_4 and O_2 is co-fed. While the ratio of CH_4 to O_2 was decreased by varying P_{O_2}, the selectivity to the produced

hydrocarbon decreased. In a number of cases the ratio of $P_{CH_4}/P_{O_2}=2$ was found to give optimum C_2 yield. All of these observations were manifested in the kinetic parameters determined by various workers over different catalytic material and under different conditions. In table 2.9.2.a, it can be seen that the order of the reaction with respect to oxygen for formation of CO_x is always larger than that for the formation of C_2. On the contrary, the order of reaction with respect to methane for the formation of C_2 is always larger than that for the formation of carbon oxide (CO_x) products. This indicate that the selectivity to C_2 will be directly dependent on CH_4 partial pressure while that to CO_x depends on the partial pressure of O_2.

Table 2.9.2.a Some kinetic data (x,y) of the oxidative reaction of methane over different catalysts. X and Y are the order of the reaction with respect to CH_4 and O_2 respectively for any particular product).

Reference	Condition	CO_2	CO_x	C_2H_6	C_2
Hinsen et.al., 1984	PbO/Al_2O_3	(0.4,1.5)	-	-	(0.8,1.1)
Asami et al., 1987a,b	PbO/Al_2O_3	-	(0.4,0.7)	-	(0.9,0.0)
Amesh and Amenomiya,1986	$Bi_2O_3/K_2CO_3/Al_2O_3$	(0.3,1.0)	-	(2.0,1.0)	-
Doi et al.,1988	Li/BeO	(0.0,1.0)	-	-	(1.0,0.4)
Tagawa and Imai, 1988	$LaAlO_3$				
	$P_{CH_4}/P_{O_2} < 4$	(0.5,1.2)	-	(1.7,-0.8)	-
	$P_{CH_4}/P_{O_2} > 4$	(0.1,1.7)	-	(1.0,0.5)	-
Lo et al., 1988	Sm_2O_3	(-1.0,1.0)	-	(0.9,0.6)	-
Miradatos and Martin, 1988	Li/MgO	-	(-0.1,0.8)	-	(0.8,0.6)

As in the high pressure homogeneous oxidative reaction of methane, the total pressure of reactant in the catalytic reactions also influences the product distribution. Otsuka et al.,1986d, observed that as the total partial pressure of reactant was

increased over $LiCl/Sm_2O_3$, the amount of methane converted increased slightly. The selectivity to C_2 hydrocarbon was however decreased significantly resulting in a lower yield of the product. The effect of the reactant pressure on the homogeneous reaction and the Li/TiO_2 catalysed reaction have been determined by Lane and Wolfe, 1988a. These workers found that for the homogeneous reactions at low pressure, high selectivity to C_2 product occurs, and it decreases significantly with pressure. Similar changes occur in the catalysed reaction, but to a smaller extent.

2.9.3 Temperature and Flow Condition

The reaction temperature and residence time of a reactant gas in the reactor is an indication of the severity of the reaction. At higher temperatures the rate of reactions are faster while at longer residence times, the reaction can proceed further.

Generally the effect of increasing temperature resulted in a greater conversion of methane, together with some variation in the product distribution. In nearly all cases the selectivity to C_2 hydrocarbon increases with temperature, especially under the oxygen limiting condition. The selectivity to ethylene was also observed to increase significantly with reaction temperature.

The effect of temperature on the reaction depends on the oxidant used. Otsuka et al.,1987 observed the advantage of using N_2O as oxidant at low temperature. At higher temperatures however, O_2 is the favoured oxidant. Hutchings et al.,1988b, 1988c, 1988d, have also studied the role of different oxidants at different temperatures. O_3 and N_2O are more oxidising than O_2 at low temperature, but at higher temperatures the use of these oxidants predominantly resulted in an exhaustive oxidation.

The nature of catalytic materials also influences the extent of temperature effects. Roos et al.,1987 observed that PbO/Al_2O_3 starts to be active, and reaches maximum activity, over a much smaller temperature range than in the Li_2O/MgO system. The Li_2O/MgO system needs a higher temperature to result in the same conversion as obtained on PbO/Al_2O_3.

Roos et al.,1988 have also observed that at fixed temperature and w/F, increasing flow resulted in the increase in both CH_4 conversion and selectivity to C_2. It was suggested that this might be caused by a lowering of the external mass transfer resistance at high gas velocity or because of better gas distribution. On the other hand, Kasteren et al., 1988 have observed that increases in post catalytic space resulted in a slight increase in methane conversion but a considerable increase in selectivity to ethene relative to ethane. This suggest that ethene formation can occur through the gaseous phase reaction of the effluent gas from the catalyst bed.

Table 2.9.3.a The effect of temperature on the kinetic parameter of reaction over PbO/Al_2O_3 (rate= $kP_{CH_4}^{m1}P_{O_2}^{m2}$, Carreiro et al.,1988)

Temp.	C_2 product			CO_x product		
°C	k	m1	m2	k	m1	m2
680	$1.5x10^{-4}$	1.1	1.4	$12.5x10^{-4}$	0.6	2.0
723	$1.1x10^{-4}$	0.8	0.7	$6.0x10^{-4}$	0.5	1.3
760	$1.9x10^{-4}$	1.3	0.4	$5.0x10^{-4}$	0.7	0.9
800	$4.8x10^{-4}$	1.2	0.6	$2.6x10^{-4}$	1.0	0.3

Another effect of temperature is on the catalytic material itself. A number of catalytic materials have significant vapour pressure (Bhasin et. al., 1988) at reaction temperatures. The sintering of Li_2CO_3/MgO and other catalysts at the high temperature have been studied by Miradatos et. al., 1987. Two modes of sintering that was pointed to be significant over these catalyst are the sintering via liquid Li_2CO_3 and the effect of H_2O and CO_2. Larkins and Nordin,1988 has observed the melting of the Li_2CO_3 of Li_2CO_3/MgO catalyst in-situ under reaction condition using the FTIR

technique. Obviously in these cases the stability of the materials are strongly affected by the reaction temperature.

Carreiro et al.,1988, have determined the effect of temperature on the kinetic parameters of catalytic oxidative reaction of methane over PbO/Al_2O catalysts, and the result is presented in Table 2.9.3.a. From these results it can be seen that the rate constant for C_2 formation increases significantly with temperature while the rate constant for the formation of CO_x decreases. This explained the increase of C_2 selectivity at higher reaction temperatures.

2.9.4 Role of additive gas

Liu et al, 1982 have observed that the presence of H_2O in the partial oxidation of methane by N_2O over Mo/SiO_2 catalyst resulted in significant formation of methanol. H_2O, however, has less effect in the higher temperature oxidative coupling reaction (Carreiro and Baerns, 1989).

As discussed earlier, the addition of Cl_2 or HCl on the partial oxidation of methane was found to result in an increase of selectivity to ethylene. In this case, the additive gas became a source of chlorine atoms which in turn promoted the formation of ethene.

The effects of CO on the oxidative coupling reaction have been studied by Larkins and Nordin, 1988a. They found that CO has a competitive effect against methane conversion. CO was preferably oxidised over the catalyst causing methane conversion to decrease. Korf et al, 1987 have studied the effect of CO_2 in the reactant stream. Its presence over Li_2CO_3/MgO resulted in a lowering of methane conversion with a slight increase in C_2 selectivity. However, when the flow was terminated the activity of the catalyst was regained. It was also found that CO_2 can be used to regenerate the catalyst after a prolonged run. However, the beneficial effect of the regeneration was found to be short lived. An interesting new concept by Aika and Nishiyama, 1988a, 1988b, is to utilise CO_2 as the source of oxygen in the partial oxidation reaction. Using a typical gas mixture flow rate of 10:10:0.1:40 ml/min for CH_4:CO_2:O_2:He respectively, up to 4% C_2 yield can be achieved.

Another additive gas that has been studied is ethane. In combustion chemistry the presence of ethane promotes methane oxidation. Similar observations were made in the catalytic reaction for the formation of oxygenates. Kastanas et al.,1988a have observed that with the presence of ethane in partial oxidation of methane over silicic acid at 560-620°C, the selectivity to formaldehyde improved and ethene was also found. The effect of the presence of ethane in the reactant stream on the oxidative reaction of methane has also been studied. Ito et al.,1985 observed that over Li/MgO, C_2H_6 reacted competitively over the catalyst against CH_4 to form ethene. These workers suggested that the formation of CO and CO_2 does not occur primarily from C_2H_4. In a similar study, Tyler,1986 compared behaviour of the oxidative reaction of ethane against that of methane and ethane mixture. The presence of methane was observed to reduce the exhaustive oxidation of the higher hydrocarbon products.

2.10 Active Site for Catalytic Reaction

The active sites responsible for the oxidative reaction of methane will be discussed according to the type of the catalytic materials. The classifications are the reducible oxidation state and the non reducible oxidation state catalytic materials.

2.10.1 Reducible Catalysts

The oxidative reactions of methane over catalysts with variable oxidation states are generally accepted to involve the redox process on the catalyst. Liu et al., 1982 have proposed the redox process involving Mo^{IV}/Mo^{V} in the partial oxidation of methane over Mo/SiO_2. Asami et al.,1988a, 1988b, also have shown that similar processes occur on PbO/Al_2O_3. Keller and Bhasin, 1982, have observed that over most reducible metal oxides, the partial oxidation of methane involve bulk oxygen indicating the reduction of the metal oxide. Sofranko et al.,1987, have made the observation that the percentage of methane conversion under feed programming mode decreases with time. This indicates that the reactions involve the bulk oxygen sites, and as these sites are depleted, the extent of reaction decreases. In the case of PbO

supported on MgO, Suleimanov et al.,1987, have observed the presence of one electron centres, the presence of which increases with PbO loading. It was also observed that methane conversion also increases with PbO loading. However it is yet to be determined whether this increase in conversion is related to the one electron centre or solely to the presence of PbO.

The redox process occurring on the reducible material can be represented by equation 2.10.1.a. The lability of the oxygen sites is directly related to the reducibility of the metal ions. The more labile the oxygen sites, the more active the material will be for the oxidation of methane. However, the actual nature of the oxygen sites is not certain; it can be either as the O^- (as in Mo/SiO_2) or as the O^{2-} type species.

Equation 2.10.1.a $\quad CH_4 + M^{(2n+)} + O_n \text{ ---> } M^{(2n-2)+} + O_{n-1} + H_2O + C_2H_6$

2.10.2 Catalysts with fixed Oxidation State

The active sites for Li_2CO_3/MgO and Na/CaO catalysts were proposed to be Li^+O^- (Wang and Lunsford,1986a) and Na^+O^- (Lin et al., 1987) respectively. Hutchings et al.,1987a have found that the O^- species on MgO was stabilised when Li was present. Various other alkali and alkali earth compounds have been found to be active for the oxidative coupling reactions especially Li/CaO, Na/MgO and $Li/SrCO_3$. It is also likely that in all these materials the O^- type species the active sites for the oxidative coupling reaction.

In the catalytic screening of Li_2CO_3/MgO, Kimble and Kolts,1987, have observed that the Li_2CO_3 phase undergoes decomposition. This indicates that for Li_2CO_3/MgO, the active site is not likely to be associated with the carbonate phase. It is possible that the carbonate phase is the direct precursor for the active sites, as was proposed by Korf et al.,1987.

Sinev et al.,1986, 1987 observed that the reaction of methane with BaO_2 resulted in high selectivity to ethane at significantly low temperatures. The O_2^{2-} species was proposed to be the redox site responsible for methane activation. Otsuka and Jinno, 1986 have also suggested the possibility of the peroxide ions, O_2^{2-} being the

sites on rare earth metal oxide and alkali promoted oxide. The O_2^{2-} can be regarded as the dimer of O^-, and it is difficult to characterise since it is diamagnetic. On lanthanum oxide Wang and Lunsford, 1986b, observed an abundant amount of O_2^-. The O_2^- species is known to be unreactive at temperatures up to 200°C. These workers argue that the fact that these superoxides are unreactive at 200°C does not necessarily indicate that they will be unreactive at temperatures greater than 327°C. The ESR spectrum of O_2^- has been observed after quenching La_2O_3 which was in air at 650°C, by immersion in liquid nitrogen, indicating that O_2^- can be present at 650°C. Kazansky, 1977, has proposed that the formation of O^{2-} can occur via O^- through the process represented by equation 2.10.2.a. The O^- can then be stabilised on an oxide surface which has a limited number of available electrons, and hence the formation of the O^{2-} species is prevented.

Equation 2.10.2.a $O_2(gas) \rightarrow O_2(ads) + e \rightarrow O_2^- + e \rightarrow 2O^- + 2e \rightarrow 2O^{2-}$

2.10.3 Catalysts made from Reducible Metal Oxide Doped with Alkali Metal Compounds

It has been noted in many works that the C_2 selectivity on materials with reducible metal oxides improves significantly when doped with alkali metal compounds. The presence of the alkali compounds on the catalyst increases its basicity. The increase in basicity result in the increase of selectivity to C_2. When alkali compounds are present another change which may occur is the reduction in the availability of labile oxygen. This causes lower methane conversion, but increases the selectivity to C_2 hydrocarbons. Over these materials the active site is likely to be the composite of that on the reducible catalyst and the non reducible materials.

2.10.4 Implication for activity

From the activity results, it has been clearly shown that the co-feed mode reactions over materials with variable oxidation states favour exhaustive oxidation in contrast to most of the non reducible materials. It should be noted however that in

contrast to most of the non reducible materials. It should be noted however that in both cases the actual active sites are not explicitly defined. It would seem that the lability of these sites determines the extent of the exhaustive oxidation. Materials with easily reducible sites, or labile adsorbed oxygen, are likely to favour the exhaustive oxidation of methane. However, the O^- sites which were stabilised on the surface are likely to generate the methyl radical intermediates more effectively. On the contrary, sites which are labile would favour the formation of methoxyl and methyl peroxy species and hence the exhaustive oxidation of methane.

2.11 Mechanism for the Catalytic Oxidative Coupling Reaction

A number of mechanisms have been proposed for the catalytic oxidative coupling reaction (Keller and Bhasin, 1982, Ito et. al., 1985, Otsuka et. al., 1986a, Sofranko et. al., 1987, Sinev at. al., 1988, and Ekstrom and Lapszewicz, 1989). These mechanisms are very similar to each other except possibly for two points. The first one is on the nature of the active sites and the second, as to whether the steps of hydrocarbon formation occur on the surface or in the gaseous phase.

Generally the oxidative coupling reaction can be outlined in a series of reactions or reaction networks. Figure 2.11.a illustrates the reaction mechanism for the catalytic oxidative reaction of methane. Interaction of methane with the active sites may result in the formation of surface hydroxyls and methyl radicals. Ekstrom and Lapszewicz, 1988a, 1988b, have suggested the possibility that this interaction involved ionic species formation as intermediates. It has also been proposed that carbene could possibly be the primary intermediate in this reaction (Martin and Miradatos, 1987; Miradatos and Martin, 1988). In the mechanism where methyl radicals was proposed to be the primary intermediate of the reaction, the radical formed would either further react to form methyl peroxy or adsorbed methoxyl species and form oxygenate, or couple to form ethane. It is more likely that the methyl radicals desorb and couple in the gaseous phase, especially at high temperatures. The recent work by Campbell et. al, 1987 on the amount of methyl radicals trapped as a function

of distance from the catalyst bed further supported the proposal that the coupling of methyl radicals in the gaseous phase is the major pathway for the formation of ethane. Nelson et. al., 1988 have obtained isotopic evidence for direct methyl coupling during the oxidative coupling reaction of methane. Under the reaction conditions, as mentioned by Labinger and Ott, 1987, the coupling reaction would be favoured due to the high spatial concentration of methyl radicals. In their molecular orbital calculations of methyl radicals present on the O^- sites of Li/MgO surfaces, Mehandru et al., 1988, found that the methyl radicals can easily desorbed allowing the recombination reaction to occur in the gaseous phase.

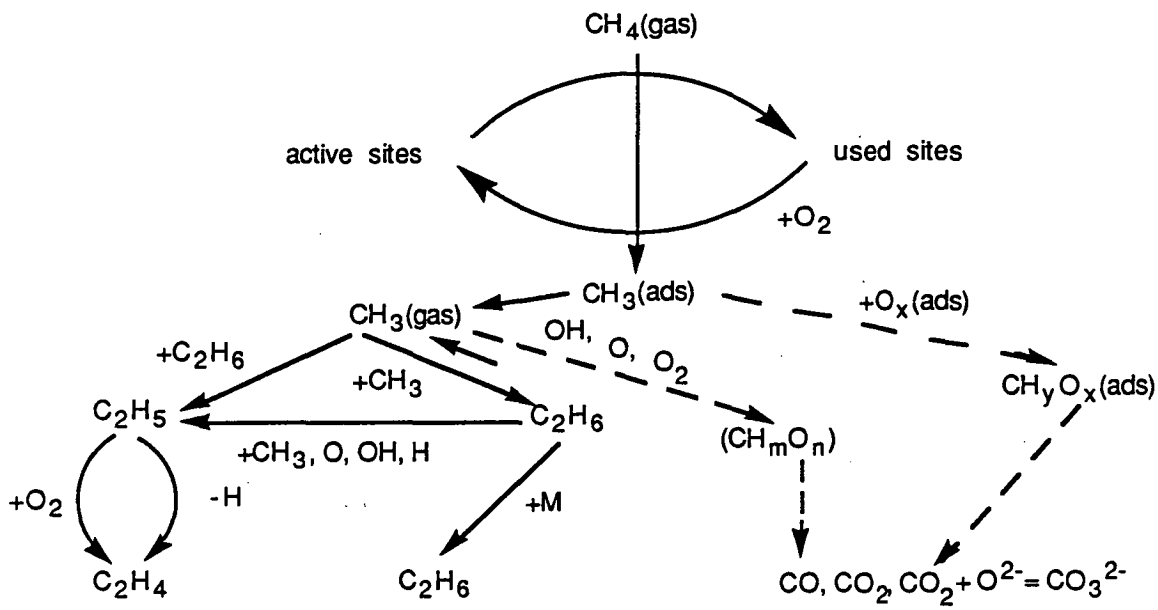

Figure 2.11.a Mechanism for the catalytic oxidative reaction of methane.

It is generally accepted that carbon oxides are also the primary product of the oxidative reaction of methane. The formation of these products has been proposed to involved surface oxidation of methyl radicals (Amorebieta and Colussi,1988). Some exhaustive oxidation can still occur in the gaseous phase through the oxygenates pathway.

The further oxidation of the hydrocarbon products with the catalyst, and also in the gaseous phase, is strongly dependent on the reaction and flow conditions. The gaseous phase reaction of C_2H_6 to C_2H_4 has been demonstrated by Kasteren et al.,1988, to be significant while Ekstrom and Lapszewicz, 1989, have suggested that on Sm_2O_3, Li/Sm_2O_3 and Pr_6O_{11}, the carbon oxides are substantially formed by the secondary oxidation of reaction products. However as shown by Lee and Oyama, 1988 the exhaustive oxidation of C_2 products, especially C_2H_4 is minimal due the relative stability of C2H4 and also because the product is further down stream, where the O_2 concentration and temperature are lower. In the catalyst screening for oxidative coupling activity, only trace amounts of oxygenates were observed in the product stream. This is because most of the oxygenates were converted to carbon oxides under the oxidising condition. It should, however, be noted that the homogeneous oxidation of the hydrocarbon products will favour formation of carbon monoxide, while surface oxidation favours the formation of carbon dioxide.

Two different reaction steps have been proposed to be the rate determining step in oxidative reaction of methane. Ito et al.,1985, and Sinev at al., 1988, have proposed that the active site regeneration is the rate determining step. On the other hand, Cant et al.,1988, and Bueskaya, et al., 1987, have shown that the kinetic isotope effect can be observed in the oxidative reaction of CH_4 and CD_4. This observation was suggested to indicate that the C-H bond breaking was the rate determining step in the reaction.

A question that remains to be fully answered is to what extent does the coupling of methyl radicals and their exhaustive reactions occur in the gaseous phase or on the catalyst surface. The most likely answer are that under the condition where homogeneous reaction are minimal, most of the exhaustive reactions occur on the catalyst surfaces while the coupling of methyl radicals occur in the gaseous phase. However since the hydrocarbon product distribution of homogeneous and catalytic reaction are broadly similar, as argued by Labinger and Ott, 1987, and Hutchings et al.,1988a the question of whether surface or gaseous phase coupling occurs may be of

no significance. The most important matter is to achieve the reduction of exhaustive oxidation and yet retain a high conversion of methane.

Table 2.12.a Oxidative Coupling of Methane over various catalysts.

Catalyst	Temp/C	CH_4:O_2:dil.#	%C_2yield	Ref.
Sm_2O_3	700	1:0.003:4.6	0.99	Otsuka et. al., 1986a
Bi_2O_3-K_2O_3/Al_2O_3	640	1:0.10:0.90	2.1	Amesh and Amenomiya,1986
La_2O_3	725	1:0.11:4.6	4.4	Lin et. al., 1986
$Mn(NO_3)_2/Al_2O_3$	800	n.s	5.0	Keller & Bhasin, 1982
PbO/SiO_2	740	1:0.1:0.33	5.4	Bytyn & Baerns, 1986
Sm_2O_3	750	1:0.19:4.4	9.2	Otsuka et. al., 1986a
PbO-NaO/Al_2O_3	549	1:0.20:0.77	10.4	Roos et. al., 1987
Na_2CO_3/CaO	707	1:0.20:0.80	10.9	Kimble and Kolts, 1987
PbO/Al_2O_3	740	1:0.10:0.33	12.1	Hinsen et. al.,1984
$LaAlO_3$	710	1:0.20:0.80	12.2	Imai and Tagawa, 1986
Sm_2O_3	750	1:0.19:4.4	13.0	Otsuka et. al,1986c
Li_2CO_3/CaO	711	1:0.20:0.80	13.2	Kimble and Kolts, 1987
BaO/CaO	800	1:0.20:1.33	14.2	Yamagata et. al., 1987
Li_2CO_3/MgO	692	1:0.2:0.80	14.7	Kimble & Kolts, 1987
LiCl/TiO_2	750	1:0.50:0.28	14.9	Otsuka et. al., 1986c
Li_2CO_3/MgO	720	1:0.62:11.5	16.8	Ito et. al., 1985
LiCl/MnO_2	750	1:0.50:0.28	17.8	Otsuka et. al., 1986c
Li_2CO_3/MgO	720	1:0.62:11.5	19.4	Ito et. al., 1985
KNO_3/$BaCO_3$	800	1:0.50:35.3	20.2	Aika et. al., 1986
Li_2CO_3/Sm_2O_3	750	1:0.40:18.5	22.3	Otsuka et. al., 1986d

mole ratio; n.s = non stoichiometric.

2.12 Comparing the Catalytic Performances

Generally the activity results published in the literature are from determinations performed under varying conditions. In most cases the reaction temperature, reactant composition and flow conditions are different. It is a well known fact that the activity of any particular catalyst is highly dependent on the screening condition and this makes the direct comparison of the performances of the oxidative

coupling catalysts dificult. However, if it is assumed that the activity reported was achieved under optimum conditions, the percentage of yield to C_2 hydrocarbons could possibly reflect the performances of these catalysts.

Lee and Oyama, 1988, have compared the performances of many catalysts reported in the literature. These workers observed that most of the high activity catalysts resulted in reaction rates greater than 10^{-5}g-mole/s cm^3 and hence satisfy the "Weisz Window" criteria (Weisz, 1982) of commercially useful chemical reactivity. It was also observed that the rate of the oxidative coupling reaction (mole.m^{-2}.s^{-1}) of irreducible oxides appeared to be lower than those of other types of catalysts. However, this trend would be different if the comparison was made on the basis of catalyst loading, since most of the irreducible catalysts have low surface areas due to the present of alkali compounds. Table 2.12.a is basically a subset of the table of literature data listed by Lee and Oyama, 1988. It is interesting to note that most of the catalysts which were reported to result in greater than 20% yield to C_2, contain alkali compounds as one of their components. Moreover these catalysts are also not very reducible.

Another general way of representing this and other data is in the form of scatter plots of the total percentage selectivity and yield to C_2 hydrocarbon versus the percentage of methane conversion plots as presented in figure 2.12.a. As indicated by figure 2.12.a, the activity points seem to scattered in a particular domain. At low methane conversion, high selectivity (~90%) to C_2 hydrocarbons can be achieved. However, as methane conversion increases, the selectivity to C_2 products decreases. There seems to be a barrier for the total selectivity to C_2 hydrocarbon at any particular percentage of methane conversion, and this is represented by the broken line drawn in figure 2.12.a.

In the case of the C_2 yield plot (figure 2.12.a), the maximum achievable yield to C_2, at any particular percentage of methane, initially increases with methane conversion. At 30% of methane conversion, a C_2 yield of about 20% can be achieved. However, further increase in methane conversion does not result in any significant

maximum achievable selectivity, and hence yield to the favoured product (C_2) with an increase of methane conversion, is suggested by figure 2.12.a. Lee and Oyama, 1988, have also observed the decrease in selectivity to C_2 hydrocarbons on various catalysts with the increase in methane conversion. This observation tends to support the proposal made by Lunsford, 1988 of the existence of an 'intrinsic limit' for the oxidative coupling reaction of methane.

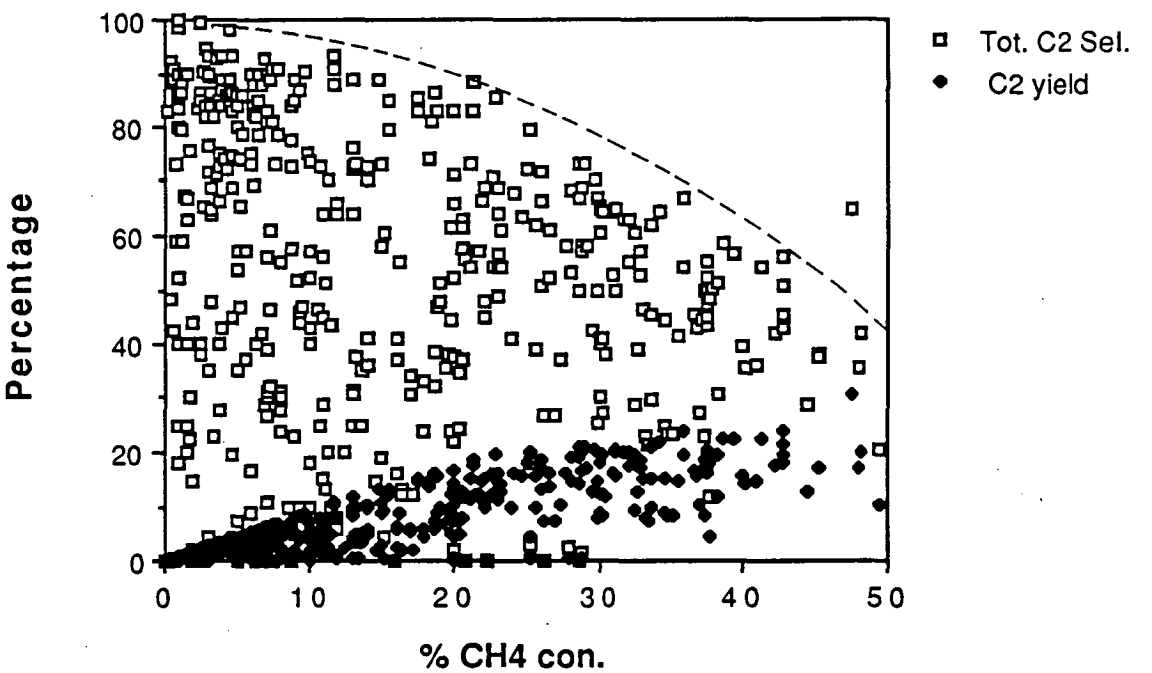

Figure 2.12.a Scatter plot of percentage of selectivity, and yield to total C_2 hydrocarbon against the percentage of methane conversion. The values used here were obtained from published catalytic activity results. The broken line in the graph represents the barrier for achieving higher total selectivity to C_2 hydrocarbon at any particular percentage of methane conversion.

Another aspect of the activity data is the percentage of C_2H_4 among the C_2 product. It is favourable to obtain higher percentage of C_2H_4 from the cataysed oxidative reaction of methane. Figure 2.12.b is a scatter plot of the percentage of C_2H_4/Total C_2 hydrocarbon data obtained from the published catalytic activity results.

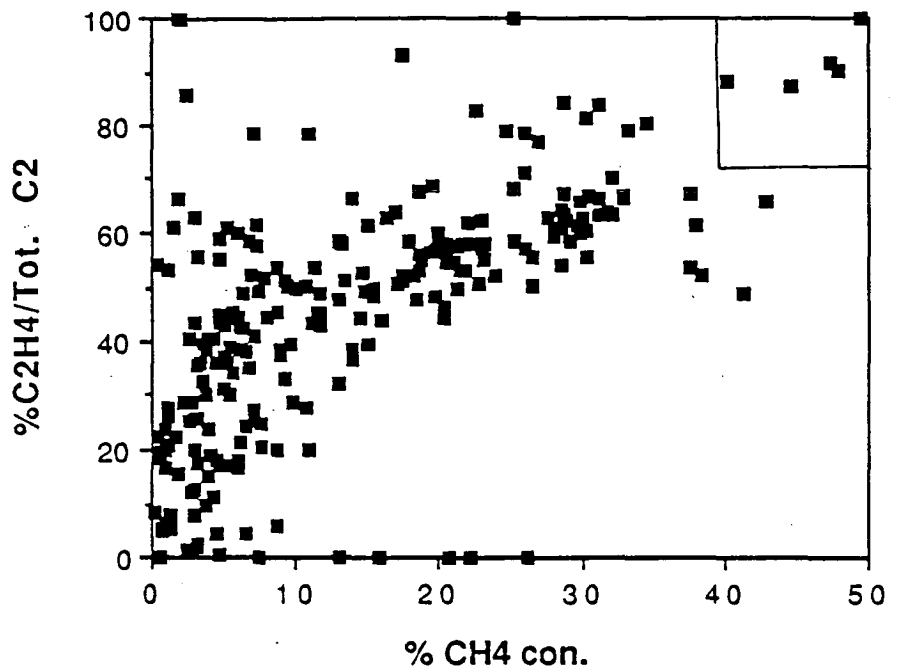

Figure 2.12.b Scatter plot of percentage of C_2H_4/Total C_2 product against the percentage of methane conversion. The values used here were obtained from published catalytic activity results.

C_2H_4/Total C_2 hydrocarbon data obtained from the published catalytic activity results. It can be generalised that the percentage of C_2H_4 in the C_2 products at lower conversion is small and as methane conversion increases, so does the percentage of C_2H_4 in the C_2 product.

Exceptions to these trends are mainly the results of reactions catalysed by materials containing chloro compounds. Moreover the five points contained in the box at the top-right hand corner of figure 2.12.b correspond to the reaction catalysed by the chloro-compound containing catalysts (Otsuka et al.,1986c,1986d). It has been established that chlorine atoms facilitate the conversion of ethane to ethylene. In this respect the chloro-compound component of the catalyst act as a reactant in the reaction.

The relationship between the percentage of C_2H_4/Tot. C_2 with percentage of methane conversion as observed in figure 2.12.b suggest that C_2H_4 is not a primary product of the catalytic oxidative reaction of methane. This indicates that the catalysts do not play any major role in determining the relative selectivity to C_2H_4 and C_2H_6. The relative selectivity to these hydrocarbon products are mainly determined by the percentage of methane conversion, which is in turn determined by catalytic activity and reaction severity.

CHAPTER 3

EXPERIMENTAL

3.1 Catalytic System

A wide cross section of materials have been reported to be active for the oxidative reaction of methane. The catalytic systems that have been most studied would probably be the Li_2CO_3/MgO and the supported transition metal oxide catalyst (Chapter 2). Generally materials which are chemically basic tend to favour the oxidative coupling reaction while supported transition metal oxide resulted in exhaustive oxidation. It has also been noted that most of the materials found to be catalytically active undergo significant physical and chemical changes under the reaction conditions.

In this work rather than embarking on purely catalytic designing and screening, efforts have also been made to investigate the nature of the catalyst more closely. Since the Li_2CO_3/MgO catalyst was the one most frequently studied, it was adopted to be the starting material in this work. Variations of this system were made and their catalytic activity was determined. The activity of various fresh chemicals have also been determined. The chemical and physical nature of these catalyst were also studied.

The list of catalyst systems studied in this work is given in table 3.1.a. The primary catalytic material is the Li_2CO_3/MgO system with different lithium loadings. However, it was found that MgO itself has significant catalytic activity and hence the activity of various MgO have been studied. The effect of different lithium salts on MgO and different support for Li_2CO_3 have also been determined. It has been reported in the literature that transition metal oxides doped with alkali metal have significant catalytic activity for the oxidative coupling reaction. In this work the effect of doping different loadings of various transition metal oxides on Li_2CO_3/MgO

systems have been studied. Other catalytic material studied are the various metal oxides and carbonates.

Table 3.1.a Catalysts studied in this work.

---

1. Li_2CO_3/MgO with different lithium loading.

2. Li_2CO_3 on various oxide supports.
Li_2CO_3/CaO, Li_2CO_3/SiO_2, Li_2CO_3/TiO_2, Li_2CO_3/γ-Al_2O_3

3. Various lithium salts on MgO
LiOH/MgO, LiCl/MgO, LiF/MgO, Li_2SO_4/MgO 49

5. Transition metal oxide on Li_2CO_3/MgO.
Oxides of Cr, Mn, Fe, Co, Ni, Cu, Zn

6. Transition metal oxide on MgO and Li_2CO_3/MgO.
Oxides of Cr,Mn,Fe and Zn (loading effect)

7. Fresh Chemicals.
MgO, $Mg(OH)_2$, $Ca(OH)_2$, SiO_2, TiO_2, γ-Al_2O_3, 12%Al_2O_3/SiO_2, $CaCO_3$, $SrCO_3$, Li_2CO_3, Na_2CO_3, K_2CO_3, Sm_2O_3, $AlPO_4$-5

3.2 Catalyst Preparation

The preparative procedure for the catalyst involved the wet aggregation and impregnation process. This procedure can be divided into three stages. First, the MgO powder was added to boiling water and the mixture was continuously stirred. Second, after an hour, the required amount of Li_2CO_3 was added. For the preparation of Li_2CO_3 doped on various supports, the MgO in the first stage was replaced by the particular support. Also in the case of various lithium salts on MgO support, the relevant lithium salt replaced the Li_2CO_3 in the second stage. The third stage is only performed in the preparation of transition metal doped Li_2CO_3/MgO catalyst. In this

step, the appropriate amount of transition metal nitrate solution was added after half an hour of the second stage.

The liquid/solid suspension was continuously heated and stirred until a thick paste formed. This paste was left under room conditions overnight before being dried at 120°C for 10 hours. A portion of this material was then removed and set aside. Another portion was then compacted at 15,000 LBS to form disc of 30 mm in diameter and about 6 mm in thickness. These discs were later broken into cubes of about 6 mm in dimension and calcined at 900°C for 10 hours. 900°C was selected as the precalcination temperature in order to achieve a stable catalytic sytem which will not sinter much under reaction condition at 700-800°C. All of this material was then ground to form powder and sieved for a particle size of less than 43 μ–meter.

3.3 Activity Determination

3.3.1 The Reactor System

The flow reactor system used in this work is illustrated in Figure 3.1.a. This reactor system consisted of mass flow controllers, a mixing coil, bypass route, the catalytic reactor, trap and connection to the analytical instrument. A total of five mass flow controllers were used. They were for controlling the flow of CH_4, 0_2, diluent gas (He or Ar) and any other additional gasses. These mass flow controllers enable a total flow rate of up to 150 ml/min to be achieved. Thorough mixing of the reactant gases was facilitated by the mixing coil.

The flow system was connected to the catalytic reactor by two ultra-torr Cajon fittings. The catalytic reactor is in the form of a tubing of 11 mm od. Initially Vycor tubing was used as the reactor body however for most of this work, Alsint tubing was used instead. The catalyst was packed between quartz wool. The length of the catalyst bed varied from 5 to 15 mm. An internal, stainless steel sheathed thermocouple touching the catalyst bed, was used to measure the reaction temperature. The tubular furnace, used together with the thermocouple, was connected to an electronic temperature controller. The temperature was regulated to ± 2.5°C.

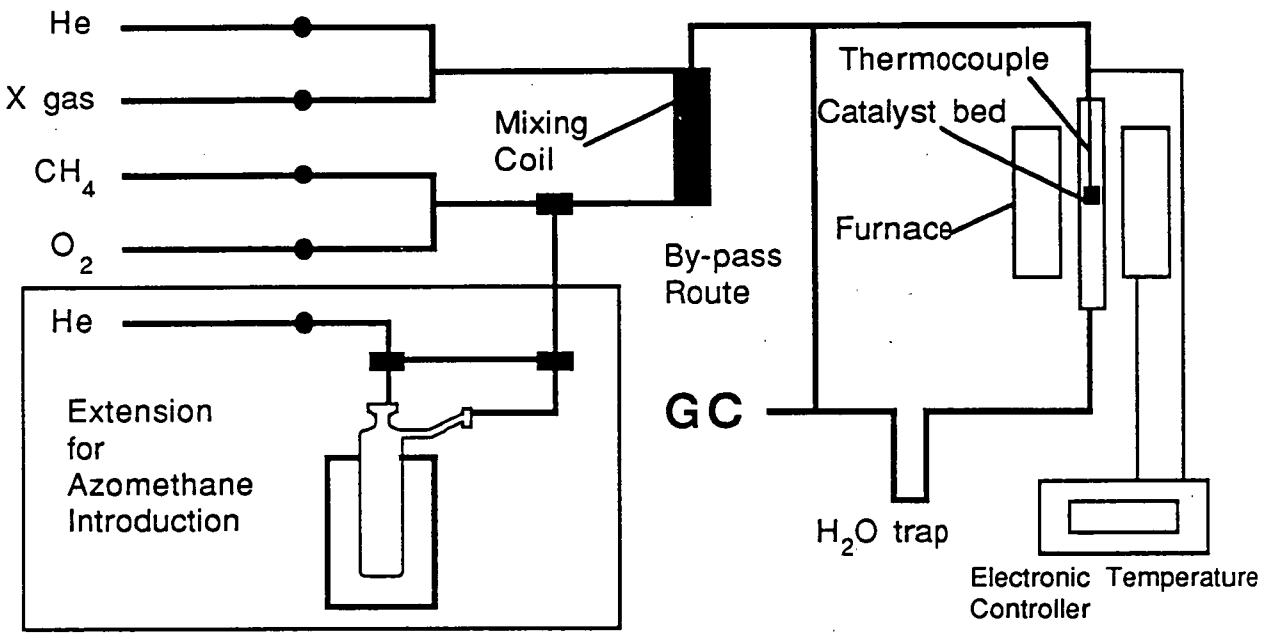

Figure 3.1.a The reactor system for catalyst screening.

The catalyst screening was normally performed with 0.2gm of catalyst and a total reactant flow rate of 25 ml/min. Catalysts which were precalcined were normally pretreated in air at 800°C for 2 hours. Uncalcined catalysts and fresh chemical compounds were not normally pretreated. The reactant gas normally was composed of about 110 torr of oxygen and 220 torr of methane, with helium making up the balance. The first activity result, at any particular temperature was determined normally after half an hour of equilibration time

3.3.2 Product Detection

The effluent from the reactor was connected to a HP 5890 gas chromatograph. The composition of this gas was analysed using the thermal conductivity detector of the g.c. Helium was used as the carrier gas at a total flow rate

of 60 ml/min and the reference flow of 30 ml/min. Temperature programmed treatment of the Carbosieve S2 column was used in order to achieve good separation between the gas components. Water is one of the major products of the oxidative dehydrogenation reaction and the presence of water speeds up the degeneration of the column. A copper coil immersed in 1-hexanol bath at -44°C was therefore used to trap out most of the water.

3.4 Catalyst Characterization

3.4.1 Composition of catalyst by Atomic Emission/Absorbance spectroscopy

The compositions of prepared catalysts prior and after calcination have been determined by the atomic emission and absorption spectroscopic method. A Varian AA-1475 series Atomic Absorption Spectrometer was used in these determinations.

Samples were first dried in a vacuum oven at 150°C for two hours. About 10 to 15 mg of a sample was first digested in hot concentrated nitric acid and then diluted to a working concentration. In the analysis of lithium, 1000 ppm of K^+ was added to the sample solution in order to minimise the atomization of the lithium. Magnesium and lithium were analysed in the emission mode while other components were analysed in the absorption mode.

The information obtained in these analyses was presented as wt.% Li/Mg and wt.% M/Mg in the case of a sample doped with transition metal oxide M. About 30 samples were analysed in duplicate, and depending on the sample, a variation of around $\pm$ 5% was observed. Such variations were due to the small amount of sample used, which was deemed necessary due to the low solubility, even in hot nitric acid, of the calcined sample.

3.4.2 Surface Area Determination

The surface area of the catalytic material prior to use was measured by means of the BET method using nitrogen at -196°C. The samples were first dried in a

vacuum oven at 150°C for six hours. Up to 2 gm of sample was used for the determination. The surface area of some samples were not measurable with this technique, and these materials were categorised as having surface areas of less than 1 m^2/gm.

3.4.3 X-Ray Powder Diffraction

X-ray powder diffraction patterns of most of the catalytic material were obtained with a Phillips powder diffractometer. A Cu Kα source was used under operating conditions of 40 kV and 20 mA.

3.4.4 Temperature Programmed Reduction Experiments

Temperature programmed reduction (TPR) was performed on catalytic materials which were doped with transition metal oxides using a laboratory-built apparatus (Roe,1988). This apparatus is represented in Figure 3.4.4.a.

The reductant gas used was hydrogen, with argon as the diluent gas. The gas flow of 0.5 ml of hydrogen, 5ml of argon was controlled by a Porter electronic mass flow controller. This gas mixture flowed into one arm of a TCD detector and onto the catalyst bed. The catalyst bed consisted of the catalyst packed between two pieces of quartz wool within a section of Alsint tubing 450 mm in length and 9 mm o.d. It was situated in the middle of an electrically heated quartz furnace 200 mm in length and 20 mm in i.d. An internal, sheathed thermocouple was used to measure the temperature of the catalyst bed. The effluent gas was passed through a cold trap to condense any water formed, and then into the other arm of the detector. A difference in conductivity indicated the changes in hydrogen concentration of the effluent gas. The operation of the mass flow controllers, reactor temperature programming and the recording of the thermal conductivity signal were controlled by a microcomputer.

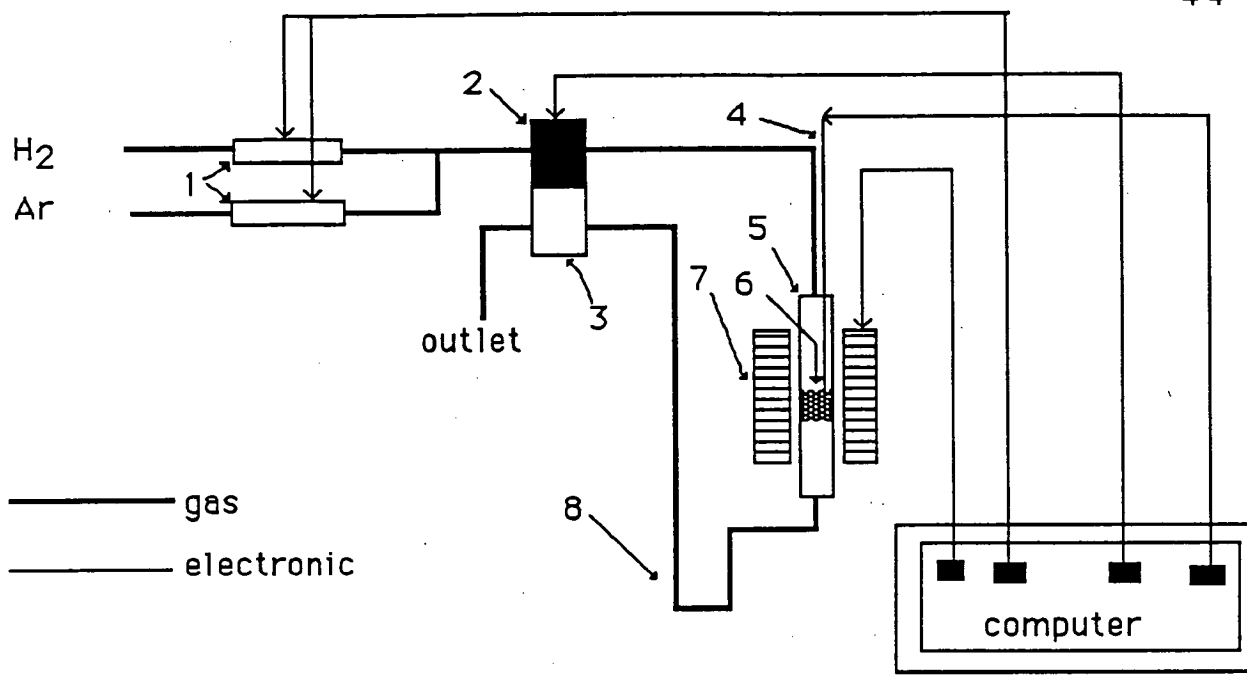

Figure 3.4.4.a Temperature Programmed Reduction Apparatus.
1 is the mass flow controller; 2 reference arm of TCD; 3 sample arm of TCD; 4 thermocouple; 5 Al_2O_3 reactor tubing; 6 catalyst bed; 7 furnace; 8 dry ice-acetone bath.

A 0.2 gm sample was normally used and was first dried in a vacuum oven at 150°C for two hours. In all of the TPR determination, the temperature was increased from RT to 850°C at a rate of 0.2°C/sec and maintained at 850°C for 20 min.

It should be realised that due to the nature of this technique, production of gases (not H_2O) by the sample (like decomposition of carbonates), will cause a dilution of H_2 in the effluent gas. This has the same effect on the TCD detector as if H_2 was consumed.

3.4.5 Thermal Gravimetric Analysis (T.G.A.)

The thermal gravimetric method was used to study the stability of Li_2CO_3/MgO catalyst under different conditions. The micro balance used was a Mettler BE-22 which was equipped with a controlled environment sample chamber.

A high temperature sample chamber with an external heater was built for this work (figure 3.4.5.a). A vacuum of about 10^{-6} Torr, and temperatures up to 1000°C can be achieved with this chamber. An all- quartz sample bucket and supporting wire was found necessary for this work. The stainless steel supporting wire was found to be not suitable, because, at the high temperature in the electrically heated furnace, it gave rise to electromagnetic interactions, masking the weight changes on the sample.

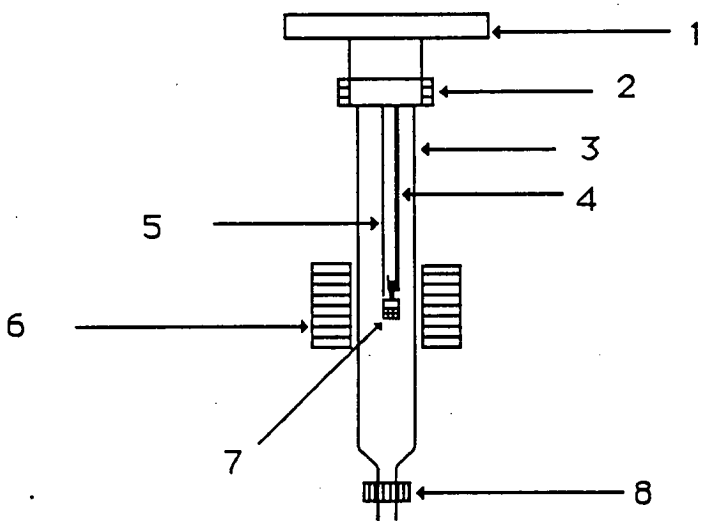

Figure 3.4.5.a High temperature attachment for TGA.

1 connecting flange to vacuum system; 2 Ultra-torr Cajon fitting; 3 quartz (Vycor) tubing; 4 quartz supporting wire; 5 thermocouple; 6 external furnace; 7 quartz sample bucket; 8 two way valve.

3.4.6 SEM, micro probe and XPS

The average particle size of the prepared catalyst, and the nature of calcined sample, was studied by scanning electron microscopy. A Phillips 505 SEM was used for this purpose. The samples, which were normally used 'as prepared' for the calcined sample, or as a pressed discs for powdered samples, were gold coated prior to being studied.

A JXA 50A electron probe micro analysis was used to study the surface composition of a selected catalyst. As in the SEM case, the samples were in the forms of 'as prepared' or pressed disk but were carbon coated.

The X-ray photo-electron spectroscopy technique was used in this work especially to study the lithium carbonate phase of Li_2CO_3/MgO catalyst. This technique has the advantage of being able to study the lithium and carbonate species which cannot be done on micro probe analysis. Moreover, the sample studied can be subjected to various treatments of interest and then probed without exposure to air.

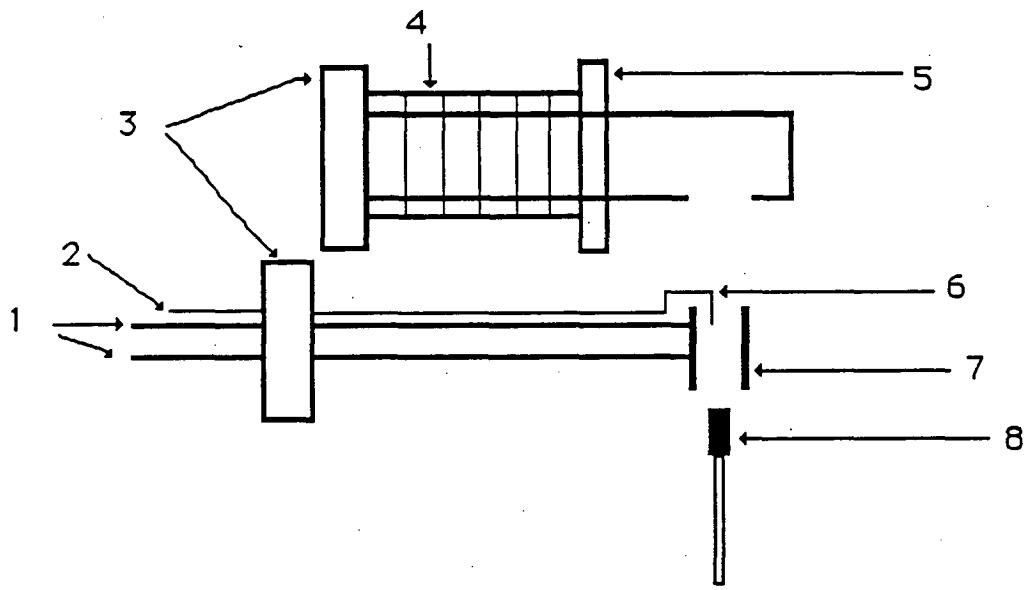

Figure 3.4.6.a Internal furnace for XPS's sample treatment.

1. electrical connection for furnace; 2 connection for thermocouple; 3 flange for the furnace; 4 bellows; 5 flange connecting furnace to sample chamber; 6 thermocouple; 7 heating element; 8 sample.

The XPS instrument used in this work was an AEI (Kratos) ES100 spectrometer, which has been modified by the addition of an UHV sample preparation chamber and an improved vacuum system, using Al $K\alpha_{1,2}$ radiation (1486.6 eV) from an X-ray gun operating at 15 Kv and 15 mA. Base pressure was better than $2x10^{-10}$

torr in the analyser and $1x10^{-9}$ torr in the sample chamber after baking at 150°C for two days. Normal working pressure in the sample preparation chamber was approximately $2x10^{-8}$ torr. Connected to the sample preparation chamber is a retractable cylindrical ceramic oven, which enables the sample to be heated up to 1000°C, together with gas inlet and outlet.

The oven was designed and made for this work, and is illustrated in figure 3.4.6.a. The heating element of the oven was of nichrome wire which was coiled and coated with a ceramic material. It was supported by two insulated metal bars. The furnace temperature was measured by means of a sheathed thermocouple with the hot junction situated in the middle of the furnace. The heating process was handled by an electronic temperature controller. The sample was pressed onto a stainless steel sample holder. Initially a gold plated sample holder was used, however it was found that under the conditions of this experiment, the gold layer evaporated. The stainless steel sample holder which was used was always polished after every experiment to remove any oxide layer which may have been formed during the experiment.

3.4.7 Infra Red Spectroscopy (IRS)

In this work the IRS technique was used to detect any reaction intermediate present in situ, and to study the catalytic material under conditions similar to that of activity studies. To enable the above objectives to be achieved, a high temperature I.R. cell with controlled environment has been designed and built.

3.4.7.1 Cell Design

Several types of IR cells have been developed by others for *in situ* catalytic studies (Peri, 1985). The most recent one was a cell which could be used to 100 atm., and 500°C (Arakawa et al.,1986). To the best of our knowledge, the present cell is the first to be used successfully for *in situ* transmission studies at temperatures as high as 800°C (Larkins and Nordin, 1988b).

There are two major problems to be faced when designing an infrared cell for studies at high temperatures in a controlled atmosphere. These are the method of sealing the cell, and the prevention of detector saturation by the unmodulated IR emissions (blackbody radiation, Brown et al., 1985) from the heating element and the hot part of the cell body. To overcome these problems, the heating was localised around the sample, and seals were located away from the heating source. The direct exposure of the detector to the emissions of the furnace was minimized. The cell which has been developed is illustrated in Fig. 3.4.7.1.a.

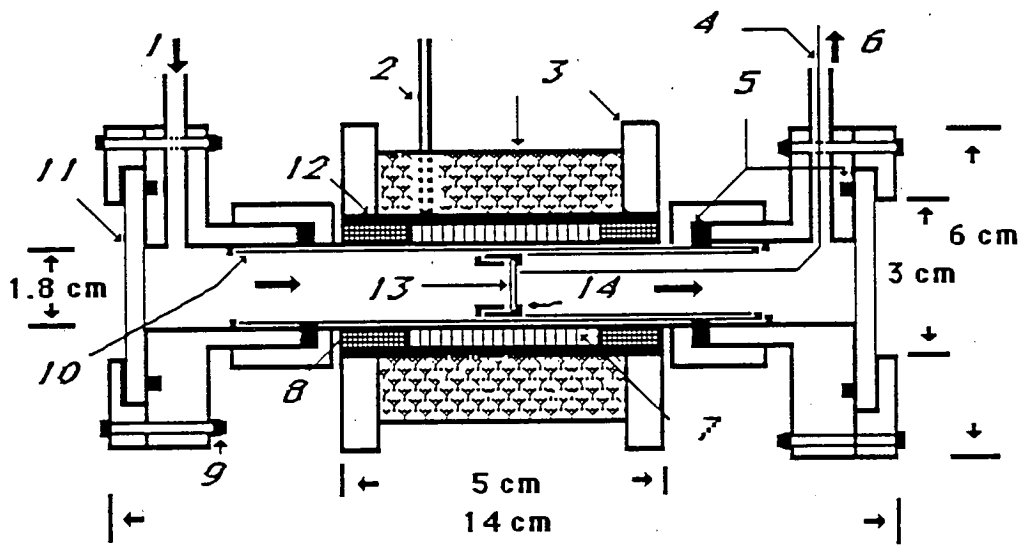

Figure 3.4.7.1.a The high temperature Infra Red Cell

1 is the gas inlet; 2 electrical connection; 3 insulating material; 4 Viton O-ring; 5 thermocouple; 6 gas outlet; 7 heating element; 8 ceramic; 9 nut and bolt; 10 Vycor tubing; 11 CaF_2 window; 12 Al_2O_3 tubing; 13 sample; 14 stainless steel sample holder.

The body of the infrared cell is of Vycor tubing (18 mm o.d.). Ultra-Torr Cajon fittings on brass flanges were used to connect the tubing and CaF_2 windows, while Viton O-rings were used for sealings. The inlet on one flange and the outlet on the other enable flow experiments to be performed. The sample, which is in the form

of a self-supporting pressed disc (11 mm in diameter), is mounted on a stainless steel structure and then placed inside the cell. A sheathed thermocouple, less than 1 mm from the sample surface, is used to measure the temperature, while an external, removable micro-furnace is used to heat the sample. The heating process is controlled by means of an electronic temperature controller accurate to ±5°C. No water cooling was found to be necessary for operation below 800°C. The cell could be evacuated to 10^{-3} torr at 800°C.

3.4.7.2 Cell Testing

In order to establish the suitability of the cell for high temperature work, the saturation level of the detector induced by the unmodulated IR radiation from the furnace and by detector heating was determined. This evaluation was achieved by monitoring the interferogram signal of the IR beam through an empty cell. The measurement was performed on an FTS-20E Fourier transform spectrometer with a triglycerine sulphate detector.

The results are summarised in Fig.3.4.7.2.a. The % signal represents the interferogram signal, normalised against the signal at room temperature. The interferogram signal is related to the sensitivity of the detector for a given experimental condition. Saturation of the detector by IR radiation from a hot object results in a decrease of the interferogram signal and hence, the loss of sensitivity. The sensitivity of the detector is also affected by temperature. It was noted that the temperature of the metal casing which supports the detector rose from 26.6°C to 32°C when the cell was heated from 26.6°C to 800°C.

Curve A on figure 3.4.7.2.a illustrates the effect of the detector temperature on the interferogram signal. In this determination, there was no contribution by the unmodulated IR beam of the furnace. This effect, namely the saturation of the detector by the unmodulated IR, together with the effect of the detector temperature is illustrated in curve B. These results indicate that , under operating conditions at 800°C, saturation of the detector due to the increase in its temperature is minimal (3%)

compared with that due to the effect of the unmodulated IR irradiation (~15%) from the furnace. The saturation due to unmodulated IR irradiation increases significantly at cell temperatures higher than 600°C. However, even at 800°C both effects reduce the sensitivity of the detector by less than 20%. The amount of sensitivity available under such operating conditions is still adequate to obtain spectra with reasonable signal-to-noise ratio. It should also be noted that the overall sensitivity for the spectroscopic studies will also be dependent on the nature of the sample. Samples which cause low scattering and absorption losses result in high sensitivity. The opposite effect will occur if the sample is itself emitting a lot of unmodulated IR irradiation.

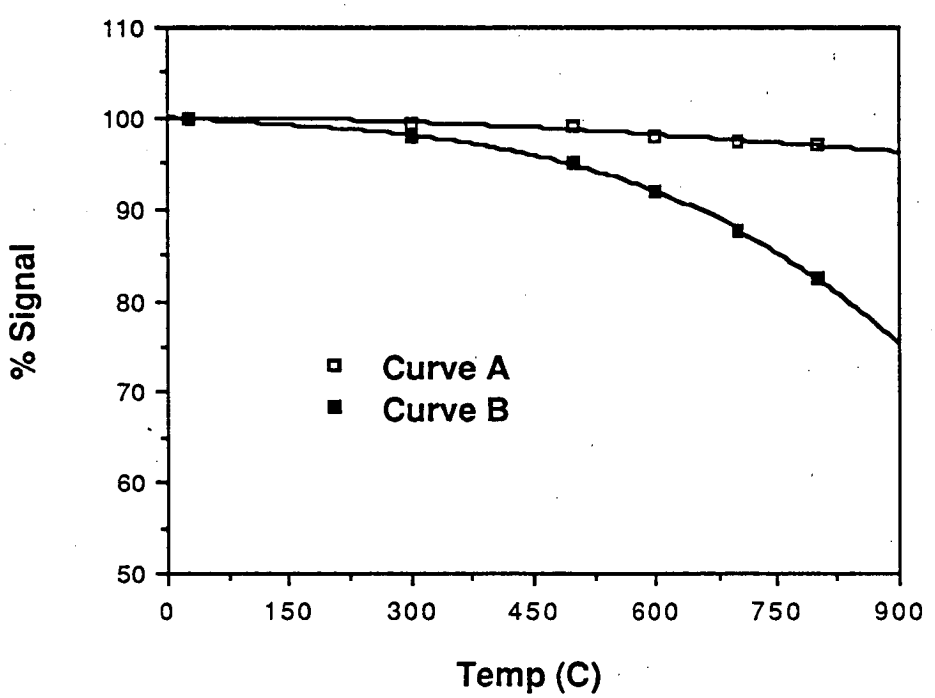

Figure 3.4.7.2.a The effect of temperature on the interferogram signal.

CHAPTER 4

ACTIVITY OF THE Li/MgO TYPE CATALYTIC MATERIAL AND FRESH CHEMICAL COMPOUNDS; RESULTS AND DISCUSSION

4.1 Homogeneous oxidative reaction of methane at different temperatures

In order to evaluate the reactor configuration, and to gauge the extent of homogeneous reaction, the gaseous phase reaction of methane and oxygen at different temperatures was determined. The reactant gas mixture of 101 torr of oxygen and 203 torr of methane in helium, was flowed at 25ml/min through the blank reactor tube. Figure 4.1.a summarizes the result of this determination. At 800°C less than 3% of methane conversion (100xCH_4 reacted/CH_4 inlet) occurs homogeneously. This suggested that the reactor configuration was suitable for studying catalytic activity under similar reaction conditions

Between 800°C to 850°C, percentage of methane conversion increases gradually with an increase in reaction temperature. At 860°C, about 12% methane conversion was observed. A further increase in reaction temperature resulted in a much higher conversion of methane. In terms of the formation of various products, the % yield of hydrocarbon (100xCH_4 in product/CH_4 inlet) decreases relative to the carbon oxides with an increase in reaction temperature. The yield of ethene with respect to ethane also increases. It was also observed that at lower temperatures, the carbon monoxide yield is lower than that of carbon dioxide, but the reverse happens at higher reaction temperature.

The % selectivity to the products (100xCH_4 in product/CH_4 reacted) are related to the severity under which the reaction was conducted. Higher reaction temperatures (more severe) resulted in higher methane conversion but more carbon oxides are formed relative to the hydrocarbon. Others (Asami et al., 19877c,1988b; Lane and

Wolfe, 1988b,1988c; Hutchings et al., 1988a) have also observed a similar correlation.

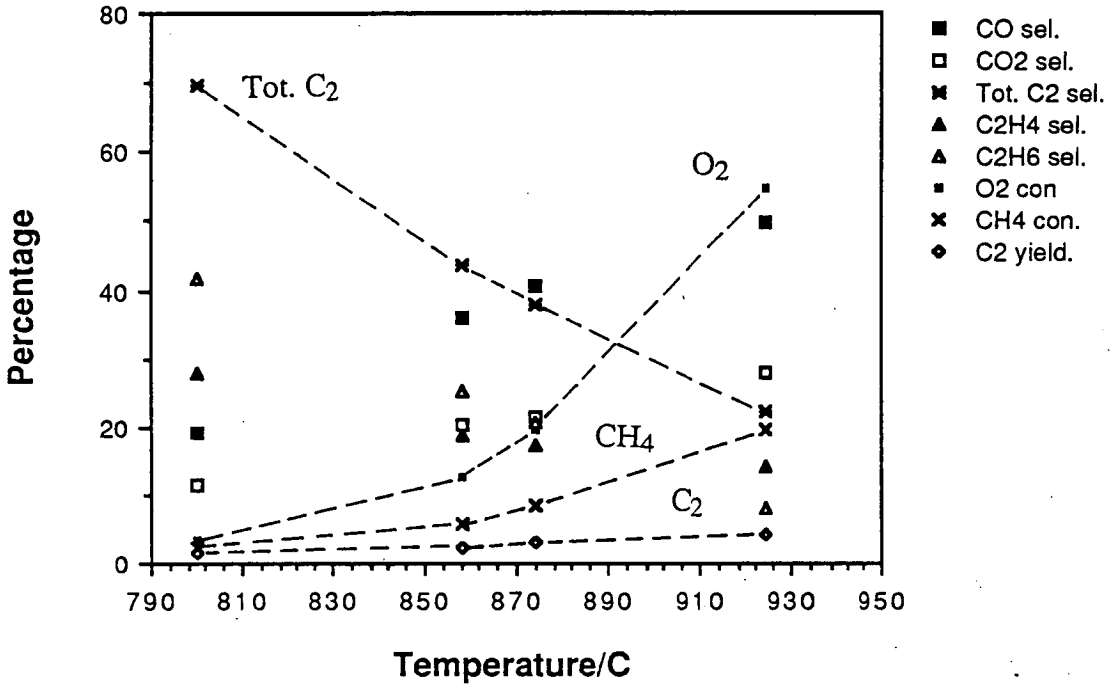

Figure 4.1.a The homogeneous reaction of methane and oxygen at different temperature (P_{O_2} 101 torr, P_{CH_4} 203 torr)

Table 4.1.a Homogeneous reaction of methane and oxygen at 800°C

Ref.	%CH_4 con;	%Sel. C_3	C_2H_6	C_2H_4	CO	CO_2	Tot.Hc.;	%Hc.yield;	%$C2^=/C_2$Tot;
a)Lane and Wolfe,1988b	30.1	-	6.1	14.1	71.4	8.5	20.2	6.1	70
b)Asami.et al.,1988b	8.3	6.4	13.7	30.6	45.2	4.1	50.7	4.2	69
c)This work	2.4	-	41.7	28.0	19.0	11.3	69.7	1.7	40

Reaction condition of a: flow rate 50ml/min; tot. pressure 1atm.; P_{CH_4}:P_{O_2}:Pdil.= 213:106:334

Reaction condition of b: flow rate 350ml/min; tot. pressure 11atm. ; P_{CH_4}:P_{O_2}:P_{N_2}=106:13:641

Reaction condition of b: flow rate 25ml/min; tot. pressure 1atm.; P_{CH_4}:P_{O_2}:P_{He}=203:101:456

Table 4.1.a compares the homogeneous reaction at 800°C, performed under varying reaction conditions in three different studies. In all three studies the amount of methane reacted differs but a correlation between selectivity to the various products with methane conversion was established. At higher methane conversion the selectivity to hydrocarbon relative to carbon oxides decreases. These results also indicate that the reaction severity, which can be in the form of reactant composition, flow rate and reactor configuration can strongly affecting the gaseous phase oxidation of methane.

4.2 Activity of calcined Li_2CO_3/MgO catalyst (7.8 wt.% Li/Mg)

As was mentioned earlier, the 7.8wt.%Li_2CO_3/MgO system is considered as the bench mark catalytic system (the value 7.8 represents the wt% Li/Mg for the catalyst). In this section the activity of this catalyst at different temperatures and different O_2/CH_4 ratios in the reactant stream was studied.

Table 4.2.1.a Activity of calcined 7.8% Li_2CO_3/MgO at different temperature (P_{O_2} 117torr, P_{CH_4} 219 torr).

Temp/°C	%con CH_4	O_2	%Sel: C_2H_6	C_2H_4	CO	CO_2	Tot.C_2;	%C_2yield;	%$C_2^=/C_2$Tot.
805	26.8	48.9	30.3	33.8	0.0	35.9	64.1	17.2	53
761	13.8	22.4	46.4	23.2	0.0	30.5	69.6	9.6	33
706	6.0	13.6	41.1	7.3	0.0	51.6	48.4	2.9	15

4.2.1 The effect of reaction temperature

Table 4.2.1.a summarizes the oxidative reaction of methane at different temperatures over a Li_2CO_3 catalyst. Under this reaction condition, full O_2 consumption does not occur. CH_4 conversion increases continuously with temperature, and so does the C_2 yield. At 805°C, 25% of methane conversion was achieved with C_2 hydrocarbon yield of 17%.

The C_2 hydrocarbon yield obtained in this experiment is comparable to that obtained by Ito et al.,1985. In their study Ito et al., 1985, used 4.0 grams of uncalcined Li_2CO_3/MgO catalyst and achieved 19.4% C_2 yield at 720°C. The selectivity to the various products varies significantly with reaction temperature (Table 4.2.1.a). C_2 selectivity increases slightly with an increase in temperature, and so does the selectivity to ethene. Unlike that of the gaseous phase reaction, the selectivity to carbon monoxide is very low. At low temperature CO_2 and C_2H_6 are the major products indicating that they are the primary products of the reaction. At higher reaction temperatures the selectivity to ethene increased suggesting that it was produced from the reactions of ethane. At higher temperature the increase in selectivity to C_2 is likely to be associated with the depletion of oxygen partial pressure.

The favoured production of CO_2 over this catalyst could proceed through the oxidation of oxygenates and carbon monoxide intermediates. Reactions of C_2H_6 with the surface are likely to occur also resulting in ethene formation and the exhaustive oxidation reactions. The oxidation of products in the homogeneous phase, after the catalyst bed, is likely to be minimal because no significant CO was observed in the product stream.

Generally the activity results and the trends with respect to reaction temperature observed here are comparable with those reported in the literature (Ito and Lunsford, 1985; Kimble and Kolts, 1985, and Roos et. al., 1987). This indicates that the reactor set up and experimental condition used are suitable for catalyst screening and other studies.

4.2.2 The effect of P_{O_2}/P_{CH_4} ratio on the activity of Li_2CO_3/MgO catalysts.at 800°C (with P_{CH_4} fixed at 210 torr)

In this experiment, the partial pressure of oxygen was varied for a fixed partial pressure of methane (210 torr). Figure 4.2.2.a shows that methane conversion increases, while total selectivity to C_2 decreases monotonically with the increase in P_{O_2}/P_{CH_4} ratio. The C_2 yield increase slightly, and further increases in oxygen partial

pressure do not cause any significant increase in C_2 yield. The selectivity to ethene increases while that to C_2H_6 decreases as the ratio increases. Figure 4.2.2.a shows that high P_{O_2}/P_{CH_4} has a detrimental effect on C_2 selectivity and favours the formation of carbon dioxide. The selectivity to CO was always negligible except at the highest ratio, where about 3% selectivity to CO occurs.

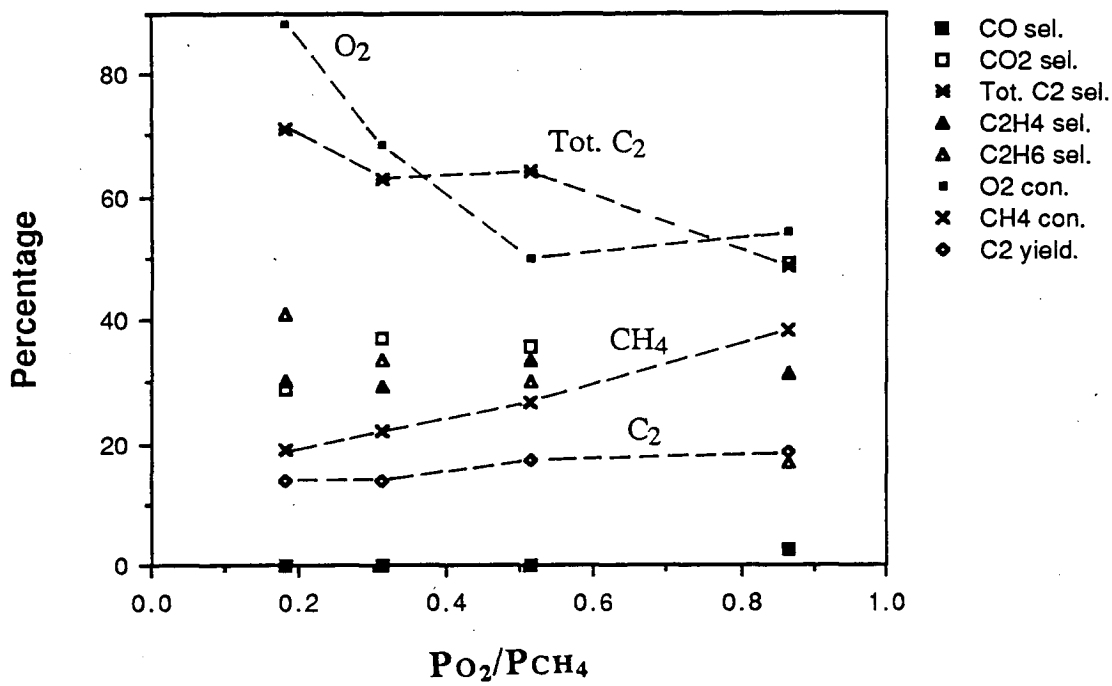

Figure 4.2.2.a Effect of changing P_{O_2}/P_{CH_4} ratio on activity at 800°C. In this experiment the partial pressure of oxygen was varied for a fixed partial pressure of methane (210 torr).

The direct effect of increasing O_2 for fixed P_{CH_4} in the reactant stream (at 800°C, 0.2 gm of catalyst) is the increase of methane conversion. However, since hydrocarbon selectivity decreases, and the C_2 yield does not increase significantly, the advantage of working at a high P_{O_2}/P_{CH_4} ratio is likely to be small. The potential for an explosion at this pressure ratio is high, thus increasing the hazard of the process. A

P_{O_2}/P_{CH_4} ratio of about 0.5 seems to be the optimum reaction flow condition, confirming the finding of Ito and Lunsford, 1985.

The amount of C_2H_4 in the product stream increases relative to C_2H_6 at higher P_{O_2}/P_{CH_4}, and hence, with methane conversion. This further suggested that ethene is a secondary product of the reaction. Since carbon dioxide still remains as the dominant carbon oxide product over Li_2CO_3/MgO, the increase in the P_{O_2}/P_{CH_4} ratio tends to facilitate the surface exhaustive reaction. However, at the higher P_{O_2}/P_{CH_4} ratios, the homogeneous exhaustive oxidation reaction would become more significant.

4.3 Effect of lithium loading on the activity of Li_2CO_3/MgO

In this section, the effect of lithium loading on Li_2CO_3/MgO catalysts is studied. The calcined catalysts are compared with the uncalcined sample, and their stability under the reaction condition monitored. The aim of the studies made here is to be more comprehensive than those performed earlier, by other workers.

4.3.1 Activity of the calcined Li_2CO_3/MgO systems of various lithium loadings at 800°C (P_{O_2} 100torr, P_{CH_4} 220 torr).

The activity results are summarised in Table 4.3.1.a. The 0% Li/MgO sample, which is MgO prepared using the same procedure as that for Li_2CO_3/MgO catalysts, resulted in 30.3% of methane conversion with a total selectivity to C_2 hydrocarbon of about 29.6%. The introduction of 0.2% Li/Mg (loading after calcination) reduced the methane conversion to 9%, with the selectivity to C_2 hydrocarbons increased from 29.6% to 83.7%. This behaviour of Li_2CO_3/MgO catalysts has not been reported in the literature . As the lithium loading was increased, methane conversion increased sharply up to 7.8wt.%, while the C_2 selectivity dropped. At a lithium loading of 1.3%, the methane conversion was 19.9%, with a selectivity to C_2 of 76%. A further increase of the lithium loading increased conversion slightly but when the loading was above 7.8%, methane conversion started to decrease while selectivity to C_2 hydrocarbons increased. C_2 yields decreased when the lithium was introduced onto

MgO at low loadings. At higher loading the C_2 yield increased and reached a maximum at a loading of 4.4%. A further increase in lithium loading resulted in a decrease in C_2 yield. It was also noted that the observations made earlier on the correlation of C_2H_4/C_2H_6 ratio in the product stream with methane conversion is also true in this experiment.

Table 4.3.1.a The activity of calcined Li_2CO_3/MgO catalyst with different lithium loading at 800°C (P_{O_2} 100 torr; P_{CH_4} 220 torr).

Wt.%Li/Mg	%con.CH_4	O_2	%Sel. C_2H_6	C_2H_4	CO	CO_2	TotC_2;	%C_2yield;	%$C_2^=/C_2$Tot.
0.0	30.3	98.3	12	17.6	2.9	67.5	29.6	9.0	59
0.2	7.0	9.4	56.2	27.5	1.3	15.0	83.7	5.8	33
0.5	7.8	11.3	52.3	26.4	1.5	19.8	78.7	6.1	34
0.6	13.4	20.4	45.7	33.4	1.9	19.0	79.1	10.6	42
1.3	19.9	34.2	38.3	37.8	2.4	21.6	76.1	15.1	50
4.4	23.9	47.3	32.9	33.9	1.7	31.5	66.8	16.0	51
7.8	24.8	53.0	29.3	32.5	1.3	36.9	61.8	15.3	53
10.6	18.3	39.6	31.6	28.8	1.0	38.6	60.4	11.0	48
12.8	11.6	19.3	46.5	25.7	0.4	27.4	71.2	8.4	36

The extent of methane conversion on Li_2CO_3/MgO catalyst is dependent on the lithium loading. The presence of Li_2CO_3 on MgO increases the selectivity to C_2 hydrocarbon significantly and causes some reduction in methane conversion. In turn, the extent of methane conversion influenced the ratio of ethene to ethane in the product stream. Since the C_2H_4/C_2H_6 ratio was found to be related to the extent of methane conversion, it further supports the contention that C_2H_4 is a secondary product from the reaction. Moreover the total selectivity to C_2 hydrocarbons is also dependent on the extent of methane conversion.

The fact that in this experiment, and that of Yamagata et. al., 1987, MgO itself was observed to have a high activity for the oxidative reaction of methane warranted further studies on the catalytic nature of MgO. The presence of Li_2CO_3 on MgO

influenced both the conversion of methane and the selectivity to C_2 hydrocarbons. Low lithium loading was seen to have deactivated MgO. It is probable that the precalcination at 900°C for 10 hours resulted in significant major chemical and physical transformations as a result of the loss of Li_2CO_3. The sintering on Li_2CO_3/MgO catalyst should be very severe since Li_2CO_3 melts at 618°C causing fusion of particles to occur. However, a further increase in Li_2CO_3 loading, where sintering is suppose to be more significant, resulted in a higher conversion. This would suggest that at lithium loading greater than 2wt%, the chemical factor plays a dominant role in the oxidative reaction of methane over these catalysts. The decrease in methane conversion at a much higher lithium loading however suggest that sintering effects become a problem at higher loading. Another interesting observation here is that the increase in lithium loading on MgO not only facilitated good selectivity of C_2 hydrocarbons, but also facilitate the full oxidation of intermediates into carbon dioxide.

In summary, it is clearly demonstrated here that the presence of Li_2CO_3 on MgO modified the activity of MgO for the oxidative reaction of methane. Lithium loadings of 4.4 to 7.8wt.% resulted in optimum performances for the oxidative coupling reaction.The results here warranted further studies on MgO itself and the physico-chemical nature of the Li_2CO_3/MgO systems.

4.3.2 Activity of uncalcined Li_2CO_3/MgO catalysts

From Table 4.3.2.a, the freshly prepared MgO resulted in 29.0% methane conversion with a selectivity to C_2 hydrocarbons of 33.7%. Unlike the calcined form, the uncalcined low loadings of Li_2CO_3 on MgO resulted in an increase of methane conversion and selectivity to C_2 products. Further increase in lithium loading resulted in decreases of methane conversion while the selectivity of C_2 increased continuously. In terms of hydrocarbon yields, significant increases in C_2 yields occurred when lithium was introduced and a maximum yield of about 20% occurred when the lithium loading was 5.2%. As before, the $\%C_2H_4/C_{2Tot.}$ ratio was also observed to increased with methane conversion. The selectivity to CO also decreases with higher lithium

loadings. These results parallel the observation made by Driscoll et. al., 1985 with respect to the amount of methyl radicals generated over Li_2CO_3/MgO catalyst to be a function of lithium loading.

Table 4.3.2.a Activity of fresh Li_2CO_3/MgO catalyst with different lithium loading at 800°C (P_{CH_4} 100 torr, P_{O_2} 220 torr)

Wt.%Li/Mg	%con.CH_4	O2	%Sel.C_2H_6	C_2H_4	CO	CO_2	Tot.C_2;%C_2	yield;%$C_2^=$/C_2Tot.	
0.0	29.0	87.9	14.2	19.5	11.5	54.8	33.7	9.8	58
0.7	36.3	93.8	17.2	30.4	7.4	45.1	47.6	17.3	64
1.3	34.9	82.5	19.4	34.7	7.3	38.7	54.1	18.8	64
1.9	36.9	93.1	18.9	32.5	3.2	45.4	51.4	18.9	63
2.3	38.4	98.2	18.4	32.8	1.3	47.5	51.2	19.7	64
5.2	36.7	88.2	22.4	33.0	0.8	43.8	55.4	20.3	60
8.4	33.6	81.9	22.1	32.2	1.3	44.4	54.3	18.3	59
11.5	28.4	63.4	27.3	34.8	1.3	36.6	62.1	17.6	56
14.0	23.6	50.7	31.5	33.1	1.0	34.4	64.6	15.3	51

In this experiment it was observed that the MgO and the Li_2CO_3/MgO catalysts are strongly affected by the preparative procedure. Generally the uncalcined Li_2CO_3/MgO catalyst resulted in a higher methane conversion. While the calcined low loading Li_2CO_3/MgO catalyst had the lowest activity, their uncalcined counterparts had the highest activity. At higher lithium loading the activity of fresh Li_2CO_3/MgO catalysts are quite similar to that of the calcined, suggesting that at the higher lithium loading, a similar extent of sintering occurs on the calcined and the uncalcined catalysts.

These results further indicate the promoting effect of Li_2CO_3 on MgO for the oxidative coupling of methane. Efforts were made to determine were made to determine wether this promoting effect is physical or chemical in nature.

4.3.3 The effect of time-on-stream on the activity of calcined MgO and the 7.8% Li_2CO_3/MgO catalyst.

From figure 4.3.3.a it can be seen that the activity of calcined MgO at 800°C is very constant with time on stream. About 26% methane conversion occurs with the selectivity to C_2, CO and CO_2 of 33%, 7% and 60% respectively. On the other hand the activity of the 7.8% Li_2CO_3/MgO catalyst changes considerably over the 21 hours on stream (figure 4.3.3.b). The percentage of methane conversion and C_2 yields decreases continuously while the selectivity to C_2 increases slightly with time. The selectivity to CO also increases slightly with time on stream.

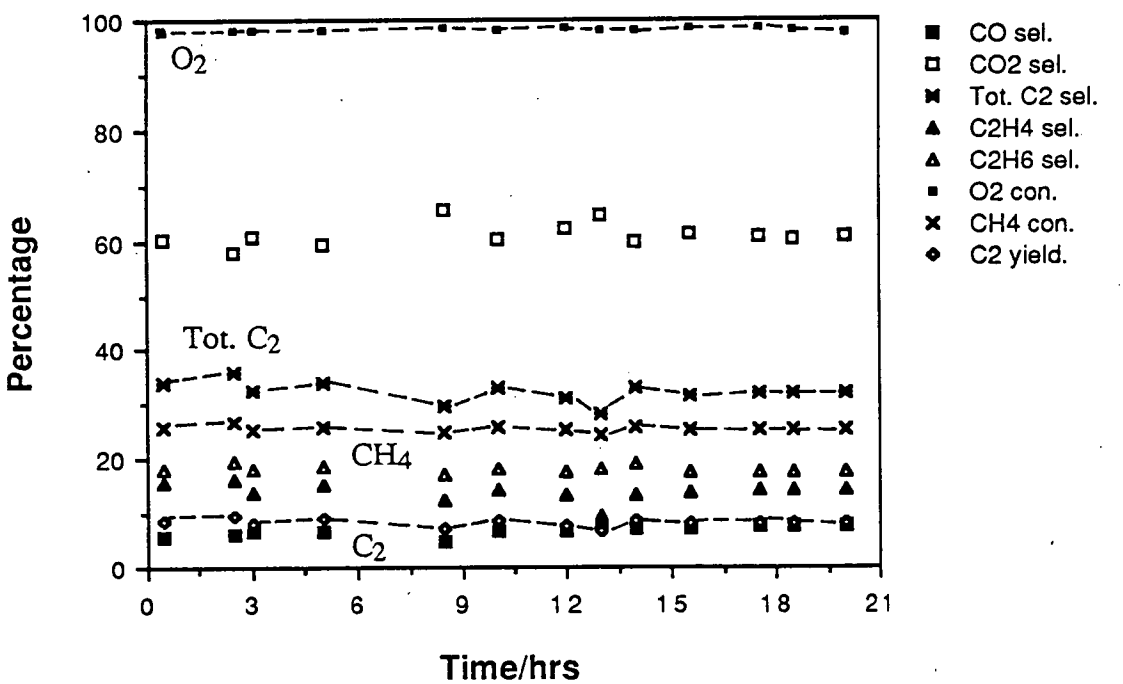

Figure 4.3.3.a The activity of calcined MgO at 800°C with time-on-stream (P_{O_2} 95 torr; P_{CH_4} 255 torr)

The stability of the oxidative reaction of methane over calcined MgO with time could indicate that no significant changes occur on the catalyst during the course of the reaction. However, the significant variation in activity of the 7.8% Li_2CO_3/MgO

catalyst with time on stream is likely to mirror the chemical and physical changes occurring on the catalyst in the course of the reaction. The possible changes happening on the Li_2CO_3/MgO catalyst are severe sintering (Miradatos et al.,1987) and the loss lithium from the catalyst surface (Kimble and Kolts,1987). The sintering would generally decrease the conversion, as was observed in 4.3.1. The loss of Li_2CO_3, however, would have a significant impact in the product distribution. As more Li_2CO_3 was lost, the catalyst surface would become less basic, and this could explain the increase in selectivity to CO.

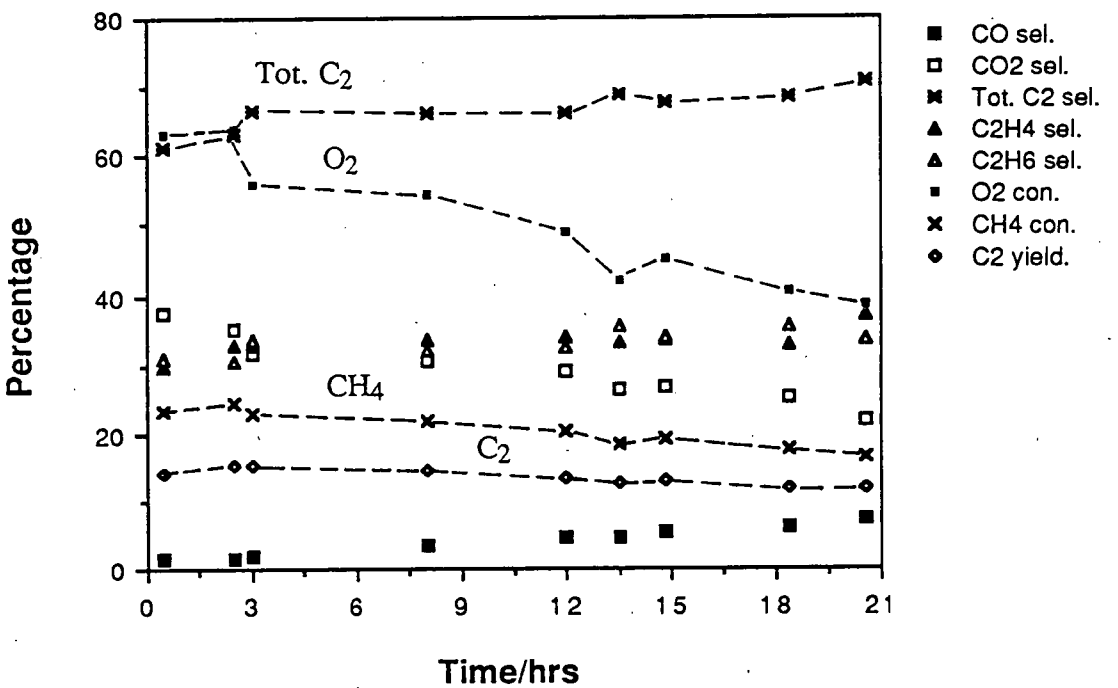

Figure 4.3.3.b Activity of 7.8% Li_2CO_3/MgO catalyst at 800°C with time-on-stream (P_{O_2} 92 torr, P_{CH_4} 249 torr)

4.3.4 Effect of the time-on-stream on activity of calcined 7.8% Li_2CO_3/MgO (P_{O_2} 200 torr; P_{CH_4} 219torr)

To better understand the time stability of the Li_2CO_3/MgO catalyst for oxidative reaction of methane, further experimentation was conducted at P_{O_2}/P_{CH_4} =1, and the results are given in Figure 4.3.4.a . In this experiment the partial pressure of oxygen is about twice that used for the studies reported in figure 4.3.3.b. The amount of

methane conversion remains about constant, at around 30%, with time-on-stream while the selectivity to C_2 hydrocarbon decreases and that to carbon dioxide increases continously. Initially the selectivity to CO rises and then thereafter decreases. It was also noted that the ratio of C_2H_4/C_2H_6 in the product stream decreases continuously with time on stream.

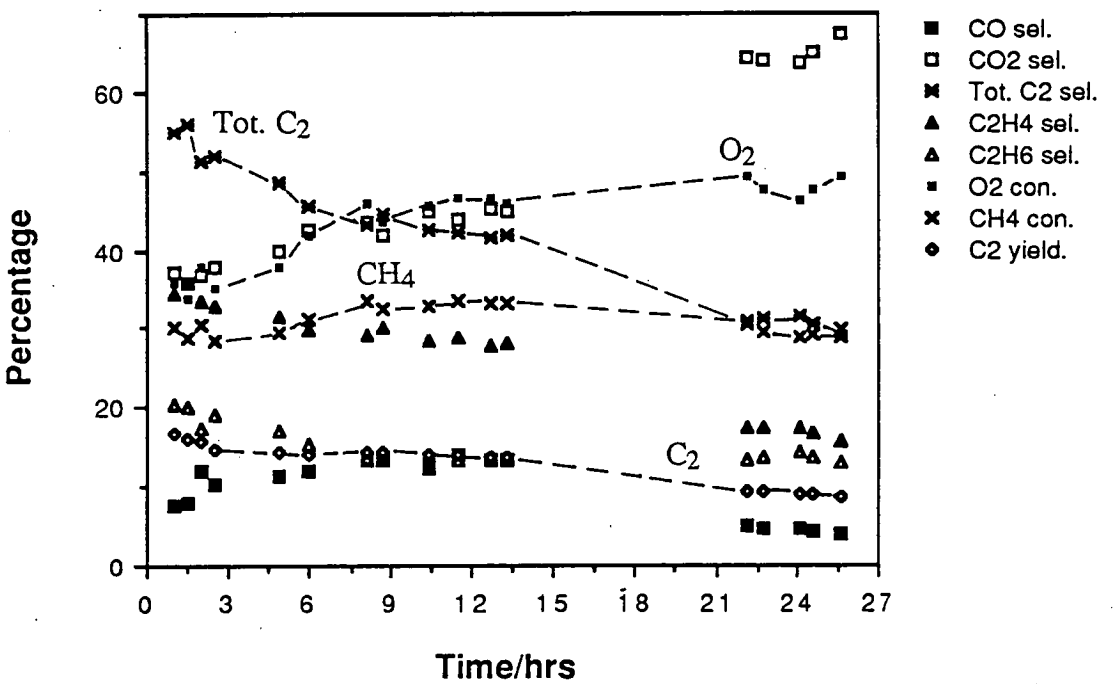

Figure 4.3.4.a Activity of calcined 7.8%Li_2CO_3/MgO catalyst at 800°C with time-on-stream (P_{O_2} 200 torr; P_{CH_4} 219 torr)

In this experiment, the relationship between methane conversion and selectivity to C_2 hydrocarbons was observed to break down. The selectivity was observed to decreased significantly with time-on-stream, although the percentage of methane conversion does not vary significantly. This result implies that significant chemical changes occurred on the catalyst. Under the conditions of this experiment the loss of selectivity to C_2 products occurs while the amount of methane conversion remains constant. Moreover, since the amount of conversion remains constant, it indicates that

under this condition the loss of active sites through sintering has less effect than the surface chemical changes. At a lower partial pressure of oxygen, the former factor might become more significant. This indicates the loss of active sites for the oxidative reaction of methane with time on stream.

Table 4.3.4.a Changes on the composition of used Li_2CO_3/MgO catalyst .

Catalyst	From micro probe % MgO	From A.A. % Li/Mg
7.8% Li_2CO_3/MgO	82	7.8
Used catalyst	88	1.2

The elemental analyses of the calcined Li_2CO_3/MgO catalysts have been determined by X-ray micro probe analysis and atomic absorbance spectroscopy. The results are given Table 4.3.4.a. In agreement with the observation made by Kimble and Kolts, 1987, the results show signifiant loss of lithium.during the catalytic reaction. The loss of lithium is likely to change the chemical nature of the catalyst surface causing the decrease in C_2 selectivity and the increase of O_2 conversion with time-on-stream without affecting the methane conversion significantly. A similar effect has also been observed on a supported PbO catalyst by Hinsen et. al. 1984.

The SEM micrograph of the various calcined 7.8%Li_2CO_3/MgO catalysts are presented in Figure 4.3.4.b. The micrographs of unused catalyst (i & ii) shows that two type of particle clusters are present; one type with average size of about 1-2 μ-metre while the other with an average size of 0.1 μ-metre. The micrographs (iii & iv) of the used sample suggests that only the larger clusters was present consistent with the sintering effect on the used catalyst. Further discussion on correlation between the physical and chemical nature of the catalyst with its activity will be made in Chapter 5.

4.3.5 Effect of time-on-stream on the activity of fresh 1.3% Li_2CO_3/MgO (0.5% calcined) and 8.4% (7.8% calcined) Li_2CO_3/MgO catalyst

The initial activity of the fresh catalysts at 800°C are much higher than their calcined counterparts. However, the activity of the uncalcined catalyst is dependent

i)

ii)

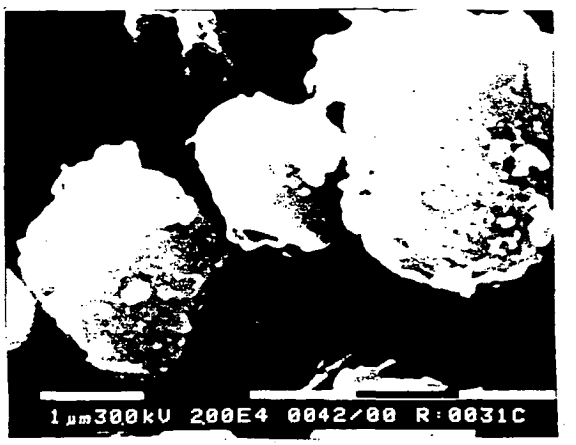

iii)

iv)

Figure 4.3.4.b SEM micrographs of Li_2CO_3/MgO catalysts.

Micrographs i) and ii) are that of the unused 7.8wt.%Li_2CO_3/MgO catalyst at magnifications of $5.0x10^2$ and $2.0x10^4$ respectively, while micrographs iii) and iv) correspond to the used catalyst under the same respective magnifications.

upon the time-on-stream. Methane conversion over 1.3% Li_2CO_3/MgO decreases from 40% to 10% after 24 hours on stream (figure 4.3.5.a). The total yield to C_2 products decreases continuously while the selectivity to C_2 hydrocarbon increases slightly. At longer time-on-stream the selectivity to CO increases and stabilises at around 7%. Similar observations have been made for the 8.4% Li_2CO_3/MgO catalyst (figure 4.3.5.b). Methane conversion drops from 36% to 16% after 20 hours on stream On the higher loading catalyst, methane conversion after 15-24 hours on stream is slightly higher while the selectivity to CO was always insignificant at on-stream times less than 24 hours. At longer times-on-stream (not in graph) a small amount of CO (3%) was present in the product stream.

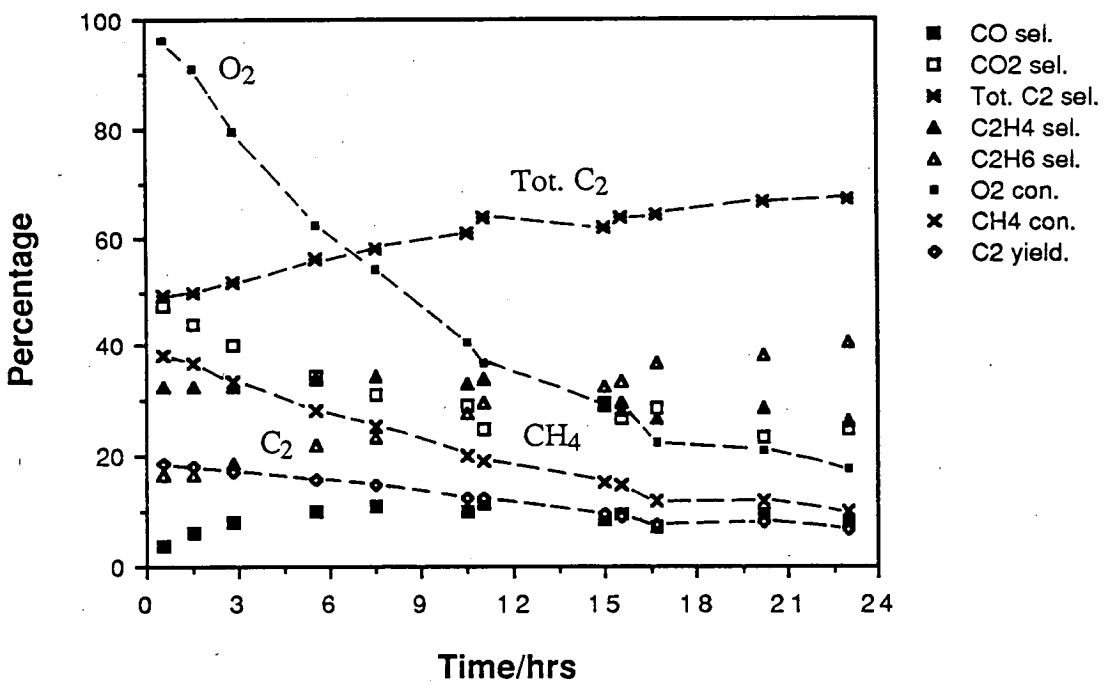

Figure 4.3.5.a The activity of fresh 1.3%Li_2CO_3/MgO at 800°C catalyst with time-on-stream (P_{O_2} 113 torr, P_{CH_4} 236 torr)

The uncalcined catalysts undergo more significant changes in activity over time-on-stream compared to calcined catalysts. The small differences observed in their

activity indicates that both catalysts undergo rapid physical and chemical changes during the reaction. The lower activity of the fresh 1.3% catalyst, after a long time-on-stream parallel the observation made in section 4.3.1 on calcined low loading catalysts that is having a low activity. Low lithium loading, together with a high temperature treatment, caused deactivation of MgO. The effect of the changes occurring on these catalyst, with time-on-stream would become more dominant if the reaction was conducted at higher P_{O_2}/P_{CH_4}.

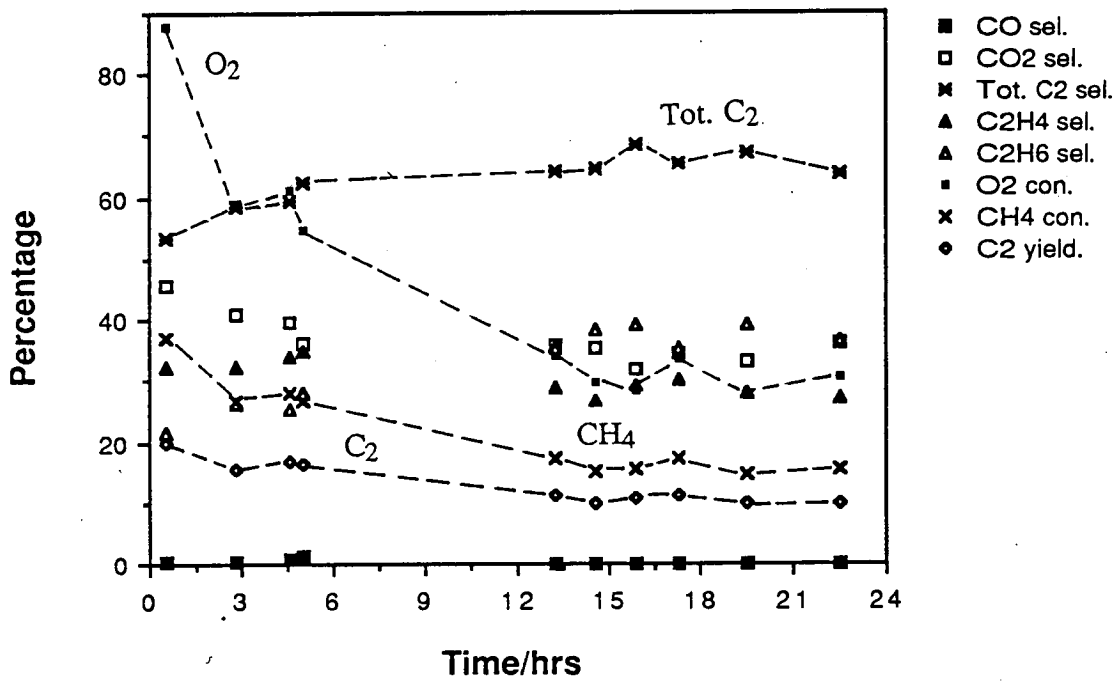

Figure 4.3.5.b Activity of 8.4% Li_2CO_3/MgO catalyst at 800°C with time on stream (P_{O_2} 117 torr, P_{CH_4} 246 torr).

The high loading catalyst also possess a slight chemically different surface since it favours formation of CO_2 over CO. This difference could be associated with the amount of lithium on the surface. The advantage of precalcination is also highlighted here: The calcined Li_2CO_3/MgO catalyst is much more stable than the fresh counterpart.

4.4 Further activity determination of MgO

4.4.1 The activity of MgO obtained from a different supplier

In this determination, 0.2 gm of MgO, was used as received. Three different MgO samples supplied by BDH, Merck and Strem have been tested. The surface area of these samples have been measured to be around 20 m^2/gm. As shown in table 4.4.1.a, all of the MgO have very similar activities, with a methane conversion of around 33% and a selectivity to C_2 of about 40%. In all cases, most of the oxygen was consumed. It was also observed that the ratio of ethene to ethane in the product was about 2. The total yield to C_2 hydrocarbons was about 16% and was higher than that for the treated MgO. Unlike the lithium doped catalyst, a significant amount of CO was produced with increasing amounts in the order of BDH, Merck and Strem.

Table 4.4.1.a Activity of fresh MgO obtained from different supplier at 800°C

Supplier	P_{CH_4}#	p_{O_2}	%con.CH_4	O_2;	%Sel.C_2H_6	C_2H_4	CO	CO_2;	Tot.C_2;	%C_2yield;	%$C_2^=/C_2$Tot.
BDH	228	100	35.3	100	16.5	30.5	5.1	48	44.0	15.5	69
Merck	225	100	36.1	100	15.1	32.2	7.9	44.9	47.3	17.1	68
Strem	230	90	34.3	100	14.4	30.1	17.0	38.5	44.5	15.3	68

total flow rate 25ml/min; # partial pressure in torr

The earlier observation of MgO being active for the oxidative reaction of methane is confirmed here. The C_2 hydrocarbon yield over these MgO samples are comparable to the yield obtained over Li_2CO_3/MgO. Since the activity observed is higher than that of the treated MgO, it would imply that the activity of MgO is fairly sensitive to its preparative and thermal history.

4.4.2 The activity of Strem MgO at 800°C with time-on-stream

The activity of the Strem MgO sample at 800°C with time-on-stream have been determined (figure 4.4.2.a). The activity was found to be very stable over 21 hours

on stream. Methane conversion stood around 35% and selectivity to C_2 hydrocarbons was about 38%. Generally the selectivity to the various products also remained fairly stable. This result indicates that, in the course of the reaction, no significant physical or chemical changes occurred over the catalyst, allowing its initial activity to be retained.

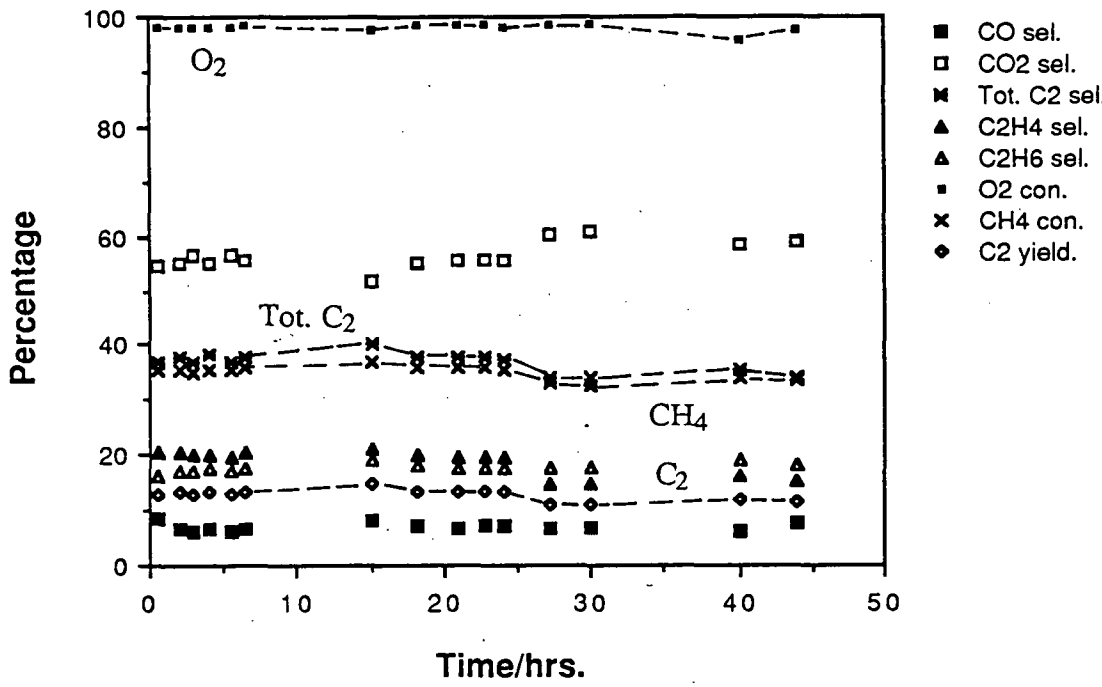

Figure 4.4.2.a The activity of 0.2g of Strem MgO at 800°C with time-on-stream (P_{O_2} 111 torr, P_{CH_4} 227 torr)

4.4.3 The effect of the amount of Strem MgO used in catalyst screening on its catalytic activity at 800°C

Generally, using a larger amount of MgO resulted in the increase of methane conversion and a decrease in C_2 selectivity (figure 4.4.3.a). The use of a larger amount of MgO did not result in a significant increase of methane conversion due to the full consumption of oxygen. It was also noted that when 0.05g of MgO was used,

the selectivity to CO was about 31%, and this decreased as the amount of catalyst used was increased.

The result obtained here indicates that increasing the amount of catalyst used in activity determination under a particular flow condition does not necessarily lead to significant benefits. Even though methane conversion increases the selectivity to C_2 hydrocarbons decreases, causing the total C_2 yield not to vary significantly. It was also demonstrated here that the maximum achievable methane conversion is limited by the availability of oxygen.

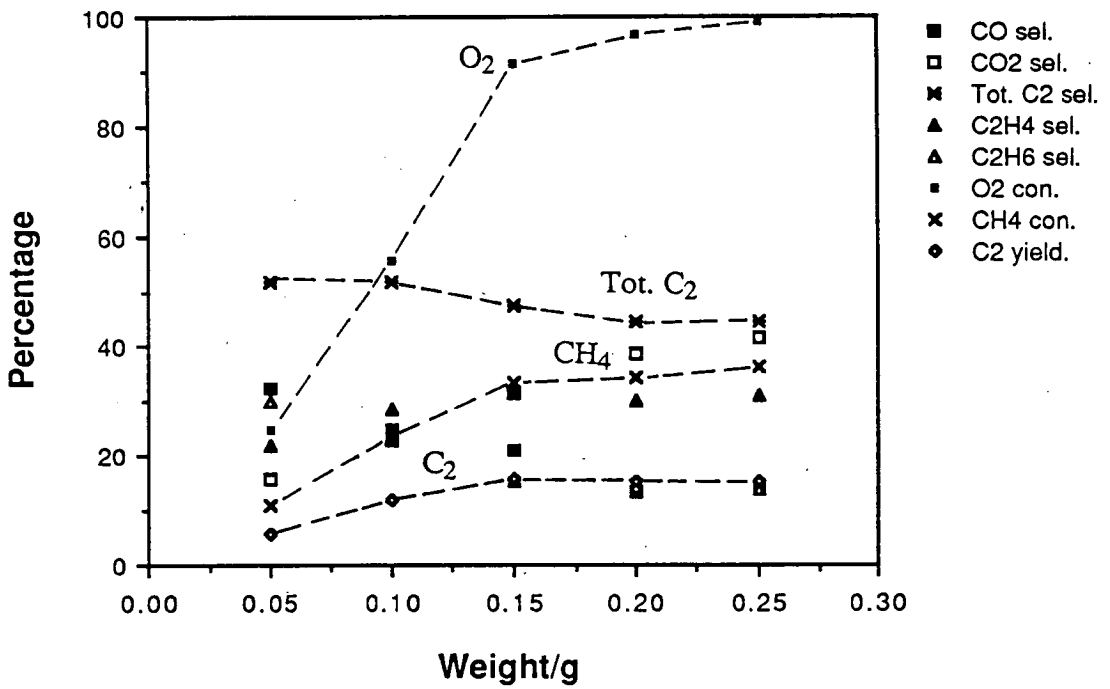

Figure 4.4.3.a The effect of the amount of Strem MgO used on the catalytic activity at 800°C (P_{O_2} 99 torr, P_{CH_4} 230 torr).

4.4.4 Activity of prepared MgO which were precalcined at different temperature.

The activities at 800°C of prepared MgO which was precalcined at different temperature for 10 hours are given in Figure 4.4.4.a. Increases in the calcination temperature resulted in similar methane conversions of about 28%, but a consistent decrease in selectivity to C_2 products. Over all of these materials oxygen consumption

in excess of 90% occurred It was also observed that the selectivity to carbon dioxide increased while CO decreased with an increase in the calcination temperature. This trend is slightly clearer when the activities at 760°C were compared instead (figure 4.4.4.b). Calcination of MgO at 900°C gave the highest methane conversion, and the lowest selectivity to C_2 and CO.

To further highlight the effect of calcination on activity of MgO, the effect of reaction temperature on MgO, calcined at the different temperatures has also been investigated. Over all reaction temperatures, a higher methane conversion occured over the catalyst calcined at 900°C. The selectivity to C_2 products increased while the selectivity to CO decreased with the reacton temperature.

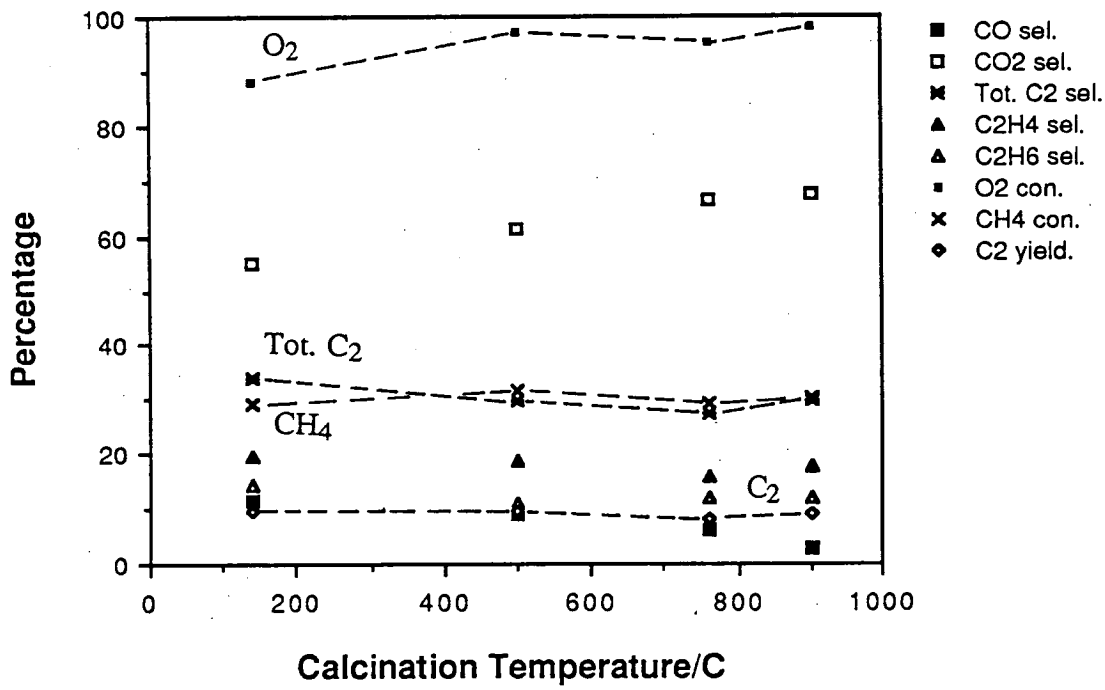

Figure 4.4.4.a The effect of precalcination temperature on the activity of MgO at 800°C (P_{O_2} 100 torr, P_{CH_4} 217 torr)

It is clearly demonstrated here that the activity of MgO is sensitive to its thermal and preparative history. This also reinforces the point that care is needed when studying and comparing any material for the oxidative reaction of methane.

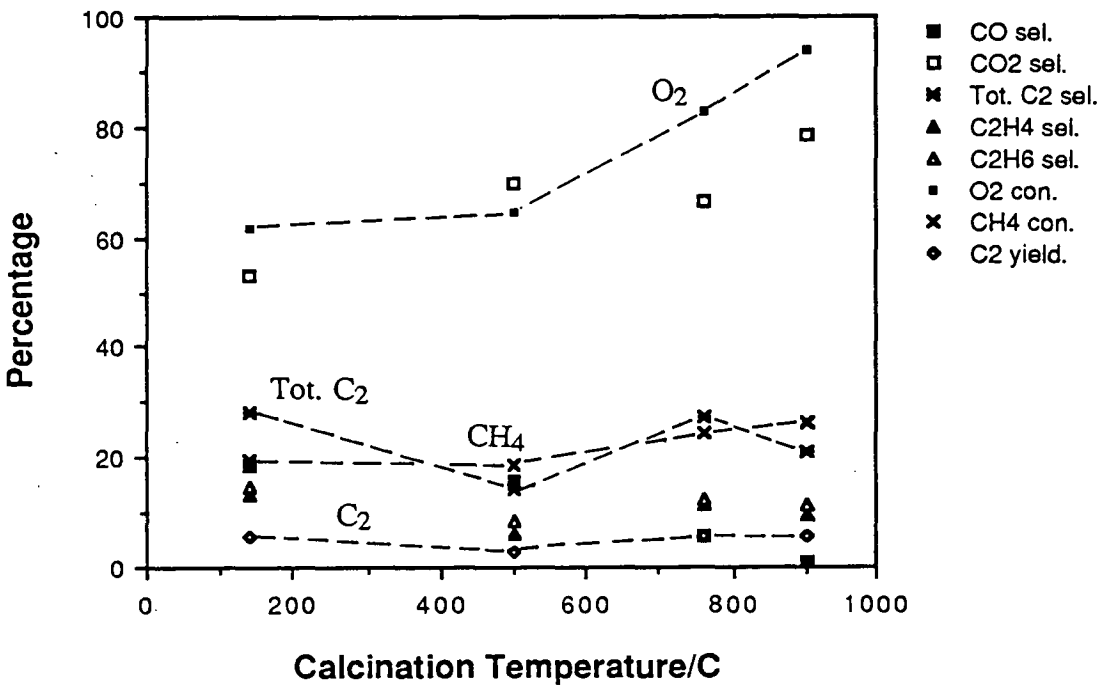

Figure 4.4.4.b Activity at 760°C of prepared MgO which was calcined at different temperature (P_{O_2} 102 torr, P_{CH_4} 219 torr)

4.4.5 Effect of length of in situ calcination time at 800°C prior to activity determination of fresh MgO.

The length of in situ calcination time at 800°C on fresh MgO has a very significant effect on the catalytic activity (Figure 4.4.5.a). Methane conversion dropped from 33% to about 14% when the fresh MgO was calcined in situ for two hours. As methane conversion decreased the selectivity to C_2 hydrocarbon increased. It was also observed that at longer in situ calcination time, the selectivity of ethane with respect to ethene increased and so did the selectivity of CO with respect to CO_2.

The changes in activity of MgO with length of in situ calcination is likely to be due primarily to changes occurring on the surface as a result of the calcination. It is likely that the in-situ pretreatment destroyed the active centre for the partial oxidation reaction. On the other hand, such deactivation does not occur on MgO during reaction at 800°C even after a long time of 24 hours on stream. A possible explanation to this behaviour is that the oxidative reaction on MgO preserves the availability of the active sites while in-situ calcination reduces the availability of these sites. Moreover, the effect of the high temperature on MgO is reversible. As observed in sections 4.3.1 and 4.4.4, MgO sample which was pretreated at high temperature and then exposed under room environment will regain its activity for the oxidative reaction of methane.

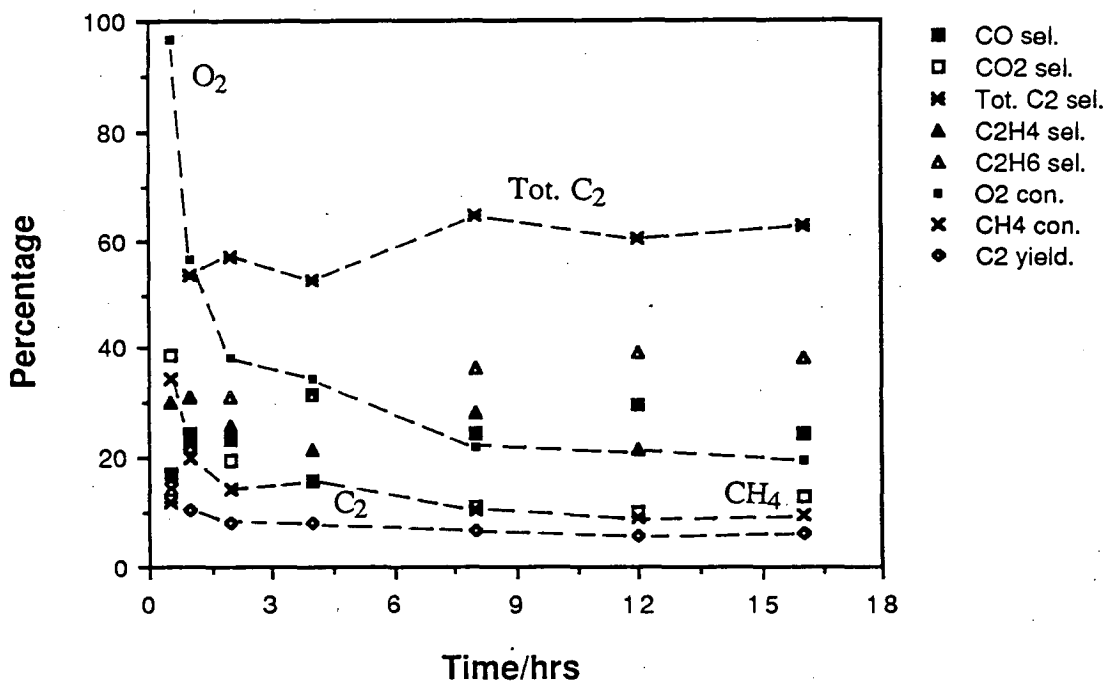

Figure 4.4.5.a The effect of length of in-situ precalcination on the activity of 0.2g Strem MgO at 800°C (P_{O_2} 110 torr, P_{CH_4} 215 torr).

The activity of raw MgO for the oxidative reaction of methane obtained in this study is comparable to the activity of the Li_2CO_3/MgO catalysts. However the activity

of MgO is very sensitive to its preparative and thermal history. This fact explains why different MgO activities were reported in the literature. The different pretreatment and screening conditions used, even on the same MgO sample, will give different activity results.

4.5 Activity determination of fresh chemicals

4.5.1 The activity of chemicals used for supporting Li_2CO_3

4.5.1.1 Activity of $Mg(OH)_2$, $Ca(OH)_2$ and CaO.

Table 4.5.1.1.a Activity of $Mg(OH)_2$, $Ca(OH)_2$ and CaO.

PO_2#	PCH_4	Temp/C	%con.CH_4	O2;	%Sel.C_2H_6	C_2H_4	CO	CO_2	Tot.C_2;	%C_2yield;	%$C_2^=/C_2$Tot.
Catalyst: $Mg(OH)_2$											
93	227	800	33.3	100	17.8	18.2	11.5	42.5	46.0	15.3	61
		760	32.4	98.3	18.0	25.1	12.4	44.6	43.0	13.9	58
		710	27.1	88.5	17.5	16.9	20.5	45.2	34.4	9.3	49
		660	21.1	75.0	14.0	9.7	29.9	46.3	23.8	5.0	41
Catalyst: $Ca(OH)_2$											
93	225	800	27.0	100.0	14.0	14.1	8.7	63.2	28.1	7.6	50
		760	26.6	100.0	13.5	12.8	9.2	64.5	26.3	7.0	49
		710	22.1	84.7	12.5	9.2	13.1	65.3	21.7	4.8	42
		660	16.2	65.0	10.9	5.3	13.8	70.0	16.2	2.6	33
Catalyst: CaO (Calcined $Ca(OH)_2$)											
96	219	800	27.1	100.0	12.3	12.8	3.8	71.1	25.1	6.8	51
		760	25.3	100.0	10.5	7.1	3.1	79.2	17.6	3.6	40
		710	21.2	86.5	8.5	4.8	3.4	83.3	13.3	2.	36
		660	15.8	64.4	7.5	5.1	2.1	85.3	12.5	2.0	41

total flow rate 25ml/min; # partial pressure in torr

$Mg(OH)_2$, fresh as received, showed a similar catalytic activity to the fresh MgO (compare Table 4.5.1.1.a with Table 4.4.1.a). At 800°C, a 32% methane conversion with 43% selectivity to C_2 hydrocarbons was observed. Fresh $Ca(OH)_2$

was also active for the oxidative reaction of methane, resulting in about 25% conversion of methane with the selectivity to C_2 about 30%. CaO used in this work was produced from calcination of $Ca(OH)_2$ at 900°C for 10 hours. This sample had been kept for a while before activity determination was performed. Its activity was similar to $Ca(OH)_2$ except that the C_2 selectivity wass slightly lower. It was also observed that, as in the case of MgO, high temperature calcination reduced the C_2 selectivity considerably.

It is clearly demonstrated here that not only is MgO active for oxidative reactions of methane, but also $Mg(OH)_2$, $Ca(OH)_2$ and CaO. The extent of methane conversion is higher than that over calcined Li_2CO_3/MgO catalyst. These materials are chemically basic. Generally, it has been observed in the literature that chemically basic materials like the alkaline and alkaline earth metal oxides show high activity for the oxidative reaction of methane.

Table 4.5.1.2.a Activity of γ-Al_2O_3, SiO_2, and TiO_2 at different temperature. The reaction conditions are also given in the table.

PO_2#	PCH_4	Temp/C	%con.CH_4	O_2;	%Sel.C_2H_6	C_2H_4	CO	CO_2	Tot.C_2;	%C_2yield;	%$C_2^=/C_2$Tot.
Catalyst: γ-Al_2O_3											
106	209	800	27.8	88.1	2.6	3.1	58.4	35.9	5.7	1.6	54
		760	23.9	75.1	1.9	1.7	67.2	29.2	3.6	0.9	47
		710	11.4	34.9	2.9	0.0	76.2	21.0	2.9	0.3	0
		660	7.2	21.2	7.0	0.0	75.1	17.9	7.0	0.5	0
Catalyst: SiO_2											
104	212	800	7.1	22.2	13.7	8.1	21.1	57.1	21.8	1.6	37
		760	3.8	10.4	21.4	12.8	14.1	51.6	34.3	1.3	37
Catalyst: TiO_2											
104	218	800	10.1	25.7	25.2	10.8	18.0	46.0	36.0	3.6	30
		760	3.3	11.7	37.1	8.7	16.3	37.9	45.7	3.3	19

total flow rate 25ml/min; # partial pressure in torr

4.5.1.2 Activity of γ-Al_2O_3, SiO_2 and TiO_2

The activity of fresh γ-Al_2O_3 for the oxidative reaction of methane at different temperatures is given in Table 4.5.1.2.a. The extent of methane conversion over γ-Al_2O_3 is comparable to that over MgO, but selectivity to C_2 hydrocarbons is much lower. Carbon monoxide is the favoured product over γ-Al_2O_3. The effect of temperature is minimal on selectivity to C_2 hydrocarbons but causes CO selectivity to decrease and CO_2 to increase significantly. Fresh SiO_2 and fresh TiO_2 resulted in lower methane conversion. Conversion of 7% and selectivity to C_2 of around 20% occurred over SiO_2 at 800°C. TiO_2 resulted in 10% methane conversion with 40% selectivity to C_2 hydrocarbons.

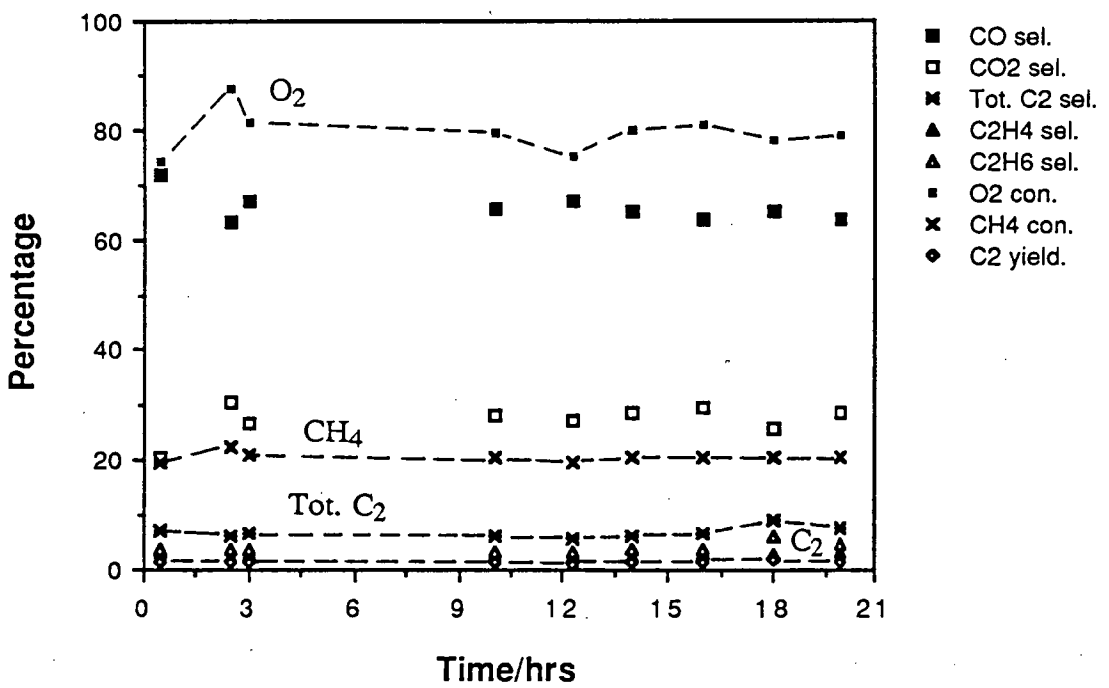

Figure 4.5.1.2.a Activity of γ-Al_2O_3 with time-on-stream (P_{O_2} 92 torr, P_{CH_4} 229 torr).

γ-Al_2O_3 shows significant activity for oxidative reactions of methane, and favours the formation of carbon oxide. This indicate that fresh γ-Al_2O_3 is not a

suitable oxidative coupling catalyst, however, it is possible that its properties can be modified. SiO_2 and TiO_2 have lower activity for oxidative reactions of methane and are not particularly selective for the production of C_2 hydrocarbons.

The effect of time on stream on stability of reaction over γ-Al_2O_3 has been determined and the result presented in Figure 4.5.1.2.a. The activity of γ-Al_2O_3 does not vary significantly with time and this indicates that the catalyst is also stable under the reaction conditions.

4.5.2 Activity of $AlPO_4$-5 and 12%Al_2O_3/SiO_2

At 800°C, the use of $AlPO_4$-5 resulted in 19% methane conversion and 74% of oxygen consumption with the selectivity to C_2 hydrocarbons of about 3% (Table 4.5.2.a). Carbon dioxide is the dominant product and no significant amount of CO was present in the product stream. Under similar conditions 12%Al_2O_3/SiO_2 gave rise to about 9% conversion of methane. Unlike the reaction over $AlPO_4$-5, over 12%Al_2O_3/SiO_2 CO was the major product - 70% , and selectivity to C_2 hydrocarbons was about 15%. However on both materials the exhaustive oxidation of methane to carbon oxide is favoured.

Table 4.5.2.a The actvity of $AlPO_4$-5 and 12%Al_2O_3/SiO_2

P_{O_2}#	P_{CH_4}	Temp/C	%con.CH_4	O_2;%Sel.C_2H_6	C_2H_4	CO	CO_2	Tot.C_2;%C_2	yield;%	$C_2^=/C_2$Tot.
Catalyst: $AlPO_4$-5										
111	218	803	19.4	74.2	3.3	0.0	0.0	96.7	3.3	0.6	0
		760	10.7	41.4	2.2	0.0	0.0	97.8	2.2	0.2	0
		711	1.7	6.7	0.0	0.0	0.0	100.0	0.0	0.0	-
Catalyst: 12% Al_2O_3/SiO_2										
101	213	800	8.7	25.0	9.8	6.6	74.1	9.6	16.3	1.4	40
		760	5.1	13.6	10.3	12.4	74.2	3.1	22.7	1.2	55

total flow rate 25ml/min; # partial pressure in torr

In this section the effects of the nature of the catalyst is further highlighted. $AlPO_4$ and $12\%Al_2O_3/SiO_2$ have been listed by Tanabe,1981, to be chemically acidic. Unlike the alkaline earth metal oxide which exibit some oxidative coupling properties, these materials resulted in mainly exhaustive oxidation of methane. It has also been suggested that both the acidic and basic sites are present on $AlPO_4$-5 (see Garnett et al.,1988). If this is so, it explain the high selectivity to CO_2 of $AlPO_4$-5 since CO_2 is the favoured carbon oxide product over basic materials.

4.5.3 Activity of Sm_2O_3

Otsuka and co-workers have extensively studied the activity of Sm_2O_3 for the oxidative reaction of methane. In this work Sm_2O_3 will also be studied under conditions similar to the studies on other catalysts. The activity of Sm_2O_3 for oxidative coupling reactions can be compared directly to that of other catalytic materials.

4.5.3.1 Temperatue effect on activity of Sm_2O_3

Generally Sm_2O_3 results in higher methane conversion (Table 4.5.3.1.a). Even at 660°C, a methane conversion of 28% and selectivity to C_2 of 17% was observed. As the reaction temperature was increased, the selectivity to C_2 hydrocarbons increased together with conversion, while selectivity to carbon dioxide decreased. At 800°C 35% methane conversion and 36% selectivity to C_2 was observed resulting in 12.5% yield to C_2. The selectivity to carbon oxides was predominantly to carbon dioxide. Carbon monoxide selectivity increases slightly at higher reaction temperature.

Sm_2O_3 has high activity for the oxidative reaction of methane. Even at 660°C, full oxygen consumption occurs. This is likely to be the reason why this compound has raised considerable interest as a possible catalyst for the oxidative coupling of methane. However, from the product distribution it is possible that

Sm_2O_3 favours the full oxidation of methane to carbon oxide. Nevertheless the selectivity to C_2 hydrocarbon can be increased by performing the reaction in an oxygen depletion environment at higher temperatures.

Table 4.5.3.1.a The activity of Sm_2O_3 at different temperature

P_{O_2}#	P_{CH_4}	Temp/°C	%con.CH_4	O_2;%Sel.C_2H_6	C_2H_4	CO	CO_2	Tot.C_2;%C_2yield;	%$C_2^=/C_2$Tot.
106	220	805	35.0	100.0	17.7	19.2	6.5	57.6	35.9	12.6	52
		763	33.0	100.0	18.5	11.8	7.2	62.5	30.3	10.0	39
		700	30.8	100.0	5.6	3.9	3.1	72.4	24.5	7.6	16
		660	28.4	100.0	16.3	1.0	0.0	81.7	17.3	4.9	6

total flow rate 25ml/min; # partial pressure in torr

It is clear from this section that higher activity to methane oxidations are detrimental to C_2 hydrocarbon yield. Even though Sm_2O_3 is active at lower temperatures, the total C_2 hydrocarbon yield is low due to the low selectivity to C_2 hydrocarbons. In order to achieve higher selectivity, the surface of Sm_2O_3 would have to be modified, possibly by an alkali promoter. Such effect has been observed by Otsuka et. al., 1986; when Li_2CO_3 was supported on Sm_2O_3, a hydrocarbon yield of 22.3% was achieved.

4.5.3.2 The influence of P_{O_2}/P_{CH_4} ratio in reactant stream on the activity of Sm_2O_3

Increasing the partial pressure of oxygen for a fixed partial pressure of methane, resulted in an increase of methane conversion and a decrease in selectivity to C_2 hydrocarbons (Figure 4.5.3.2.a). The effect of the P_{O_2}/P_{CH_4} ratio on the selectivity to C_2 hydrocarbon over Sm_2O_3 is more severe than that over Li_2CO_3/MgO. Over the entire range of oxygen partial pressure examined, full consumption of oxygen occurred. When the ratio of P_{O_2}/P_{CH_4} on Sm_2O_3 was 0.84 the selectivity to C_2 was 16%. On Li_2CO_3/MgO, the selectivity was 48% when the ratio was 0.86.

Moreover, under this condition the C_2 yield over $Li_2/CO_3/MgO$ was 18.6% while over Sm_2O_3 it was 8%. Carbon dioxide was the most prominent product over Sm_2O_3

The results here confirm that Sm_2O_3 is a very active material for the oxidative reaction of methane. Due to its high activity, full oxidation of methane to carbon dioxide occurs. The extent to which methane conversion occurs on Sm_2O_3 is only limited by the amount of oxygen available. In terms of hydrocarbon yields, MgO and CaO are a better oxidative coupling catalysts than Sm_2O_3. In its original form, Sm_2O_3 is unlikely to be a suitable catalyst for oxidative coupling of methane.

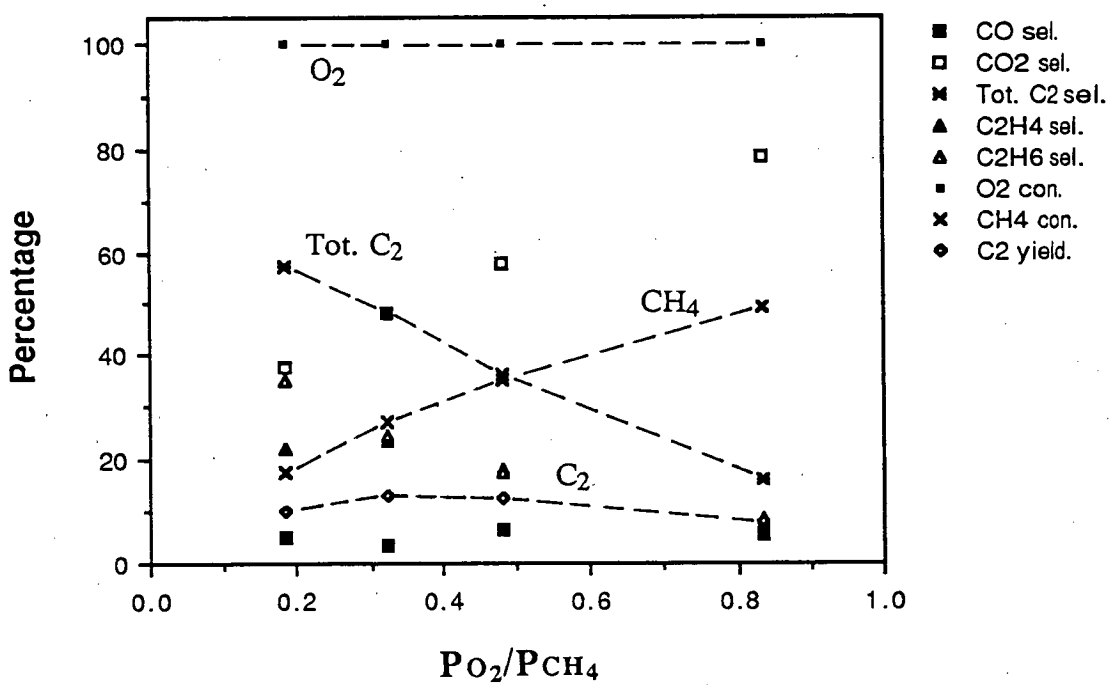

Figure 4.5.3.2 a The effect of P_{O_2}/P_{CH_4} ratio on the activity of Sm_2O_3 at 800°C (with the P_{CH_4} fixed at 220 torr).

4.5.3.3 Time stability of Sm_2O_3 at 800°C

The stability of the oxidative reaction of methane on Sm_2O_3 at 800°C has been determined. The reactant flow contained 199 and 236 torr partial pressures for O_2 and CH_4 respectively. As presented in Figure 4.5.3.3.a the activity only varies

slightly with reaction time. This indicates that the material was stable under reaction conditions for up to 21 hours.

To confirm the assertion made above, regarding the nature of the catalyst during the reaction, the physical structure of fresh and used catalyst was studied by SEM (Figure 4.5.3.3.b). As shown in Figure 4.5.3.3.b, the morphology of the unused Sm_2O_3 (micrograph i & ii) is similar to that of the used catalyst (micrographs iii & iv). This suggest that the physical nature of Sm_2O_3 catalyst do not change significantly under the condition of oxidative reaction of methane is possibly the reason why Sm2O3 have stable activity with time-on-stream.

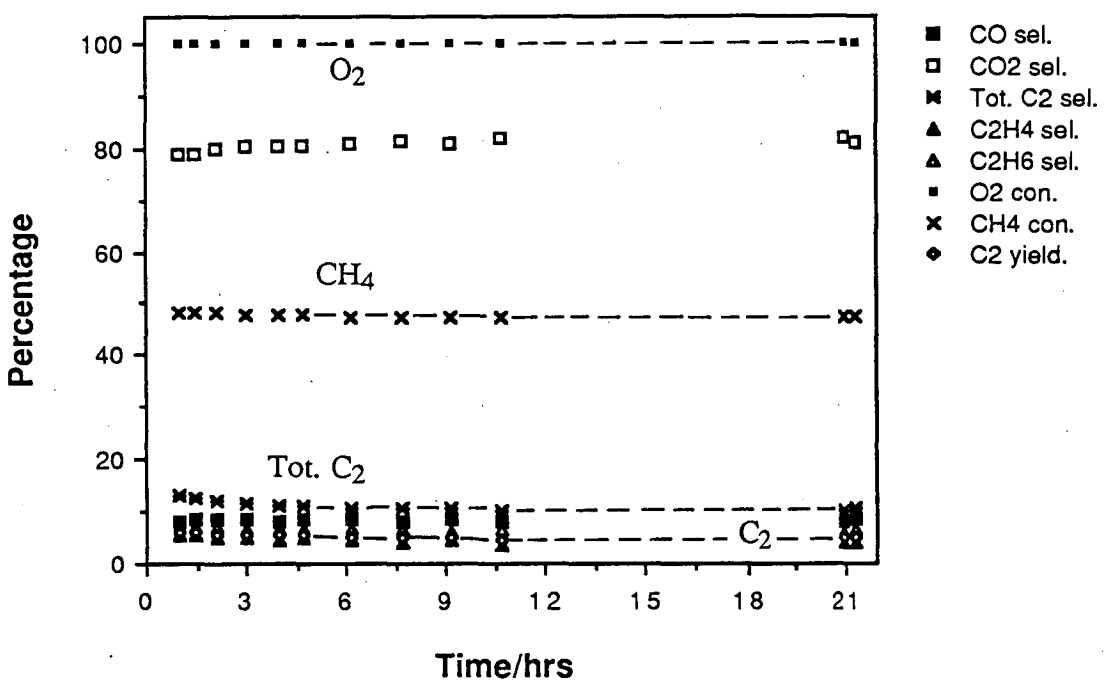

Figure 4.5.3.3.a The activity of Sm_2O_3 at 800°C with time-on-stream (P_{O_2} 199 torr, P_{CH_4} 236 torr)

4.5.4 The activity of various carbonates.

4.5.4.1 Activity of the first row carbonates at 800°C

Na_2CO_3 and K_2CO_3 resulted in 7-8% methane conversion with a selectivity to C_2 hydrocarbons of 65-50%. Selectivity to CO over these materials is low (Table 4.5.4.1.a).

i)

ii)

iii)

iv)

Figure 4.5.3.3.b SEM micrographs of Sm_2O_3 catalysts.

Micrographs i) and ii) are that of the unused Sm_2O_3 catalyst at magnifications of $5.0x10^2$ and $2.0x10^4$ respectively, while micrographs iii)and iv) correspond to the used catalyst under the same respective magnifications.

Since the melting temperature of Na_2CO_3 is 854°C, and 897°C for K_2CO_3, it is likely that these materials undergo significant transformation at reaction temperatures. The question is whether the instability of these materials under reaction conditions influences their catalytic activity.

Table 4.5.4.1.a Activity of Na_2CO_3 and K_2CO_3 at 800°C.

P_{O_2}#	P_{CH_4}	Temp/°C	%con.CH_4	O_2;%Sel.C_2H_6	C_2H_4	CO	CO_2	Tot.C_2;	%C_2 yield;	%$C_2^=/C_2$Tot.
Catalyst: Na_2CO_3										
108	220	800	7.0	12.6	48.2	18.5	0.0	33.3	66.7	4.7	28
Catalyst: K_2CO_3										
108	226	800	8.2	18.1	36.3	14.7	11.6	37.4	51.0	4.2	29

total flow rate 25ml/min; # partial pressure in torr

4.5.4.2 Activity of second row carbonates at 800°C

$CaCO_3$ shows a high activity for the oxidative reaction of methane (Table 4.5.4.2.a). At 800°C, about 30% methane was converted with a total selectivity to C_2 of around 37%. $SrCO_3$ and $BaCO_3$, had similar methane conversion of about 10% while the C_2 selectivity over $SrCO_3$ was 30% and over $BaCO_3$ 50%. For all of the three compounds the selectivity to CO was less than 10%.

$CaCO_3$ decomposes at 900°C while $BaCO_3$ and $SrCO_3$ decompose at 1350°C. In the case of $CaCO_3$, it is likely that some decomposition occurs under the reaction conditions to form calcium oxide. From the results of this, and the previous experiments, it would seem that the oxidative reaction of this material is related to their stability. It is possible that the active site is formed by the decomposition of the carbonate.

Carbonates which undergo decomposition and do not melt will have more active sites since the surface area is retained. The formation of the active sites can be

tentatively represented by the equation 4.5.4.2.a, and its reversal indicates the loss of active sites causing a decrease in catalytic activity.

Equation 4.5.4.2.a MCO_3 <-----> (CO_2) + MO <-----> (active site)

Table 4.5.4.2.a The activity of second row carbonates at 800°C.

P_{O_2}#	P_{CH_4}	Temp/°C	%con. CH_4	O_2	%Sel.C_2H_6	C_2H_4	CO	CO_2	Tot.C_2	%C_2	yield;%$C_2^=/C_2$Tot.
Catalyst: $CaCO_3$											
98	224	800	30.4	98.2	15.9	18.9	4.8	60.4	34.8	10.6	54
		760	29.6	98.3	15.5	16.2	5.9	62.4	31.7	9.4	51
		710	16.1	60.8	10.8	4.8	17.9	66.4	15.6	2.5	31
		660	12.7	48.6	9.2	5.2	18.1	67.5	14.4	1.8	36
Catalyst: SrCO3											
101	213	800	11.2	6.0	18.5	9.5	6.6	65.4	28.1	3.1	34
		760	6.0	18.6	19.3	10.5	6.3	63.9	29.9	1.8	35
Catalyst: BaCO3											
98	211	800	10.8	25.8	32.9	17.9	8.2	41.1	50.8	5.5	35
		760	6.4	15.8	34.6	13.2	9.9	42.3	47.8	3.1	28

total flow rate 25ml/min; # partial pressure in torr

4.6 Activity of various lithium salts on MgO

In order to probe further the role of the catalyst nature on its activity for oxidative reaction of methane, the effect of various lithium salts on MgO have been studied. The activity of fresh and calcined samples has been compared, so that the extent of chemical and physical effects can be gauged.

4.6.1 Activity of the calcined sample at 800°C

The activity of calcined LiOH/MgO (Table 4.6.1.a) is very similar to that of Li_2CO_3/MgO (section 4.2) with a methane conversion of about 25% and C_2 yield of 15%. The ratio of ethene to ethane in the product stream is about 1 while carbon dioxide is the dominant carbon oxide product. LiCl/MgO also results in high methane

conversion with the selectivity to C_2 of around 50%. A distinct difference between the activity of LiCl/MgO to that of Li_2CO_3/MgO is that the selectivity to C_2H_4 is nearly twice that of C_2H_6. LiF/MgO and Li_2SO_4/MgO have low catalytic activity. It was also observed that the activity of LiCl/MgO changes very rapidly with time on stream suggesting a significant transformation occurs on the catalyst.

The similarity in the catalytic activity of LiOH/MgO and Li_2CO_3/MgO suggests the resemblance in their physical and chemical nature. This is supported by the fact that not only the amount of methane conversion is similar, but the overall product distribution is nearly the same. In the case of LiCl/MgO, a distinct difference exists. Preliminary results suggest that this material is unstable with time on stream. Otsuka and co-workers, have studied extensively the activity of LiCl supported catalysts and they proposed that the chlorine atom from the catalyst participated in the reaction with the hydrocarbon and facilitated the conversion of ethane to ethene. On the other hand the presence of LiF and Li_2SO_4 on MgO seemed to destroy the catalytic activity of MgO.

Table 4.6.1.a The activity of calcined lithium salts on MgO at 800°C.

P_{O_2}#	P_{CH_4}	Temp/C	%con.CH_4	O_2;%Sel.C_2H_6	C_2H_4	CO	CO_2	Tot.C_2;%C_2	yield;%$C_2^=$/C_2Tot.
Catalyst: Li_2CO_3/MgO									
96	207	800	24.8	53.0	29.3	32.5	1.3	36.9	61.8	15.3	53
Catalyst: LiOH/MgO									
101	203	800	26.8	53.9	26.5	33.0	2.6	37.9	59.5	15.9	55
Catalyst: LiCl/MgO									
104	210	800	37.2	100	12.9	30.2	0.0	56.9	43.2	16.0	70
Catalyst: LiF/MgO									
108	194	800	2.5	2.1	63.3	28.1	1.5	7.1	91.4	2.3	31
Catalyst: Li2SO4/MgO									
108	194	800	4.3	6.93	48.8	17.0	0.6	33.6	65.8	2.8	26

total flow rate 25ml/min; # partial pressure in torr

4.6.2 Activity of uncalcined sample at 800°C

The activity of fresh LiOH/MgO is also similar to that of uncalcined Li_2CO_3/MgO (Table 4.6.2.a). Generally the uncalcined catalyst results in higher methane conversion relative to its calcined counterpart. However, the activity of LiF/MgO and Li_2SO_4/MgO is much lower than the activity of MgO indicating that the calcinations are not a necessity for the destruction of MgO activity.

The relatively higher activity of uncalcined LiOH/MgO and Li_2CO_3/MgO are likely to be associated with the higher surface area of the uncalcined sample. However surface area per se is not the determining factor as to whether a material is catalytically active or not. Fresh Li2SO4/MgO and LiF/MgO have higher surface area than calcined Li_2CO_3/MgO or LiOH/MgO (section 5.6.1) and yet their activity is lower. For an active material however higher surface area will result in higher activity.

Table 4.6.2.a The activity of fresh lithium salts on MgO at 800°C.

P_{O_2}#	P_{CH_4}	Temp/°C	%con.CH_4	O_2;%Sel.C_2H_6	C_2H_4	CO	CO_2	Tot.C_2;%C_2yield;	%$C_2^=/C_2$Tot.
Catalyst: Li_2CO_3/MgO									
105	228	800	33.6	81.9	22.1	32.2	1.3	44.4	54.3	18.3	59
Catalyst: LiOH/MgO									
103	234	800	37.0	93.0	20.7	34.3	0.9	44.1	55.1	20.1	62
Catalyst: LiCl/MgO									
103	234	800	29.5	75.3	20.1	30.5	13.5	35.9	50.6	14.9	60
Catalyst: LiF/MgO									
103	234	800	4.5	10.8	38.0	17.7	1.1	42.9	55.7	2.5	32
Catalyst: Li2SO4/MgO									
103	234	800	5.5	10.9	46.8	19.5	4.3	29.4	66.3	3.7	29

total flow rate 25ml/min; # partial pressure in torr

Not only is the activity of calcined Li_2CO_3/MgO similar to that of LiOH/MgO but their uncalcined form also results in similar activity. This indicates that high temperature precalcination is not a prerequisite for creating an active material. It also

Not only is the activity of calcined Li_2CO_3/MgO similar to that of LiOH/MgO but their uncalcined form also results in similar activity. This indicates that high temperature precalcination is not a prerequisite for creating an active material. It also indicates that irrespective of whether Li_2CO_3 or LiOH was used, active material was formed and selectivity to C_2 products was promoted. This observation infers that neither LiOH nor Li_2CO_3 is the active species for the oxidative coupling reaction. These chemicals could serve as the precursor for active sites and also cause significant physico-chemical changes on the catalyst, and thus influence the nature of the reaction.

The uncalcined LiCl/MgO also shows significant activity with high C_2 selectivity. Some CO was also present in the product stream. Due to the observation made earlier on LiCl/MgO, this material was studied further (section 5.6.3) in order to highlight the role of the catalyst on the oxidative reaction of methane. 4

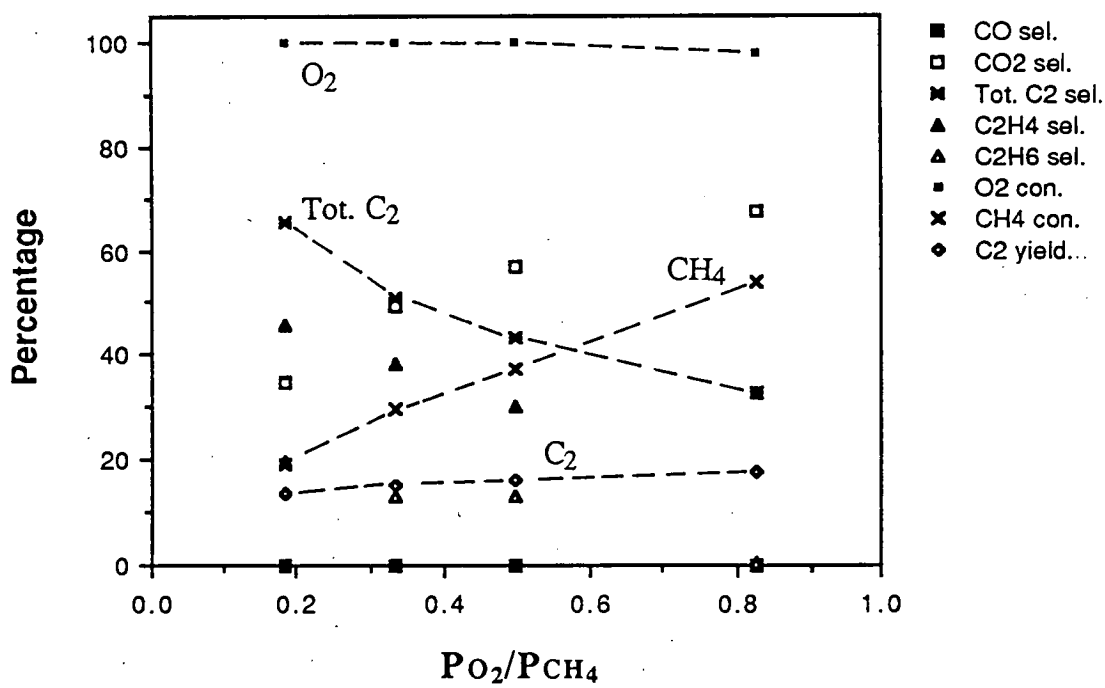

Figure 4.6.3.1.a The effect of the P_{O_2}/P_{CH_4} ratio on the activity of LiCl/MgO at 800°C (with the partial pressure of CH_4 fixed at 200 torr)

4.6.3 Further studies on calcined LiCl/MgO

4.6.3.1 Effect of O_2/CH_4 ratio at fixed partial pressure of methane (P_{CH_4} 200 torr) on the reaction over LiCl/MgO

As the partial pressure of oxygen increases methane conversion increases while selectivity to C_2 hydrocarbon decreases continously (figure 4.6.3.1.a). Higher selectivity to ethene than ethane is observed at all partial pressures of oxygen. At the highest partial pressure of oxygen only C_2H_4 exists as C_2 hydrocarbon product. At all partial pressures of oxygen carbon dioxide is the dominant carbon oxide product.

The similarity in carbon oxide product distribution over Li_2CO_3/MgO and LiCl/MgO catalysts indicate that both catalysts have similar reactivity for the exhaustive reaction. In terms of selectivity to C_2 hydrocarbons, LiCl/MgO, unlike Li_2CO_3/MgO promote the formation of ethene relative to ethane.

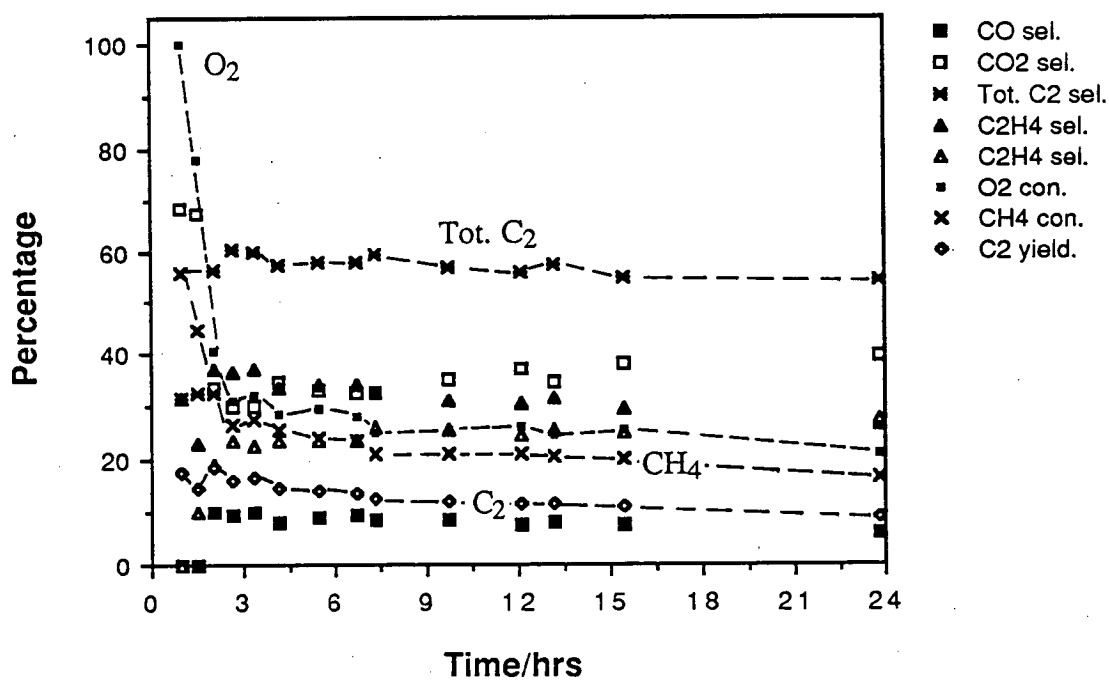

Figure 4.6.3.2.a The effect of time-on-stream on the activity of LiCl/MgO catalyst at 800°C (P_{O_2} 195 torr, P_{CH_4} 230 torr).

4.6.3.2 The effect of time on stream on the activity of LiCl/MgO catalyst (P_{O_2} 195 torr, P_{CH_4} 230 torr)

LiCl/MgO activity undergoes very significant changes during the time on stream (figure 4.6.3.2.a). Methane conversion decreases rapidly in the first five hours during on stream. When the reactant was first introduced, selectivity to C_2 product was about 30% and predominantly consisted of ethene. After 2 hours on stream the selectivity to C_2 rises drastically to about 55% and decreased slightly with further on stream time. The ratio of ethene to ethane in the product stream approached 1. It was also observed that following the rapid decreases in methane conversion, the selectivity to CO rose and remained at about 8%.

This result basically confirms earlier observations of rapid changes in activity of LiCl/MgO catalysts with time on stream. In their studies on the activity of LiCl doped transition metal oxide, Otsuka et al.,1988a, have also made similar observation. They proposed that in the presence of O_2, CH_4 will react with LiCl to form LiOH and CH_3Cl. The CH_3Cl will then decompose in the gaseous phase to into methyl and chlorine radicals. The methyl radicals recombine to form ethane. Reactions between the chlorine with ethane facilitate the formation of ethene. The role of chlorine is significant at the early stages of the reaction due to its high concentration. With time on stream, the effect of chlorine decreases and the behaviour of the catalyst approaches that of $LiCO_3$/MgO. It is possible that the chemical and physical behaviour of LiCl/MgO after prolonged use is similar to that of Li_2CO_3/MgO.

4.6.3.3 Physical and chemical changes on LiCl/MgO after 25 hours on stream.

The nature of LiCl/MgO catalysts have been studied by micro-probe analysis, atomic absorbtion spectroscopy and scanning electron microscopy. The wt% Li/Mg of uncalcined, calcined and used catalysts have been determined by AAS and presented in table 4.6.3.3.a

Table 4.6.3.3.a The composition of various LiCl/MgO catalysts

Catalyst sample	Wt % Li/Mg
Uncalcined LiCl/MgO	6.2
Calcined LiCl/MgO	2.9
Used, 25 hrs on stream	0.3

Significant losses of lithium occured as a result of the calcination procedure and after time-on-stream. In order to determine the changes with respect to chlorine content, x-ray microprobe analysis on calcined and used samples has been performed, and the results presented in table 4.6.3.3.b.

Table 4.6.3.3.b The composition on unused and used LiCl/MgO catalysts.

Sample	Wt % MgO	Wt % Cl
Calcined LiCl/MgO	77	10.4
Used 25 hrs onstream	94	0.0

The result indicated that after 25 hours on stream most of the LiCl decomposed, resulting in a chlorine free sample. However since 0.3% of the Li was still present, it must have existed in the form of an oxide or carbonate. This suggests that the chemical composition of used LiCl/MgO is similar to that of Li_2CO_3/MgO catalyst. This result also implies that Cl is responsible in promoting the selectivity to ethene during the oxidative reaction of methane on a LiCl/MgO catalyst.

The physical nature of calcined and used LiCl/MgO catalysts have been studied by SEM. The particle clusters of LiCl/MgO, after calcination are less distinct and seem to be covered by a layered structure. Used catalysts have a distinct and well defined particle boundary (figure 4.6.3.3.a). The micrographs of used LiCl/MgO and Li_2CO_3/MgO are quite similar (compare micrographs iii & iv of figure 4.6.3.3.a with

i)

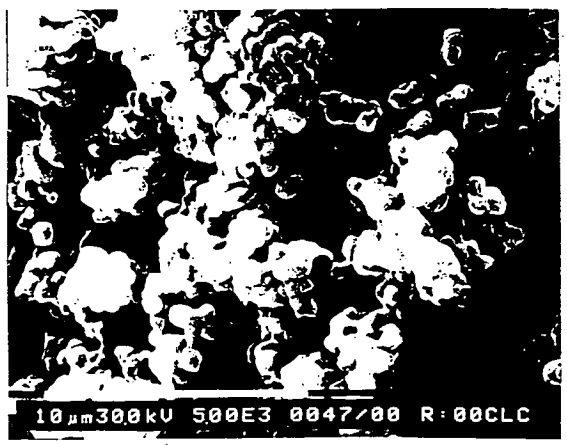

ii)

iii)

iv)

Figure 4.6.3.3.a SEM micrographs of LiCl/MgO catalysts.

Micrographs i) and ii) are that of the unused LiCl/MgO catalyst at magnifications of $5.0x10^2$ and $2.0x10^4$ respectively, while micrographs iii) and iv) correspond to the used catalyst under the same respective magnifications.

micrographs iii & iv of figure 4.3.4.b), and further suggest the similarity in the chemical and physical nature of the used catalyst. This explains the similarity in their activity after long time-on-stream. The nature of other catalytic materials after calcination and activity determination will be discussed further in chapter 5.

4.7 Activity of Li_2CO_3 supported on various oxide

4.7.1 The activity of calcined Li_2CO_3/M_xO_y at 800°C

As expected, the activities of catalysts prepared from Li_2CO_3 and $Mg(OH)_2$ are very similar to that of Li_2CO_3/MgO (Table 4.7.1.a). The use of $Li_2CO_3/Ca(OH)_2$ resulted in higher methane conversion but lower selectivity to C_2 hydrocarbons than the Li_2CO_3/MgO catalyst. About 18% total C_2 yield was achieved over $Li_2CO_3/Ca(OH)_2$. Li_2CO_3/γ-Al_2O_3 also showed high methane conversion of about 21% and a C_2 selectivity of about 30%. The use of Li_2CO_3/TiO_2 resulted in methane conversion of about 7% and a C_2 selectivity of around 38% but Li_2CO_3/SiO_2 is not significantly active. Over all of these catalysts the selectivity to carbon oxides is predominantly for carbon dioxide.

The $Li_2CO_3/Ca(OH)_2$ system has been proposed by Wang and Lunsford,1986, to be unsuitable for the formation of Li^tO^- sites due to the differences in ionic radii of Li^+ and Ca^{2+} ions. However since this system shows significant oxidative coupling behaviour it would imply that a different active site can also be responsible for the oxidative reaction. This is further supported by the fact that CaO itself shows significant activity. The presence of Li_2CO_3 on CaO was observed to have only a small effect on the activity of CaO. This implies that the presence of Li^+O^- type sites may not be necessary for achieving high methane conversion.

The activity of Li_2CO_3/γ-Al_2O_3 is very different from γ-Al_2O_3. The doping of Li_2CO_3 on γ-Al_2O_3 is supposed to reduce the acidity of γ-Al_2O_3, besides causing physical changes on the support. These changes result in an increase in selectivity to C_2 hydrocarbons and promote the formation of carbon dioxide instead of carbon

monoxide. The low activity of Li_2CO_3/TiO_2 and Li_2CO_3/SiO_2 are analogous to the activity of the corresponding untreated support.

Table 4.7.1.a The activity of calcined lithium carbonate on various support at 800°C.

PO_2#	PCH_4	Temp/°C	%con.CH_4	O_2;%Sel.C_2H_6	C_2H_4	CO	CO_2	Tot.C_2;%C_2	yield;%$C_2^=/C_2$Tot.
Catalyst: Li_2CO_3/MgO									
113	219	800	26.8	49.8	30.3	33.8	0.0	35.9	64.1	17.2	53
Catalyst: $Li_2CO_3/Mg(OH)_2$									
98	212	800	24.0	52.8	27.8	31.8	2.5	37.9	59.6	14.3	53
Catalyst: $Li_2CO_3/Ca(OH)_2$									
104	224	800	32.2	73.3	21.7	36.8	3.3	38.2	58.5	18.9	63
Catalyst: Li_2CO_3/SiO_2									
102	198	800	3.0	6.1	34.0	18.7	17.7	29.6	52.7	1.6	35
Catalyst: Li_2CO_3/TiO_2									
100	205	800	7.8	22.3	26.1	9.9	0.3	63.7	36.0	2.8	28
Catalyst: Li_2CO_3/γ-Al_2O_3									
100	221	800	27.6	96.5	9.8	16.9	0.2	73.2	26.7	7.4	63

total flow rate 25ml/min; # partial pressure in torr

4.7.2 The activity of uncalcined Li_2CO_3/M_xO_y at 800°C

The use of uncalcined $Li_2CO_3/Ca(OH)_2$ (table 4.7.2.a) resulted in slightly lower methane conversion than the calcined form, but still a good oxidative coupling property was present. In the case of Li_2CO_3/γ-Al_2O_3, the oxidative coupling properties are not exactly the same as in the calcined form. Compared to raw γ-Al_2O_3, the C_2 selectivity was higher while the CO selectivity was lower. The fresh Li_2CO_3/SiO_2 and Li_2CO_3/TiO_2 had low catalytic activity.

The results from these experiments, and others in this chapter show that chemically basic materials have significant oxidative coupling properties. These materials not only promote the formation of C_2 hydrocarbons but also the formation of carbon dioxide. γ-Al_2O_3, which is acidic in nature, results in mainly the oxidation of

methane to carbon monoxide, but when Li_2CO_3 was doped on it carbon dioxide became the sole carbon oxide product and the selectivity to C_2 hydrocarbons increased significantly. The presence of Li_2CO_3 increased the basicity of γ-Al_2O_3, and this facilitated the oxidative coupling reaction of methane.

In this study the nature of the active site for the oxidative coupling reaction occurring is yet to be elucidated. However, this site is not likely to be specifically the Li^+O^- type site, since many catalysts which do not contain lithium also show significant oxidative coupling properties. The presence of Li_2CO_3 on a number of oxides does however promote C_2 hydrocarbon selectivity. Since the precalcination is not a significant factor in determining whether the supported catalyst is active or not, it then implies that the presence of Li_2CO_3 on these oxides under reaction conditions influences the chemical and the physico-chemical nature of the catalyst and its surfaces.

Table 4.7.2.a The activity of uncalcined lithium carbonate on various support at 800°C.

P_{O_2}#	P_{CH_4}	Temp/°C	%con.CH_4	O_2;%Sel.C_2H_6	C_2H_4	CO	CO_2	Tot.C_2;%C_2yield;	%$C_2^=/C_2$Tot.
Catalyst: Li_2CO_3/MgO									
105	229	800	33.6	81.9	22.1	32.2	0.8	44.4	54.3	18.3	59
Catalyst: $Li_2CO_3/Mg(OH)_2$									
105	223	800	33.4	93.3	9.6	36.2	1.1	53.1	45.8	15.3	79
Catalyst: $Li_2CO_3/Ca(OH)_2$									
105	223	800	28.9	59.3	25.7	38.2	1.8	34.3	63.9	18.4	60
Catalyst: Li_2CO_3/SiO_2									
105	223	800	2.1	3.1	49.0	27.5	3.0	20.5	76.5	1.6	36
Catalyst: Li_2CO_3/TiO_2									
105	223	800	4.2	5.8	49.6	25.2	19.1	6.0	74.9	3.1	34
Catalyst: Li_2CO_3/γ-Al_2O_3									
105	223	800	26.0	88.5	7.7	11.4	14.7	1.5	19.1	5.0	60

total flow rate 25ml/min; # partial pressure in torr

4.7.3 Further studies on the Li_2CO_3/CaO System

4.7.3.1 Effect of reaction temperature on the activity of Li_2CO_3/CaO catalyst (P_{O_2} 104 torr; P_{CH_4} 224 torr)

The effects of temperature on the activity of Li_2CO_3/CaO have been studied and the results are presented in Table 4.7.3.1.a. The temperature dependence of Li_2CO_3/CaO is similar to that of Li_2CO_3/MgO catalysts. Methane conversion increases with temperature and so does the selectivity to ethene with respect to ethane. The selectivity to carbon oxides is predominantly to carbon dioxide at all reaction temperatures.

Table 4.7.3.1.a The activity of Li_2CO_3/CaO at 800°C.

P_{O_2}#	P_{CH_4}	Temp/°C	%con.CH_4	O_2;%Sel.C_2H_6	C_2H_4	CO	CO_2	Tot.C_2;	%C_2yield;	%$C_2^=/C_2$Tot.
104	224	800	32.2	73.3	21.7	36.8	3.3	38.2	58.5	18.9	63
		760	10.6	19.4	47.1	21.9	0.0	30.9	69.1	10.6	32
		710	4.3	8.8	48.4	13.3	0.0	38.3	61.7	2.7	22

total flow rate 25ml/min; # partial pressure in torr

This result shows that the presence of Li_2CO_3 on CaO and MgO increases the selectivity to C_2 hydrocarbons and decreases the amount of methane conversion at any particular temperature. The effect of Li_2CO_3 is more significant on MgO than on CaO.

At 700°C the use of fresh MgO and $Ca(OH)_2$ resulted in methane conversion in excess of 20%, but on the doped analogue a conversion of less than 10% was observed. However, at higher reaction temperature the conversion over the doped catalysts increased and so did the C_2 hydrocarbon yield.

4.7.3.2 The effect P_{O_2}/P_{CH_4} ratio on the activity of the Li_2CO_3/CaO at 800°C

Increasing the partial pressure of oxygen for a fixed partial pressure of methane (P_{CH_4} 210 torr) resulted in the increase of methane conversion. (Figure

4.7.3.2.a) Methane conversion seemed to be linearly related to the oxygen partial pressure. However the selectivity to C_2 hydrocarbons decreased as the partial pressure of oxygen increased. The total C_2 yield initially increased with an increase in oxygen partial pressure, but at higher partial pressures no significant increase of C_2 yield occured. A P_{O_2}/P_{CH_4} ratio of 0.5 seemed to be the optimum reactant condition for the production of C_2 hydrocarbons.

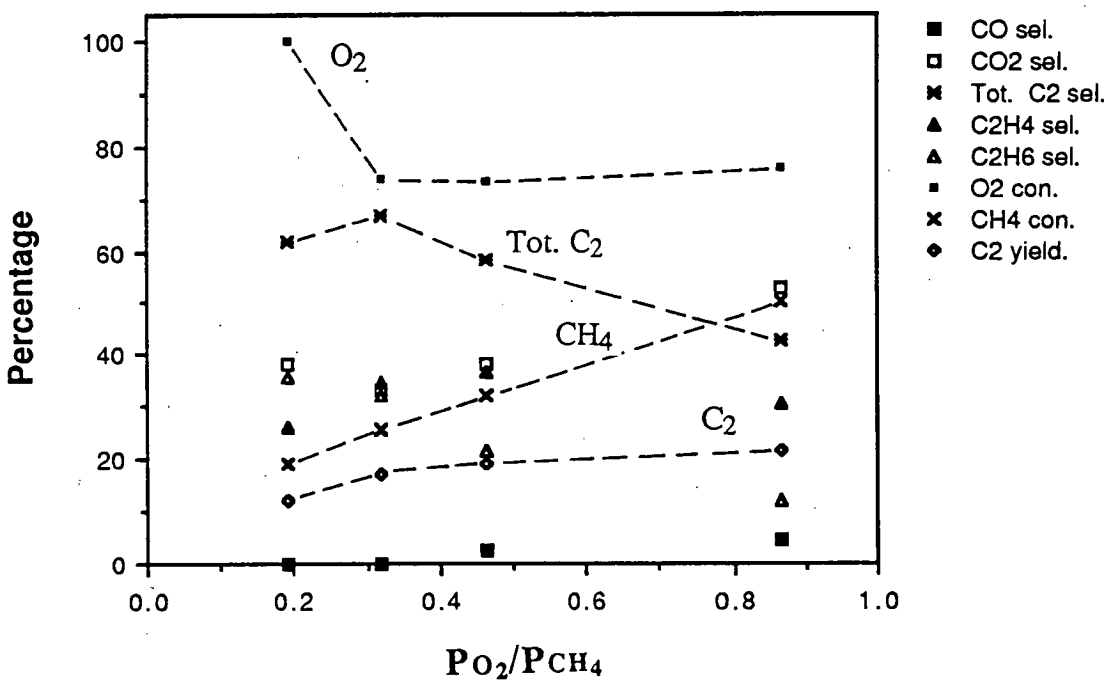

Figure 4.7.3.2.a The effect of P_{O_2}/P_{CH_4} ratio on the activity of Li_2CO_3/CaO at 800°C (with P_{CH_4} fixed at 210 torr)

4.7.3.3 Activity of Li_2CO_3/CaO catalyst at 800°C with time-on-stream (P_{O_2} 194, P_{CH_4} 224 torr)

The activity of Li_2CO_3/CaO changes considerably with time-on-stream (Figure 4.7.3.3.a). Methane conversion decreases, together with the selectivity to C_2 hydrocarbons at longer times-on-stream. The ratio of ethene to ethane in the product stream also decreases with time.

The changes in activity of Li_2CO_3/CaO occurs gradually with time on stream. Since the product distribution also changes, this indicates that the material undergoes physical and chemical changes. In order to highlight the effect of Li_2CO_3/ CaO nature on its catalytic activity, the chemical and physical nature of various Li_2CO_3/CaO catalysts have been determined.

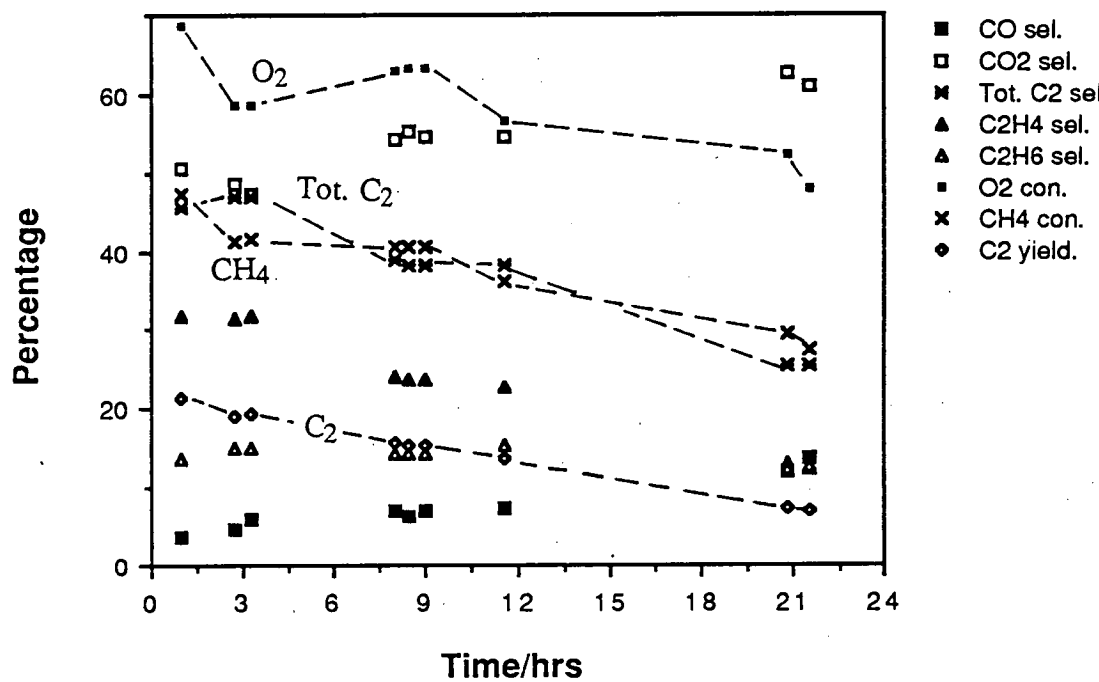

Figure 4.7.3.3.a The activity of Li_2CO_3/CaO catalyst at 800°C with time-on-stream (P_{O_2} 194, P_{CH_4} 224 torr)

4.7.3.4 Physical and chemical nature of various Li_2CO_3/CaO catalysts

The result of micro-probe analysis and AAS for various forms of Li_2CO_3/CaO is given in table 4.7.3.4.a. These results indicate that precalcination causes a significant loss of lithium from the Li_2CO_3/CaO sample.

Further removal of lithium occurs during the long time-on-stream. This indicates that CaO, is not a suitable support for stabilising Li_2CO_3. The wt % of CaO as

determined by micro-probes analysis, indicates indirectly the amount of carbonate present in the catalyst surface. After calcination, only 50% of the surface is composed of CaO indicating a significant presence of carbonate. Even after reaction, some carbonate is likely to still be present possibly in the form of calcium carbonate.

Table 4.7.3.4.a The composition of various Li_2CO_3/CaO catalysts.

Sample	Wt % CaO microprobe	%Li/Ca (AAS)
Fresh Li_2CO_3/CaO	n.d	3.9
Calcined Li_2CO_3/CaO	52	2.6
Used Li_2CO_3/CaO	80	0.1

n.d not determined

The nature of the catalyst particles before and after a catalytic run have been studied by S.E.M. The SEM micrographs of these catalysts are given in figure 4.7.3.4.a. The particle cluster of the unused Li_2CO_3/CaO catalyst (micrographs i & ii) is much smaller and less well defined than Li_2CO_3/MgO (micrograph i & ii of figure 4.3.4.b). This indicates that Li_2CO_3/CaO is not as good a solid matrix as in Li_2CO_3/MgO. The used catalyst also seem to result in a larger cluster and flaky-like structure (micrograph iii & iv) probably due to the formation of high surface area $Ca(OH)_2$ and $CaCO_3$.

The loss of lithium from Li_2CO_3/CaO must have altered the product's distribution on Li_2CO_3/CaO. Loss of lithium might have caused the decrease in C_2 selectivity while the sintering of this catalyst during the time-on-stream must have caused the general decrease in methane converison.

i)

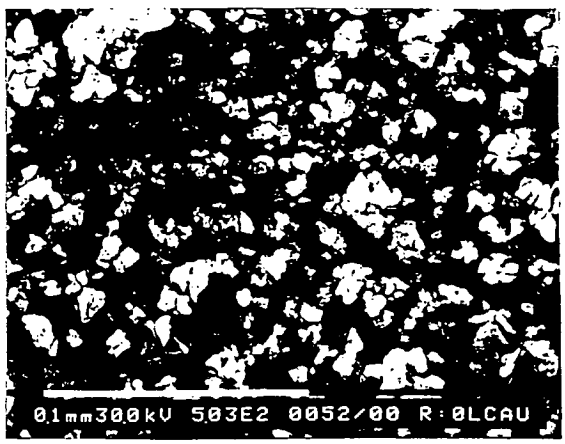

ii)

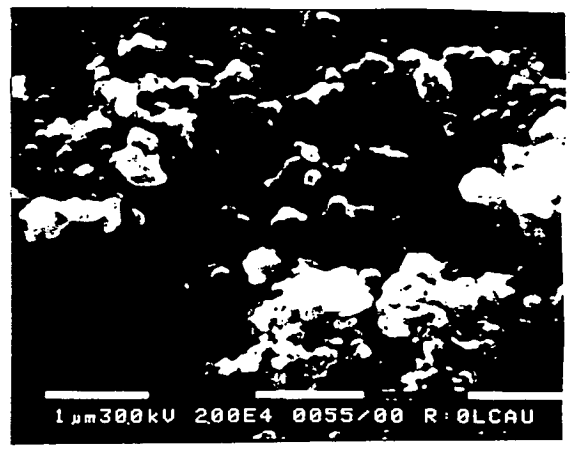

iii)

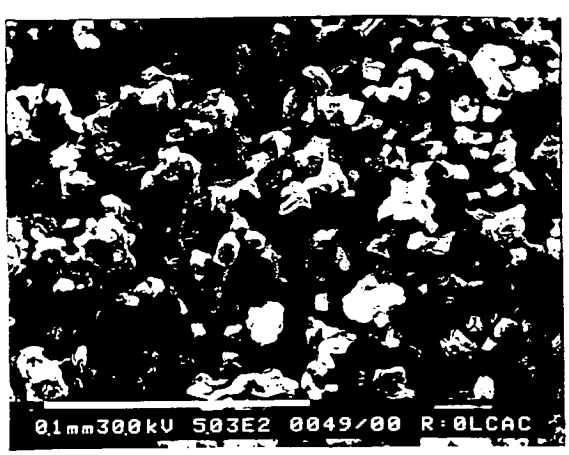

iv)

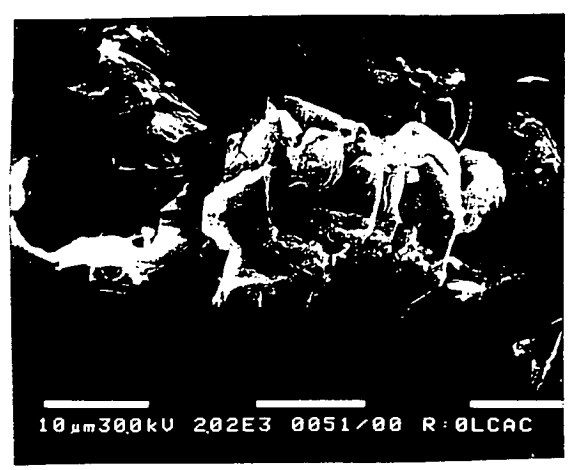

Figure 4.7.3.4.a SEM micrographs of Li_2CO_3/CaO catalysts.

Micrographs i) and ii) are that of the unused Li_2CO_3/CaO catalyst at magnifications of $5.0x10^2$ and $2.0x10^4$ respectively, while micrographs iii) and iv) correspond to the used catalyst under the same respective magnifications.

4.8 SUMMARY OF FINDINGS

1. The major difference between homogeneous and catalytic oxidative reactions of methane is in the selectivity to the carbon oxide products. The homogeneous reaction favoured the production of CO while most catalytic reactions favoured the formation of CO_2. However the correlation between the selectivity to various C_2 products with methane conversion existed in both the homogeneous and the catalytic reaction (section 4.1).

2. The presence of Li_2CO_3 on MgO increased C_2 selectivity but resulted in a reduction of methane conversion. The precalcination of Li_2CO_3/MgO catalyst, with Li loading less than one percent, at 900°C for 10 hours resulted in significantly lower methane conversion compared to that of the higher lithium loading catalyst. Generally, the uncalcined catalysts resulted in higher methane conversion than the calcined catalysts (section4.3).

3. MgO itself was demonstrated to have high activity for oxidative reactions of methane, and a C_2 yield of up to 17% can be achieved at 800°C. However, it was also shown in this study that the activity of MgO is highly sensitive to the pretreatment exposed to it (section 4.4).

4. Under the conditions of this experiment, the Li_2CO_3/MgO catalyst loses its activity significantly with time-on-stream. The deactivation of the uncalcined catalyst is more rapid than the calcined catalysts (section 4.3.4).

5. When the Li_2CO_3/MgO catalyst was studied at 800°C with P_{O_2}/P_{CH_4} ratio of about 0.5, the methane conversion decreased while the selectivity to C_2 increased with time-on-stream. However when the P_{O_2}/P_{CH_4} was about 1, methane conversion remained about 30% but the selectivity to C_2 still decreased with time on-stream. This result highlighted the role of sintering and the loss of Li_2CO_3 on the activity of Li_2CO_3/MgO catalyst, and possibly on other alkali doped catalysts. When the P_{O_2}/P_{CH_4} ratio was about 0.5, the effect of sintering is more prominent. However when the ratio was about 1, the effect of Li_2CO_3 loss, favouring the exhaustive oxidation of methane, was magnified (section 4.3.5).

6. Generally chemically basic metal oxides resulted in a higher C_2 yield (section 4.5).

7. The Sm_2O_3 is very active for the oxidative reaction of methane but favours the exhaustive oxidation to carbon oxide. The reaction over Sm_2O_3 was observed to be very sensitive the P_{O_2}/P_{CH_4} ratio in the reactant stream. The potential of Sm_2O_3 lies in its ability to cause high methane conversion, even at 660°C (section 4.5.3.1).

8. The alkali and alkali earth metal carbonates show significant activity for the oxidative reaction of methane. Their activity seems to increase with respect to their relative instability under the reaction condition. Moreover the carbonates which undergo decomposition rather than melting at temperatures similar to catalyst screening conditions resulted in higher conversion (section 4.5.4.2).

9. Li_2CO_3 and LiOH on MgO resulted in nearly identical catalytic performances. The presence of LiF and Li_2SO_4 on MgO resulted in the loss of methane conversion. The presence of LiCl on MgO promoted the production of C_2H_4. However, it was shown in this study that the LiCl/MgO catalyst lose its 'favoured' performances rapidly with time-on-stream (section 4.6).

10. The amount of methane conversion over the supported Li_2CO_3 catalyst is always slightly lower than that over the support material itself. The presence of Li_2CO_3 over the support materials seems to moderate the activity of the support and to result in an increase of selectivity to C_2. Generally, the methane conversion over these catalysts is derived from that of the support materials. This result suggests that the Li^+O^- type sites are not a necessary condition to achieve high methane conversion (section 4.7).

CHAPTER 5

CHEMICAL AND PHYSICAL PROPERTIES OF OXIDATIVE COUPLING CATALYSTS; RESULTS AND DISCUSSION

5.1 Introduction

It has been observed that most of the lithium doped catalysts used in chapter 4, undergo significant physical and chemical changes as a result of the precalcination and exposure to the conditions of the oxidative reaction of methane. The changes occurring on these catalysts illustrates their relative instability under the high temperature conditions of pretreatment and the catalyst screening. In this chapter, the effect of the high temperature process on the physical and chemical stability of the lithium doped catalysts and other catalysts were investigated further.

5.2 Li_2CO_3/MgO Catalysts

5.2.1 Effect of calcination on the physical nature of Li_2CO_3/MgO

The precalcination of the Li_2CO_3/MgO catalyst precursor at 900°C for 10 hours resulted in extensive sintering causing the sample to become harder and to change colour from white to pinkish. The hardness and colour change increase with lithium loading (from 0 wt.% to 14wt.%).

The calcined samples with different lithium loadings have been studied by SEM and the micrographs at high magnifications are given in Figure 5.2.1.a. Generally it was observed that the amount of lithium loading influenced the nature and cluster size of particles formed on the surface of the calcined samples. The presence of Li_2CO_3 initially increases the cluster size of the particles formed on the calcined samples. When the loading of lithium was 0.5wt.%, the distinct clusters formed on the sample surface have an average size of around 0.3 μ-metre (micrograph ii of figure 5.2.1.a). Increasing in lithium loading initially resulted in the increase of the mean cluster size. At a loading of 1.3wt.% the mean cluster size was about 2 μ-metre

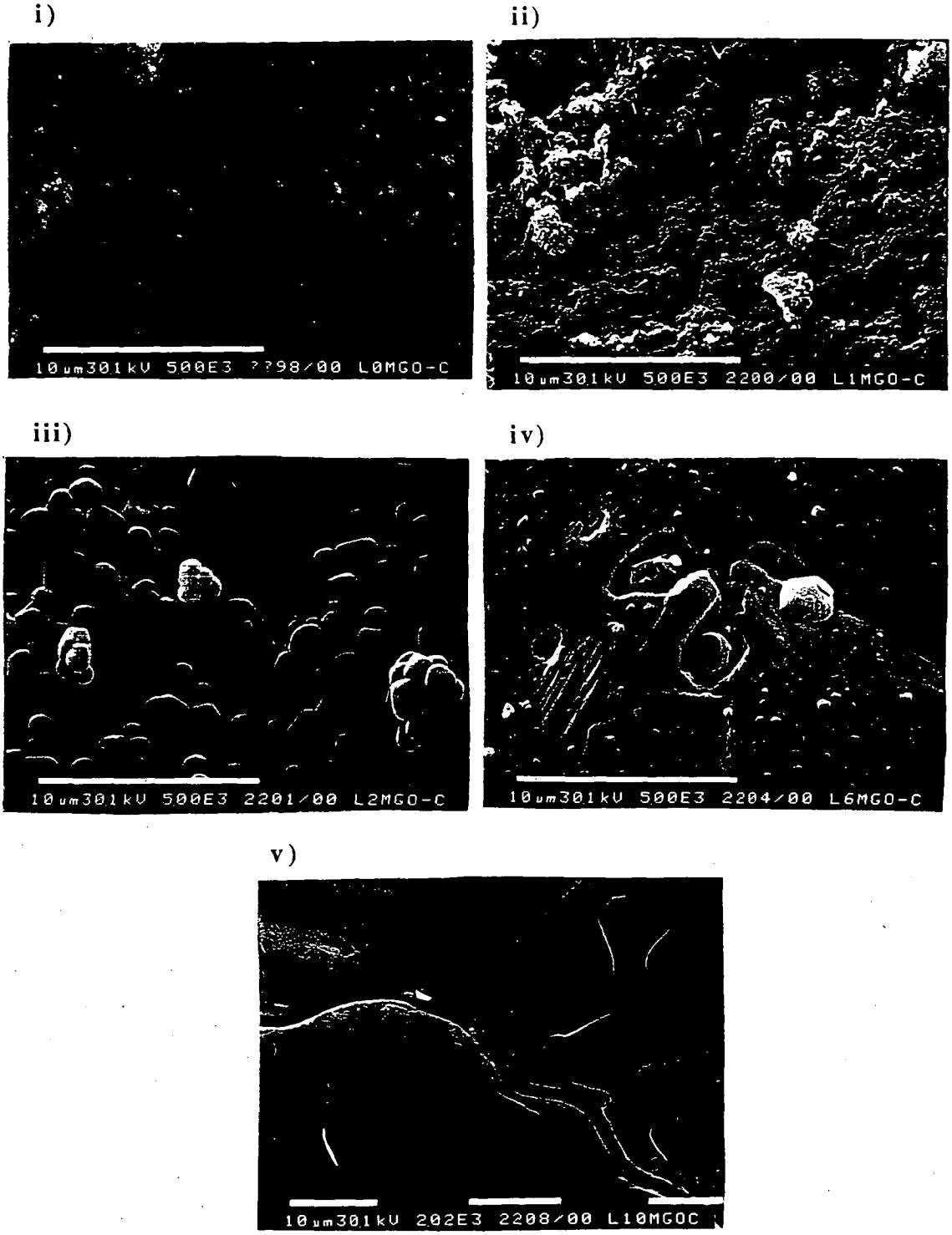

Figure 5.2.1.a SEM micrographs of i) MgO, ii) 0.5wt.%Li_2CO_3/MgO, iii) 1.3 wt.%Li_2CO_3/MgO, iv) 7.8wt.%Li_2CO_3/MgO, and v) 12.8%Li_2CO_3/MgO samples after precalcination at 900°C in air for 10 hours. Micrographs i), ii), iii) and iv) were taken at magnification of $5x10^3$ while micrograph v) at magnification of $2x10^3$.

(micrograph iii). The distinctly shaped clusters disappeared at higher loading (micrographs iv and v). Under this condition the samples seem to be coated by a layer of material.

In order to probe further the effects of precalcination on the nature of Li_2CO_3/MgO, a sample of 7.8wt.% Li_2CO_3/MgO containing a section of its surface which was pierced, prior to carbon coating was studied by SEM. The SEM micrographs of this sample are presented in figure 5.2.1.b. From micrograph i of figure 5.2.1.b it is apparent that the formation of the surface layer does occur not only on the upper most layer of the surface but also on the other exterior surfaces of the calcined samples. Moreover the physico-chemical nature of the layer of the calcined 7.8%Li_2CO_3/MgO seem to be different from the bulk (micrograph ii). The layer consists of particle's clusters which are not well defined, presumably amorphous, while the particle's in the bulks are well defined and have a mean diameter of around 2 μ-metre.This difference is highlighted in micrograph iii. The differences in the physical nature and possibly the chemical nature between the surface layers and the bulk of the calcined 7.8%Li_2CO_3/MgO is probably related to the surface and bulk composition.

The SEM micrographs of the calcined Li_2CO_3/MgO samples (figure 5.2.1.a and figure 5.2.1.b) indicate that migration of a certain component of the sample to the surface occurs during the precalcination process. This can be the cause of the surface layer formation. Since Li_2CO_3 and MgO are the two components of the sample and Li_2CO_3 has the lowest melting point, it is likely that migration of Li_2CO_3 to the surface gives rise to the layer formation. Moreover it was observed that the extent of the surface layer formation increased with lithium loading.

In the preparative procedure (refer section 3.2), the calcined samples were always crushed and sieved for particle size less than 43 μ-metre, prior to being screened for catalytic activity. The sieved Li_2CO_3/MgO catalyst with different lithium loadings have also been studied by SEM and their micrographs are given in figure 5.2.1.c. MgO (micrograph i), which is prepared in the same manner as other materials, have clusters which are regular and cubic in shapes. The average cluster

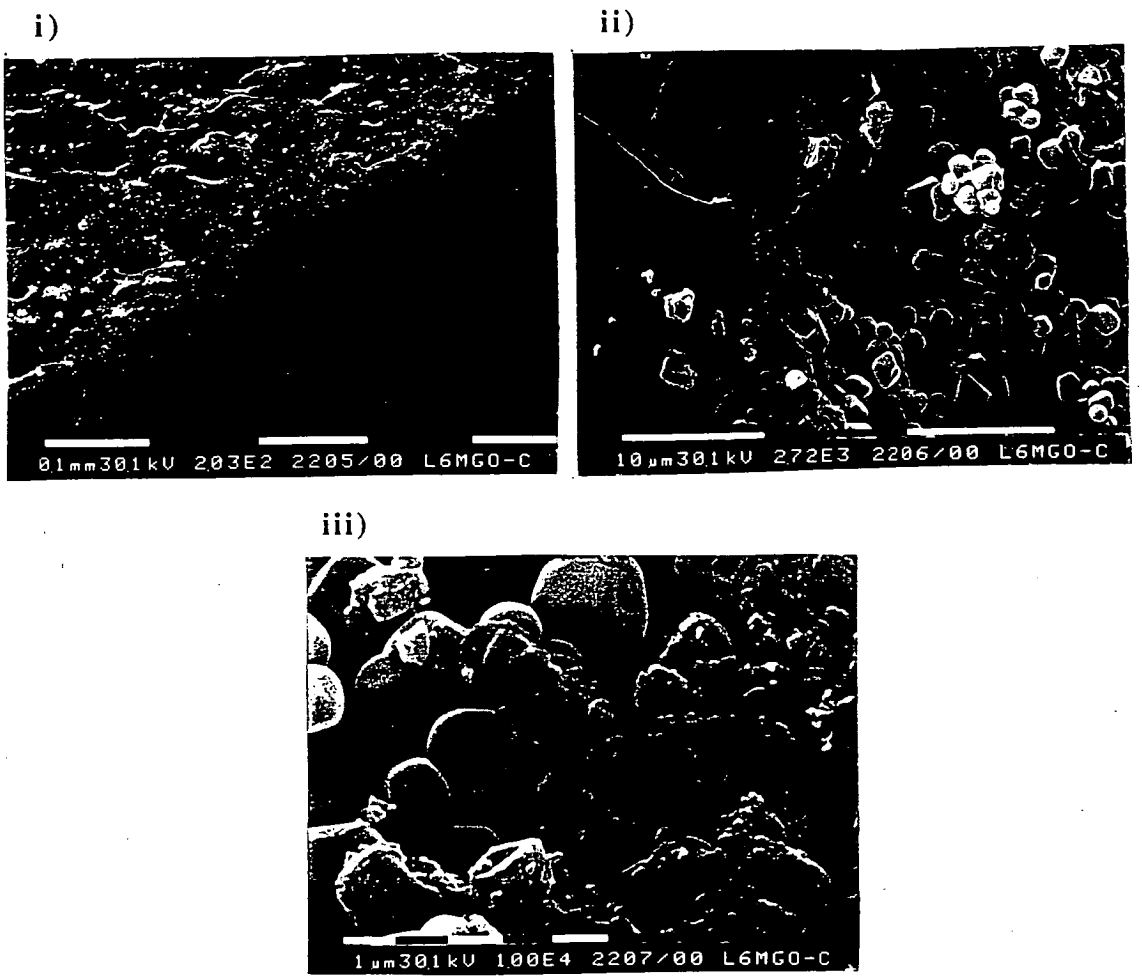

Figure 5.2.1.b SEM micrographs of 7.8wt.%Li_2CO_3/MgO after precalcination at 900°C in air for 10 hours. The magnifications for micrograph i), ii) and iii) are $2.0x10^2$, $2.7x10^3$ and $1.0x10^4$ respectively.

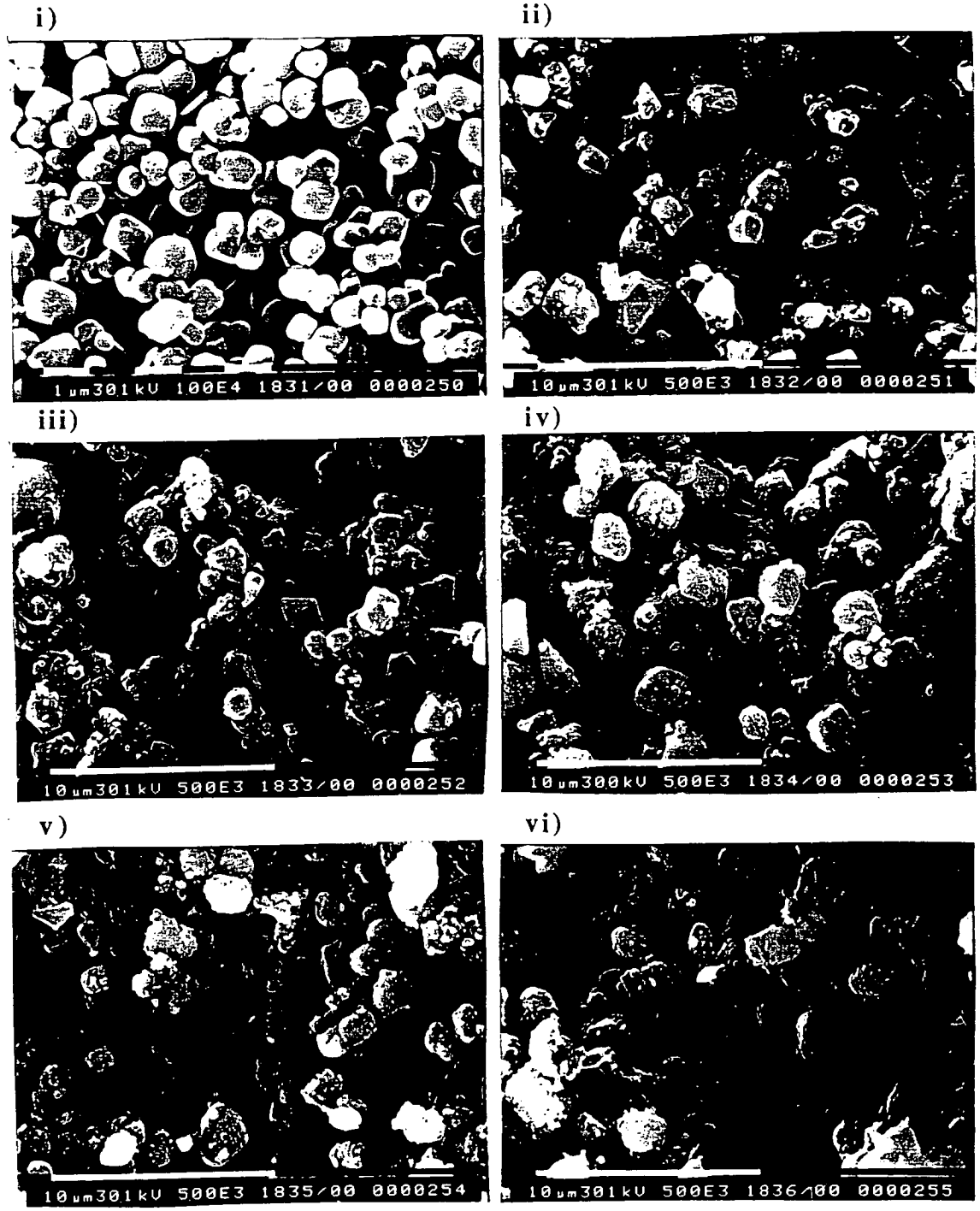

Figure 5.2.1.c SEM micrographs of calcined, grinded and sieved Li_2CO_3/MgO with i) 0.0 wt.%, ii)1.3wt.%; iii)4.4wt.%, iv) 7.8wt.%, 10.6 wt.%, and 12.8 wt.% lithium loading. Micrograph i) is at a magnification of $1.0x10^4$ while ii), iii), iv), v) and vi) are at magnification of $5.0x10^3$.

size was about 1 μ-metre. On the other hand the clusters of the crushed Li_2CO_3/MgO are not very regular in shape and have sharp edges. Two types of cluster size seem to be present on the crushed Li_2CO_3/MgO catalysts, the larger clusters with about 3 μ-metres in diameter and the smaller clusters with around 0.3 μ-metre. In line with the observation made in micrograph ii and iii of Figure 5.2.1.b, the extent of the finely divided particle's clusters seems to increase with higher lithium loading. This suggest that the smaller clusters are derived from the surface layer and hence are probably Li_2CO_3 rich. The larger particle would compose mainly of MgO with some lithium being substituted in the lattice. The fact that sharp edges were formed on the crushed particles of the calcined samples suggest that Li_2CO_3 acted as cement forming good solid matrix with MgO, making it hard and hence difficult to be crushed.

Table 5.2.1.a The wt% of MgO on various 7.8%Li_2CO_3/MgO samples as studied by x-ray micro-probe analysis.

Sample	Wt % MgO	Av. Deviation*
Calcined, uncrushed	16.0	0.2
Calcined and crushed	81.0	1.2

* from three analysis

In order to probe further the nature of the calcined and crushed Li_2CO_3/MgO samples, the two forms of 7.8wt% Li_2CO_3/MgO catalyst (calcined and powdered catalysts) have been studied by micro-probe analysis. The composition of the calcined sample should indicate the nature of the layer formed after precalcination while the composition of the crushed calcined sample should represent that of the bulk. Since both lithium and carbon cannot be analysed with this technique, the weight % of MgO on the sample (as detected by the micro-probe analysis) should indirectly indicate the amount of the Li_2CO_3 phase on the surface of the sample (ie. amount of Li_2CO_3 could be proportional to 100 - % MgO).

MgO made up of only 16 % of the surface of the uncrushed calcined sample while for the crushed 81% MgO was detected (table 5.2.1.a). The result indicates that the major components of the layer formed on calcined Li_2CO_3/MgO are Li_2CO_3 and possibly some magnesium carbonates. The enrichment of the surface with Li_2CO_3 can only occur through its migration during the high temperature calcination. This result highlighted the difference in the composition of the surface layer of the calcined Li_2CO_3/MgO sample to that of its bulk.

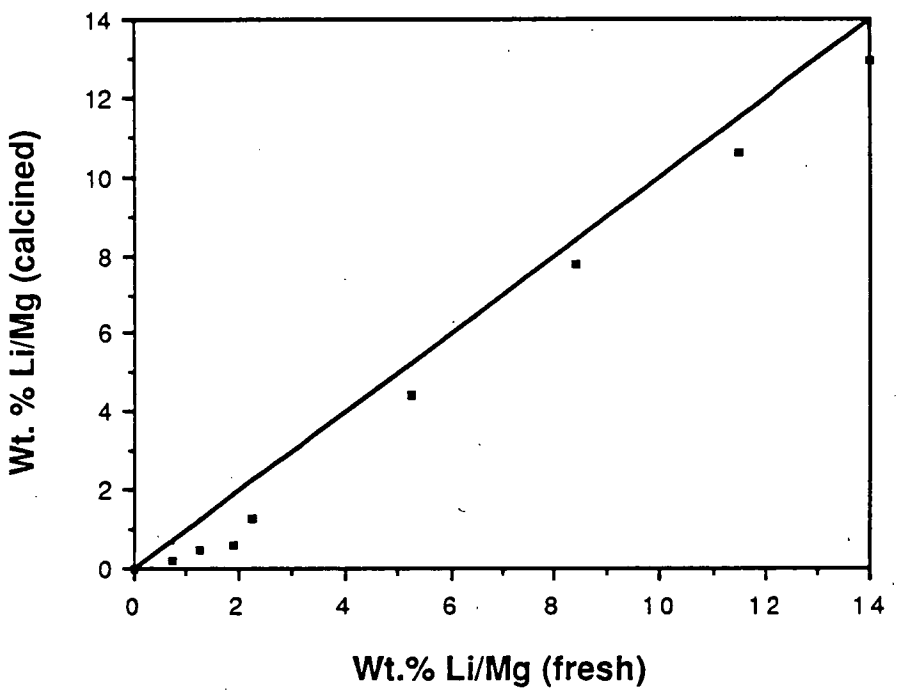

Figure 5.2.2.a The wt% Li/Mg in Li_2CO_3/MgO samples which were precalcined at 900°C for 10 hours, against that of the corresponding fresh samples

5.2.2 Effect of precalcination on the bulk composition of Li_2CO_3/MgO systems

The bulk composition of fresh and calcined Li_2CO_3/MgO systems have been determined by Atomic Absorption Spectroscopy (AAS) and the results are presented in Figure 5.2.2.a. For catalysts with low lithium loading, significant losses of lithium as a result of precalcination occurs. In the case of freshly prepared 1.9wt.%Li_2CO_3/MgO

catalysts, the precalcination process resulted in the loss of 68% of lithium. When the initial loading was higher than 2 wt % the percentage of lithium loss as a result of precalcination decreased. At 8.4wt.% of initial lithium loading, only 8% of lithium was lost as a result of the precalcination. The retention of lithium on MgO. at the higher lithium loading parallel the extent of layer formation on the calcined samples. This suggest that the layer formation could promote the stabilisation of the Li_2CO_3 phase on MgO.

The exact nature of the carbonate phase on Li_2CO_3/MgO catalysts have been determined by transmission FTIR and the results are presented in Figure 5.2.2.b. The transmission FTIR spectra of self-supporting 7.8wt.% Li_2CO_3/MgO catalysts at room temperature (spectrum iii) were compared with those of Li_2CO_3 (spectrum ii) and $MgCO_3$ (spectrum i). The absorbance bands near 2900, 2500, 1800 and 1500 cm^{-1} are characteristic of the carbonate phase. The peak position of the 1800 cm^{-1} band for the Li_2CO_3/MgO catalyst is similar to that of Li_2CO_3. This indicates that most of the carbonate phase in the calcined Li_2CO_3/MgO catalyst is actually in the form of Li_2CO_3.

The spectra of Li_2CO_3/MgO catalysts at different temperatures are also presented in figure 5.2.2.b (spectra iii to vii). As the temperature was increased, the absorption bands associated to the carbonates broaden and shift to lower wave number, while their intensities decreases. These changes are associated with the increase in the thermal excitation of the carbonate phase. Since Li_2CO_3 was known to melt at 618°C (Aylward and Findlay, 1971), this transformation could well illustrate the melting process of Li_2CO_3 component of the catalytic materials. Moreover at 800°C, not only does the carbonate phase of Li_2CO_3/MgO melt but it also undergoes decomposition when heated in air at the temperature as evidenced by the increasing amount of gaseous CO_2 (spectrum vii).

5.2.3 The nature of calcined 7.8%Li_2CO_3/MgO catalyst at high temperature.

Figures 5.2.3.a, b and c show the transmission FTIR spectra of calcined Li_2CO_3/MgO catalysts of different lithium loading in air at RT, at 750°C after 1 hour

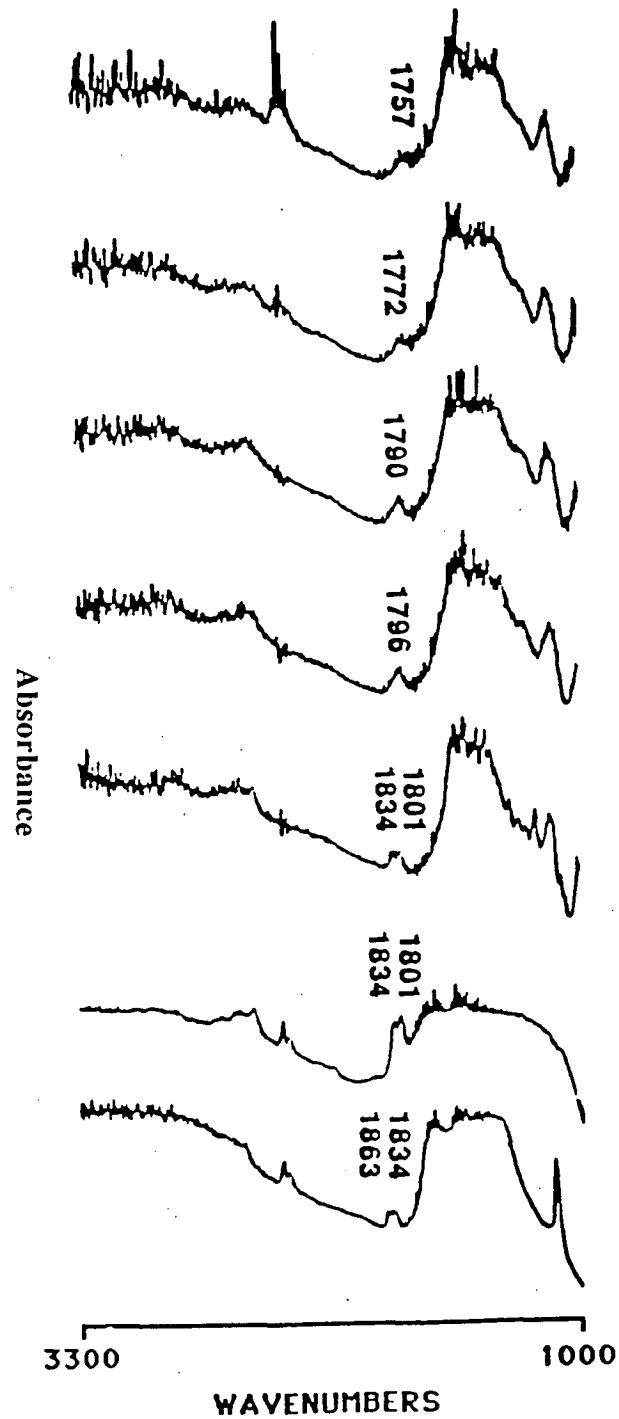

Figure 5.2.2.b Transmission FTIR spectra of i) $MgCO_3$, ii)Li_2CO_3, iii)7.8wt.% Li_2CO_3/MgO catalyst at RT and that of the catalysts at iv)500°C, v)600°C, vi)700°C and vii)800°C. These spectrum were accumulated with 100-500 scans and at a resolution of $4cm^{-1}$.

of equilibration time, and at RT after the 750°C temperature exposure, respectively. The major regions of interest in these spectra are in the 1200-1800cm^{-1} and the 3500 - 3800 cm^{-1} regions corresponding to the carbonates and the hydroxyl species respectively. However, the presence of adsorbed H_2O will also gave rise to absorption band in these regions.

The spectra of the calcined 0.5% Li_2CO_3/MgO (spectra ii) catalyst differ significantly from that of pure MgO (spectrum i) while. the spectra of the higher loading Li_2CO_3/MgO materials show the predominance of Li_2CO_3 phase. At RT (figure 5.2.3.a), the spectra of pure MgO showed the presence of adsorbed H_2O but not on the spectra of the lithium doped samples. It was also observed that sharp absorption peaks in the region of 3500-3800 cm-1 were present in the spectra of Li_2CO_3/MgO material. These absorption peak can be assigned to the LiOH species (Smyrl et al.,1983) and to the cation vacancy defects on the calcined sample which are normally present on alkali earth oxides (Freund et al.,1983).

The spectra of MgO at 750°C (Figure 5.2.3.b) suggested that most of the adsorbed H_2O on MgO surfaces was removed. In the case of the 0.5%Li_2CO_3/MgO catalyst (spectra ii), the spectral feature shows the absence of adsorbed H_2O and carbonate species. The spectra of higher lithium loading catalyst at 750°C (spectra iii-v) however show the prominence of the Li_2CO_3 phase. The absence of absorption bands in the spectra of low loading Li_2CO_3/MgO materials corresponding to the Li_2CO_3 phase is consistent with its instability. All of Li_2CO_3 added during the preparation of these catalysts was lost in the precalcination stage and during treatment at 750°C in the I.R cell. On the catalysts with higher lithium loading the Li_2CO_3 phase was still present. The formation of the Li_2CO_3 rich surface layer as observed in figure 5.2.1.a could probably be the major factor which facilitates the stabilisation of Li_2CO_3 phase.

The transmission FTIR spectra of Li_2CO_3/MgO catalysts, cooled to RT from 750°C, (spectra ii-v of figure 5.2.3.c) show an increase in the intensity of absorption bands associated with the Li_2CO_3 phase. This indicates that aggregation of the Li_2CO_3

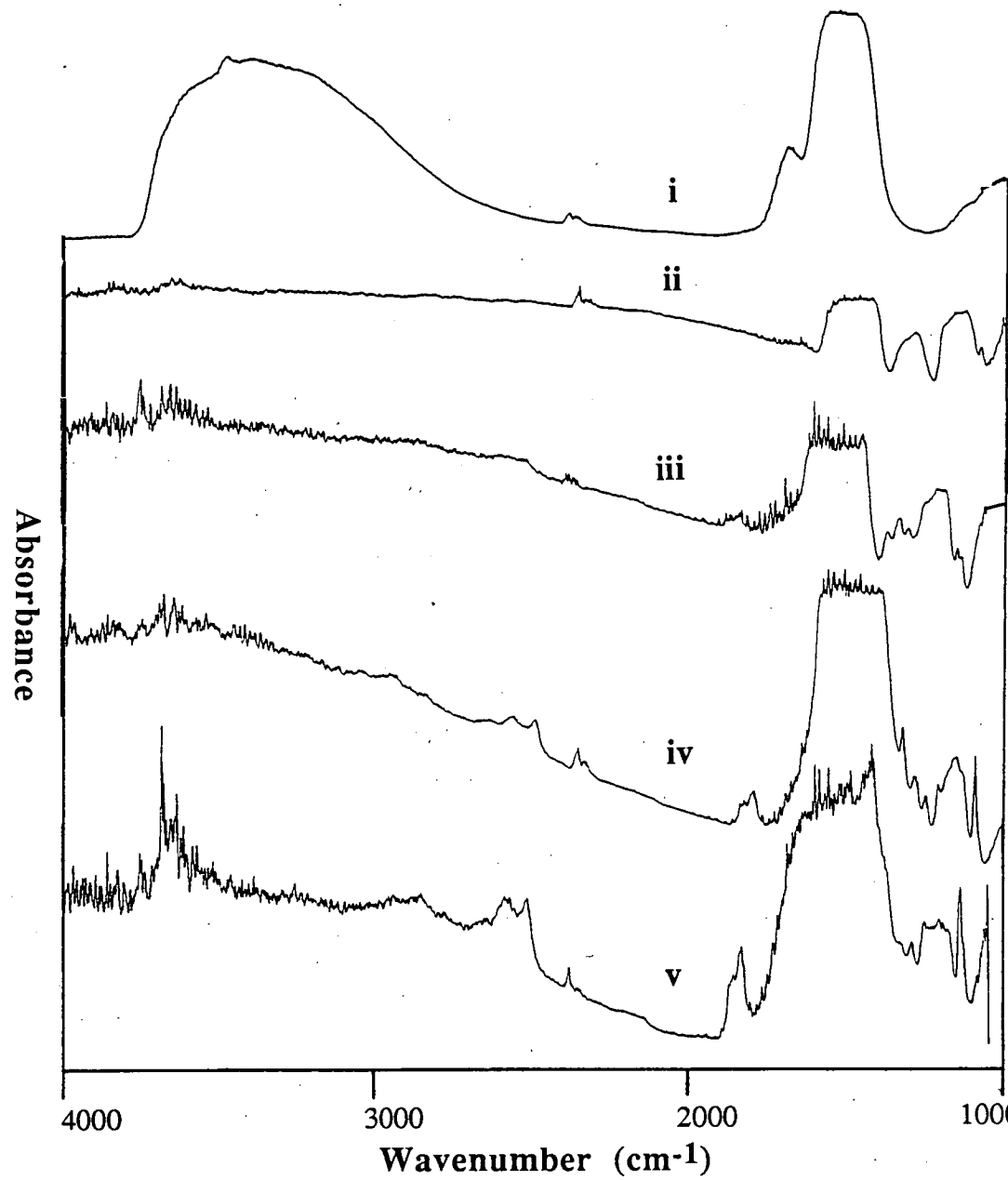

Figure 5.2.3.a Transmission FTIR spectra of calcined Li_2CO_3/MgO catalysts of different lithium loading after evacuation at RT for 2 hours. Spectra i), ii), iii), iv) and v) correspond to that of the catalyst with lithium loading of 0.0, 0.5,4.4, 7.8 and 10.6wt.% respectively. These spectra were accumulated with 100-500 scans and with a resolution of $4cm^{-1}$.

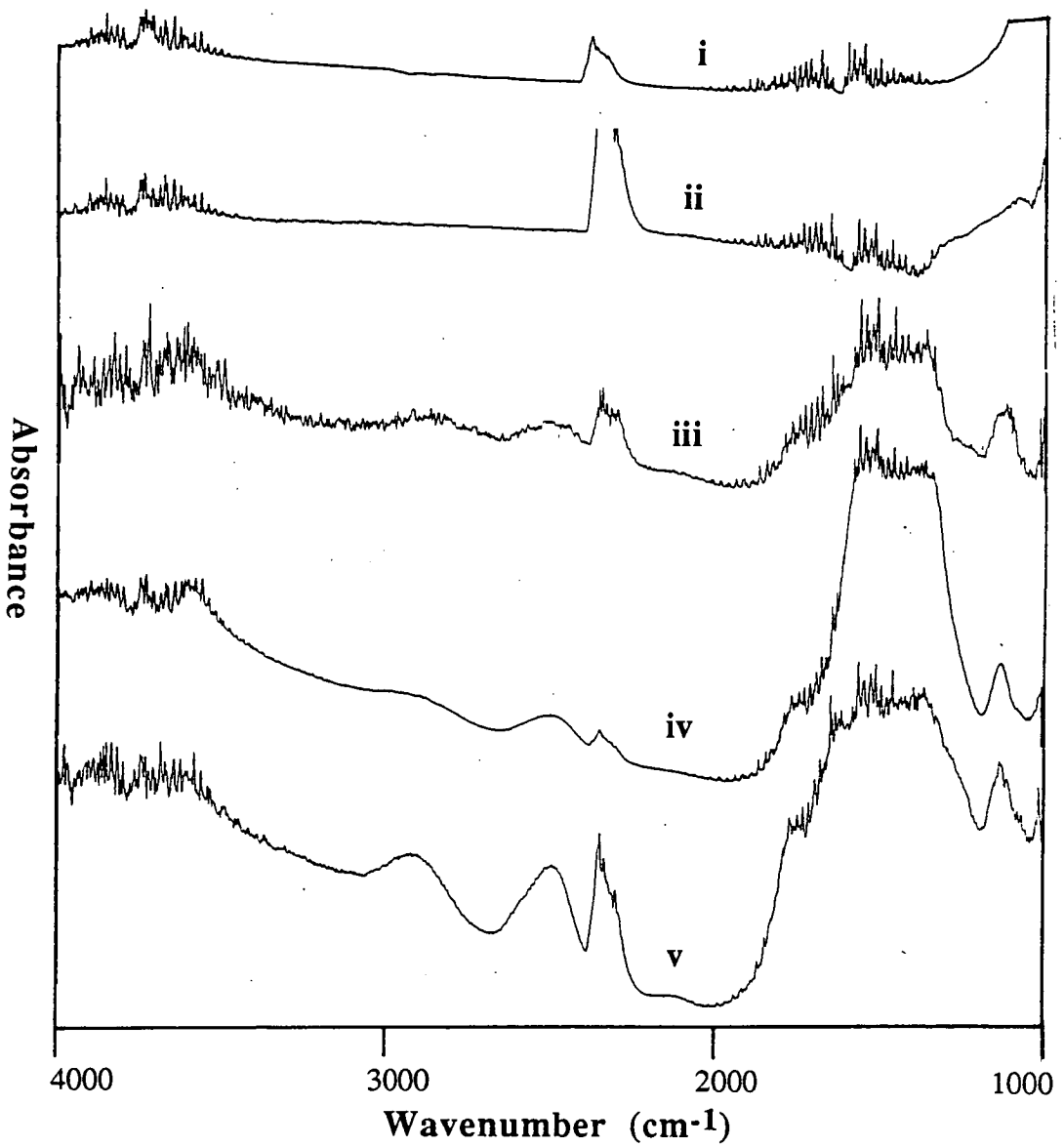

Figure 5.2.3.b Transmission FTIR spectra of calcined Li_2CO_3/MgO catalysts of different lithium loading at 750°C after one hour of equilibration time. Spectra i), ii), iii), iv) and v) correspond to that of the catalyst with lithium loading of 0.0, 0.5,4.4, 7.8 and 10.6wt.% respectively. These spectra were accumulated with 100-500 scans and with a resolution of $4cm^{-1}$.

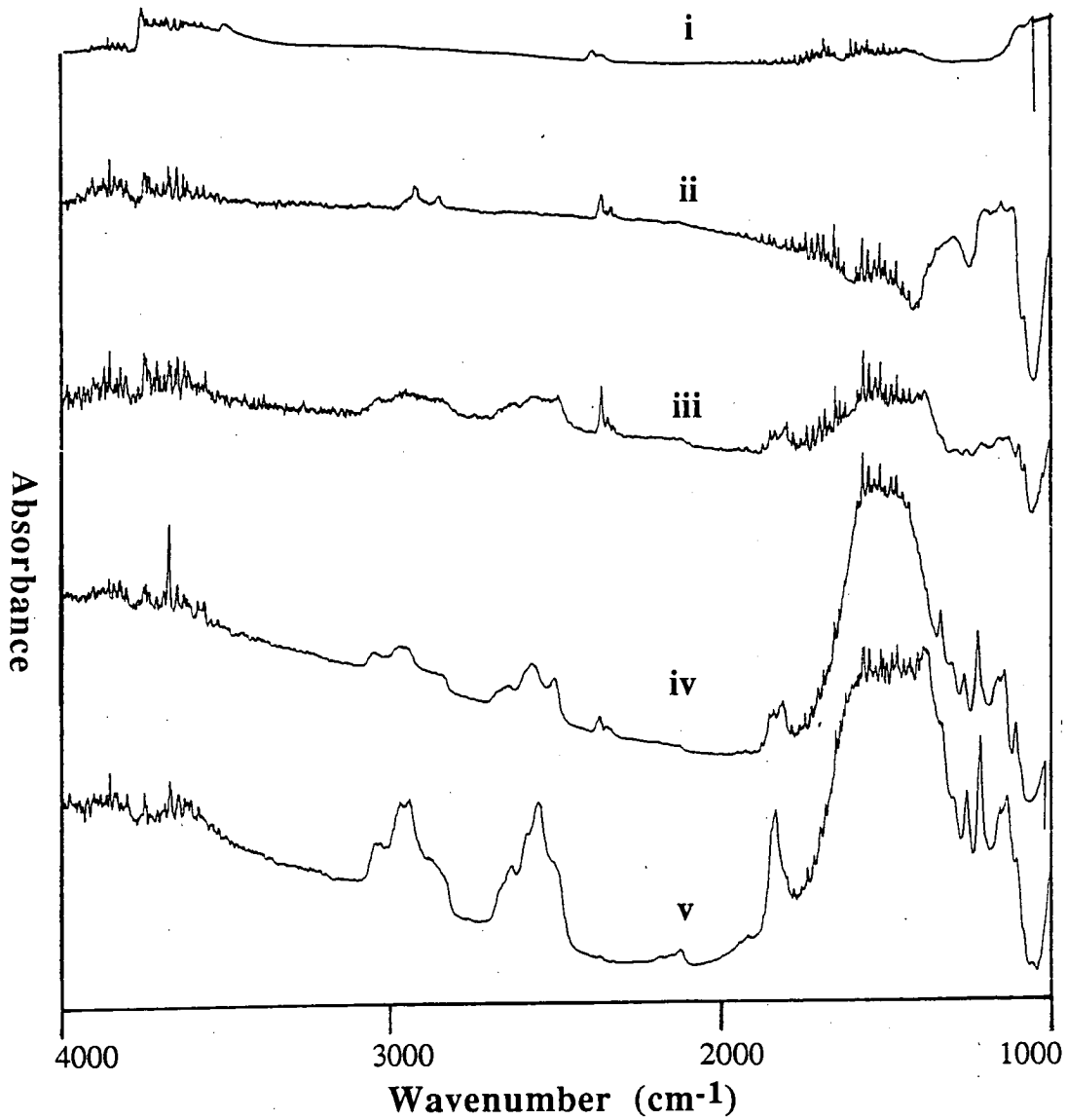

Figure 5.2.3.c Transmission FTIR spectra of calcined Li_2CO_3/MgO catalysts of different lithium loading at RT after the 750°C exposure. Spectra i), ii), iii), iv) and v) correspond to that of the catalyst with lithium loading of 0.0, 0.5,4.4, 7.8 and 10.6wt.% respectively. These spectra were accumulated with 100-500 scans and with a resolution of $4cm^{-1}$.

phase in the catalysts occurs as a result of it being treated at high temperature (ie. at 750°C for 1hour). This is in line with the proposal that enrichment of Li_2CO_3 on the surface of the Li_2CO_3/MgO catalytic samples occurs under high temperature conditions.

Table 5.2.3.a The ratio of various elemental peaks from figure 5.2.3.d. and figure 5.2.3.e

Conditions	Figure 5.2.3.d: O_{1s}/Mg_{2s}	O_{1s}/Mg_{2s}	Figure 5.2.3.e Li_{1s}/Mg_{2s}	Li_{1s}/O_{1s}	$Li_{1s}/C_{1s}(CO_3^{-2})$
i	0.64	1.11	0.38	0.34	0.36
ii	0.56	0.75	0.17	0.23	0.50
iii	0.52	1.53	0.77	0.50	0.69
iv	0.49	1.03	0.59	0.58	1.55
v	1.57			0.82	
vi	1.88			0.55	

In order to further verify the observation made above, the effect of high temperature on freshly prepared catalysts have been investigated by the X-ray Photoelectron Spectroscopy (XPS) technique. The sample was exposed to different pretreatment conditions in the sample preparation chamber. The pretreatments used were: evacuation (10^{-5} torr) at 150°C for 48 hours (i), calcination in dry air for 2 hours at 600°C, 700°C, 800°C (ii-iv) and under evacuation (10^{-5}Torr) at 800°C for 2 and 4 hours (v,vi) respectively. Prior to recording the XPS spectra, the sample was cooled down to room temperature in the sample pretreatment chamber and transferred to the XPS chamber. The Mg_{2p}, Mg_{2s} and O_{1s} spectra of MgO sample were accumulated with 1 scan each, and are presented in figure 5.2.3.d. For the Li_2CO_3/MgO sample, Li_{1s}, Mg_{2p}, Mg_{2s}, C_{1s} and O_{1s} spectra were accumulated with 1 scan each and are presented in figure 5.2.3.e. TheLi_{1s}, Mg_{2p}, Mg_{2s}, C_{1s} (contamination), C_{1s} (CO_3^{-2}) and O_{1s} are assigned to peak number i to vi respectively.

The peak-width at half height of O_{1s} spectra of MgO and Li_2CO_3/MgO after the first pretreatment were about 4eV and this indicates the presence of at least two oxygen species on the catalysts surface. In the C_{1s} spectrum of Li_2CO_3/MgO catalysts two distinct peaks were observed. Analogous to the assignment made by Vinek et al.,1978 to the C_{1s} spectra of $MgCO_3$ and contamination carbon, the peak with higher electron binding energy (B.E), 291 eV, is assigned to the carbon of the carbonate phase while the lower B.E (285 eV) peak to the carbon impurities on the sample. After the pretreatment at 600°C on the Li_2CO_3/MgO catalyst, the O_{1s}/Mg_{2s}, Li_{1s}/Mg_{2s} and Li_{1s}/O_{1s} peaks ratio decreases (see table 5.2.3.a) indicating the loss of water from the sample and leaving more MgO component exposed on the surface. It was also observed that the C_{1s} due to the carbonates and the Li_{1s} signals decreases, indicating that the Li_2CO_3 migrating into the bulk of the sample.

Subjecting the MgO and the Li_2CO_3/MgO catalysts to pretreatment at higher temperatures resulted in the appearance of a shoulder in the O_{1s} spectra at higher binding energy (533 eV). This shoulder peak was assigned to the O^-/OH type oxygen species and to the oxygen of the carbonate, while the major peak is due to O^{2-} species (Vinek et al.,1978;Inque and Yasumori,1981). The $Li_{1s}/C_{1s}(CO_3^{2-})$ and Li_{1s}/O_{1s} ratios (see table 5.3.3.a) in the spectra of Li_2CO_3/MgO sample were observed to increased continuously when the sample was treated at high temperature suggesting the increase in carbonate phase decomposition. In the case of the O_{1s}/Mg_{2s} and Li_{1s}/Mg_{2s} ratios, initially they decreases when the sample was pretreated at 600°C and rises at 700°C but decreases again at 800°C. The increase in the ratios at 700°C indicate the migration of Li_2CO_3 back to the surface as a result of its increase vapour pressure while the decrease after pretreatment at 800°C is consistent with the volatilisation of lithium from the surface. When the sample was heated at 800°C under vacuum, the Mg_{2s} and Mg_{2p} peak were diminished. This observation proved that the migration of Li_2CO_3 occurs at the high temperatures and was facilitated by the evacuation. Not does the Li_2CO_3 phase melts, as evidence by the migration of Li_2CO_3, but it also undergoes

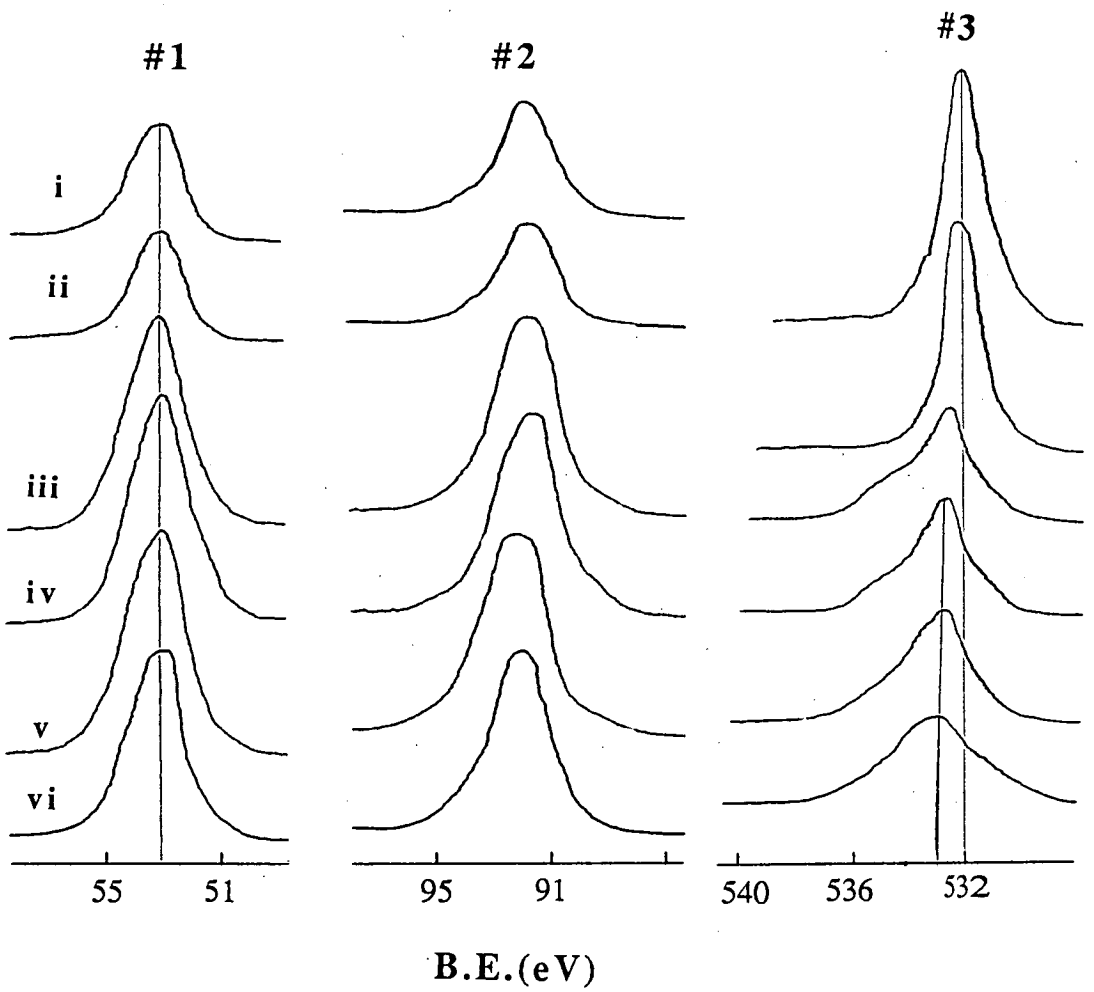

Figure 5.2.3.d XPS spectra of MgO after i) evacuation at 140°C for 48 hours, calcination in dry air for 2 hours at ii)600°C, iii)700°C, iv)800°C and being evacuated at 800°C for v)2 and vi)4 hours respectively. Peaks 1, 2 and 3 were assigned to Mg_{2p}, Mg_{2s} and O_{1s} spectra respectively.

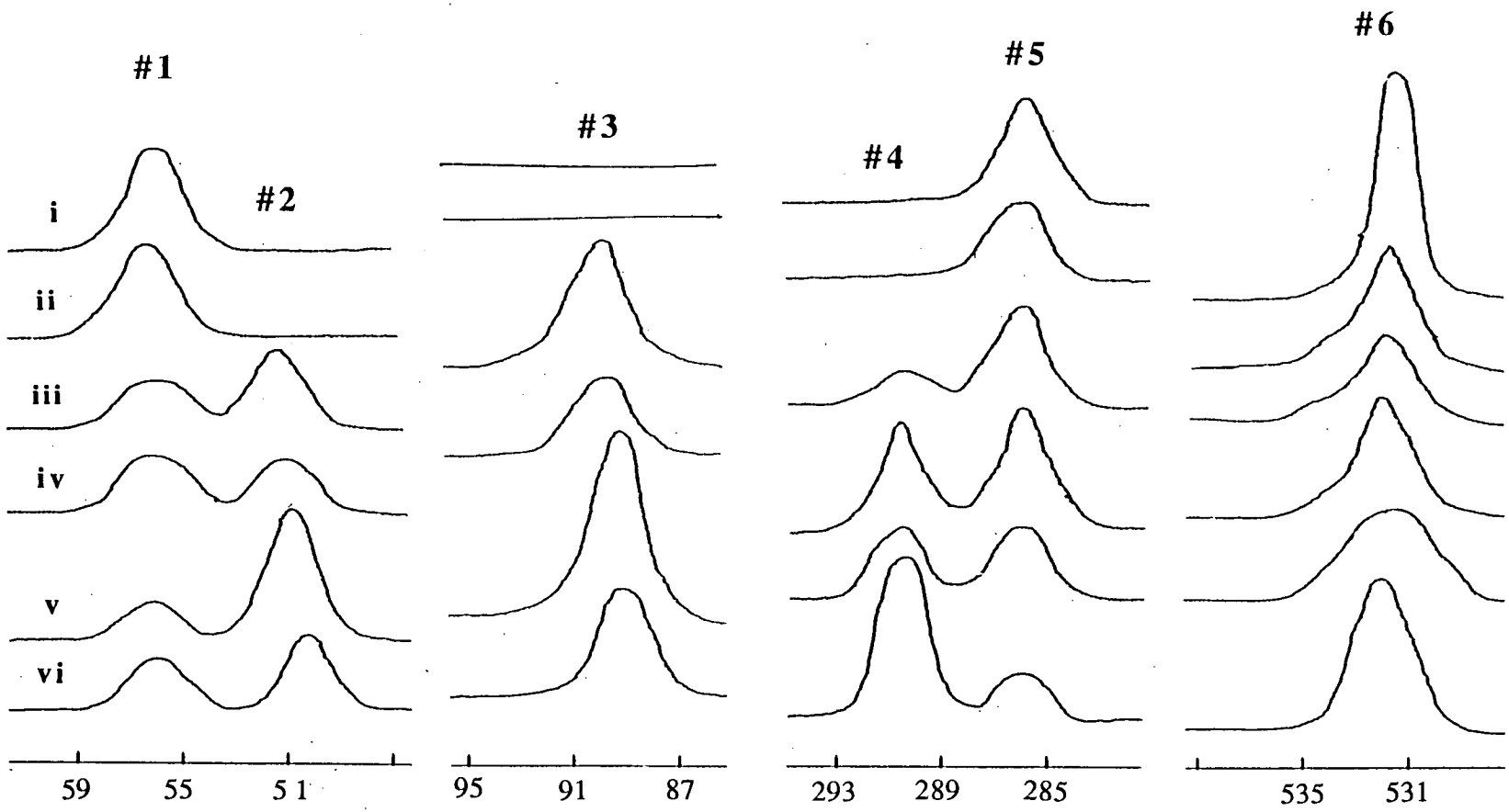

Figure 5.2.3.e XPS spectra of Li_2CO_3/MgO catalyst after i) thermal vacuum treatment at 140°C for 48 hours, calcination in dry air for 2 hours at ii)600°C, iii)700°C, iv)800°C, and thermal vacuum treatment at 800°C for v)2 hours and vi)4 hours respectively. Peaks 1, 2, 3, 4, 5, and 6 were assigned correspondingly to Li_{1s}, Mg_{2p}, Mg_{2s}, C_{1s}(contaminant), $C_{1s}(CO_3^{-2})$ and O_{1s}.

decomposition to form Li_2O, as evidence by the continual decrease of the $Li_{1s}/C_{1s}(CO_3^{-2})$ ratio.

When MgO was evacuated at 800°C for 2 and then 4 hours (spectra v and vi of figure 5.2.3.d), the O_{1s} spectra revealed only peak namely that of the O^{2-} species. The O_{1s}/Mg_{2s} peak area ratio increases from about 0.6 to 1.5 when MgO sample was heated under vacuum. The increase in the intensity of the O_{1s} signal would suggest that significant surface reconstruction on MgO also occurs as a result of the high temperature evacuation.

On Li_2CO_3/MgO catalyst, evacuation for 2 hours, did not remove the shoulder peak of the O_{1s} spectrum completely (figure 5.2.3.e, spectra v). However after the next four hours evacuation only the main O_{1s} peak was present. The Mg_{2p} peak of Li_2CO_3 disappears completely after the evacuation of the Li_2CO_3/MgO catalyst at 800°C for two hours. The evacuation at 800°C increases the Li_{1s} peak significantly. The carbon peak associated with the carbonate species disappears after evacuation. This indicates that the carbonate phase undergoes complete decomposition to form Li_2O. After the six hours evacuation at 800°C the surface of Li_2CO_3/MgO sample was covered totally by Li_2O. An interesting observation made here is the presence of the shoulder peak in the O_{1s} spectra of Li_2CO_3/MgO catalyst which was vacuum heated at 800°C for 2 hours (spectra v). Since no carbonates species were present and the surface was mainly covered with Li_2O, this shoulder peak can be assigned to the O^- species. Because the species were eliminated at longer evacuation time, this infers that the O^- species is an intermediate species formed during the decomposition of carbonates.

The results obtained from the X.P.S. experiments confirmed the migration and decomposition of the Li_2CO_3 phase on the Li_2CO_3/MgO catalyst at 800°C. These results also shed some light on the nature of the active sites on the MgO and the Li_2CO_3/MgO catalysts. As proposed by other workers (Che and Tench,1982; Ito et al.,1985), the active site is likely to be O^- type species which was present after high temperature treatment. On MgO, the O^- sites is however unstable under continuous

treatment at high temperature in air or in vacuum. It has been observed in the catalytic studies that MgO loses its activity if pretreated in-situ at 800°C over about 2 hours prior to activity determination (section 4.4.5). Under the reaction condition, these sites are likely to be stabilised since the activity of MgO does not vary significantly after 45 hours on-stream (section 4.4.2).

On Li_2CO_3/MgO catalysts the decomposition of the Li_2CO_3 phase resulted in the formation of O^- type species. Since enrichment of Li_2CO_3 occurs on the Li_2CO_3/MgO catalyst surface, it is possible that a high active sites density can be present at the portion of the surface which is rich in Li_2CO_3. High methyl radicals 'concentration' over these sites could occur and this could help explain the promotion of C_2 selectivity by Li_2CO_3 when doped on MgO. Complete decomposition of the carbonate phase resulted in the removal of O^- species and in severe sintering. The removal of O^- species and other oxygen sites on MgO and Li_2CO_3/MgO through high temperature treatment would cause the catalysts to lose its activity.

5.2.4 Further studies on the stability of Li_2CO_3/MgO at high temperature

It was observed that in a TGA experiment, 11 mg of the fresh Li_2CO_3 lost 6.8 mg of weight over two hours period when treated in air at 680°C (figure 5.2.4.a). This weight loss corresponds to the decomposition of Li_2CO_3 to form Li_2O. In the case of the calcined 7.8wt% Li_2CO_3/MgO catalyst, the amount of weight loss in the two hours period was only about 0.2mg. This suggest that the stabilisation of the residual Li_2CO_3 phase on the calcined Li_2CO_3/MgO catalysts occurs relative to the unsupported Li_2CO_3. This is not suprising in view of the pretreatment conditions (900°C, 10 hour in air).

The stability of fresh, uncalcined 8.4%Li_2CO_3/MgO relative to the calcined sample in air at 750°C have also been studied by FTIR. As in the other studies 0.02gm of self supporting pressed catalyst disks was used in this work. As illustrated in figure 5.2.4.b, it was observed that on the uncalcined Li_2CO_3/MgO catalyst, most of the Li_2CO_3 phase decomposed after one hour at 750°C (spectrum ii). On the contrary, the

calcined catalyst (see figure 5.2.3.b) retained most of its carbonate phase after the 1 hour exposure at 750°C. This indicate that the precalcination process resulted in the stabilisation of Li_2CO_3 phase of the Li_2CO_3/MgO catalysts probably through the formation of good solid matrix between Li_2CO_3 and MgO.

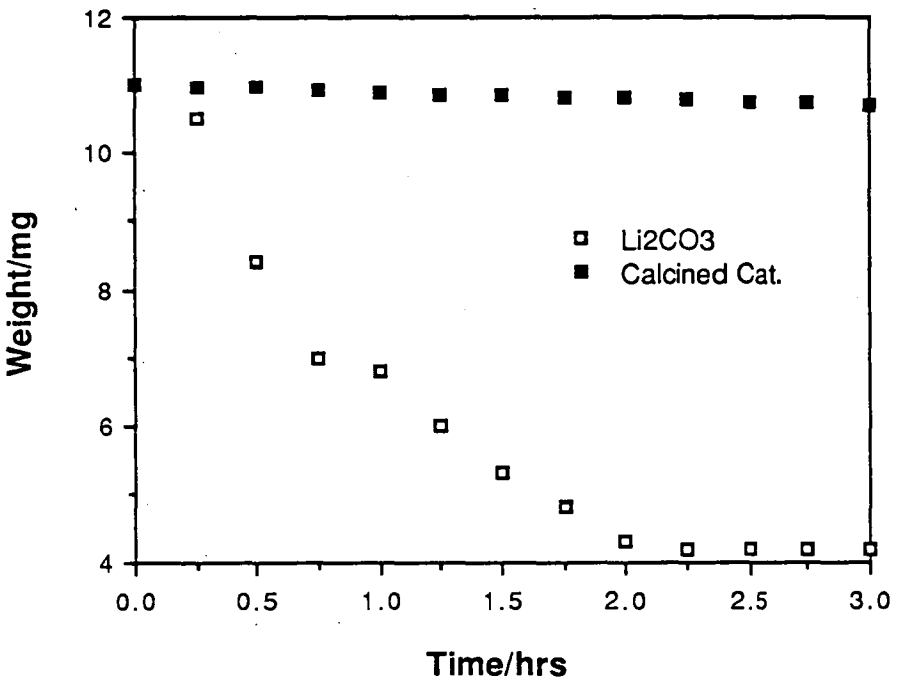

Figure 5.2.4.a The effect of exposure time at 680°C on 11mg of calcined (900°C in air, for 10 hours) 7.8wt.%Li_2CO_3/MgO and fresh Li_2CO_3 samples.

The rate of decomposition of Li_2CO_3 phase in calcined 7.8wt.% Li_2CO_3/MgO catalyst at 750°C in air and under dynamic vacuum has been determined (figure 5.2.4.c). These were achieved by monitoring the rate of loss in peak areas of the 1200-1800cm^{-1} band which is associated with the carbonate phase from the F.T.I.R. spectra. The rate of carbonate loss on the calcined catalyst in air is quite steady with time, at least over three hours at 5%carbonate/20min. Under vacuum (10^{-3} torr) the decomposition occurs at a faster and more variable rate especially in the first 100 min. Complete loss of carbonate species occurred after about two hours. The spectra of the

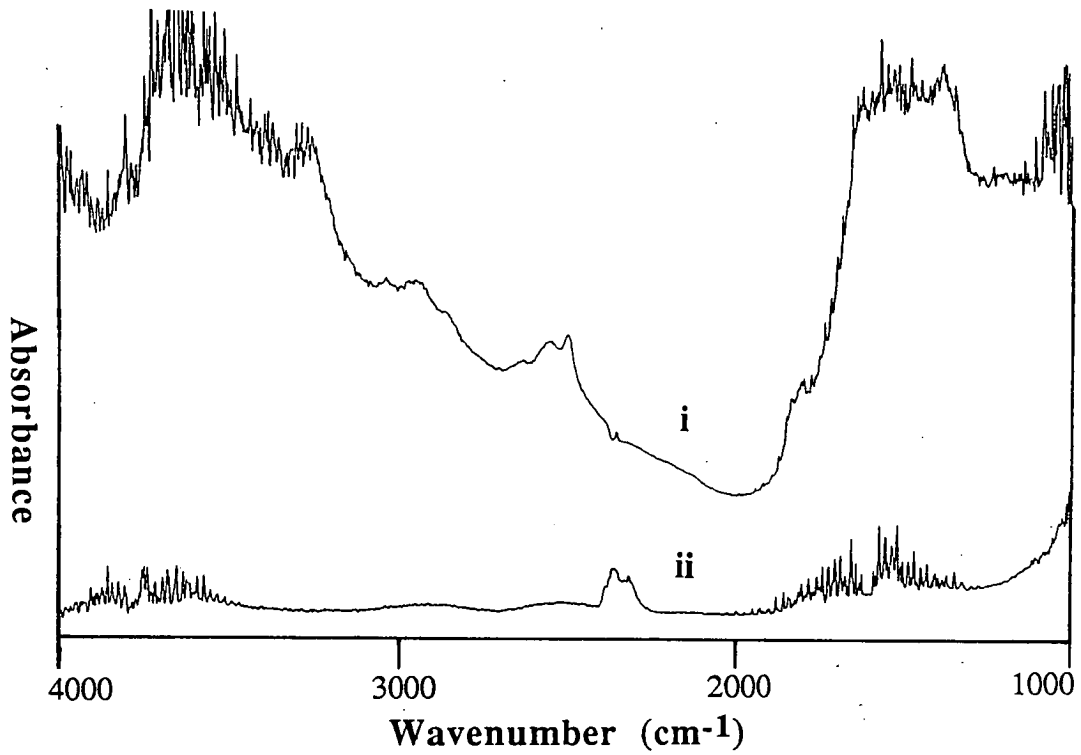

Figure 5.2.4.b The effect of pretreatment in air at 750°C on fresh 8.4wt.%Li_2CO_3/MgO catalysts. Spectrum i) is that of the catayst at RT after being evacuated (10^{-3}Torr) for 2 hours, while spectrum ii) was accumulated after 1 hour at 750°C. These spectra were accumulated with 500 scans and with a resolution of 4cm^{-1}.

catalyst at the various times under evacuation at 750°C are also given in Figure 5.2.4.d.

The effect of temperature on the rate of % weight loss due to carbonate decomposition on 11 mg of calcined Li_2CO_3/MgO catalysts have also been studied and the result given in figure 5.2.4.e. At temperatures less than 750°C the rate of % weight loss is less than 4% in every 20 minutes. At 800°C the rate of weight loss increases to about 7%, while further increase in temperature resulted in the exponential increase of rate of carbonate decomposition. However it has been observed that the rate of carbonate decomposition can be suppressed by flowing CO_2 over the catalyst at the high temperature.

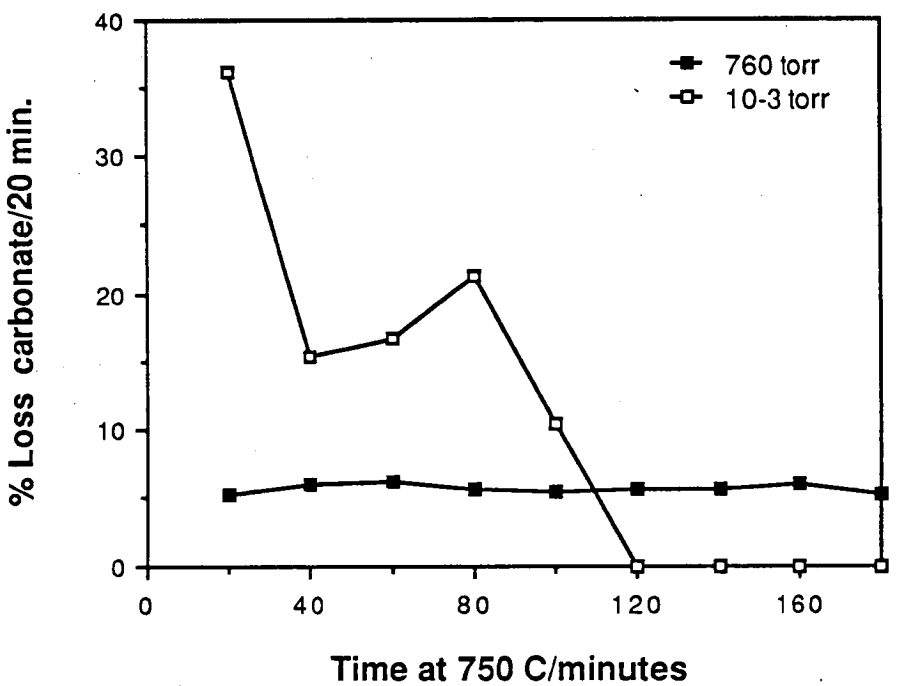

Figure 5.2.4.c The rate of carbonate loss from 0.02g of calcined 7.8%Li_2CO_3/MgO at 750°C in air and under evacuation.

These results clearly confirm that Li_2CO_3 is unstable and undergoes melting and decomposition at the temperature normally used for catalyst screening. To some

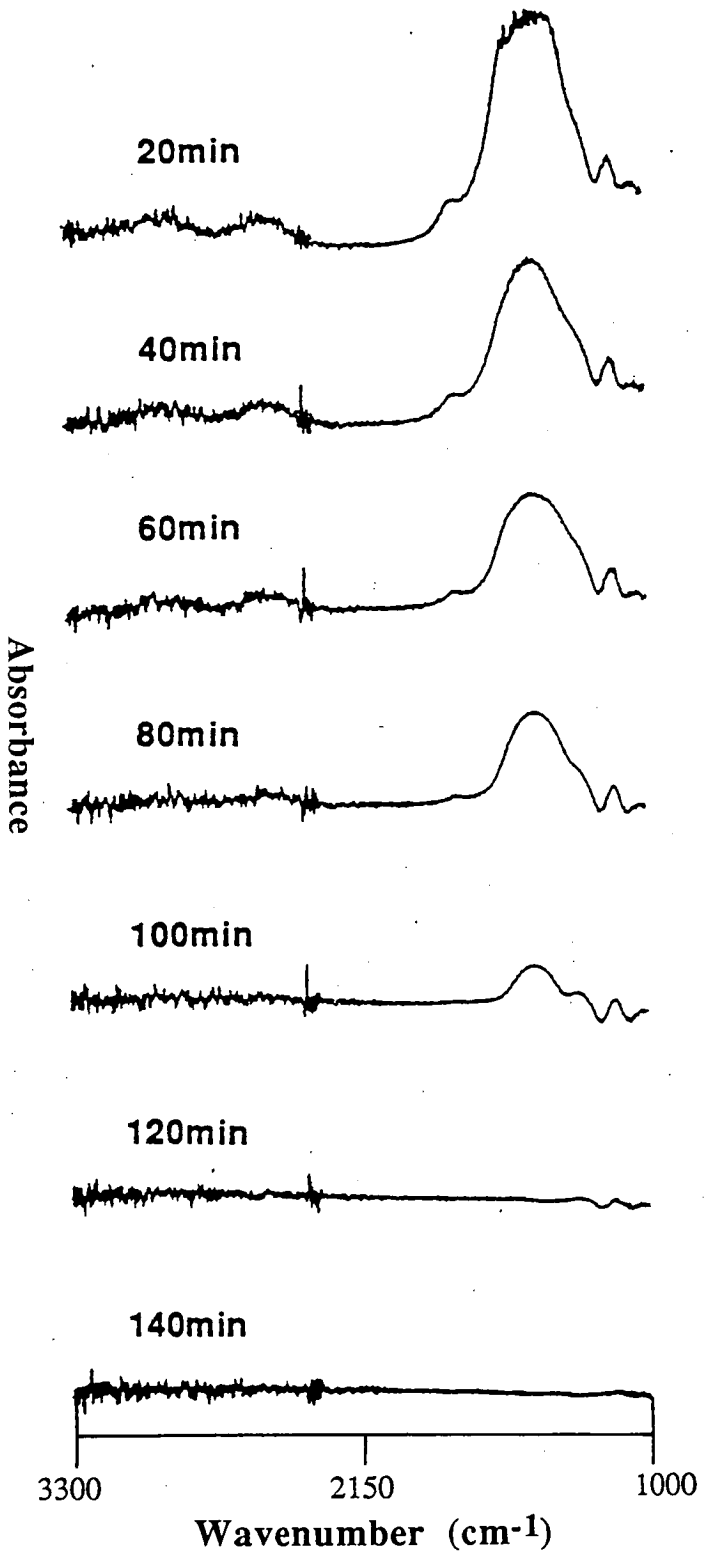

Figure 5.2.4.d The transmission FTIR spectra of calcined 7.8wt.%Li_2CO_3/MgO catalyst at 750°C in 10^{-3}torr of dynamic vacuum at different times.

extent the stabilization of the Li_2CO_3 phase on MgO can be achieved through precalcination. The physico-chemical nature of Li_2CO_3/MgO catalyst at high temperature is likely to influence its catalytic activity significantly.

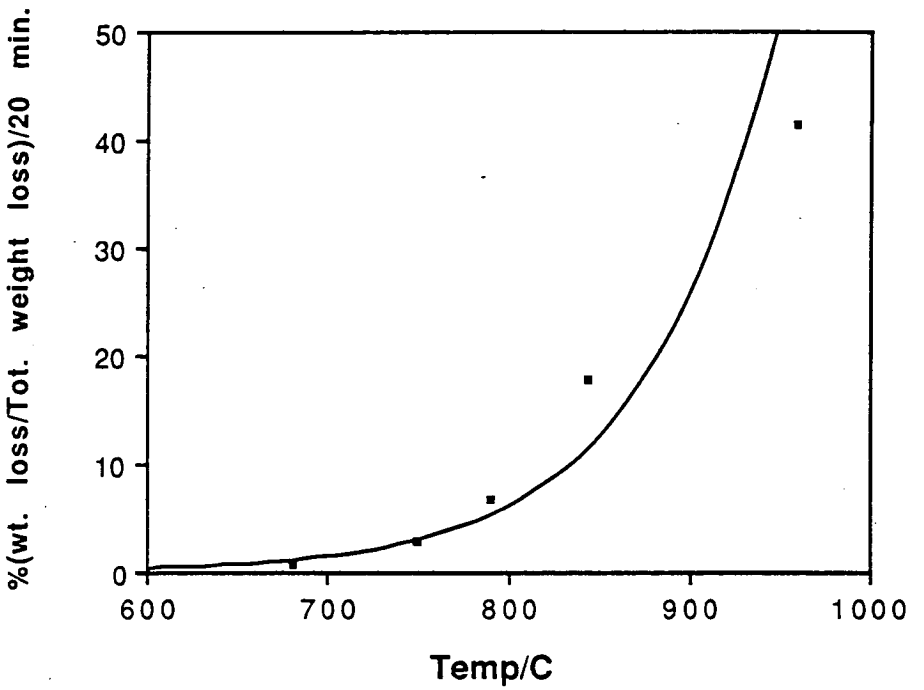

Figure 5.2.4.e The rate of % weight loss due to carbonate decomposition from 11 mg of 7.8wt.% Li_2CO_3/MgO catalyst when treated at different temperature in air.

5.3 The nature of MgO doped with different lithium salt

5.3.1 SEM studies on calcined samples.

The SEM micrographs of LiOH/MgO, LiCl/MgO, Li_2SO_4/MgO and LiF/MgO after precalcination at 900°C for 10 hours are given in figure 5.3.1.a. The micrograph of the calcined LiOH/MgO (micrograph i) is very similar to that of Li_2CO_3/MgO (micrograph iv of figure 5.2.1.a); the surface layer formation also occurs on the calcined LiOH/MgO. This suggest that the Li_2CO_3/MgO and LiOH/MgO catalysts have similar physical properties.

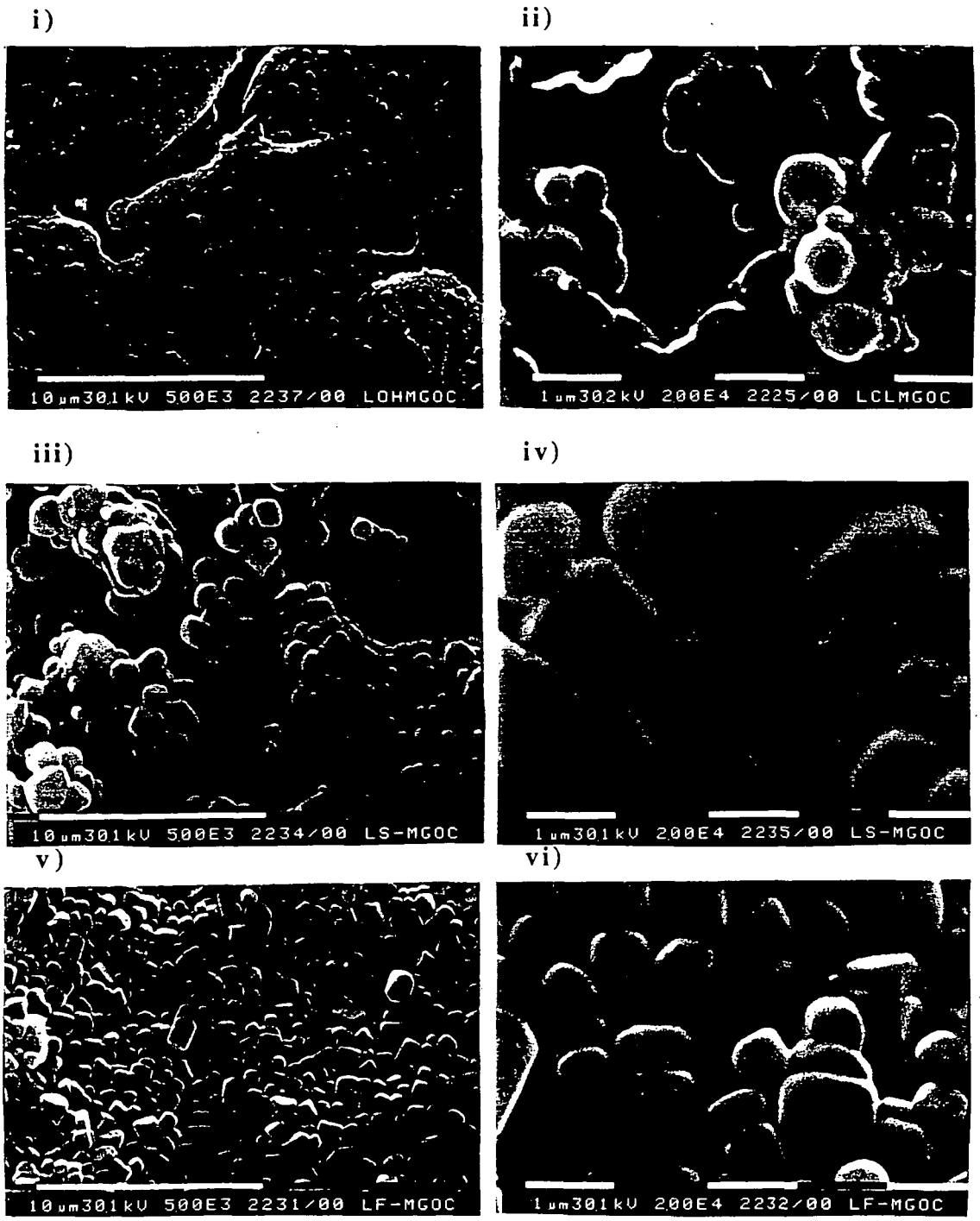

Figure 5.3.1.a SEM micrographs of i)LiOH/MgO, ii)LiCl/MgO, Li_2SO_4/MgO (iii & iv)and LiF/MgO (v & vi) after precalcination at 900°C for 10 hours. Micrographs i), ii) and iv) are take at a magnification of $5x10^3$ while micrographs ii), iv) and vi) at a magnification of $2.0x10^4$.

On LiCl/MgO (micrograph ii) no extensive layer formation was observed to occur. Instead the clusters seems to be bound together and coated by a layer of fluffy materials. In section 4.6.3.3 it was observed that the fluffy layers were removed when the catalyst was used onstream for 20 hours. An elemental analysis of the used catalyst showed the losses of both Li and Cl. This indicate that the fluffy material is mainly composed of LiCl.

The SEM micrograph of the calcined Li_2SO_4/MgO (micrograph iii) shows that some layer formation seem to be present on this sample. However at a magnification of $2x10^4$ (micrograph iv) the particles are distinctly cubic in shape. No layer formation was observed at all for calcined LiF/MgO (micrograph v). The material existed as clearly defined particle structures of cubic shapes corresponding to the crystals of MgO and LiF (micrograph vi).

It would seem from these observations that the layer formations are related to the melting point of the lithium salt. LiCl and Li_2CO_3 which melt at about 610°C and 618°C respectively (Aylward and Findlay, 1971), must exist in molten state and have a considerable vapour pressure when calcined at 900°C. Migration of these salts will occur causing their enrichment on the catalysts surface. Such changes do not occur on Li_2SO_4/MgO and LiF/MgO because of their relatively higher melting points. Li_2SO_4 and LiF melts at 857°C and 870°C respectively. As a result the formation of the LiF and Li_2SO_4 rich surface layer on the respective catalyst during precalcination does not occurs.

It was also observed that the calcined samples of Li_2CO_3/MgO and the LiOH/MgO are much harder than that of the other salt on MgO. This indicate that in Li_2CO_3/MgO the dispersion of Li_2CO_3 phase also acted as a cement resulting in a formation of solid matrix with MgO. The formation of this solid matrix in the precalcined samples must contribute significantly to the stability of Li_2CO_3 phase compared to the uncalcined samples. However the formation of the solid matrix per se is not likely to control the activity of material. Although Li_2SO_4 and LiF does not seem to form a solid matrix with MgO the presence of Li_2SO_4 and LiF on MgO before

precalcination, causes a decrease in methane conversion. These salts seem to poison the activity of MgO for the oxidative reaction of methane.

5.3.2 The composition of various lithium doped MgO catalysts

The composition of the various fresh and calcined lithium doped MgO catalysts have been determined by AAS and are presented in table 5.3.2.a in the form of wt % Li/Mg. Generally, most of the calcined sample lose some lithium due to the calcination. The LiCl/MgO system was most affected by calcination; more than half of the lithium originally present was lost. This is mainly due to the volatility of LiCl under the calcination temperature. In the case of LiF/MgO and Li_2SO_4/MgO, the high decomposition temperature of these salt cause smaller loss of lithium (table 5.3.2.a). On the LiOH/MgO system as in Li_2CO_3/MgO, the formation of solid matrix between MgO and Li_2CO_3 and the formation of lithium carbonate rich layer on the surface of the calcined sample could probably be the cause which hinders any significant loss of lithium.

Table 5.3.2.a The composition of fresh and calcined lithium salt supported on MgO

Sample	Wt.% Li/Mg	
	Fresh	Calcined
LiOH/MgO	4.6	4.5
LiCl/MgO	6.2	2.9
Li_2SO_4/MgO	8.3	8.0
LiF/MgO	7.9	6.9

The XRD patterns of the various calcined lithium doped MgO have been determined and are presented in figure 5.3.2.a. Comparing the patterns of Li_2CO_3/MgO (pattern iii) to that of pure Li_2CO_3 (pattern ii) and MgO (pattern i), the Li_2CO_3 and MgO phases are the main components of the calcined catalysts. The

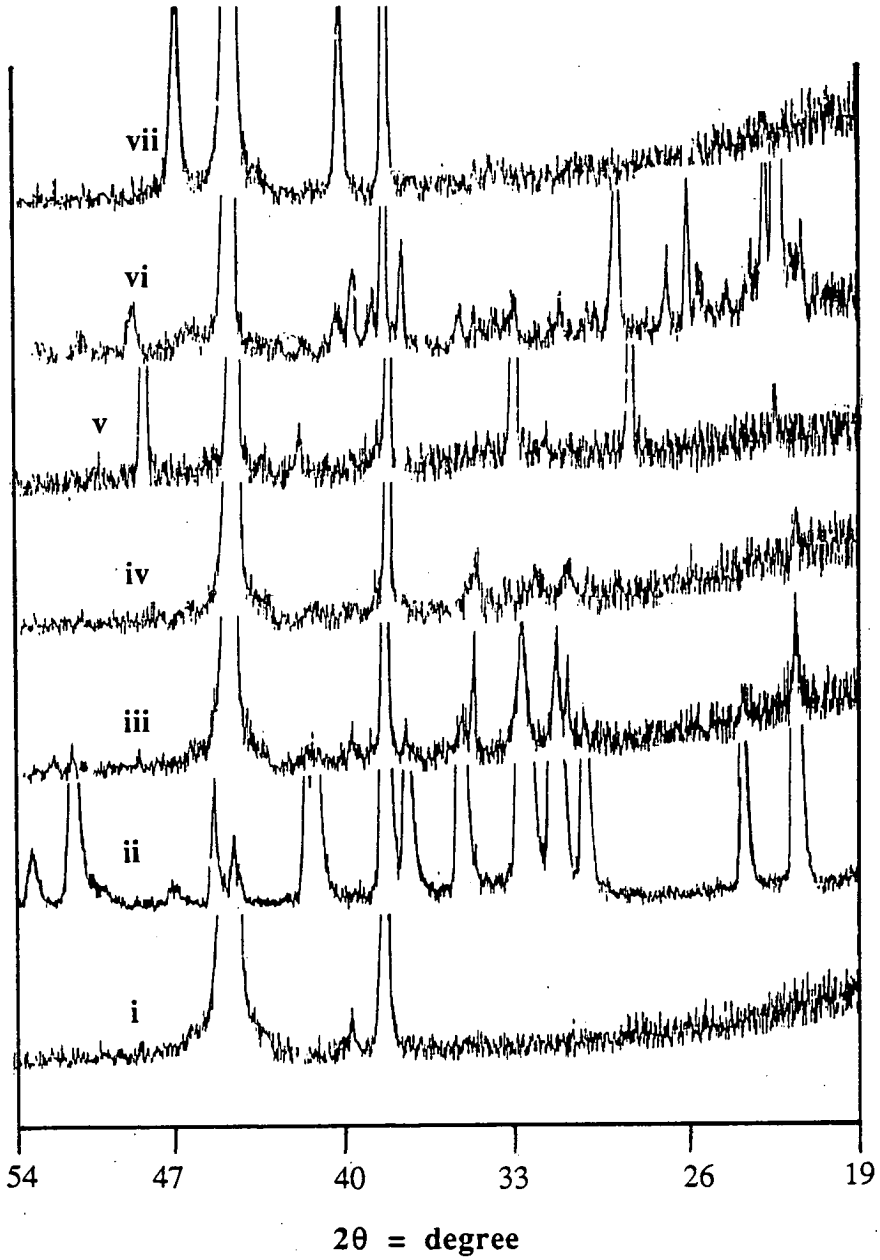

Figure 5.3.2.a XRD pattern of i)MgO, ii)Li_2CO_3, and of calcined iii)Li_2CO_3/MgO, iv)LiOH/MgO, v)LiCl/MgO, vi)Li_2SO_4/MgO and vii)LiF/MgO catalysts for 2θ in the range of 19-54°.

Li_2CO_3 phase was also observed on the calcined LiOH/MgO catalyst. The peaks due to the Li_2CO_3 on LiOH/MgO is smaller than on Li_2CO_3/MgO indicating the relatively smaller quantities of Li_2CO_3 on LiOH/MgO or that over this catalyst the Li_2CO_3 phase was well dispersed. No significant Li_2CO_3 phase was present on the other catalyst.

These results provide the basis for some understanding on the nature of active site for oxidative reaction of methane. The presence of Li_2CO_3 on the support for both the Li_2CO_3/MgO and LiOH/MgO catalysts resulted in the promotion of oxidative coupling properties. However the presence of LiCl also has similar effects. This infers that Li_2CO_3 is not likely to be the active species per se. However in both of the LiCl and Li_2CO_3 doped catalysts, the lithium salt might serve as the precursor for the active site. This is facilitated by the decomposition of the salt on MgO to form the O^- type species. Such reactions is not likely to occur on LiF/MgO and Li_2SO_4/MgO catalysts due to the stability of these salts.

5.3.3 FTIR study on calcined Lithium salt/MgO catalysts

Transmission FTIR spectra of the calcined LiOH/MgO and LiF/MgO catalysts at RT, at 750°C and at RT after cooling down from 750°C have been accumulated and are presented in spectra 5.3.3.a. Absorption bands typical of Li_2CO_3 phase (at 2800, 2500, 1800 and 1500 cm^{-1}) were observed to be present on the spectrum of calcined LiOH/MgO at RT (spectrum i of set A). Li_2CO_3 formation must have occurred through carbon dioxide absorption during the preparation stage of the catalyst. The spectra of LiF/MgO (set B of figure 5.3.3.a) however does not show any evidence of Li_2CO_3.

The broadening of absorption bands of Li_2CO_3 on the LiOH/MgO occurs when it was heated to 750°C (spectra ii of set A) as on Li_2CO_3/MgO catalyst. Significant amounts of hydroxyl species were still present on the LiOH/MgO catalysts at 750°C (spectrum i in set A). On LiF/MgO however, the band associated with adsorbed H_2O was absent at 760°C and no significant hydroxyl peaks were observed. When the sample was cooled, the spectrum of LiOH/MgO (number iii of set A) shows

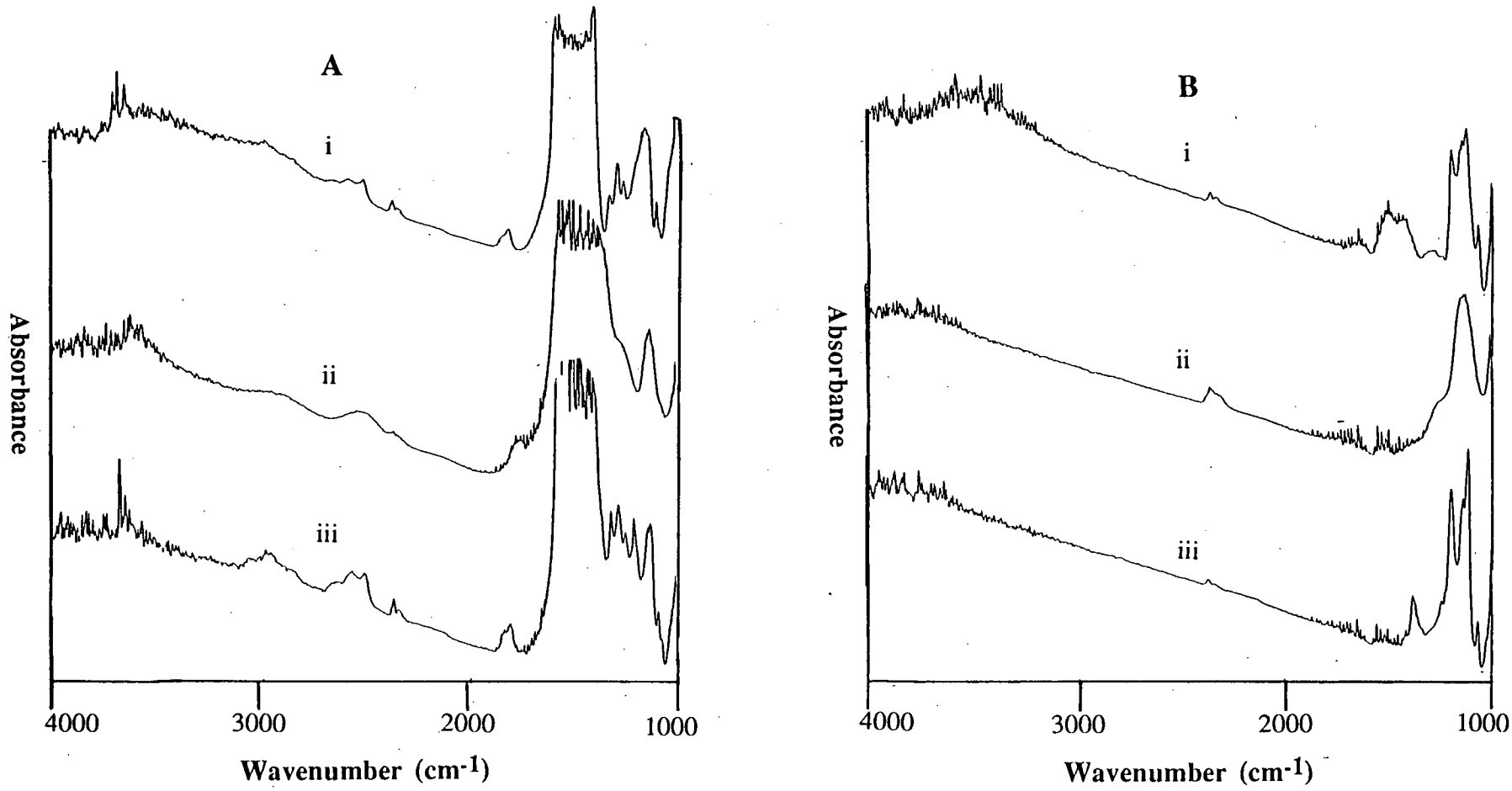

Figure 5.3.3.a Transmission FTIR spectra of calcined LiOH/MgO (set A) and LiF/MgO catalysts (set B) at i)RT after 2 hours of evacuation, ii) 750°C after 1 hour of equilibration time and at iii) RT after the 750°C treatment.

the increased intensity for the carbonate bands indicating the aggregation of Li_2CO_3 phase during the high temperature pretreatment.

The spectra of calcined LiOH/MgO (set A) are very similar to that of Li_2CO_3/MgO (see figure 5.2.3.a) suggesting that the two materials have similar chemical composition and chemical nature. The significant similarity in the physical (see section 5.3.1) and the chemical properties of LiOH/MgO and Li_2CO_3/MgO explained why these catalyst have identical catalytic activity. These studies also showed that under the conditions of this experiment, not only carbonate melting and decomposition occurs but a significant amount of the hydroxyl species was present at the high temperature. The presence of hydroxyl species on these catalysts at the high temperature indicate the presence of oxygen sites with higher basicity such as the O^- species. Such a phenomenon occurs on LiOH/MgO and Li_2CO_3/MgO catalyst but not on LiF/MgO. This further suggest that the Li_2CO_3 phase when supported on MgO is responsible for the generation and stabilisation of O^- type sites at high temperature. Driscoll et al.,1985 and Ito et al.,1985, have proposed that the Li^+O^- site are responsible for the oxidative coupling activity over Li_2CO_3/MgO catalyst.

5.3.4 XPS experiment on Li_2SO_4/MgO catalyst

To further investigate the nature of oxygen sites, the calcined Li_2SO_4/MgO catalyst was also studied by XPS under the pretreatment conditions applied in section 5.2.3. The Li_{1s}, Mg_{2p}, Mg_{2s}, S_{2p} and O_{1s} spectra, denoted by #1 to #5 were accumulated after each pretreatment and are given in figure 5.3.4.a. After evacuation of 140°C, both lithium, magnesium as well as sulphur and oxygen were observed to be present on the catalyst surface .The O_{1s} peak after evacuation at 140°C is broad indicating the presence of more than one oxygen species. After the sample was treated at 600°C, the Li_{1s} peak diminishes while that of Mg increases relative to the spectra after the first treatment. The S_{2p} peak also decreases in intensity while that of oxygen broadens. Treating the sample at 700°C and 800°C for two hours each does not significantly change the surface composition. When the sample was treated under

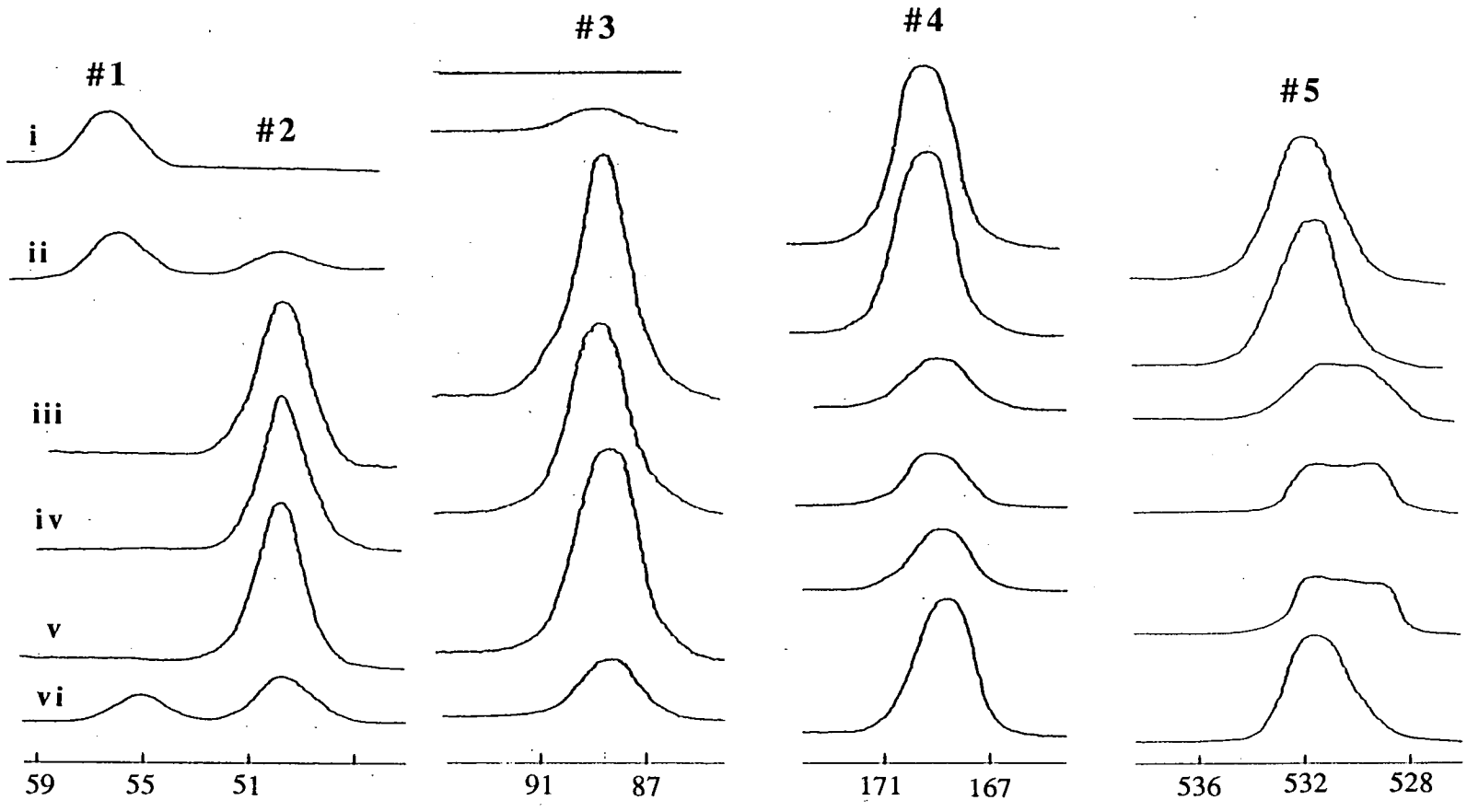

Figure 5.3.4.a XPS spectra of Li_2SO_4/MgO catalyst i) after thermal vacuum treatment at 140°C for 48 hours, after calcination in dry air at ii)600°C, iii)700°C, iv)800°C and after thermal vacuum treatment at 800°C for v)2 hours and vi)4 hours respectively. Peaks 1, 2, 3, 4, and 5 were assigned correspondingly to Li_{1s}, Mg_{2p}, Mg_{2s}, $S_{2p3/2}$ and O_{1s}.

vacuum (10^{-5} torr) at 800°C for two hours, relative to the spectra after pretreatment in air at this temperature the Li_{1s} peak increased together with that of sulphur and O_{1s} while the Mg peak decreased. After 6 hours of treatment in vacuum at 800°C no Mg peak was observed.

These results indicate that after calcination at 900°C both Li and Mg are present on the catalyst surface. When the sample was treated at 600, 700 and 800°C some of the lithium migrated into the bulk leaving only MgO and some sulphate on the surface. The migration caused the decrease in sulphate concentration while increasing the concentration of MgO on the surface and this is the probable explanation for the broadening of O_{1s} peak. When the sample was evacuated at 800°C however, the migration of Li_2SO_4 back to the surface of the sample was facilitated and the enrichment of the surface with Li_2SO_4 occurs. As a result the amount of MgO present on the surface diminishes. The corresponding increase of S_{2p} and O_{1s} peaks indicate that in the O_{1s} spectra the dominant oxygen species is that from the SO_4^{2-} species.

When MgO was doped with Li_2SO_4, most of the oxygen species present on the surface of Li_2SO_4/MgO is due to the SO_4^{2-} species. This could hinder the formation of basic oxygen sites and help explain why MgO doped with Li_2SO_4 has low activity for the oxidative reaction of methane.

5.4 The nature of Li_2CO_3 on various supports

5.4.1 SEM studies on calcined Li_2CO_3 on various supports

The physical nature of calcined $Li_2CO_3/Mg(OH)_2$, Li_2CO_3/CaO, Li_2CO_3/γ-Al_2O_3, Li_2CO_3/SiO_2, and Li_2CO_3/TiO_2 have been studied by SEM. As shown in figure 5.4.1.a, these materials differed significantly from each other. These differences signify the effect of the various oxides on the stability Li_2CO_3 phase.

A great similarity was observed between the physical texture of $Li_2CO_3/Mg(OH)_2$ (micrograph i of figure 5.4.1.a) to that of Li_2CO_3/MgO (micrograph iv of figure 5.2.1.a) and $Li(OH)_2$/MgO (micrograph i of figure 5.3.1.a). This indicate that all the three sample are physically and chemically similar and this fact is reflected

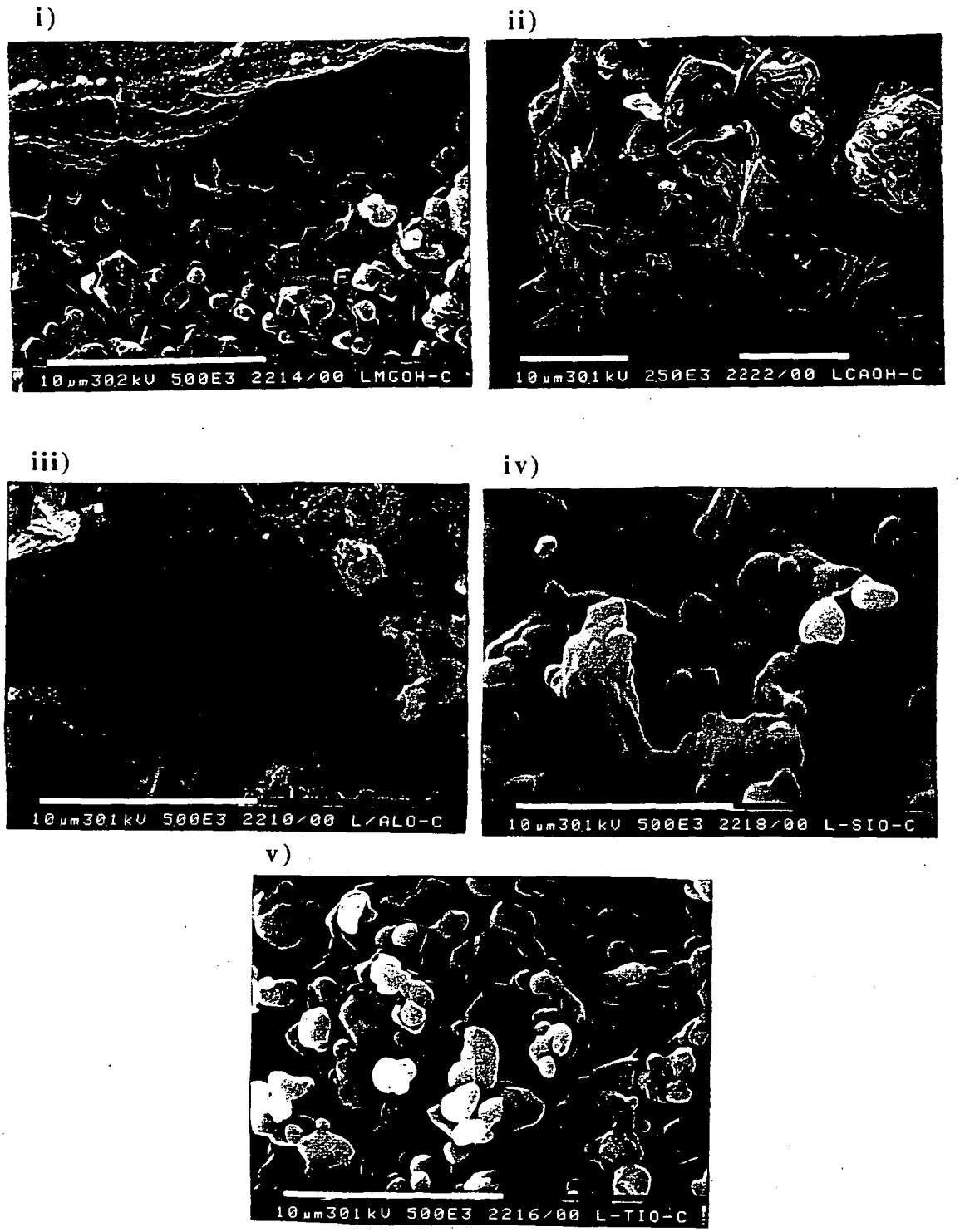

Figure 5.4.1.a SEM micrographs of i)$Li_2CO_3/Mg(OH)_2$, ii)Li_2CO_3/CaO iii)Li_2CO_3/γ-Al_2O_3 iv)Li_2CO_3/SiO_2 and v) Li_2CO_3/TiO_2 after precalcination at 900°C for 10 hours. Micrograph ii) is at magnification of $2.5x10^3$ while the others are at magnification of $5x10^3$.

by the similarity of their catalytic performances. In the case of Li_2CO_3/CaO (micrograph ii) and Li_2CO_3/γ-Al_2O_3 (micrograph iii), a totally different morphology was observed. No distinct clusters shapes were present. Instead the samples seem to be in flaky form. These samples have been observed to be quite soft and can be powdered very easily. The surface area of these samples were determined (see Table 5.6.1.a) and found to be higher than that of the other samples. The flaky structure of the material contributed to their relatively higher surface area.

No layer formation as on Li_2CO_3/MgO was observed on Li_2CO_3/SiO_2 (micrograph iv)and Li_2CO_3/TiO_2 (micrograph v). On these materials clearly defined but irregularly shaped particles were fused together in three dimension. The extent of particle fusion is more significant on Li_2CO_3/SiO_2 than on Li_2CO_3/TiO_2. These micrograph showed that the layer formation is not favoured on SiO_2 and TiO_2 and that the formation of Li_2CO_3 rich surface layer does not occur on these oxides.

5.4.2 AAS and XRD studies

To further understand the nature of these materials, the effect of calcination on their decomposition has been determined by AAS and XRD. The composition of these materials prior and after calcination are presented in table 5.4.2.a in the form of wt % Li/M, where M is the mass of metal M. Generally it can be seen that some losses of lithium occur as a result of precalcination.

The XRD patterns of the various materials are presented in figure 5.4.2.a. No significant Li_2CO_3 phases were observed to be present on calcined Li_2CO_3/γ-Al_2O_3 (pattern vi), Li_2CO_3/SiO_2 (pattern v), Li_2CO_3/TiO_2 (pattern iv) and Li_2CO_3/CaO (pattern iii). This indicates that most of the carbonate phase must have decomposed during precalcination. The lithium present on the calcined sample will then have to be in the form of the oxide and are integrated in the lattice. The transmission FTIR of some of these catalysts at RT have also been determined (Figure 5.4.2.b) and the absence of Li_2CO_3 phase on supports other than MgO was confirmed.

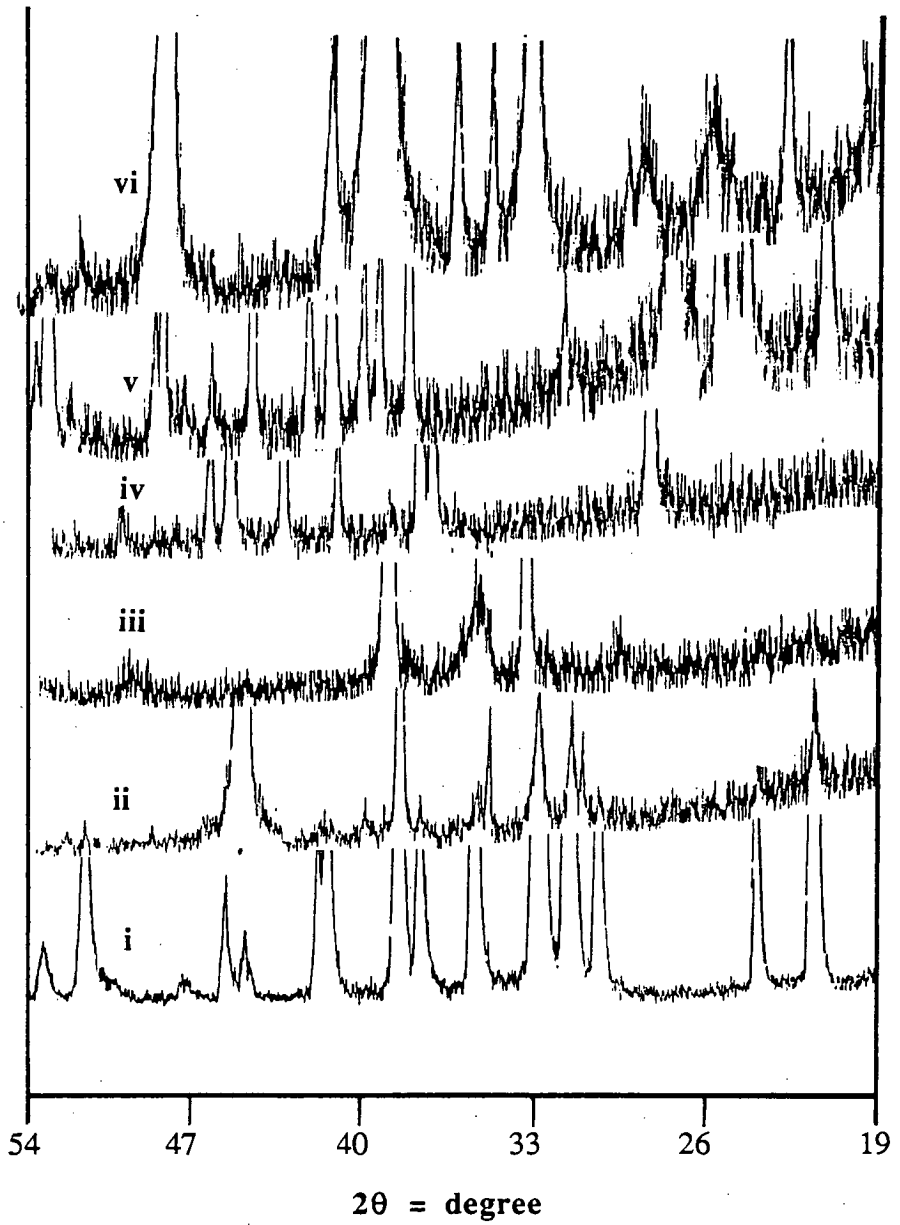

Figure 5.4.2.a XRD pattern of i)Li_2CO_3 and of calcined ii)Li_2CO_3/MgO, iii)Li_2CO_3/CaO, iv)Li_2CO_3/TiO_2, v)Li_2CO_3/SiO_2 and vi)Li_2CO_3/γ-Al_2O_3 catalysts for 2θ in the range of 19-54°.

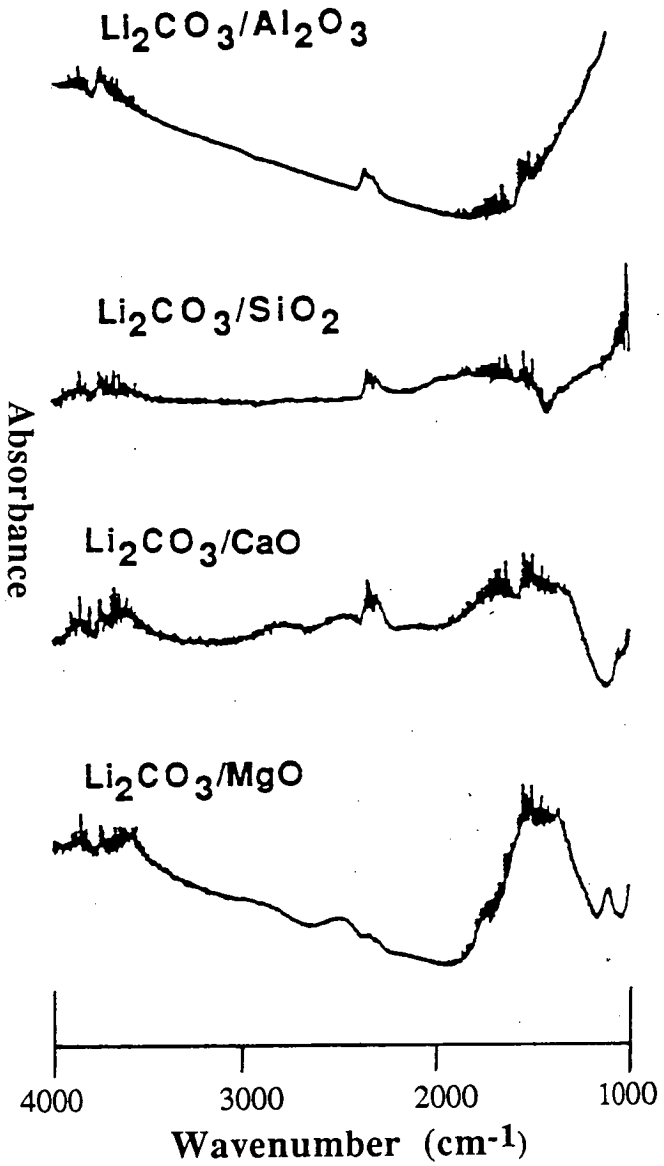

Figure 5.4.2.b Transmission FTIR spectra at 750°C of Li_2CO_3/γ-Al_2O_3, Li_2CO_3/SiO_2, Li_2CO_3/CaO and Li_2CO_3/MgO catalysts which have been calcined at 900°C for 10 hours. These spectra were accumulated with 100-500 scans and with a resolution of $4cm^{-1}$.

The results obtained in this section suggest the possible role of ionic radii in stabilising the Li_2CO_3 phase. According to the values listed by Aylward and Findlay,1971 the ionic radii of Mg^{2+} (72pm-see table 6.5.a) is similar to Li^+ (74pm) but differ significantly to that of Ca^{2+} (99pm), Al^{3+} (53pm), Si^{4+} (40pm) and Ti^{4+} (61pm). Due to the similarity in the ionic radii of Mg^{2+} and Li^+, Li_2CO_3 can form a better solid solutioon with MgO than with the other oxides. This could be the reason why the Li_2CO_3 phase of Li_2CO_3/MgO catalyst was relatively stable when exposed to high temperature while on other oxides it undergoes decomposition.

Table 5.4.2.a The composition of fresh and calcined Li_2CO_3 supported on various metal oxide.

Wt% Li/M where M_xO_y is the support for Li_2CO_3.		
Sample	Fresh	Calcined
Li_2CO_3/MgO	8.4	7.8
Li_2CO_3/$Mg(OH)_2$	3.6	3.1
Li_2CO_3/$Ca(OH)_2$	3.9	2.6
Estimated values (support not totally dissolved)		
Li_2CO_3/TiO_2	3.4	2.9
Li_2CO_3/SiO_2	5.6	4.4
Li_2CO_3/γ-Al_2O_3	6.6	5.4

* calcined at 900°C in air for 10 hours

5.5 Further FTIR studies on catalytic materials.

The transmission FTIR spectra of Li_2CO_3/SiO_2, Li_2CO_3/γ-Al_2O_3, CaO, $CaCO_3$ and Li_2CO_3/CaO catalyst at RT, 750°C and RT after 750°C pretreatment are presented in figures 5.5.a, 5.5.b and 5.5.c respectively. The RT spectra of Li_2CO_3/SiO_2 (spectrum i) does not show any significant amount of Li_2CO_3 phase or

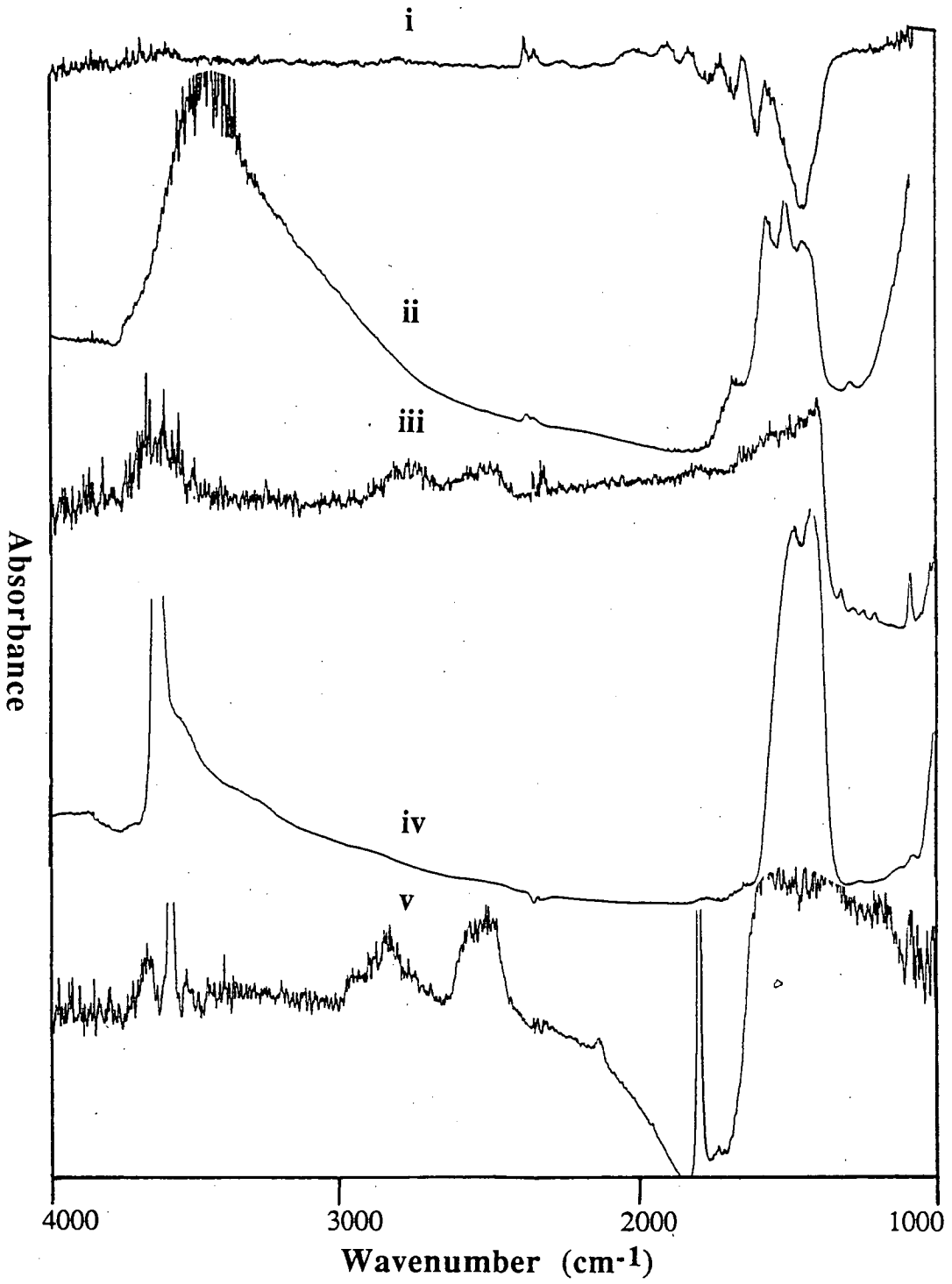

Figure 5.5.a Transmission FTIR spectra of i)Li_2CO_3/SiO_2, ii)Li_2CO_3/γ-Al_2O_3, iii)Li_2CO_3/CaO, iv) CaO and iv)$CaCO_3$ at RT after evacuation for 2 hours. These spectra were accumulated with 100-500 scans and a resolution of $4cm^{-1}$.

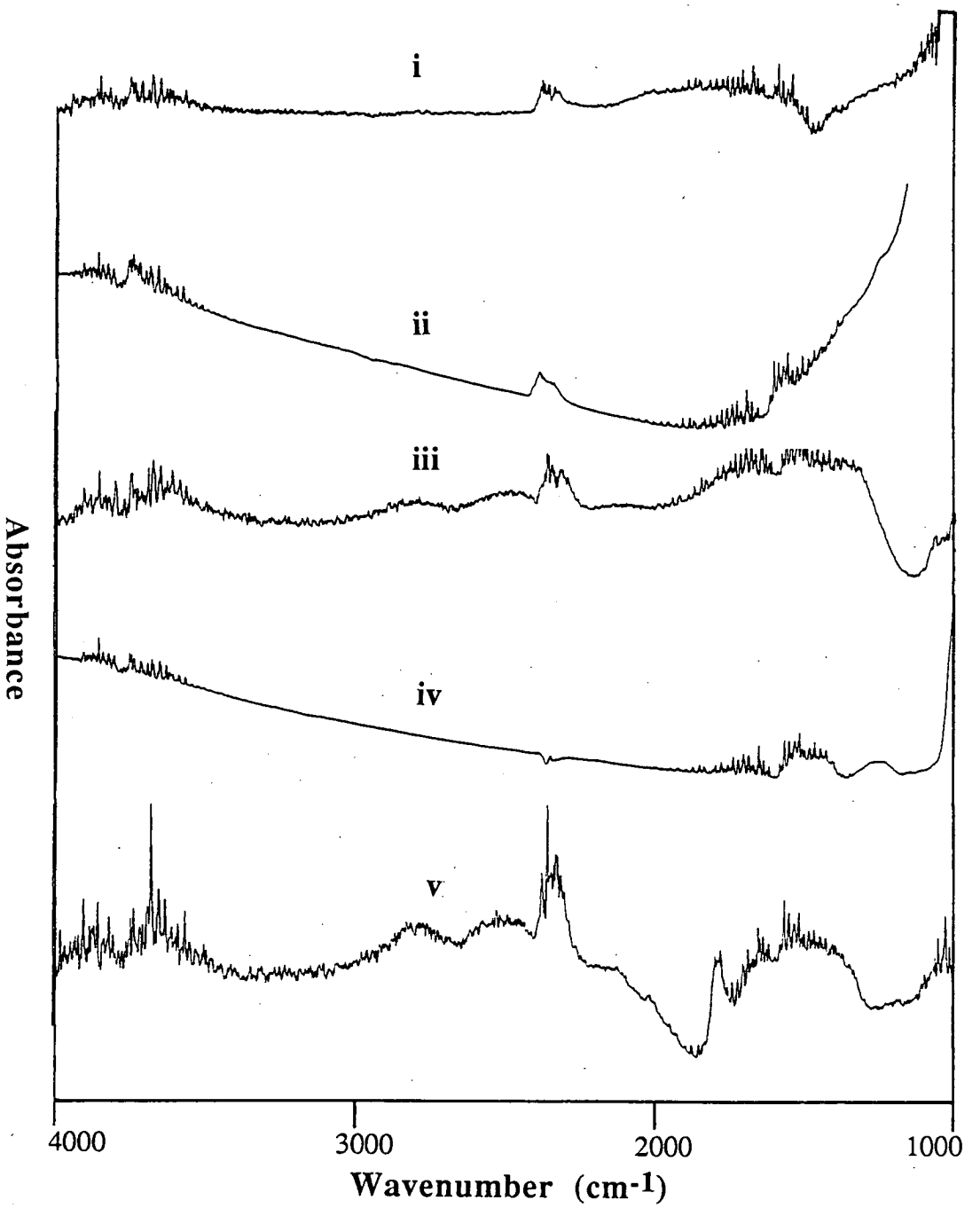

Figure 5.5.b Transmission FTIR spectra of i)Li_2CO_3/SiO_2, ii)Li_2CO_3/γ-Al_2O_3, iii)Li_2CO_3/CaO, iv) CaO and iv)$CaCO_3$ at 750°C after 1 hour of equilibration time. These spectra were accumulated with 100-500 scans and a resolution of $4cm^{-1}$.

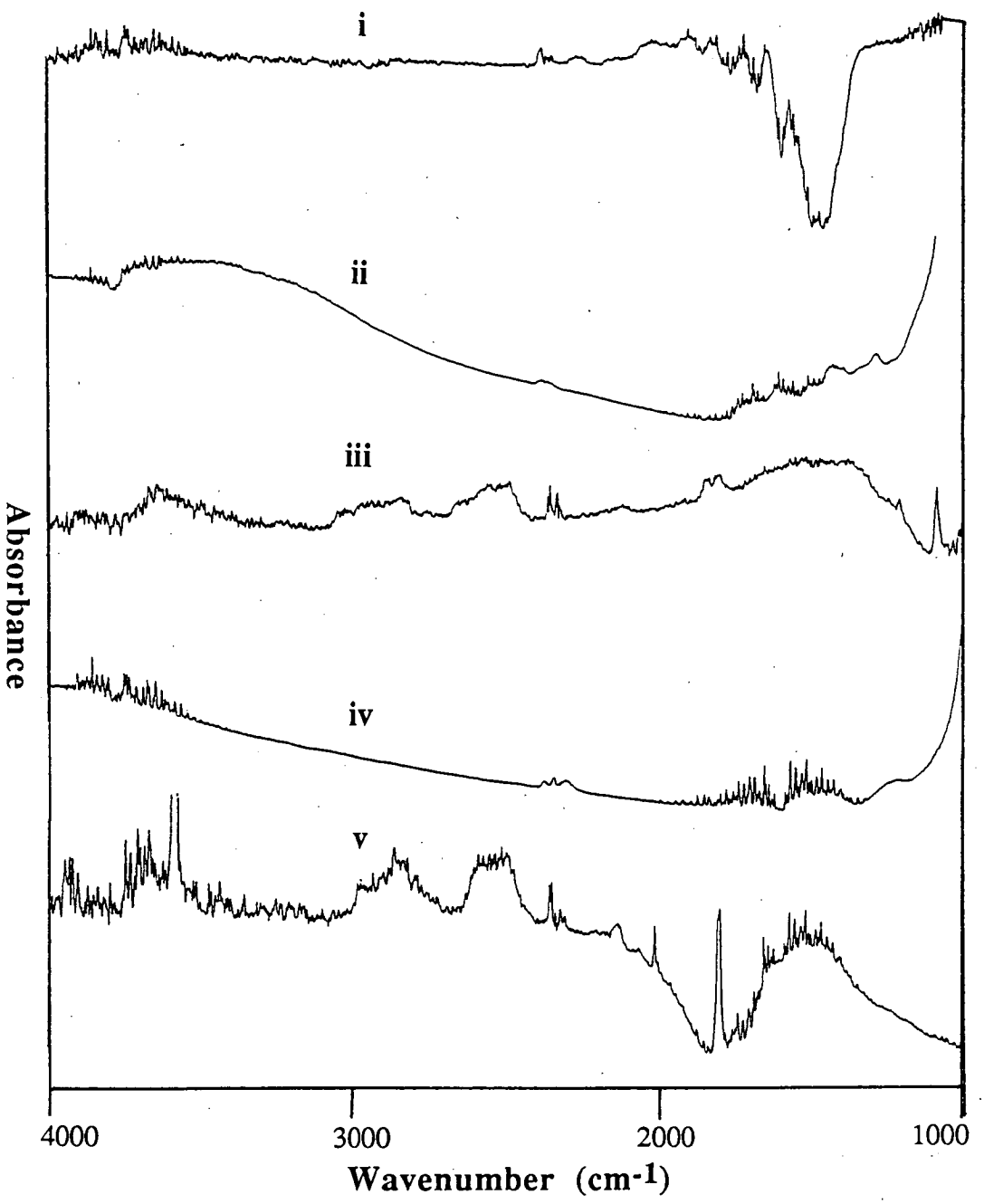

Figure 5.5.c Transmission FTIR spectra of i)Li_2CO_3/SiO_2, ii)Li_2CO_3/γ-Al_2O_3, iii)Li_2CO_3/CaO, iv) CaO and iv)$CaCO_3$ at RT after the 750°C treatment. These spectra were accumulated with 100-500 scans and a resolution of $4cm^{-1}$.

adsorbed H_2O while on Li_2CO_3/γ-Al_2O_3 (spectrum ii) some amount of absorbed H_2O and hydroxyl species was present. This is likely to be due to the surface area of these materials since Li_2CO_3/γ-Al_2O_3 has a surface area of $31m^2/g$ while the surface area of Li_2CO_3/SiO_2 is less than $1m^2/g$. At 750°C most of the water and hydroxyl species on Li_2CO_3/γ-Al_2O_3 (spectrum ii of figure 5.5.b) was removed. No significant hydroxyl species were present on Li_2CO_3/SiO_2 at 750°C (spectrum i of figure 5.5.b). When the samples were cooled to RT, the hydroxyl species on MgO and Li_2CO_3/γ-Al_2O_3 reformed again. Some hydroxyl species also formed on Li_2CO_3/MgO at RT. Comparing the spectra of MgO, Li_2CO_3/γ-Al_2O_3 and Li_2CO_3/MgO the absorption band due to hydroxyl species on Li_2CO_3/MgO are different from that of the other two catalysts. Broader absorption band was observed on MgO and Li_2CO_3/γ-Al_2O_3 while on Li_2CO_3/MgO the bands are sharper. It is likely that on Li_2CO_3/MgO, the formation of OH species are associated with particular oxygen sites and this site is not as numerous as that on the other two catalysts. On MgO and Li_2CO_3/γ-Al_2O_3 however the oxygen sites which generate the hydroxyl species are numerous and this explains the broad OH band observed. The presence of Li_2CO_3 on MgO has drastically changed the amount of hydroxyl species formed on MgO.

Spectrum iii, iv and v in figure 5.5.a-c are that of Li_2CO_3/CaO, CaO and $CaCO_3$ respectively. Similar to that on MgO, it was also observed that the presence of Li_2CO_3 on CaO reduces the amount of hydroxyl species and absorbed water on CaO. At 750°C most of the absorbed H_2O and the hydroxyl species on CaO was removed while some hydroxyl species are still present on $CaCO_3$ and Li_2CO_3/CaO. It was also observed that some decomposition of $CaCO_3$ occurs at this temperature as evidence by the increase in CO_2 absorption band (spectrum iv of figure 5.5.b).

In this experiment the modification of MgO and CaO with respect to hydroxyl species formation occurs when Li_2CO_3 was present. Since the presence of Li_2CO_3 on these oxides also increase their oxidative coupling activity while reducing the general activity of the oxide, it is then possible that these phenomena are related. The effect of the Li_2CO_3 doping on CaO and MgO could possibly be two fold. Firstly it decreases

the surface area of the sample (see table 5.6.1.a) relative to the undoped oxide, making less active sites per unit weight available for oxidative reaction of methane. The moderation in the activity of the catalyst was facilitated by the reduction of surface area. This effect is reflected by the decrease in absorbed H_2O and hydroxyl species form on the doped catalysts. The second effect could possibly be the increase in the number of sites on the sample which have higher basicity and the destruction of unselective sites. It has been observed that the presence of Li_2CO_3 on CaO and MgO resulted in the existence of hydroxyl species even at 750°C. This would indicate that the presence of Li_2CO_3 on the oxides generate O^- type sites which are more basic than those intially present on the raw oxide. Such sites would have stronger interaction with oxygenate and CO intermediates and would cause the oxidation of these intermediates to carbon dioxide. Generally it has been observed in the catalytic studies that the increase in oxidative coupling activity also results in high selectivity to carbon dioxide in the carbon oxide products.

5.6 The influence of physical and chemical properties on catalytic activity

5.6.1 Surface area and activity.

In their studies on the alkali doped metal oxide catalyst, Iwamatsu et al., 1988b, found that the amount of C_2 yield is related to the surface area of these catalysts. High C_2 yields were observed over catalysts with low surface area. The oxidative reaction of methane over various catalytic systems with different surface area at 800°C as determined in this work are summarised in table 5.6.1.a. The total reactant flow rate used in the activity determination was 25 ml/min with the partial pressure of He, CH_4, and O_2 at about 430, 220, and 110 torr respectively. The actual reactant composition used in each determination are given in table 5.6.1.a.

Figure 5.6.1.a shows scatter plots of percentages of methane conversion and C2 yield against surface area from data given in table 5.6.1.a. In these plots no direct correlation can be drawn between methane conversion or C_2 yield with surface area

data. This would suggest that the surface area does not determined whether a material will have high activity or not. High C_2 yield can be achieved on materials which have low surface area. The calcined Li_2CO_3/MgO catalysts have surface area of less than $1m^2/g$ but yet resulted about 16% yield to C_2 hydrocarbon. Uncalcined Li_2SO_4/MgO and LiF/MgO (table 5.6.1.a) have surface area in excess of 34 m^2/g but resulted in methane conversion of only about 8% while $CaCO_3$ which has a surface area less than 1 m^2/g, cause higher than 30% of methane conversion at 800°C. However for an active material, the selectivity to C_2 hydrocarbon is generally higher for the lower surface area material.

Table 5.6.1.a The effect of surface area on catalytic activity. 0.2 g of catalyst was used together with reactant total flow rate of 25 ml/min.

Catalyst	SA(m2/g)	Temp/°C	PO_2#	PCH_4	%CH_4con.	%O_2con	%C_2 sel	%$C_2^=/C_2$Tot	%C_2yield
a) Uncalcined Li_2CO_3/MgO with different wt.% Li/Mg									
0.0	22	800	102	209	28.9	87.9	33.7	59.5	9.8
0.7	20	800	96	216	36.3	93.8	47.6	63.9	17.3
1.3	23	800	99	212	34.9	92.5	54.1	64.2	18.8
1.9	30	800	98	217	36.9	93.2	51.4	63.2	18.9
2.3	41	800	94	215	38.4	98.3	51.2	64.0	19.7
5.2	40	800	95	206	36.7	88.2	55.4	59.5	20.3
8.4	28	800	96	207	33.6	81.9	54.3	59.3	18.3
11.5	32	800	97	207	28.4	63.4	62.1	56.1	17.6
14.0	30	800	98	204	23.6	50.7	64.6	51.2	15.3
b) Calcined Li_2CO_3/MgO with different wt.% Li/Mg.									
0.0	15	800	102	219	30.3	98.3	29.6	59.5	8.9
0.2	<1	800	96	216	7.0	9.4	83.7	32.9	5.8
0.5	<1	800	99	212	7.8	11.3	78.7	33.8	6.1
0.6	<1	800	98	217	13.4	20.4	79.1	42.2	10.6
1.3	<1	800	94	215	19.9	34.2	76.0	49.7	15.1
4.4	1	800	95	206	23.9	47.3	66.8	50.7	16.0
7.8	1	800	96	207	24.8	53.0	61.8	52.6	15.3
10.6	1	800	97	207	18.3	39.6	60.3	47.6	11.0
12.8	2	800	98	204	11.6	19.3	71.2	35.5	8.4

c) As supplied MgO									
Strem	19	800	90	230	34.3	100	44.5	67.7	15.3
BDH	22	800	100	228	35.3	100	47.0	64.9	16.6
Merck	25	800	100	225	36.1	100	47.3	67.7	17.1
d) Uncalcined Li_2CO_3 supported on various oxide									
SiO_2	1	800	105	223	2.1	3.1	76.5	35.9	1.6
TiO_2	1	800	105	223	4.2	5.8	74.9	33.8	3.1
$Ca(OH)_2$	9	800	105	223	25.7	59.3	63.9	59.8	11.8
γ-Al_2O_3	166	800	105	223	26.0	88.5	19.1	59.5	5.0
e) Calcined Li_2CO_3 supported on various oxide									
SiO_2	<1	800	102	198	3.0	6.1	52.7	35.5	1.6
TiO_2	<1	800	100	205	7.8	22.3	36.0	27.5	2.8
CaO	1	800	104	224	32.2	73.3	58.5	62.8	18.9
γ-Al_2O_3	31	800	99.7	221	27.6	96.5	26.7	63.2	7.4
f) Uncalcined form of various lithium salts on MgO									
LiCl	31	800	103	234	29.5	75.3	50.6	60.0	14.9
Li_2SO_4	34	800	103	234	5.5	10.9	66.3	29.6	3.7
LiF	35	800	103	234	4.5	10.8	55.7	31.5	2.5
LiOH	42	800	103	234	36.6	81.9	54.3	59.3	18.3
g) Calcined form of various lithium salts on MgO									
LiCl	3.4	800	104	219	37.2	100	43.2	70.1	16.0
Li_2SO_4	<1	800	104	209	4.3	6.9	65.8	25.9	2.8
LiF	<1	800	108	193	2.5	2.1	91.4	30.6	1.3
LiOH	1	800	100	202	26.8	53.9	59.5	32.9	15.9
h) Fresh chemicals									
SiO_2	<1	800	104	212	7.1	22.2	21.8	37.1	1.6
TiO_2	<1	800	104	218	10.1	25.7	36.0	30.1	3.6
$CaCO_3$	<1	800	98	224	30.4	98.2	34.8	54.3	10.6
$SrCO_3$	1	800	101	213	6.0	11.2	28.4	33.8	3.1
Sm_2O_3	2	805	106	220	35.0	100	35.9	50.7	12.6
$BaCO_3$	4	800	98	211	10.8	25.8	50.8	35.1	5.5
$Ca(OH)_2$	9	800	93	225	27.1	97.4	25.1	51.0	6.8
$Mg(OH)_2$	19	800	93	227	33.3	98.0	46.0	61.2	15.3
$AlPO_4$-5	79	800	111	218	19.4	74.2	3.3	0.0	0.6
12%AL_2O_3/SiO_2									
	128	800	101	213	8.7	25.0	16.3	40.1	1.4
γ-Al_2O_3	245	800	106	209	27.8	88.1	5.7	54.8	1.6

* partial pressure in torr.

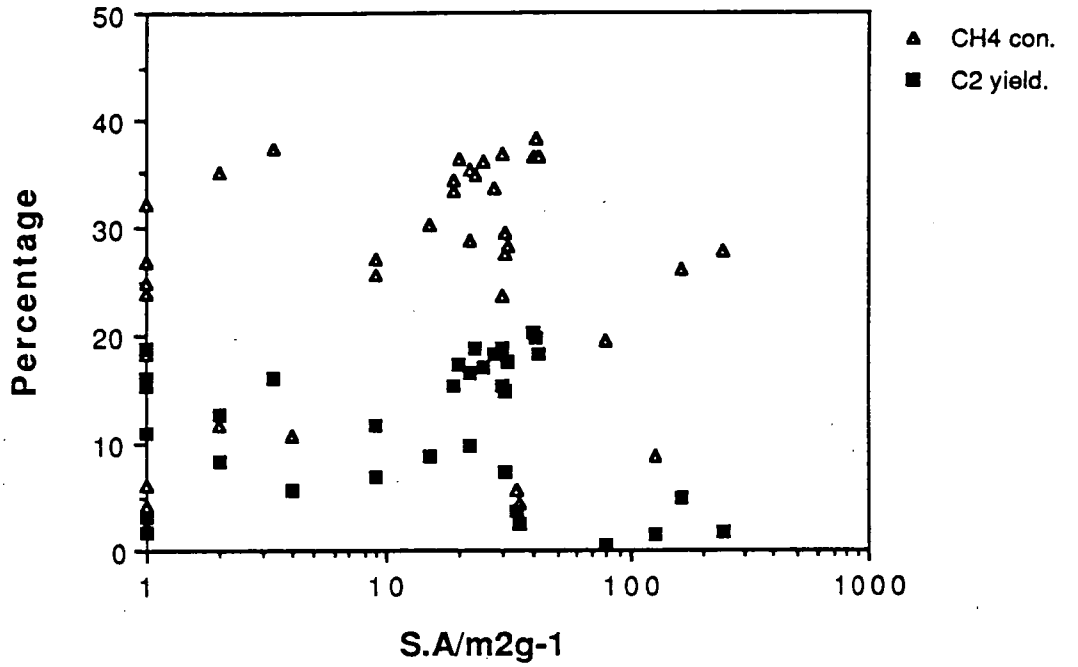

Figure 5.6.1.a The scatter plot of percentages of methane conversion and C_2 yield against surface area of various catalyst. The data used was derived from table 5.6.1.a

The role of surface area in the case of active catalysts is to provide more active site per unit mass. In this case the rate of exhaustive oxidative reaction will be faster over a material with high surface area compared to the same material but having lower surface area. Yamagata et. al., 1987 have shown that lower surface area MgO and CaO resulted in higher C_2 yield than in their higher surface area analogue. Generally for a particular catalyst increase in surface area would indicate that more active site will be available for the reaction. However, in the oxidative reaction of methane, the desired product is more reactive than methane. On the higher surface area catalyst, the products are more likely to be oxidised further to carbon dioxide. On a low surface area catalysts the amount of secondary reaction with the surface will be less and a higher C_2 selectivity can be achieved.

The scatter plots of percentages of selectivity to C_2, C_2 yield and $C_2^=$/Tot. C_2 against percentage of methane conversion of data given in table 5.6.1.a are presented in figure 5.6.1.b. The maximum achievable selectivity to C_2 hydrocarbonat any particular conversion decreases with the increase in methane conversion. In terms of C_2 yield, initially it increase with methane conversion but at higher methane conversion further increase in methane conversion does not leads to significant increase in C_2 yield. Moreover, the percentage of C_2H_4 in the C_2 product increase with methane conversion. These trends have been obseved in section 2.12, and they highlights the inherent nature of oxidative reaction of methane.

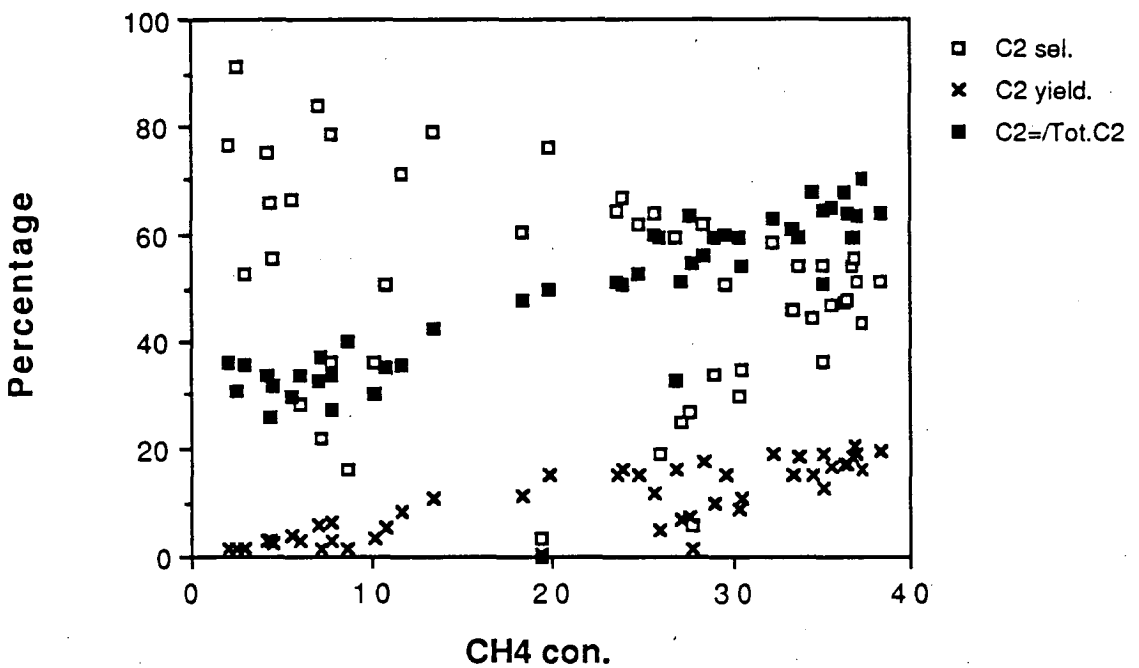

Figure 5.6.1.b The scatter plots of percentages of selectivity to C_2, C_2 yield and $C_2^=/C_{2\ Tot}$ against percentage of methane conversion (data from table 5.6.1.a)

5.6.2 Basicity and activity

Generally it has been reported in the literature (see section 2.12), that chemically basic compounds favours the oxidative coupling to hydrocarbons while

acidic materials favour the exhaustive oxidation of methane. Similar observations were also made in this work. MgO, CaO, Li_2CO_3/MgO, Li_2CO_3/CaO, $CaCO_3$ and other materials prepared from alkali and alkali earth compounds are chemically basic (Tanabe,1981) and showed significant oxidative coupling activity. On the other hand, 12% Al_2O_3/SiO_2 and γ-Al_2O_3 which are acidic in nature resulted in exhaustive oxidation of methane to carbon monoxide and carbon dioxide.

Basicity influenced the selectivity to C_2 hydrocarbons and also changes the product distribution with respect to carbon monoxide and carbon dioxide. Basic materials favour higher selectivity to C_2 hydrocarbon and carbon dioxide. It has been observed in this work that γ-Al_2O_3 promoted the exhaustive oxidation of methane to form mainly carbon monoxide with a total selectivity to C_2 hydrocarbon of 5.7%. When Li_2CO_3 was doped on γ-Al_2O_3, C_2 selectivity increases to 26.7% and carbon dioxide was formed as the major carbon oxide product (see table 5.6.1.a). The doping of the alkaline earth carbonate or oxide on metal oxide should normally increase the basicity of the resulting materials and generally it was found that a better oxidative coupling behaviour resulted.

5.6.3 The effect of catalyst stability on its activity

The question of catalyst stability is important in all catalytic work. A chemically and physically stable catalyst under reaction condition is important in ensuring a consistent activity after a long time on stream. In this work it was observed that a number of the oxidative coupling catalysts are chemically unstable under the reaction condition. The instability of these catalysts can influence their catalytic activity. LiCl/MgO was observed to lose its activity with time on stream due to the loss of LiCl through decomposition (section 4.6.3). Similarly Li_2CO_3/MgO also undergoes phase transformations, at high reaction temperatures due to the melting of Li_2CO_3 (section 5.2.1). The deactivation of Li_2CO_3/MgO catalyst with time onstream is associated with the complete decomposition of the Li_2CO_3 phase. However catalysts

like MgO and γ-Al_2O_3 which do not undergo significant chemical and physical changes under reaction conditions have steady activity with time on stream.

Table 5.6.3.a The correlation between decomposition temperature of alkali carbonates and catalytic activity

Carbonates	Decomposition Temp./°C*	$\%CH_4$ con.	$\%C_2$ yield.
$CaCO_3$	900	30.4	10.6
$BaCO_3$	1350	10.8	5.5
$SrCO_3$	1350	6.0	3.1

*Aylward and Findlay, 1971

Another correlation that was observed is between the activity of the alkali carbonates with their chemical stability. The carbonates which decompose at temperature similar to that under reaction conditions have higher activity for the oxidative reaction of methane (table 5.6.3.a). While there is no direct evidence available it is tempting to suggest that the formation of active sites on these materials are associated with the decomposition of the carbonate species as represented by equation 5.6.3.a

Equation 5.6.3.a MCO_3 <===> (CO_2 +) MO <===> active site

Less active site formation will occur on carbonate with high decomposition temperature. These carbonates have lower catalytic activity compared to that which undergoes decomposition at lower temperatures. The presence of carbon oxide in the enviroment of the carbonates could slow down the decomposition process. Therefore, the presence of CO_2 in the reactant stream may shift the equilibrium to the left, causing less active sites to be formed. Korf et al.,1987 have observed that under these conditions, lower catalytic activity was observed on Li_2CO_3/MgO catalysts. This indicate that the carbonate phase itself is not an active site for oxidative reaction of methane, but served as a precursor for the formation of active sites.

5.7 Summary of findings

1. The formation of a Li_2CO_3 rich layer structure was observed to occur on calcined Li_2CO_3/MgO samples. The extent of the layer formation increases with lithium loading. On crushing the calcined Li_2CO_3/MgO samples, two types of cluster was observed. The large clusters had sharp edges and dimension of about 3 μ-metres while the finer particles were about 0.3 μ-metre in diameter (section 5.2.1).

2. The elemental analysis shows that precalcination caused a higher percentage of lithium lost from Li_2CO_3/MgO materials with initial lithium loadings of less than 2wt.%. Most of the carbonate phase on the calcined Li_2CO_3/MgO catalyst was confirmed to be Li_2CO_3 and it existed in a molten state at reaction temperatures in excess of 700°C (section 5.2.2).

3. The migration and decomposition of Li_2CO_3 phase of the Li_2CO_3/MgO catalyst at high temperature was confirmed in an XPS experiment. The presence of O^- oxygen species was observed on MgO and Li_2CO_3/MgO catalyst after high temperature treatment. On the Li_2CO_3/MgO catalyst, the amount of O^- species diminishes when all of the Li_2CO_3 phase decomposed under evacuation. Since all the surface of the sample was totally covered by lithium oxide, this indicates that the O^- species was an intermediate product of the decomposition of Li_2CO_3 phase on MgO (section 5.2.3).

4. Supporting Li_2CO_3 on MgO resulted in the stabilisation of Li_2CO_3 phase relative to pure Li_2CO_3. The precalcination of Li_2CO_3/MgO sample also enhanced the stabilisation of Li_2CO_3 phase at high temperature. The decomposition of Li_2CO_3 in the Li_2CO_3/MgO catalyst increases under evacuation. The rate of Li_2CO_3 decomposition was observed to increase exponentially with temperature (section 5.2.4).

5. The similarity in the phyiscal and chemical nature of LiOH/MgO and Li_2CO_3/MgO explained their near identical catalytic performances. On LiCl/MgO the 'fluffy' material formed on the catalyst surface was rich in LiCl. This material was lost when the catalyst was used onstream due to the decomposition of LiCl. For

Li_2SO_4/MgO and LiF/MgO, minimal surface layer formation occurs on the calcined materials due to the high melting temperature of Li_2SO_4 and LiF salts (section 5.3.1).

6. In XPS experiments with the Li_2SO_4/MgO catalyst, the O_{1s} spectra showed the prominence of SO_4^{2-} oxygens. The presence of the sulphate ions on MgO prevented the formation of basic oxygen sites and this help explain why Li_2SO_4/MgO catalyst have low activity for oxidative reaction of methane (section 5.3.4).

7. When Li_2CO_3 was supported on various metal oxides, with the exception of MgO, most of the carbonate phase was decomposed when calcined at 900°C for 10 hours. Since most of the lithium was retained in the calcined sample the lithium must exist in oxide forms and was fused into a solid solution with the particles of the magnesium oxide. the stability of Li_2CO_3 on MgO is related to the similarity of the ionic radii of Li^+ and Mg^{2+} ions (section 5.4.1).

8. The presence of OH group on Li_2CO_3 supported on some metal oxides, at high temperature as observed in their high temperature FTIR spectra suggested that the number of higher basicity oxygen sites on these oxide was increased as a result of lithium doping (section 5.5).

9. Surface area per se do not determine whether a particular meterial will be active for the oxidative reaction of methane or not. Materials with low surface area has been shown to demonstrate good oxidative coupling properties. For materials which catalysed the oxidative reaction of methane low surface area will normally results in higher selectivity to C_2 hydrocarbon (section 5.6.1).

10. The increase in selectivity to C_2 hydrocarbons when Li_2CO_3 was supported on γ-Al_2O_3 is likely to be associated with the increase in basicity of the catalyst (section 5.6.2).

11. In the alkaline earth carbonates, higher activity for oxidative reaction of methane was observed on carbonate samples with the lower decomposition temperature (section 5.6.3).

CHAPTER 6

TRANSITION METAL OXIDE DOPED MgO AND Li_2CO_3/MgO CATALYSTS; RESULTS AND DISCUSSION

6.1 Introduction

In chapter 4 it was established the Li_2CO_3/MgO catalyst showed the most promising performance for the oxidative coupling of methane of all the catalysts investigated. In order to improve the performance of this catalyst the effect of doping transition metal oxides on its activity was investigated. The activity of MgO doped with various transition metal oxides were also determined. The physico-chemical nature of these catalysts were studied by the XRD, SEM, X-Ray microprobe analysis and TPR techniques. Correlations between the physico-chemical nature of the catalysts and their catalytic activity were drawn.

6.2 Activity Studies

6.2.1 Preliminary studies on the doping effect of different transition metal oxide on the activity of fresh and calcined Li_2CO_3/MgO catalysts

6.2.1.1 Composition and activity of fresh and calcined catalysts

The preparation of the catalysts was performed according to the procedure outlined in section 3.2. The composition of these catalysts was determined by the AAS and presented in table 6.2.1.1.a, in the form of weight (wt.) and mole percentage of Li/Mg and M/Mg, where M is the transition metal . The average wt.%Li/Mg of the catalyst was 8.7 corresponding to 30.5 mole% of Li/Mg while the average wt.% of M/Mg was only 2.6% corresponding to around 1 mole %. The purpose of adding of such a small amount of transition metal oxide relative to lithium carbonate is to study any promoting effect of these oxides on the activity of Li_2CO_3/MgO catalysts.

Generally, the weight and mole percentages of Li/Mg and M/Mg of the calcined catalysts are slightly lower than that of fresh (uncalcined) samples suggesting the loss of these ions during the precalcination process.

Table 6.2.1.1.a The composition calcined (Cal.) and fresh (Uncal) Li_2CO_3/MgO catalysts doped with various transition metal oxide (M_xO_y)

Catalyst	Li/Mg				M/Mg			
	Wt.%		Mole%;		Wt.%		Mole%	
	Cal.	Uncal.	Cal.	Uncal.	Cal.	Uncal.	Cal.	Uncal.
Li_2CO_3/MgO	8.4	7.8	27.3	29.4	-	-	-	-
$Fe/Li_2CO_3/MgO$	8.4	8.0	29.4	28.0	2.7	2.5	1.2	1.1
$Cu/Li_2CO_3/MgO$	8.5	8.1	29.8	28.4	3.4	3.3	1.3	1.3
$Ni/Li_2CO_3/MgO$	8.7	8.3	30.5	29.1	3.3	3.1	1.4	1.3
$Co/Li_2CO_3/MgO$	8.2	7.4	28.7	25.9	2.7	2.6	1.1	1.1
$Cr/Li_2CO_3/MgO$	8.1	7.6	28.4	26.6	1.1	1.0	0.5	0.5
$Mn/Li_2CO_3/MgO$	9.0	7.9	31.5	27.7	2.6	2.3	1.2	1.0
$Zn/Li_2CO_3/MgO$	9.5	7.4	33.3	25.9	3.6	3.3	1.3	1.2

The oxidative reaction of methane over calcined, Li_2CO_3/MgO doped with different transition metal oxide at 800°C have been determined and are given in table 6.2.1.1.b. In these determination, 0.2 g of catalyst was always used. The catalyst was normally pretreated in air at 800°C for 2 hours before the exposure to reactant gas and the first gas sampling for analysis was normally done after half an hour on stream. The results presented in this chapter were that after 2 hours on-stream. The total reactant flow rate was 25 ml/min with helium being used as the diluent gas. A P_{O_2}/P_{CH_4} ratio of approximately 0.5 was always used. The actual reactant compositions in the screening of each catalyst are also given in the table.

The preliminary results (table 6.2.1.1.b) show that the doping of Li_2CO_3/MgO with Mn, Fe, Co and Cu oxides causes higher methane conversions (by about 6%) than that over Li_2CO_3/MgO catalyst. On the other hand, the presence of Ni and Zn oxides resulted in lower methane conversion. When Li_2CO_3/MgO catalyst was

doped with manganese, iron and cobalt oxides, the C_2 yields were 18.1, 20.0 and 19.2% respectively. These yields are slightly higher than that over Li_2CO_3/MgO (17.2%). The presence of nickel, copper and zinc oxides resulted in lower C_2 yield relative to the blank Li_2CO_3/MgO catalyst while the presence of chromium oxide on Li_2CO_3/MgO resulted in C_2 yield of 1.8% only.

Table 6.2.1.1.b The activity of calcined Li_2CO_3/MgO catalyst doped with different transition metal oxide.

M*	P_{O_2}#	P_{CH_4}	%con.CH_4	O_2;	%sel.C_2H_6	C_2H_4	CO	CO_2	Tot.C_2;	%C_2yield;	%$C_2^=$/Tot.C_2
-	117	219	26.8	48.9	30.3	33.8	0.0	35.9	64.1	17.2	52.7
Cr	100	212	25.0	100.0	4.7	2.4	0.0	92.9	7.1	1.8	3.4
Mn	93	251	32.2	92.6	25.3	32.6	0.0	42.1	57.9	18.7	56.3
Fe	89	228	31.6	78.9	29.5	33.7	0.0	36.8	63.2	20.0	53.3
Co	91	229	29.7	70.9	31.3	33.6	0.0	35.1	64.9	19.2	51.7
Ni	97	233	21.3	48.7	32.6	31.1	1.8	34.4	63.7	13.6	48.8
Cu	91	243	28.3	91.6	23.7	24.4	0.0	51.9	48.1	13.6	50.7
Zn	101	217	18.8	37.4	36.2	29.7	0.0	34.2	65.8	12.4	45.1

* transition metal existing as oxide M_xO_y, # partial pressure in torr with a total flow rate of 25 ml/min

Generally, it was observed (table 6.2.1.1.b) that the product distribution over Li_2CO_3/MgO catalysts doped with transition metal oxides, other than chromium oxide, is quite similar to that over the undoped Li_2CO_3/MgO catalyst. The selectivity to C_2 over these catalysts, was about 60% and carbon dioxide is the favoured carbon oxide product. The percentage of ethene in the C_2 product over these catalysts was about 50%.. The similarity in the product distribution of oxidative reaction of methane over these catalysts suggest that the presence of the transition metal oxides (except chromium oxide) results in mainly physical changes on the Li_2CO_3/MgO catalyst.. The presence of chromium oxide, however, drastically changes the nature of the oxidative reaction of methane, favouring the oxidative reaction of methane to carbon

dioxide. This suggests that chromium oxide causes significant chemical changes on the surface of the doped Li_2CO_3/MgO catalyst.

Table 6.2.1.1.c The activity of fresh Li_2CO_3/MgO catalyst doped with different transition metal oxide.

M*	P_{O_2}	#P_{CH_4}	%con. CH_4	O_2;	%sel.C_2H_6	C_2H_4	CO	CO_2	Tot.C_2;	%C_2yield;	%$C_2^=$/Tot.C_2
-	105	228	33.6	81.9	22.1	32.2	1.3	44.4	54.3	18.3	59.3
Cr	97	235	26.1	98.2	16.5	10.9	0.0	72.6	27.4	7.2	39.9
Mn	97	235	35.1	98.1	21.3	31.7	0.0	47.0	53.0	18.6	59.8
Fe	97	228	35.5	98.3	20.9	33.0	0.0	46.1	53.9	19.1	61.2
Co	97	235	32.6	87.7	23.9	32.9	0.0	43.3	56.7	18.5	57.9
Ni	97	235	24.6	54.6	30.3	36.6	1.8	31.3	66.9	16.5	54.7
Cu	97	235	33.8	92.1	21.6	33.0	1.2	44.2	54.6	18.5	60.5
Zn	97	235	30.8	77.7	25.4	34.6	2.5	37.5	60.0	18.5	57.6

* transition metal oxide existing as M_xO_y, # partial pressure in torr

The activity data of the uncalcined Li_2CO_3/MgO catalysts doped with different transition metal oxides at 800°C are presented in table 6.2.1.1.c. Higher methane conversion (>30%) was observed over these catalysts compared to that over the corresponding calcined analogue. Except for the chromium oxide doped catalysts, the C_2 selectivity over the fresh catalysts (50%) are generally slightly lower than that over their calcined analogues (60%). In the case of the chromium oxide doped catalyst, C_2 selectivity of 27.4% was observed and this which is higher than that of the calcined analogue. C_2 yield of around 18% was observed over most of the uncalcined catalysts. The fresh chromium oxide doped catalyst, however, resulted in only 7.2% yield to C_2, indicating that, as in the calcined sample, the exhaustive oxidation of methane to carbon dioxide was favoured.

The doping of Li_2CO_3/MgO with transition metal oxide (about 2.6wt.%) is most likely to influence its catalytic activity. Depending on the nature of the transition

metal oxide, the oxidative coupling activity of Li_2CO_3/MgO can be increased, reduced or destroyed. Manganese, iron and cobalt oxides increase, while nickel,copper and zinc oxides decrease the oxidative coupling activity of Li_2CO_3/MgO catalyst. The presence of chromium oxide on Li_2CO_3/MgO catalyst, however, destroyed most of the oxidative coupling activities of the catalyst, causing the exhaustive oxidation of methane.

An interesting observation made in this study is that generally the overall product distribution of the oxidative reaction of methane over the calcined and uncalcined doped catalysts are similar to that over Li_2CO_3/MgO. The precalcination mainly resulted in the decrease of methane conversion but only has a slight effect on the product distribution. Over the uncalcined catalysts a slightly higher methane conversion occurs together with slightly higher C_2H_4/Tot. C_2 ratio (60%), while selectivity to carbon oxide over both the calcined and uncalcined catalysts is still predominantly to carbon dioxide.

These results indicate that the methane conversion in oxidative coupling reaction over Li_2CO_3/MgO catalyst can be improved through the doping of transition metal oxid, especially manganese oxide. However, since the presence of about 2.6wt.% of transition metal oxide on Li_2CO_3/MgO (except for chromium oxide), does not significantly change the product distribution, it is likely that only the physical nature of the catalyst is affected by the doping. In this respect the transition metal oxide presence on Li_2CO_3/MgO does not seem to play any direct role in the oxidative reaction of methane.

Over the chromium doped catalyst, however, the chromium oxide is likely to play the dominant role in facilitating the exhaustive reaction of methane to carbon dioxide. It was observed that the C_2 hydrocarbon yield over fresh chromium doped Li_2CO_3/MgO catalyst (7.2%) was higher than that over the calcined analogue (1.8%). The Li_2CO_3 content of the uncalcined catalyst relative to the calcined analogue could be responsible for the higher oxidative coupling activity of the fresh catalyst. This can

happen through the fomation of the carbonate layer on the catalyst surface which limit the availability of chromium oxide on the surface of the catalysts during the reaction.

6.2.1.2 The effect of temperature on the activity of calcined catalysts

The effect of temperature on the activity of the calcined transition metal oxide doped Li_2CO_3/MgO catalysts have been determined and are presented in table 6.2.1.2.a. Except for the chromium oxide doped catalyst, a similar trends between product selectivity with reaction temperature was observed over all the catalysts. The relative selectivity to the various hydrocarbon product over these catalysts at any particular reaction temperature is also quite similar. The selectivity to C_2H_4 relative to total C_2 selectivity increase with temperature. Carbon dioxide is the major carbon oxide product over these catalysts at all reaction temperatures. Over chromium oxide doped Li_2CO_3/MgO, carbon dioxide was the major product (>80%) at all reaction temperatures. The selectivity to C_2 hydrocarbon over this catalyst at 710°C was only 17%, and it decreased with the reaction temperatures.

In terms of methane conversion, the catalyst doped with manganese oxide resulted in the highest methane conversion at all reaction temperatures while the one doped with zinc oxide showed the lowest conversion. The C_2 hydrocarbon yields over manganese oxide doped catalyst at 760°C is similar to that over Li_2CO_3/MgO catalyst at 800°C. In this respect the
presence of manganese oxide on Li_2CO_3/MgO caused the oxidative reaction of methane to occur at relatively lower temperature.

The presence of about 3 wt % (about 1 mole%) of transition metal oxide on Li_2CO_3/MgO catalysts does affect the catalytic activity of Li_2CO_3/MgO. Chromium oxide caused the most significant changes causing the catalyst to favour exhaustive oxidation of methane to carbon dioxide. On the other hand the other transition metal oxide only affects the extent of methane conversion while maintaining the selectivity to the various products. Manganese oxide promotes the conversion of methane while zinc oxide does the reverse. Since the product distribution from the oxidative reaction

Table 6.2.1.2.a The effect of temperature on the activity of calcined Li_2CO_3/MgO catalyst doped with different transition metal oxides.

T/°C	P_{O_2}#	P_{CH_4}	%con. CH_4	O_2;	%sel.C_2H_6	C_2H_4	CO	CO_2	Tot.C_2;	%C_2yield;	%$C_2^=$/Tot.C_2
Catalyst: Li_2CO_3/MgO											
800	117	219	26.8	48.9	30.3	33.8	0.0	35.9	64.1	17.2	52.7
760			13.8	22.4	46.4	23.2	0.0	30.5	69.6	9.6	33.3
710			6.0	13.6	41.1	7.3	0.0	51.6	48.4	2.9	15.1
Catalyst: Cr*/Li_2CO_3/MgO											
800	100	212	24.8	99.1	4.7	2.4	0.0	92.9	7.1	1.8	34.3
760			14.3	55.8	5.8	3.8	0.0	90.4	9.6	1.4	39.3
710			5.8	21.3	10.9	6.0	0.0	83.1	16.9	1.0	35.6
Catalyst:Mn/Li_2CO_3/MgO											
800	93	251	32.2	92.6	25.3	32.6	0.0	42.1	57.9	18.7	56.4
760			28.2	76.7	29.3	31.8	0.0	38.9	61.1	17.2	52.1
710			9.1	23.3	39.2	24.1	0.0	36.7	63.3	5.6	38.0
Catalyst:Fe/Li_2CO_3/MgO											
800	89	228	31.6	78.9	29.5	78.9	0.0	36.8	63.2	20.0	53.2
760			20.9	40.3	40.6	30.4	0.0	29.0	71.0	14.8	42.8
710			7.0	13.0	57.1	18.1	0.0	24.9	75.2	5.3	24.1
Catalyst: Co/Li_2CO_3/MgO											
800	91	229	29.7	70.9	31.3	33.6	0.0	35.1	64.9	19.2	51.7
760			15.5	29.2	48.0	27.5	0.0	24.5	75.5	11.7	36.4
710			5.8	11.4	57.3	14.7	0.0	27.9	72.0	4.2	20.4
Catalyst: Ni/Li_2CO_3/MgO											
800	97	235	21.3	48.7	32.6	31.1	1.8	34.4	63.7	13.6	48.8
760			14.7	29.0	42.3	28.4	1.8	32.5	70.8	10.4	40.0
710			4.0	8.2	51.8	15.7	0.0	32.5	67.5	2.7	23.3
Catalyst: Cu/Li_2CO_3/MgO											
800	91	243	28.3	91.6	23.7	24.4	0.0	51.9	48.1	13.6	50.7
760			19.2	56.6	31.7	22.3	0.0	46.0	54.0	10.4	41.3
710			8.1	23.1	41.2	13.7	0.0	45.1	54.9	4.4	25.0
Catalyst: Zn/Li_2CO_3/MgO											
800	101	217	18.8	37.4	36.2	29.7	0.0	34.2	65.8	12.4	45.1
760			11.2	18.6	49.1	24.6	0.0	26.3	73.7	8.2	33.4
710			4.6	9.1	80.8	13.0	0.0	36.21	63.8	2.9	20.4

partial pressure in torr; *transition metal oxide existing as M_xO_y

of methane over most of these catalysts at any particular reaction temperature are similar, this suggests that the transition metal oxides are not directly involved in the reaction, especially as a redox sites. However the presence of these transition metal oxide on Li_2CO_3/MgO could results in the variation physical nature of the catalysts and hence influencing the extent of methane conversion.

Driscoll et al., 1985a, have proposed the role of ionic radii in the formation and stability of Li^+O^- type active sites. In chapter 5 it was observed that the ionic radii factor is important in determining whether a stable solid matrix can be formed between the support metal oxide and Li_2CO_3. Li_2CO_3 forms a good solid matrix with MgO because Li^+ and Mg^{2+} have similar ionic radii (section 5.4.1). On other supports, due to the differences in the ionic radii of Li^+ and the metal ion, Li_2CO_3 is not stabilised and undergoes decomposition at high temperature. When a third component was added onto the Li_2CO_3/MgO system it is likely that it will intefere in the formation of the solid solution. As observed in this work, the presence of the third component does affect the catalytic activity of Li_2CO_3/MgO catalysts. In order to probe further the physical and chemical nature of the transition metal oxide doped Li_2CO_3/MgO catalyst and its effects on the oxidative reaction of methane, the effects of different loading of Fe, Zn, Mn, and Cr oxides on Li_2CO_3/MgO have been investigated. The effects of the 'ionic radii factor' will also be monitored since Fe^{2+}, Zn^{2+}, Mn^{2+} and Cr^{3+} have ionic radii spanning from lower to higher than that of Li^+ (74 pm, where $1pm=10^{-12}m$, see table 6.5.a).

6.2.2 Different loadings of Iron oxide on Li_2CO_3/MgO and MgO

6.2.2.1 Catalyst composition

The composition of the iron oxide doped Li_2CO_3/MgO and MgO catalysts have been studied by AAS and the results are presented in table 6.2.2.1.a and table 6.2.2.1.b. respectively. These catalysts are marked with a number and alphabet C for sample which was calcined at 900°C for 10 hours, or F for the fresh, uncalcined samples. Generally the percentage of Li/Mg and Fe/Mg of the calcined catalysts are

lower than that of the corresponding uncalcined catalyst. This indicates that some loss of the lithium and iron compound relative to MgO could have occurred.

Table 6.2.2.1.a: Composition of calcined (C) and fresh (F) Li_2CO_3/MgO catalysts doped with different loadings of iron oxide

Sample	Li/Mg		Fe/Mg	
	Wt%	Mole%	Wt.%	Mole%
1C	5.9	20.7	0.4	0.2
1F	7.9	27.7	0.7	0.3
2C	6.9	24.2	1.0	0.4
2F	8.2	28.7	1.1	0.5
3C	6.7	23.5	6.0	2.6
3F	7.8	27.3	6.3	2.7
4C	7.2	25.2	28.6	12.4
4F	7.1	24.9	30.0	13.1

Table 6.2.2.1.b: Composition of calcined (C) and fresh (F) MgO catalysts doped with different loadings of iron oxide

Sample	Fe/Mg	
	Wt.%	Mole%
5C	0.6	0.3
5F	0.8	0.4
6C	1.1	0.5
6F	1.4	0.6
7C	5.4	2.4
7F	5.8	2.5
8C	34.2	14.9
8F	35.4	15.4

6.2.2.2 The activity of iron oxide doped Li_2CO_3/MgO and MgO catalysts

The activity of the various iron oxide doped Li_2CO_3/MgO catalysts at 805°C are presented in table 6.2.2.2.a. Over the catalysts with iron oxide loading of less than

6.0 wt % (1C-3C), methane conversion and C_2 selectivity of about 30 and 60% was observed respectively with about 60% O_2 consumption. Generally the percentage of C_2 yield over these catalysts were higher than 18%. The highest C_2 yield of 19.3% was observed on the 28.6wt.% (4C) iron oxide doped catalyst.

Table 6.2.2.2.a The activity of calcined Li_2CO_3/MgO catalyst doped with different loading of iron oxide.

T/°C	P_{O_2}#	P_{CH_4}	%con. CH_4	O_2;	%sel.C_2H_6	C_2H_4	CO	CO_2	Tot.C_2;	%C_2yield;	%$C_2^=$/Tot.C_2
Catalyst: 1C*											
805	105	210	30.64	63.2	26.1	33.9	1.7	38.3	60.0	18.4	56.5
760			18.5	35.3	43.6	21.1	0.0	35.3	64.7	12.0	32.5
710			6.7	29.4	52.2	18.3	0.0	29.4	70.6	4.8	26.0
Catalyst: 2C											
805	102	206	28.3	54.8	28.9	54.8	0.0	35.4	64.4	18.3	55.5
760			13.1	18.6	51.3	26.7	0.0	22.0	78.0	10.2	34.3
710			4.0	4.0	69.8	20.9	0.0	9.0	91	3.6	23.1
Catalyst:3C											
800	102	209	30.9	66.2	27.0	32.2	0.0	40.8	59.2	18.3	54.4
760			15.5	26.5	44.1	26.1	0.0	32.5	70.1	10.8	37.2
710			4.4	4.8	65.2	21.7	0.0	13.0	87.0	3.8	25.0
Catalyst:4C											
800	102	216	36.9	96.4	20.6	27.2	0.0	52.2	47.8	19.3	56.8
760			20.5	51.1	30.3	19.9	0.0	49.9	50.1	10.3	42.8
710			5.4	11.9	43.7	13.7	0.0	42.6	57.4	3.1	23.9

partial pressure in torr; * see table 6.2.2.1.a for catalysts composition

The activity of the iron oxide doped MgO at 805°C as given in table 6.2.2.2.b. The results are in contrast to that of the doped Li_2CO_3/MgO catalysts in Table 6.2.2.2.a. The exhaustive oxidation of methane to carbon oxide was favoured over these catalysts. Full consumption of oxygen occurs even over the catalysts which was doped with 0.6wt% (5C) of iron oxide. The highest selectivity to C_2 of 30% was observed over 0.6wt.% iron oxide doped MgO catalyst and a much lower C_2

selectivity was observed at higher loading of iron oxide. It was also observed that the amount of methane conversion decreased, while selectivity to carbon dioxide increased at higher loading of iron oxide. This suggested that at higher loading of iron oxide, the exhaustive oxidation reaction becomes more favoured, causing less oxygen being available for methane oxidative coupling.

Table 6.2.2.2.b The activity of MgO catalyst doped with different loading of iron oxide at 805°C

N*	P_{O_2}#	P_{CH_4}	%con. CH_4	O_2;	%sel.C_2H_6	C_2H_4	CO	CO_2	Tot.C_2;	%C_2yield;	%$C_2^=$/Tot.C_2
5C	112	223	28.5	100.0	8.8	1.0	12.6	77.7	9.8	2.8	10.3
6C	113	220	28.1	100.0	4.2	0.0	17.5	78.3	4.2	1.2	0.0
7C	110	220	25.9	100.0	1.4	0.0	8.3	90.3	1.4	0.4	0.0
8C	109	229	25.2	100.0	4.6	1.0	3.1	91.6	5.3	1.3	13.2

* see table 6.2.2.1.b for catalysts composition, # partial pressure in torr

These results indicate the major difference in the nature of iron oxide doped Li_2CO_3/MgO and MgO catalysts. The iron oxide doped on Li_2CO_3/MgO catalysts retained the oxidative coupling properties while the doped MgO doped resulted in the the exhaustive oxidation of methane to form carbon oxide. For the iron oxide doped MgO catalysts, the iron oxide is likely to serve as a redox centre during the oxidative reaction of methane. The oxygen transfer on this catalyst will be facilitated and hence the exhaustive oxidation of methane to carbon oxide occurred. In the case of the iron oxide doped Li_2CO_3 catalysts as was discussed earlier, the iron oxide are not directly involved in the reaction. The iron oxide phases are not available for the surface reaction possibly due to the formation of the Li_2CO_3 layer on the surface of the catalysts.

The effect of temperature on the activity of different loading of iron oxide on Li_2CO_3/MgO catalysts have been determined and the results are presented in table 6.2.2.2.a. Similar trends were observed with respect to the product distribution over all of these catalysts with reaction temperature. At low temperature ethane is the major C_2 product and it decreases at higher temperature. As the selectivity to C_2H_6 decreases

at higher temperature, selectivity to ethene increases. At all reaction temperatures, carbon dioxide is the major carbon oxide product. With respect to C_2 yield it normally increases with the increase in reaction temperature. It was also observed that on the 28.6wt% iron oxide doped catalyst, higher conversion of methane and lower selectivity to C_2 relative to the other catalyst was observed at any particular temperature.

This result further highlighted that the present of iron oxide on Li_2CO_3/MgO at a loading less than 28.6% only effected the percentage of methane conversion. In the case of iron oxide doped on MgO, the exhaustive oxidation of methane to carbon dioxide was promoted. Since the product distribution from iron oxide doped Li_2CO_3/MgO catalyst was not drastically changed even at a loading of 28.6%, this indicated that the iron oxide did not play any major role in the oxidative reaction of methane over the doped Li_2CO_3/MgO catalysts.

In chapter 5 it has been shown that the Li_2CO_3/MgO catalyst surface is enriched in Li_2CO_3 phase at high temperature. Such situation could also happened on the iron oxide doped Li_2CO_3/MgO catalysts. Iron can exist in oxidation state of +2 and +3 with the ionic radiis of 78 and 64 pm respectively (see table 6.5.a). Since the ionic radii of these ions is similar to that of Li^+ (74 pm) and Mg^{2+} (72 pm) respectively, the presence of iron oxide will not significantly alter the physical nature of the catalysts. As in the undoped Li_2CO_3/MgO catalyst the Li_2CO_3 rich layer will also be formed on the iron oxide doped Li_2CO_3/MgO catalysts making the iron oxide inaccessible to the reactant. This would make the the nature of oxidative reaction of methane on the iron oxide doped catalyst similar to that on the Li_2CO_3/MgO catalyst.

6.2.3 Different loadings of zinc oxide on Li_2CO_3/MgO and MgO

6.2.3.1 Catalysts composition

The composition of zinc oxide doped Li_2CO_3/MgO and MgO catalysts have been determined by AAS and the result presented in table 6.2.3.1.a and 6.2.3.1.b. respectively.

Table 6.2.3.1.a: Composition of calcined (C) and fresh (F) Li_2CO_3/MgO catalysts doped with different loading of zinc oxide

Sample	Li/MgO		Zn/Mg	
	Wt%	Mole%	Wt.%	Mole%
9C	6.1	21.4	0.7	0.3
9F	8.0	28.0	0.7	0.3
10C	4.8	16.8	1.6	0.6
10F	6.8	23.8	1.6	0.6
11C	6.9	24.2	6.9	2.6
11F	7.5	26.3	7.1	2.6
12C	6.1	21.4	32.1	11.9
12F	6.9	24.2	35.0	13.0

Table 6.2.3.1.b: Composition of calcined (C) and fresh (F) MgO catalysts doped with different loading of zinc oxide

Sample	Zn/Mg	
	Wt.%	Mole%
13C	0.7	0.30
13F	1.2	0.5
14C	1.6	0.6
14F	1.8	0.7
15C	5.9	2.2
15F	6.5	2.4
16C	25.4	9.4
16F	28.8	10.7

6.2.3.2 The activity of zinc oxide doped Li_2CO_3/MgO and MgO catalysts

In the preliminary catalyst screening (section 6.2.1.1) it was observed that the presence of zinc oxide on Li_2CO_3/MgO caused a slight decrease in methane conversion. In this section the effect of zinc oxide loading on the activity of Li_2CO_3/MgO catalyst has been determined and the activity data are presented in table

6.2.3.2.a. Comparing the activity of these catalysts at 805°C it is observed that the percentage of methane conversion over the catalysts with low loading of zinc oxide are less than that over the comparable iron oxide doped catalyst. It was also observed that when the zinc oxide loading was 6.9wt.% (11C), a lowest methane conversion of around 23% occurred.

The activity of zinc oxide doped MgO catalyst at 805°C has been determined and the results are presented in table 6.2.3.2b. Exhaustive oxidation reaction, favouring the formation of carbon dioxide also occurs on these catalysts as in the iron oxide doped MgO. A slight decrease in methane conversions occurs with the increase in Zn loading and full oxygen consumption occurs over all of these catalysts.

Table 6.2.3.2.a The activity of calcined Li_2CO_3/MgO catalyst doped with different loadings of zinc oxide.

T/°C	PO_2#	PCH_4	%con. CH_4	O_2;	%sel.C_2H_6	C_2H_4	CO	CO_2	Tot.C_2;	%C_2yield;	%$C_2^=$/Tot.C_2
Catalyst: 9C*											
805	116	234	26.6	58.0	29.7	25.7	1.9	42.4	55.7	14.8	46.2
760			16.6	41.7	35.5	9.3	0.0	55.3	44.7	7.4	20.7
710			8.0	21.5	33.3	5.4	0.0	61.3	38.7	3.1	13.9
Catalyst: 10C											
805	112	225	30.4	60.9	28.1	33.7	1.6	36.6	61.8	18.8	54.5
760			14.6	27.3	47.6	15.9	0.0	36.6	63.4	9.2	25.0
710			4.9	7.9	57.9	12.7	0.0	29.4	70.6	3.5	17.9
Catalyst:11C											
805	107	214	22.4	41.6	32.5	33.4	0.0	34.1	65.9	14.8	54.4
760			11.5	17.7	51.1	22.7	0.0	26.2	73.8	8.5	37.2
710			3.3	2.0	77.3	22.7	0.0	0.	100	2.0	25.0
Catalyst:12C											
800	107	224	32.2	74.9	28.0	26.1	1.6	43.3	54.1	17.4	48.2
760			16.6	35.9	45.8	10.8	0.0	43.3	56.6	9.4	19.1
710			4.7	5.9	68.6	10.3	0.0	18.1	81.9	3.8	16.2

partial pressure in torr; * see table 6.2.3.1.a for catalysts composition#

Table 6.2.3.2.b The activity of MgO catalyst doped with different loadings of zinc oxide at 805°C

N*	P_{O_2}#	P_{CH_4}	%con. CH_4	O_2;	%sel.C_2H_6	C_2H_4	CO	CO_2	Tot.C_2;	%C_2yield;	%$C_2^=$/Tot.C_2
13C	107	199	29.1	100	9.3	0.0	0.0	90.7	9.3	2.7	0.0
14C	109	215	27.8	100	8.1	0.0	6.3	85.6	8.1	2.2	0.0
15C	105	207	27.9	100	7.3	0.0	10.0	82.7	7.3	2.0	0.0
16C	105	217	27.0	100	10.6	0.0	4.9	84.5	10.6	2.9	0.0

* see table 6.2.2.1.b for catalysts composition,; # partial pressure torr

The effect of reaction temperature on the activity of different loading of zinc oxide on Li_2CO_3/MgO catalysts were also given in table 6.2.3.2.a. Generally, similar trends between the product distribution and temperature was observed over these catalysts. At low temperature, ethane and carbon dioxide are the major products. At higher reaction temperature the overall C_2 yield and selectivity to C_2H_4 increases while that to C_2H_6 decreases. However, it was also observed that for the 6.9% (11C) catalysts, methane conversion was lower than that over all the other catalysts at any reaction temperature. These results confirm that the presence of zinc oxide on Li_2CO_3/MgO resulted in a slight decrease in methane conversion. However since a similar product distribution was observed, it is likely that the present of zinc oxide on Li_2CO_3/MgO also resulted in only physical changes on the catalysts.

Zinc has a singular oxidation state of +2 with an ionic radii of 74 pm (see table 6.5.a). In this respect the presence of zinc oxide on the Li_2CO_3/MgO catalysts should cause minimal changes on the physical nature of Li_2CO_3/MgO. However, due to the similarity in the ionic radii of Zn^{2+} and Li^+ (each at 74pm), it is likely that the Li_2CO_3 will form a better solid matrix with ZnO than with MgO. Enrichment of zinc oxide with Li_2CO_3 phase should occur on the zinc oxide doped Li_2CO_3/MgO catalysts and this could possibly explain the variation of zinc oxide doped catalyst with loading. Matsuura et. al., 1986 has observed that the Li_2CO_3/ZnO have a good oxidative coupling activity. In this work it was observed that the presence of zinc oxide on

Li_2CO_3/MgO catalyst resulted in activity similar to the blank Li_2CO_3/MgO catalyst. It is possible that the activity of the Li_2CO_3/ZnO catalyst are associated with the stabilisation of the Li_2CO_3 phase on the zinc oxide phase due to the similarity between the ionic radii of Zn^{2+} and Li^+.

In the case of the zinc oxide doped MgO catalyst it was observed that the exhaustive oxidation is favoured as in the iron oxide doped MgO. Since zinc ion predominantly exists in the oxidation state of +2 and is not reducible under the reaction condition (Bhasin, 1988), a redox process involving ZnO is highly unlikely. The presence of ZnO could result in the increase of surface defects on MgO resulting in the increase of exhaustive oxidation of methane to carbon oxide.

6.2.4 Different loadings of manganese oxide on Li_2CO_3/MgO and on MgO

6.2.4.1 Catalyst composition

The composition of different loadings of manganese oxide on Li_2CO_3/MgO and MgO have been studied by AAS and the analysis given in Table 6.2.4.1.a and Table 6.2.4.1.b respectively. As it was observed in the other catalytic system, the calcination resulted in a slight loss of lithium and manganese compounds relative to MgO.

Table 6.2.4.1.a Composition of calcined (C) and fresh (F) Li_2CO_3/MgO catalysts doped with different loadings of manganese oxide

Sample	Li/Mg		Mn/Mg	
	Wt%	Mole%	Wt.%	Mole%
17C	6.2	21.7	0.2	0.1
17F	7.2	25.2	0.2	0.1
18C	5.9	20.7	0.6	0.3
18F	6.9	24.2	0.6	0.3
19C	6.4	22.4	4.6	2.0
19F	7.0	24.5	5.0	2.2
20C	6.9	24.2	19.8	8.8
20F	7.1	24.9	26.6	11.8

Table 6.2.4.1.b: Composition of calcined (C) and fresh (F) MgO catalysts doped with different loadings of manganese oxide

Sample	Mn/Mg	
	Wt.%	Mole%
21C	0.3	0.1
21F	0.4	0.2
22C	1.0	0.4
22F	1.0	0.4
23C	4.5	2.0
23F	5.3	2.3
24C	20.7	9.2
24F	21.0	9.3

6.2.4.2 The activity of the manganese oxide doped Li_2CO_3/MgO and MgO catalysts

The activity of Li_2CO_3/MgO doped with different loadings of manganese oxide at 805°C is strongly affected by the loading (see table 6.2.4.2.a). The presence of manganese oxide on Li_2CO_3/MgO resulted in a siginificant increase in methane conversion. At a loading of 0.2%Mn (17C), 36% of methane conversion occurred and the highest methane conversion of 39% occured over the 0.6wt.%Mn (18C) catalyst. A further increase in loading resulted in a decrease in amounts of methane conversion together with an increase in the selectivity to carbon dioxide. The carbon oxide products over all the catalyst is mainly in the form of carbon dioxide. The selectivity to C_2 hydrocarbon decreases continuously with manganese loading and a maximum C_2 yield of 20.7% occurred over the 0.6wt%Mn (18C) catalyst.

The activity of different loading of manganese oxide on MgO at 805°C have been determined and are presented in table 6.2.4.2.b. These catalysts favour the exhaustive oxidation of methane to carbon dioxide. Full oxygen consumption occurs even at low manganese loading. It was also observed that at higher manganese loading the amount of methane converted decreased slightly while selectivity to carbon dioxide increased.

Table 6.2.4.2.a The activity of calcined Li_2CO_3/MgO catalyst doped with different loadings of manganese oxide.

T/°C	P_{O_2}#	P_{CH_4}	%con. CH_4	O_2;	%sel.C_2H_6	C_2H_4	CO	CO_2	Tot.C_2;	%C_2yield;	%$C_2^=$/Tot.C_2
Catalyst: 17C*											
805	112	233	36.1	83.9	23.6	31.4	0.0	45.1	55.0	19.8	57.1
760			23.5	48.8	35.0	25.9	0.0	39.1	60.9	14.3	42.5
710			8.1	15.4	48.6	15.8	0.0	6.7	64.5	5.2	24.6
Catalyst: 18C											
805	109	228	39.1	94.5	22.0	31.0	0.0	47.0	53.0	20.7	58.4
760			28.4	60.2	31.3	29.7	0.0	39.1	60.9	17.3	48.7
710			9.5	17.9	48.9	16.6	0.0	34.5	65.5	6.2	25.4
Catalyst:19C											
805	111	237	38.3	100.0	21.6	26.3	0.0	52.1	47.9	18.3	54.8
760			28.3	73.0	28.4	19.4	0.0	52.2	47.8	13.5	40.6
710			11.1	27.7	37.4	11.4	0.0	51.2	48.8	5.4	23.4
Catalyst:20C											
800	108	227	30.6	100.0	16.5	10.4	0.0	73.1	26.9	8.2	38.6
760			27.4	96.5	13.8	5.5	0.0	80.7	19.3	5.3	28.3
710			18.7	73.5	5.4	1.9	0.0	92.7	7.3	1.4	26.0

* see table 6.2.4.1.a for catalysts composition, # partial pressure torr

Table 6.2.4.2.b The activity of MgO catalyst doped with different loadings of manganese oxide at 805°C

N*	P_{O_2}#	P_{CH_4}	%con. CH_4	O_2;	%sel.C_2H_6	C_2H_4	CO	CO_2;	Tot.C_2;	%C_2yield;	%$C_2^=$/Tot.C_2
21C	114	218	28.2	100	4.6	0.0	14.3	81.1	4.6	1.3	0.0
22C	105	217	27.7	100	6.3	0.7	10.0	81.3	8.7	2.4	8.0
23C	113	222	27.3	100	4.6	0.3	4.1	87.6	5.6	1.5	5.4
24C	111	223	25.8	100	3.1	1.4	0.0	94.5	4.5	1.7	31.0

*see table 6.2.2.1.b for catalysts composition, # partial pressure in torr

Generally higher methane conversion at all reaction temperature was observed over Li_2CO_3/MgO doped with manganese oxide catalysts compared to the iron and zinc oxides doped catalytic systems (section 6.2.2.2 and 6.2.3.2) while the selectivity

to C_2 were generally lower. A decrease in reaction temperature resulted in a decrease of methane conversion but was not necessarily followed by the increase in C_2 selectivity. On the catalyst with manganese oxide loading of 0.2 (17C) and 0.6wt.% (18C) the selectivity to C_2 increases with a decrease in reaction temperature. The C_2 selectivity over 4.6wt.% (19C) catalyst does not vary significantly with temperature while that over 19.8% catalysts decreases with the decrease in reaction temperature. The selectivity to carbon oxide over these catalyst at all temperature is mainly to carbon dioxide.

These results clearly show that the presence of manganese oxide on Li_2CO_3/MgO promotes the overall oxidative reaction of methane over the catalysts. Depending on the loadings, the presence of manganese does not only influence methane conversion but also the selectivity to the various products This is likely to be associated with the physical and chemical changes occurring on the manganese oxide doped Li_2CO_3/MgO catalysts. At a loading of less than 4.6wt.%, the high C_2 selectivity and the similar product distribution trends with reaction temperature suggest that the surface of these catalysts are chemically similar to that on undoped Li_2CO_3/MgO catalyst. The increase in methane conversion over these catalysts relative to the undoped Li_2CO_3/MgO can be explained in terms of physical changes. Over the 19.8wt.% catalysts (20C), however, the catalysts surface would be chemically different from that at lower loading. The increase in exhaustive oxidation of methane over this catalysts suggested that manganese oxide are present on the surface during the reaction. The manganese ions will facilitate the oxygen transfer and hence increase the conversion of methane to carbon dioxide.

The changes happening on the manganese oxide doped catalyst can be associated with the ionic radii factor since the ionic radii of manganese ions are very different (Mn^{2+} 83pm, Mn^{7+} 46pm, see table 6.5.a) from Mg^{2+} (72pm) and Li^+ (74pm). The presence of manganese oxide on the surface is likely to hinder the formation of solid matrix between MgO, and Li_2CO_3 and to minimise the formation of a Li_2CO_3 rich surface layer. Low loadings of manganese oxide on Li_2CO_3/MgO would

significantly affect the physical nature of the catalysts; such as causing the calcined catalysts to have smaller particle clusters, and hence a higher surface area and this can cause the increase in methane conversion. Higher loading of manganese oxide would however result in some manganese oxide being exposed on the surface under the reaction condition. The manganese oxide will then participate as a redox site facilitating oxygen transfer and hence promoting the exhaustive oxidation of methane to carbon dioxide. On the manganese oxide doped MgO, however, the manganese oxide would certainly be accessible to the reactant and hence favouring the exhaustive reaction of methane.

The relationship between methane conversion and C_2 selectivity over the oxidative coupling catalysts was further highlighted in this experiment. On catalyst with good oxidative coupling activity higher methane conversion was always followed by a decrease in selectivity to C_2 hydrocarbon. However, over the catalysts where exhaustive oxidation of methane is favoured, the higher conversion normally results in an increase in C_2 selectivity.

These results confirm the observation made earlier on the promoting effect of manganese oxide on the catalytic activity of Li_2CO_3/MgO catalysts. A loading of 0.6wt.% (18C) seem to result in the highest C_2 yield of 20.7%, but a higher loading causes the exhaustive reaction to become more favoured.

6.2.5 Different loadings of chromium oxide on Li_2CO_3/MgO and MgO

6.2.5.1 Catalyst composition

It was found in section 6.2.1.1 that the presence of 1.0 wt % of chromium oxide on Li_2CO_3/MgO resulted in the exhaustive oxidation of methane to carbon dioxide. In this experiment the effect of lower chromium oxide loading was investigated. The composition of the chromium oxide doped on Li_2CO_3/MgO and MgO catalysts, after calcination, were studied by AAS. These results are presented in table 6.2.5.1.a and table 6.2.5.1.b. respectively.

6.2.5.2 Activity of chromium oxide doped Li_2CO_3/MgO and MgO catalysts at 805°C

The activity of chromium oxide doped Li_2CO_3/MgO catalysts at 805°C are given in table 6.2.5.2.a. The presence of even 0.1wt.% chromium oxide on Li_2CO_3/MgO (25C) resulted in methane conversion of 30.6%, and only 29.1% selectivity to C_2 hydrocarbon. Further increases in Cr loading to 0.4 wt % (26C) resulted in a decrease of methane conversion to 25.5% and a significant loss of C_2 selectivity to only 5.5%. At 2.6wt.% (27C) loading methane conversion and C_2 selectivity decreases to 23.1 and 4.4% respectively. CO_2 was formed as the sole carbon oxide products while full oxygen consumption occurs over all of the catalysts.

Table 6.2.5.1.a Composition of calcined (C) and fresh (F) Li_2CO_3/MgO catalysts doped with different loadings of chromium oxide

Sample	Li/MgO		Cr/Mg	
	Wt%	Mole%	Wt.%	Mole%
25C	5.5	19.3	0.1	0.1
26C	4.7	16.5	0.4	0.2
27C	7.5	26.3	2.2	1.0

Table 6.2.5.1.b Composition of calcined (C) and fresh (F) MgO catalysts doped with different loadings of chromium oxide

Sample	Cr/Mg	
	Wt.%	Mole%
28C	0.1	0.1
29C	0.4	0.2
30C	1.6	0.8

The oxidative coupling reaction of methane over MgO doped with chromium oxide are not favoured at all (see table 6.2.5.2.b). Methane was oxidised to carbon monoxide and carbon dioxide. Over 0.1wt% (28C) chromium oxide doped catalyst an equal amount of carbon monoxide and carbon dioxide was observed in the product

stream. At higher loading the selectivity to carbon dioxide increases while that to carbon monoxide decreases. It was also observed that methane conversion also decreases with the increases in chromium oxide loading.

Table 6.2.5.2.a The activity of Li_2CO_3/MgO catalyst doped with different loading of chromium oxide at 805°C

N*	P_{O_2}#	P_{CH_4}	%con. CH_4	O_2;	%sel.C_2H_6	C_2H_4	CO	CO_2	Tot.C_2;	%C_2yield;	%$C_2^=$/Tot.C_2
25C	106	227	30.6	100	15.9	13.3	0.0	70.9	29.1	8.9	45.7
26C	113	231	25.5	100	3.4	2.1	0.0	94.5	5.5	1.4	38.6
27C	111	231	23.1	100	2.7	1.7	0.0	95.5	4.4	1.0	38.5

* see table 6.2.5.1.b for catalysts composition, # ipartial pressure in torr

These results confirmed the detrimental effect of chromium oxide on the oxidative coupling properties of Li_2CO_3/MgO catalysts. The presence of chromium oxide on Li_2CO_3/MgO catalyst even at a loading of 0.1% (28C), resulted in the increase of exhaustive oxidation of methane to carbon dioxide. The ionic radii of chromium ions, 63pm for Cr^{3+} and 52pm for Cr^{6+} (see table 6.5.a), are very different from that of Mg^{2+} and Li^+ ions.

Table 6.2.5.2.b The activity of MgO catalyst doped with different loading of chromium oxide at 805°C

N*	P_{O_2}#	P_{CH_4}	%con. CH_4	O_2;	%sel.C_2H_6	C_2H_4	CO	CO_2;	Tot.C_2;	%C_2yield;	%$C_2^=$/Tot.C_2
28C	111	210	28.2	100	0.0	0.0	49.5	50.5	0.0	0.0	-
29C	104	200	27.7	100	0.0	0.0	33.9	66.1	0.0	0.0	-
30C	113	218	27.3	100	0.0	0.0	14.6	85.4	0.0	0.0	-

* see table 6.2.5.1.a for catalysts composition, # partial pressure in torr

The presence of chromium even at low loadings is likely to disrupt the formation of the Li_2CO_3 rich layer covering the surface of the catalyst under the reaction condition. This should enable some of the chromium oxide species to be exposed on the catalysts surface and be involved in the oxidative reaction of methane. On the chromium oxide doped MgO catalysts, virtually no C_2 hydrocarbon product

was achieved and this illustrates the effectiveness of chromium oxide for converting methane to carbon oxide. Over the 1.6wt.% (30C) doped MgO catalyst the conversion of methane is predominantly to carbon dioxide.

6.3 Further studies on the nature of reaction on transition metal doped catalyst

6.3.1 The effect of reactant composition on activity of 0.6wt % of manganese oxide doped Li_2CO_3/MgO catalysts

In section 6.2.4.2 it has been confirmed that the presence of manganese oxide on Li_2CO_3/MgO promoted the oxidative reaction of methane to C_2 hydrocarbons at a lower reaction temperature. In order to establish the nature of reaction happening on the manganese oxide doped Li_2CO_3/MgO catalysts, the effect of reactant composition on the activity of 0.6wt % manganese oxide doped Li_2CO_3/MgO catalyst (18C) has been studied.

The increase in oxygen partial pressure (at constant partial pressure of methane) over the catalyst at 805°C resulted in an increase in methane conversion with full oxygen consumption occurring at all reactant composition. Selectivity to C_2 hydrocarbons (see figure 6.3.1.a) decreases while that to carbon dioxide increases continously at the higher oxygen partial pressure. Virtually no carbon monoxide was present in the product stream. The increase in P_{O_2}/P_{CH_4} ratio initially resulted in the increase of C_2 yield which reached a maximum value of 20.7% when the P_{O_2}/P_{CH_4} ratio was 0.5. A further increase in the partial pressure of oxygen relative to methane resulted in a decrease of C_2 yield. It was also observed that the percentage of ethene in the C_2 product formed increased continuously with the increase of P_{O_2}/P_{CH_4} ratio.

These results further supported the correlation between methane conversion and C_2 selectivity in the catalytic oxidative reaction of methane to C_2 hydrocarbons. The increase in methane conversion and decrease in C_2 selectivity when oxygen partial pressure (at a fixed partial pressure of methane) was increased indicates the critical role of oxygen in the reaction. Oxygen is required for the reaction to occur but excess

of it will favour the exhaustive oxidation of methane to carbon dioxide. The increase in percentage of ethene in the C_2 products at higher oxygen partial pressure again show that ethene selectivity are significantly controlled by the extent of the reaction. This further indicates that ethene is a secondary product of the catalytic oxidative reaction of methane to C_2 hydrocarbons.

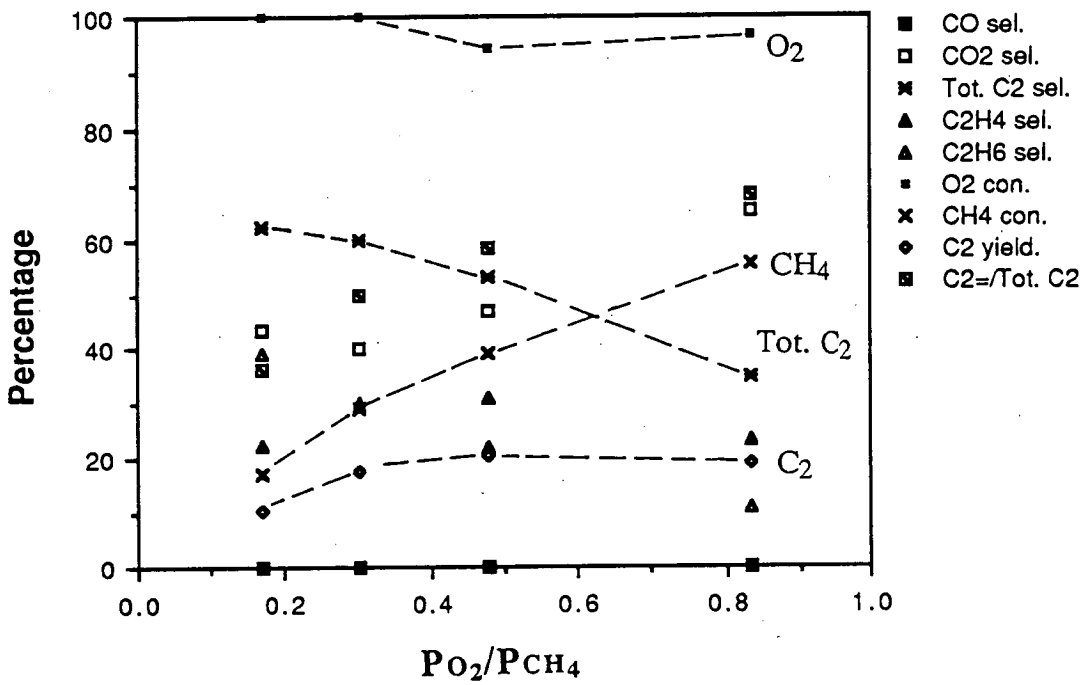

Figure 6.3.1.a The effect of P_{O_2}/P_{CH_4} ratio on the activity at 805°C of 0.6wt.% manganese oxide doped Li_2CO_3/MgO (P_{CH_4} 230 torr)

6.3.2 The activity of 0.6wt.% (18C) manganese oxide doped Li_2CO_3/MgO catalyst at 805°C with time-on-stream

The effect of time-on-stream on the oxidative reaction of methane over 0.6wt% (18C) catalyst at 805°C and under two different reactant composition have been determined. The results of the reaction with partial pressures of oxygen and methane of 92 and 260 torr respectively are given in figure 6.3.2.a. Under this condition 32.2% methane conversion and 58.9% selectivity to C_2 occurs after 0.5

hour onstream. At longer time-on-stream, methane conversion and the percentage of ethene in C_2 products decreases continuously while the total C_2 selectivity increase slightly. The percentage of C_2 yield decreases continuously with time-on-stream. It was also observed that the selectivity to CO_2 decreased significantly with reaction time while that to carbon monoxide increased slightly. After 21 hours of reaction, methane conversion and C_2 yield decreased to 19.5% and 13.1% respectively while the total C_2 selectivity increased to 67.4%.

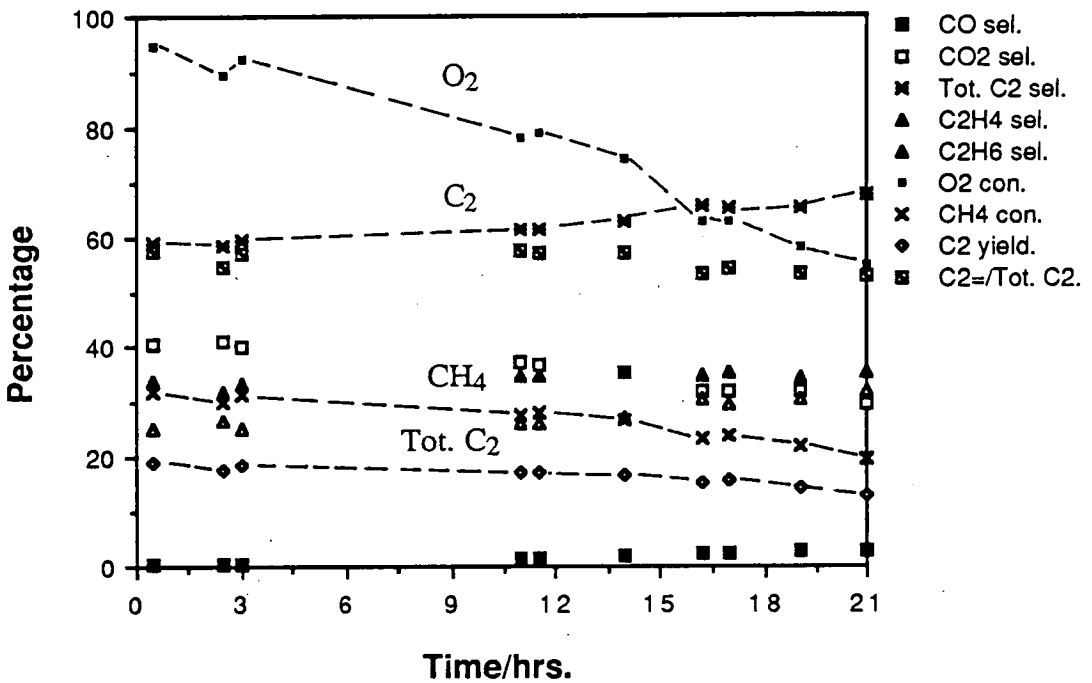

Figure 6.3.2.a The activity of 0.6wt.% manganese oxide doped Li_2CO_3/MgO catalyst at 805°Cwith time-on-stream (P_{O_2} 92 torr, P_{CH_4} 257 torr)

Some changes in activity with time onstream were also observed on the 0.6 wt % catalyst when the P_{O_2} and P_{CH_4} were 197 torr and 240 torr respectively. After 1 hour on-stream, methane conversion and C_2 selectivity over the catalyst were 52.7% and 39.8% respectively. Methane and oxygen conversion decreases continously with time onstream and so is the total selectivity to C_2 hydrocarbon. After 26 hours on-

stream, methane conversion dropped to 41.1% while the total selectivity decreased to 29.5%. The percentage of C_2 yield and the percentage of ethene in the C_2 products decreased continously with time-on-stream.

The decrease of methane conversion with time-on-stream suggested that significant changes are occurring on the catalyst under the reaction condition. Similar observation have been made over the undoped Li_2CO_3/MgO catalysts (section 4.3.3). On both catalysts, physical changes as a result of sintering are likely to be the main cause of the loss of activity. In the reaction with the higher oxygen partial pressure (pO_2/pCH_4 of about 1) however, the total selectivity was observed to decrease with time-on-stream. This suggest that beside the sintering effect, some chemical changes also occurred on the surface of the catalyst. These results also illustrate the dominant role of oxygen partial pressure in controlling the nature of oxidative reaction of methane.

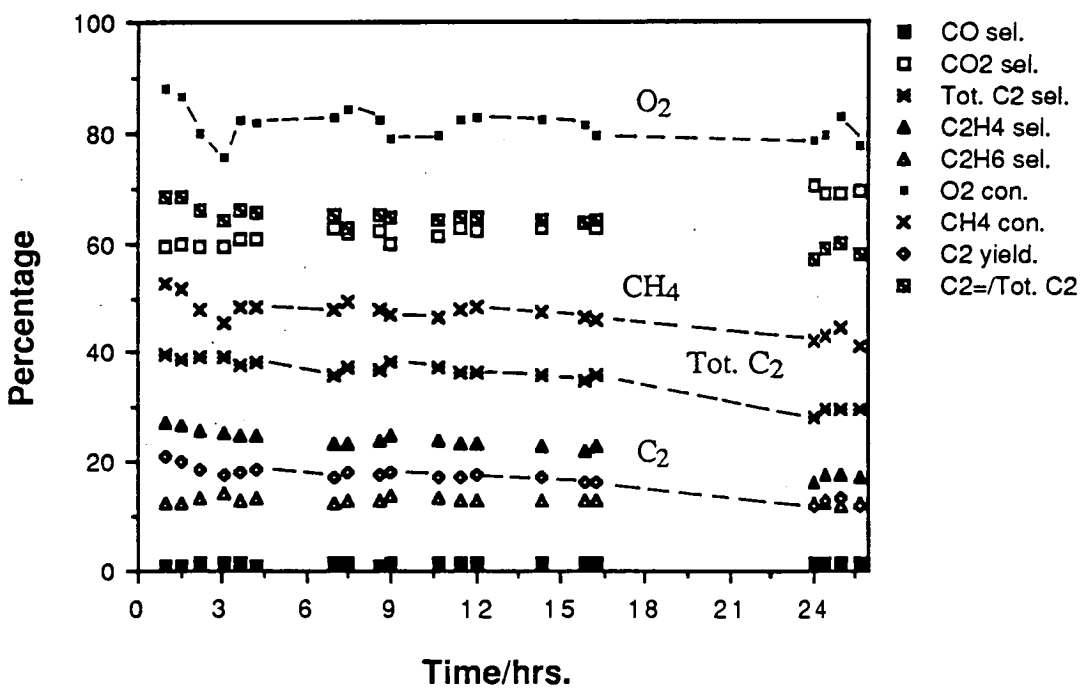

Figure 6.3.2.b The activity of 0.6wt.% manganese oxide doped Li_2CO_3/MgO at 805°C with time-on-stream (P_{O_2} 197torr,P_{CH_4} 240 torr).

In order to investigate the changes occurring on the 0.6wt.% manganese oxide doped Li_2CO_3/MgO catalyst after 27 hours on stream, the used and unused catalysts were studied by SEM. Figure 6.3.2.c contained the SEM micrographs of the various 0.6wt.% catalyst. The micrograph of the unused catalysts (ii and ii) indicate that the mean particle cluster size of about 0.2 μ-metre which is much smaller than that of the undoped Li_2CO_3/MgO catalysts (3 μ-metre). On the used catalysts the particles cluster size increases to about 0.4 μ-metre (micrograph iii and iv). indicating that the used catalyst have undergone significant physical changes from the fresh sample. The increase in the particle cluster size would lead in the reduction of the catalysts surface area which is presumably responsible for the decrease in methane conversion at longer time-on-stream.

To investigate the changes occurring on the catalysts the composition of the unused and used catalysts have been determined by AAS and microprobe analysis. The result of this analysis are presented in Table 6.3.2.a.

In the microprobe analysis the amount of magnesium and manganese was determined as the weight percentage of MgO and MnO respectively. The amount of lithium present cannot be studied by this technique but the value of (100-Wt.%MgO-Wt.%MnO) can be taken as an indication of the amount of Li_2CO_3 present on the samples. In table 6.3.2.a the weight percentage of MgO in the used catalyst increases to 87wt% from 81wt.% while the MnO components only increase by only 0.1wt.%. This suggests the decrease in amount of Li_2CO_3 phase on the used catalysts.

The composition of the catalyst as studied by AAS confirmed the significant loss of lithium on the used catalysts as were observed on the undoped Li_2CO_3/MgO (section 4.3.4 and Kimble and Kolts,1987). 81.4% of lithium originally present on Li_2CO_3/MgO catalysts was lost after 27 hours of reaction. The results of the microprobe analysis is also consistent with the loss of lithium from the used catalyst. The loss of Li_2CO_3 phase from the catalysts resulted in more exposed MgO sites and this could be related to the decrease in total selectivity to C_2 with time-on-stream in the

i) ii)

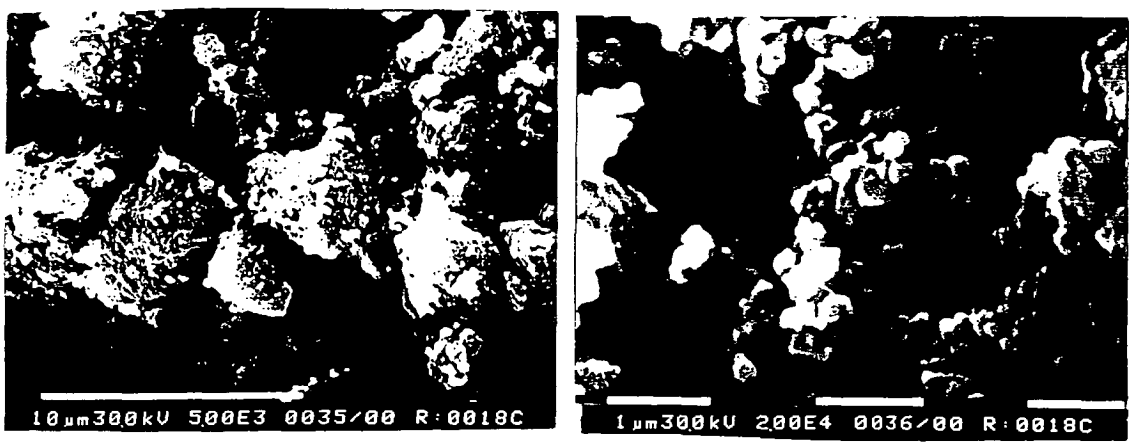

iii) iv)

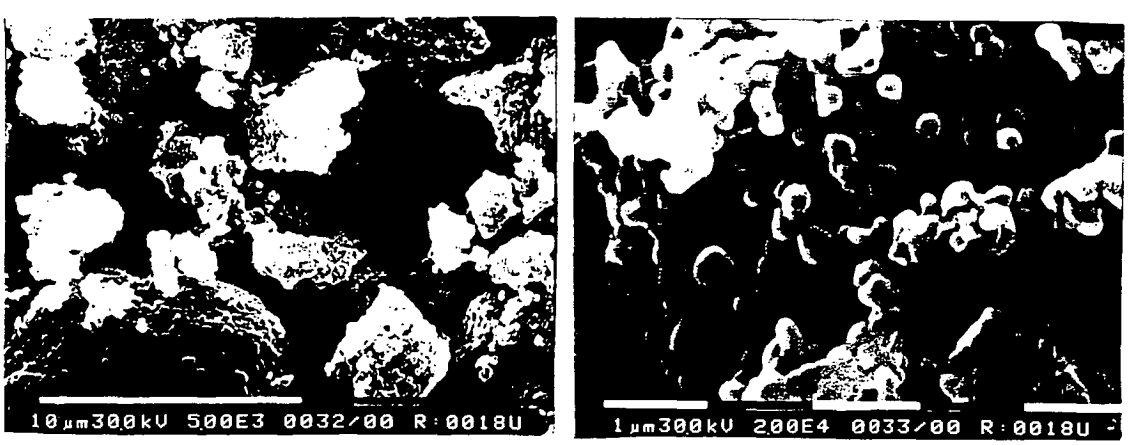

Figure 6.3.2.c SEM micrographs of the 18C catalysts (0.6wt.% Mn/Mg-18C). Micrographs i) and ii) are that of the unused catalyst at magnifications of $5.0x10^3$ and $2.0x10^4$ respectively, while micrographs iii) and iv) correspond to the used catalyst under the same respective magnifications.

experiment when P_{O_2}/P_{CH_4} was about one. The fact that the effect of the chemical changes on the product selectivity was observed at the high oxygen partial pressure suggest the significant role of physical changes in changing the activity of this catalysts. On the other hand Hinsen et al.,1984 have observed that the loss of PbO from PbO/Al_2O_3 catalysts with time-on-stream increases the exhaustive reaction of methane. In this respect the chemical changes on the catalyst surface caused alter the catalytic activity significantly.

Table 6.3.2.a The composition of unused and used 0.6wt.% manganese oxide doped Li_2CO_3/MgO catalyst

Sample	Wt% (microprobe)		A.A.S.	
	MgO	MnO	Li/Mg	Mn/Mg
18C(unused)	81.3(1.3*)	0.7(0.02)	5.9	0.6
18C(used)	87.4(0.7)	0.8(0.10)	1.1	0.6

*average deviation from three analysis

These results indicate that significant changes in the physical and chemical nature of 0.6wt.% (18C) manganese oxide doped Li_2CO_3/MgO catalysts occur during the 27 hours on-stream. Similar observation was made for the undoped Li_2CO_3/MgO catalysts (section 4.3.4).

6.4 The physico-chemical characteristics of transition metal oxide doped Li_2CO_3/MgO catalysts and its correlation to catalytic activity

6.4.1 Introduction

In section 6.2 and 6.3 it was shown that the presence of transition metal oxide on Li_2CO_3/MgO affected its catalytic activity. Attempts have been made to elucidate the effect of the transition metal oxide in terms of 'ionic radii factor'. In this section the

results of studies or the changes in physical and chemical nature of the transition metal oxide doped Li_2CO_3/MgO relative to the undoped catalysts will be reported.

The characteristics of the transition metal oxide doped catalysts was studied by SEM, XRD, TPR and microprobe analysis. The SEM micrographs of the catalysts samples should illustrate the physical nature of the materials while XRD analysis should give the type of phases present in the catalysts. The reducibility of the catalysts and the thermal stability of the carbonate phase should be manifested in the temperature programme reduction experiment. Studies using SEM and microprobe should enlighten further the physical and chemical nature of the various catalysts.

6.4.2 Iron oxide doped on MgO and Li_2CO_3/MgO system

Figure 6.4.2.a shows the photomicrographs of iron oxide, with different loading on Li_2CO_3/MgO sample after the precalcination at 900°C for 10 hours. At a loading of 0.4wt.% (1C, micrograph i), the formation of surface layer covering the calcined samples, as on the undoped Li_2CO_3/MgO sample (figure 5.2.1.a), was observed. Increase in iron oxide loading to 1.0wt.% (2C, micrograph ii) decreases the extent of the surface layer formed and at a loading of 28.6wt% (4C, micrograph iv) no significant surface layer formation was observed on the surface of the calcined sample. The SEM micrograph of the 28.6wt% (4C) sample shows that the surface was covered by clusters of particles which were abour 0.3 μ-metre in size. These micrographs suggest that the presence of high loading of iron oxide reduces the formation of surface layer during the precalcination of the samples.

The micrographs of calcined iron oxide doped Li_2CO_3MgO catalyst after crushing are given in figure 6.4.2.b. These micrographs do not show any significant effect of iron oxide loading on the size of particle cluster of the ground catalysts. In all of the samples the cross section of the particle cluster size range from 0.5 to 1 μ-metre. An interesting feature of the ground catalysts is that the particles do not have regular shapes and can be seen to have sharp edges. Such observation have also been made on the undoped Li_2CO_3/MgO catalysts even though the particle cluster size of the iron

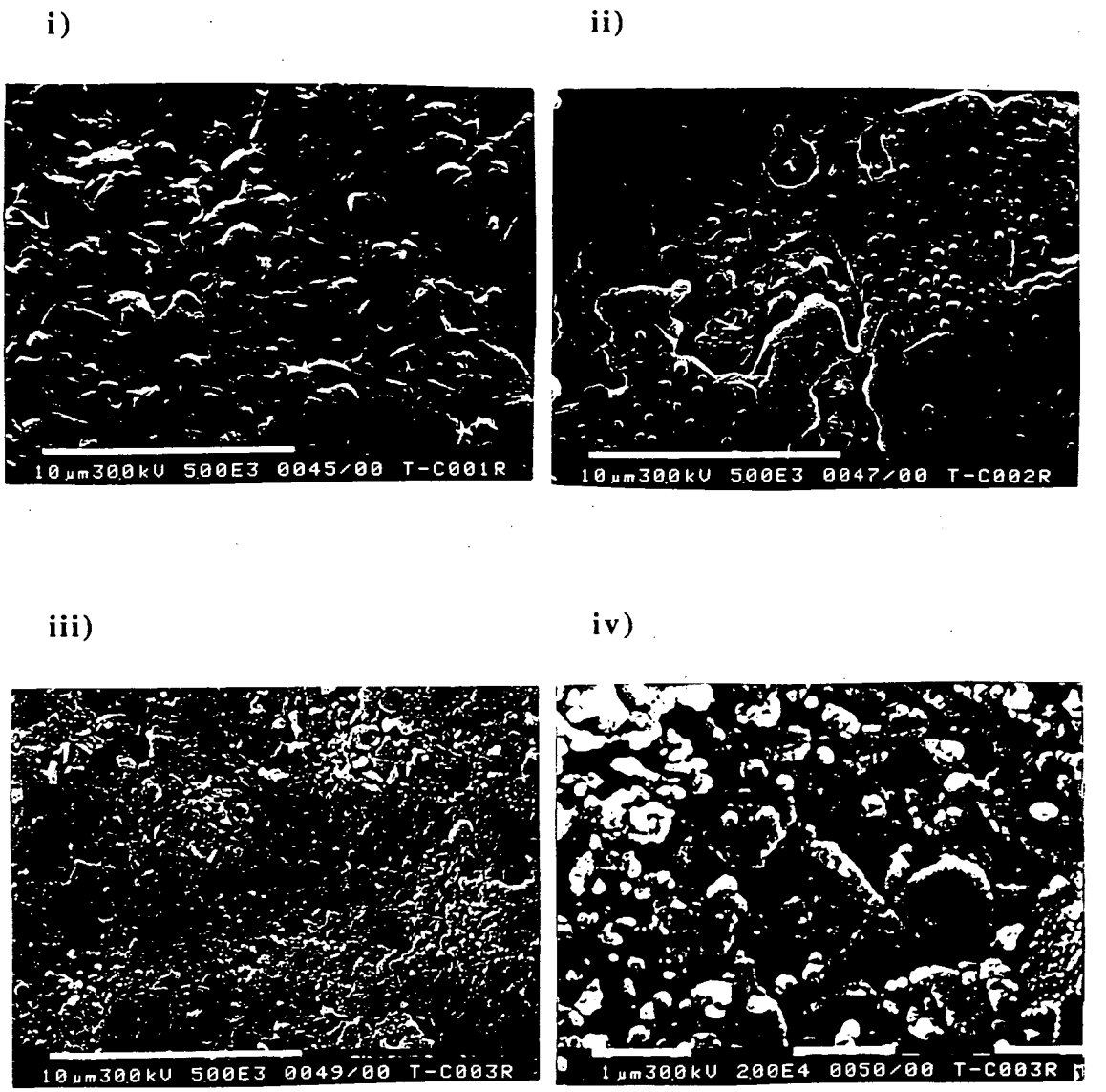

Figure 6.4.2.a SEM micrographs of the Li_2CO_3/MgO doped with different loadings of iron oxide after precalcination at 900°C for 10 hours. Micrograph iv) correspond to catalytic sample 4C at a magnification of $2x10^4$, while i), ii) and iii) are micrographs of 1C, 2C and 3C respectively at a magnification of $5x10^3$. The composition of these catalytic sample is given in Table 6.2.2.1.a.

i)

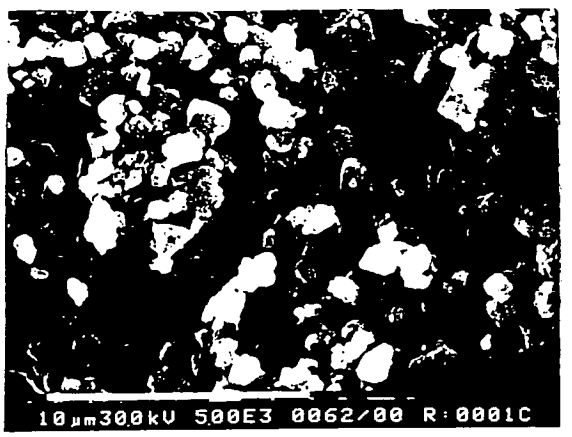

ii)

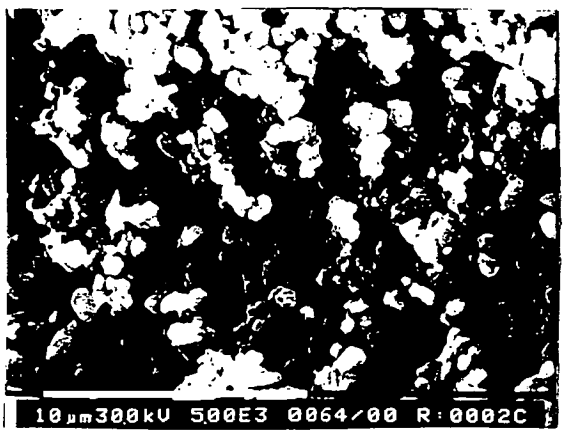

iii)

iv)

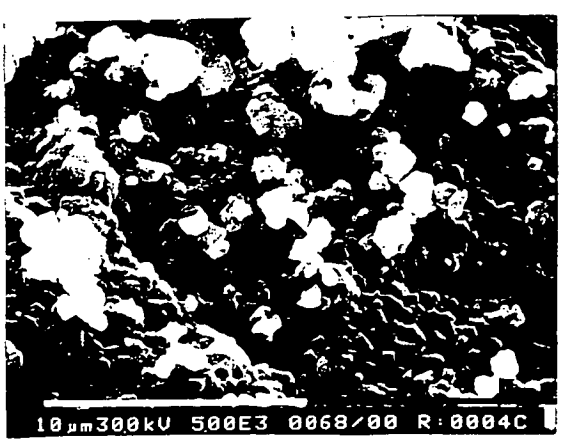

Figure 6.4.2.b SEM micrographs of calcined, ground and sieved Li_2CO_3/MgO doped with different loadings of iron oxide. Micrograph iii) correspond to catalytic sample 3C at a magnification of $1x10^4$, while i), ii) and iv) are micrographs of 1C, 2C and 4C respectively at a magnification of $5x10^3$. The composition of these catalytic sample is given in Table 6.2.2.1.a.

oxide doped catalyst is much smaller than the undoped catalysts. This suggest that the presence of iron oxide on Li_2CO_3/MgO reduces the formation of solid matrix between MgO and Li_2CO_3 making it softer and easier to ground.

The XRD patterns recorded with the angle of diffraction, 2θ, spanning from 5 to 45°, of iron oxide with different loading on MgO and Li_2CO_3/MgO after precalcination and grinding are given in figures 6.4.2.c and 6.4.2.d respectively. In the XRD patterns of iron oxide doped MgO (figure 6.4.2.c), iron oxide loading of 0.6wt% (5C, pattern i) and less shows the pattern due to MgO phase only. When iron oxide loading was increased to 5.4wt.% (7C, pattern ii), two new peaks were observed at 2θ of 30.2 and 35.5° which correspond to the d-spacing value of 2.96 and 2.53 respectively. The intensity of this peaks increases with iron oxide loading (pattern iii). These new XRD lines can be assigned to that of Fe_3O_4 (2.53_x, 1.49_4,2.97_3, ie. whose three major peaks occurs at d-spacing of 2.53, 1.49 and 2.97 with their relative intensity of 1.0, 0.4 and 0.3 respectively, (Powder Diffraction File, 1975), $MgFe_2O_4$ (2.53_x,1.49_4,2.97_4) and γ-Fe_2O_3 (2.52_x,1.48_5, 2.95_3) phases which have similar XRD patterns. It was also observed that the XRD peaks associated with the MgO phase decreases in intensity at higher iron oxide loading.

In the case of iron oxide doped Li_2CO_3/MgO (figure 6.4.2.d), the major phase present in the low loading catalysts (pattern i and ii) are MgO and Li_2CO_3. The increase in iron oxide loading decreases the intensity of XRD peaks of the MgO and Li_2CO_3 phase. In the sample with iron oxide loading of 28.6wt.%, the peaks related to the Li_2CO_3 phase disappeared and those to MgO were much weaker compared to those of lower loading catalysts. No peaks that can be assigned to the iron oxide phase were present.

In XRD technique, the effective crystallite size, L, of any sample are related to the breadth of a diffraction profile at half maximum by equation 6.4.2.a (known as the Scherrer formula, Matyi et. al.,1987) where $B_{1/2}$ is the breadth measured in radians, λ is the wavelength of the x-radiation, k is a constant and θ^o is the angular position of the peak maximum. Despite the limitation of Sherrer formula (Matyi et. al.,

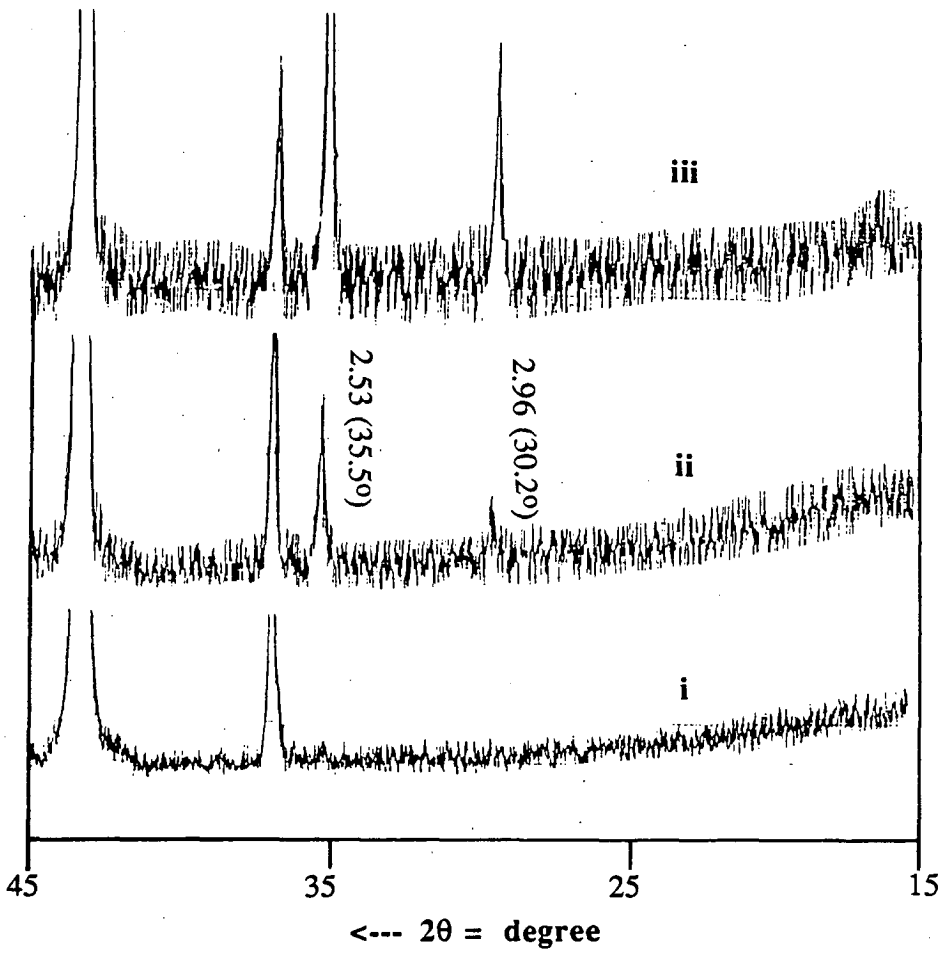

Figure 6.4.2.c XRD patterns of calcined, ground and sieved MgO catalysts doped with different loadings of iron oxide. Patterns i), ii) and iii) correspond to catalytic sample 6C, 7C, and 8C respectively, whose composition are given in Table 6.2.2.1.b. The value presented at any particular peak correspond its d-spacing.

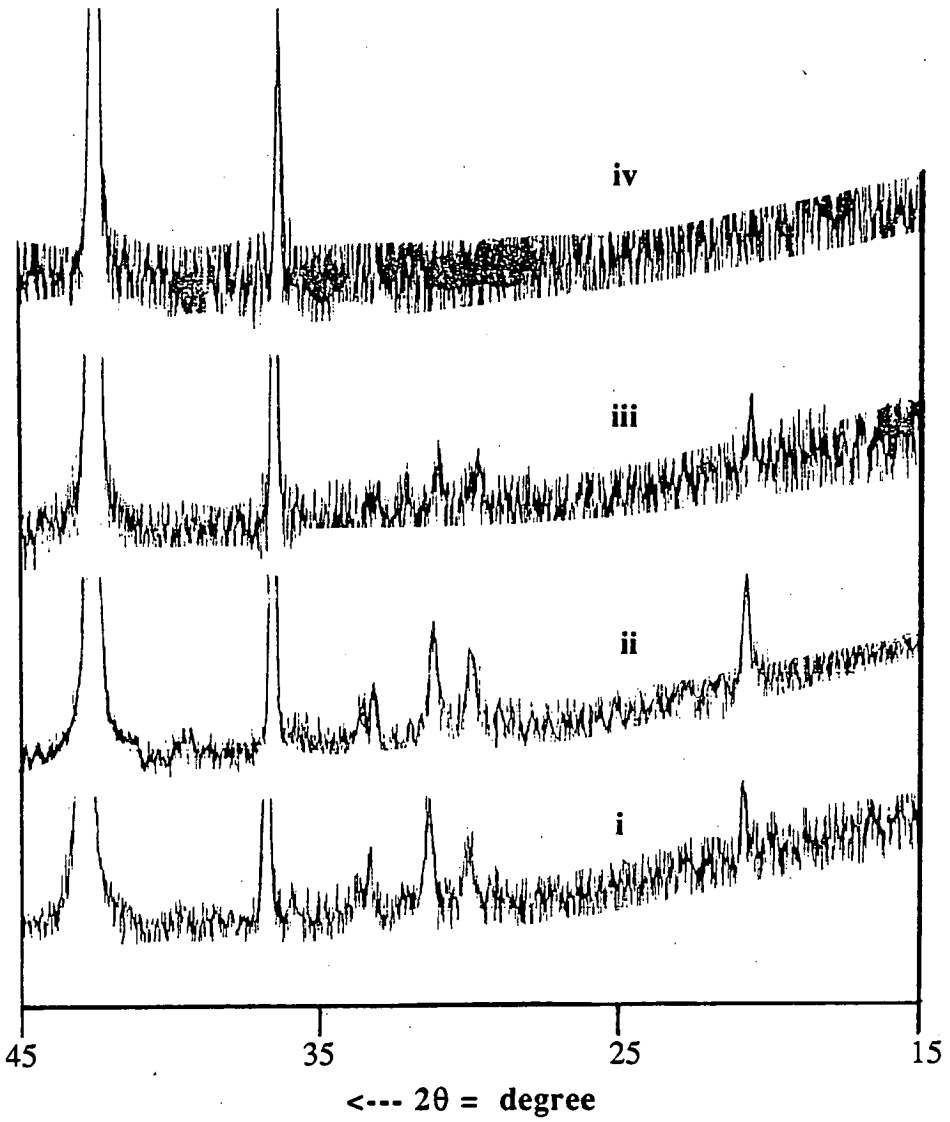

Figure 6.4.2.d XRD patterns of calcined, ground and sieved Li_2CO_3/MgO catalysts doped with different loadings of iron oxide. Patterns i), ii), iii) and iv) correspond to catalytic sample 1C, 2C, 3C, and 4C respectively, whose composition are given in Table 6.2.2.1.a.

1987), the breadth at half maximum can be taken to be inversely related to the effective particle size in a sample.

Equation 6.4.2.a $B_{1/2}=k*\lambda/(L*\cos(\theta^o)$

The decrease in the breadth of the XRD profiles of MgO when iron oxide was present on MgO and Li_2CO_3/MgO catalyst, according equation 6.4.2.a, could indicate the increase in the particle size of MgO for the doped catalysts. The decrease in the intensity of MgO profile is also in-line with the decrease in percentage of MgO present on the catalysts as the loading of iron oxide was increased.This could also suggest that in the presence of a higher loading of iron oxide the crystallinity of MgO decrease or that most of the particle size are small to result in a coherent scattering pattern. In the case of XRD profiles of iron oxide doped MgO, the increase in the intensity of the peaks associated with Fe_3O_4, $MgFe_2O_4$ and γ-Fe_2O_3 occurs with loading. These phases are however not present on the doped Li_2CO_3/MgO catalysts. The absence of XRD peaks assignable to iron oxide phases on the doped Li_2CO_3/MgO suggest that the iron oxide, together with MgO and Li_2CO_3 formed amorphous solid solution.

The presence of the Fe_3O_4, $MgFe_2O_4$ and γ-Fe_2O_3 phases on the iron oxide doped MgO catalysts should increase the redox capability of the catalysts under reaction condition. In the activity studies, it has been observed that the iron oxide doped MgO favours the exhaustive oxidation of methane while the doped Li_2CO_3/MgO still retained the high oxidative coupling properties. This tends to suggest that the iron oxide phases are responsible for the exhaustive oxidation of methane to carbon oxide. On the doped Li_2CO_3/MgO catalysts however, its oxidative coupling behaviour seems to be related to the Li_2CO_3/MgO component of the catalysts.

The TPR profiles of different loading of iron oxide doped MgO catalysts are given in figure 6.4.2.e. In the TPR profile of the 1.0wt % catalyst (curve i), a broad reduction profile between 280°-600°C and a distinct peak at 725°C was observed. The reduction peaks increases in intensities at higher iron oxide loading. In the TPR profiles of 5.4wt % catalysts (curve ii) a reduction peak shoulder at 460°C, a distinct

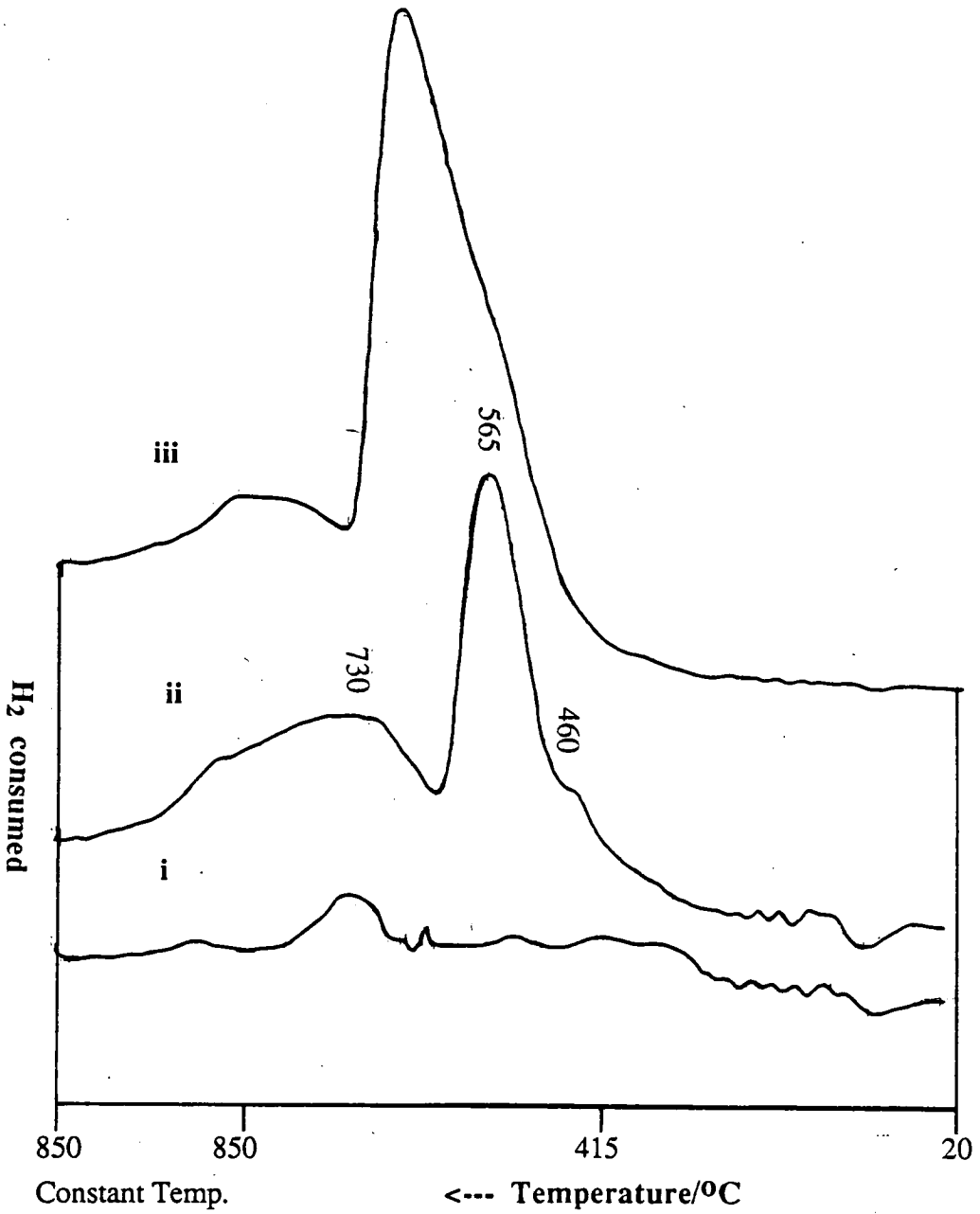

Figure 6.4.2.e TPR profiles of calcined, ground and sieved MgO catalysts doped with different loading of iron oxide. Profiles i), ii) and ii) correspond to catalytic sample 6C, 7C and 8C respectively, whose composition are given in Table 6.2.2.1.b.

peak at 565°C, and a broad peak centred around 730°C were observed. At a loading of 28.6wt.% these three peaks were still present but have shifted to higher temperatures.

Equation 6.4.2.b $H_2 + Fe_2O_3 \rightarrow 2\ Fe_3O_4 + H_2O$

Equation 6.4.2.c $4H_2 + Fe_3O_4 \rightarrow 3Fe + 4H_2O$

The first reduction peak can be assigned to the reduction of Fe_2O_3 to form Fe_3O_4 (equation 6.4.2.b) while the second peak is due to the reduction of the Fe_3O_4 to metallic iron (equation 6.4.2.c). The broad peak at the high temperature was assigned to the reduction of $MgFe_2O_4$ phase (Alan and McNicol,1986). The last assignment is supported by the fact that significant amount of this phase was present at low loading when the formation of the $MgFe_2O_4$ is more likely to occur.

Before the TPR profiles of any of the metal oxide doped on Li_2CO_3/MgO catalysts were determined, the TPR profiles of unused and used (800°C for 2 hours) Li_2CO_3/MgO were first investigated The profiles of the unused and used Li_2CO_3/MgO catalysts are given in figure 6.4.2.f. A large peak was observed in these profiles at temperature above 700°C and is due to the decomposition of the carbonate phase. The carbon dioxide produced in the decomposition resulted in the dilution of the hydrogen in the sample arm of the TCD (see figure 3.4.4.a) relative to that in the reference arm. This gave rise to the difference signal and hence to TPR peaks similar to that as if hydrogen was consumed by the sample.

The TPR profiles of different loadings of iron oxides on Li_2CO_3/MgO (compare figure 6.4.2.g with figure 6.4.2.e) are very different to that of the iron oxide doped MgO catalysts. Two peaks were observed at 630°C and one at around 840°C. The position of these peaks does not vary significantly with iron oxide loading loading. The decrease in the size of these peak on the 28.6wt.% (4C) catalyst (curve iii) is agreement with the decrease in the amount of Li_2CO_3 phase in this catalyst. The peaks observed in the TPR of iron oxide doped Li_2CO_3/MgO catalyst correspond to that due to the decomposition of Li_2CO_3 phase indicating that no reduction of the iron oxide phase occurs on these catalysts. The likely explanation for this is that the iron oxide in the doped Li_2CO_3/MgO catalyst are not present on the catalyst surface. It has

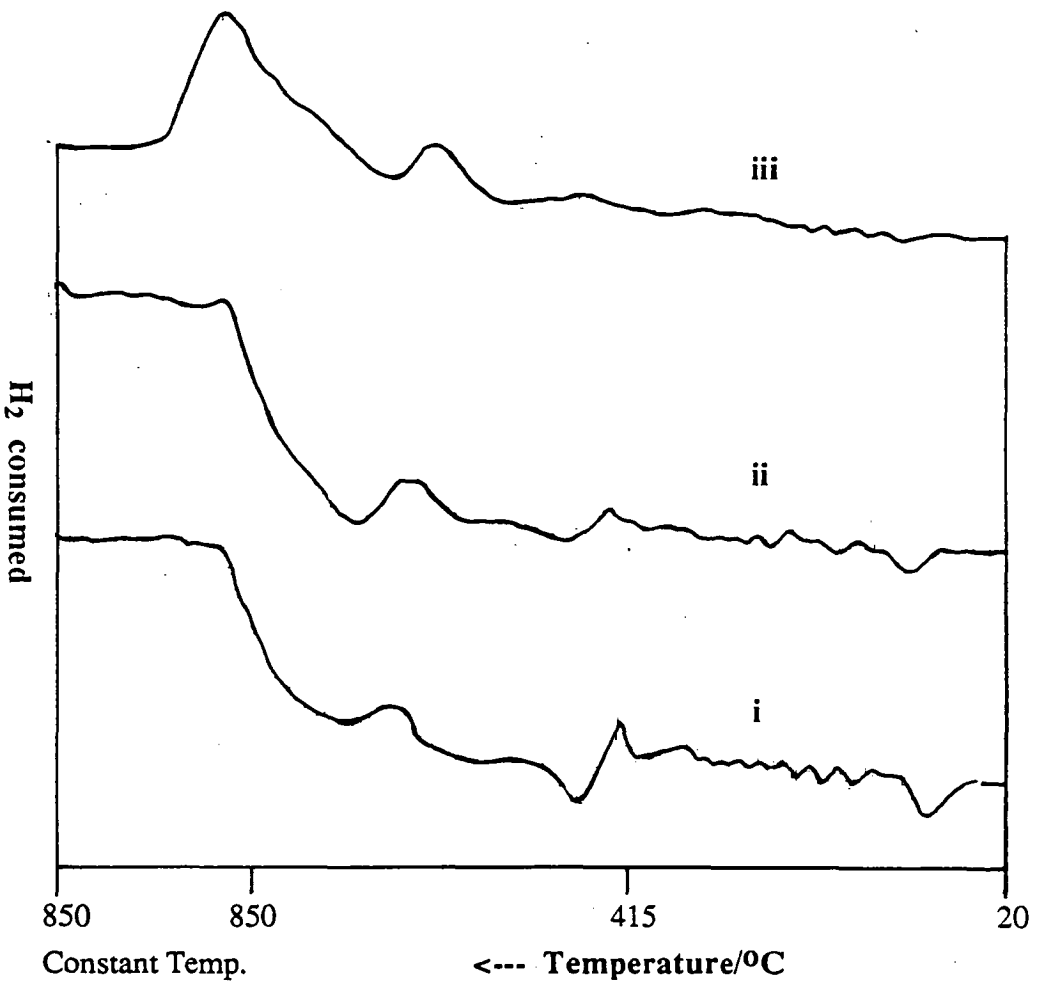

Figure 6.4.2.g TPR profiles of calcined, ground and sieved Li_2CO_3/MgO catalysts doped with different loadings of iron oxide. Profiles i), ii) and iii) correspond to catalytic sample 2C, 3C and 4C respectively, whoese composition are given in Table 6.2.2.1.a.

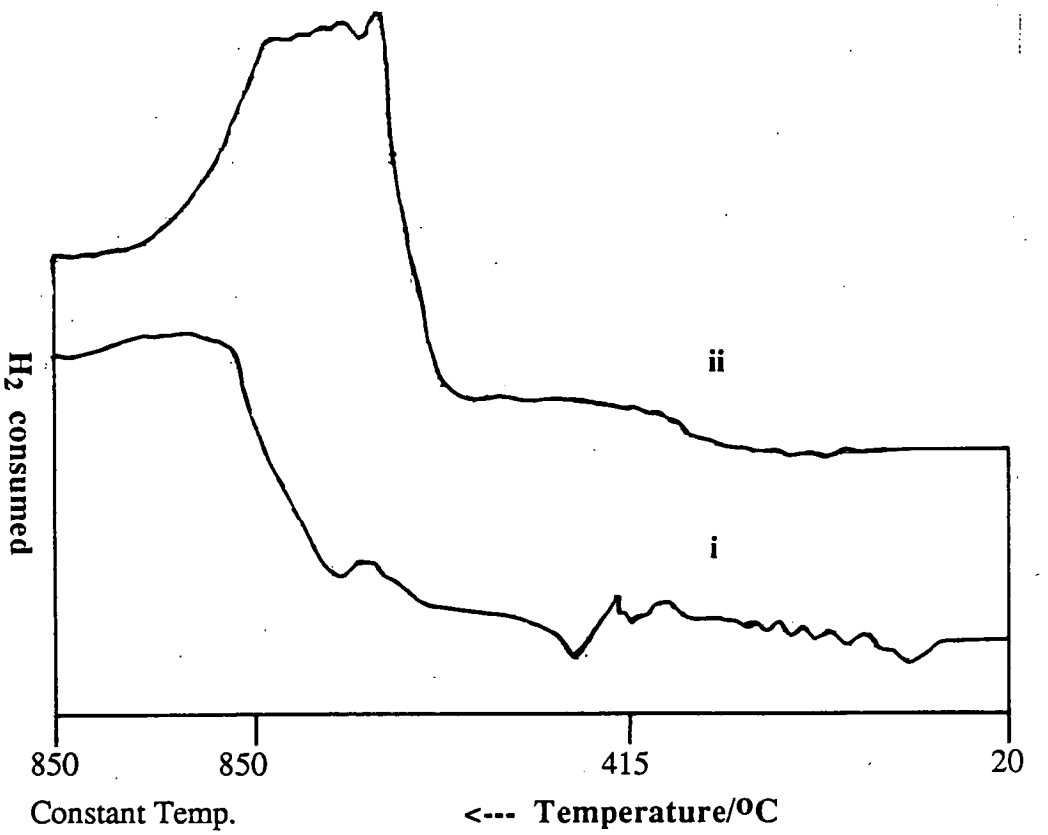

Figure 6.4.2.f TPR profiles of i)unused and ii) used 7.8wt.%Li_2CO_3/MgO catalysts. The used catalysts was esposed for 2 hours to the oxidative reaction of methane at 800°C

been observed in the SEM work that to some extent the formation of surface layer during the high temperature precalcination are facilitated on these catalysts. Under these circumstances the enrichment of Li_2CO_3 phase on the catalysts surface occurs preventing the availability of iron oxide on the surface. As a result no reduction of iron oxide occurs under the TPR condition and this also explained the similarity in the activity of the iron oxide doped Li_2CO_3/MgO catalysts with the undoped Li_2CO_3/MgO catalysts.

In order gain some understanding on the nature of the catalysts under the catalytic condition, the TPR profiles of the used catalysts were determined. In these determinations the catalysts were exposed to the reactant gas at 800°C for two hours, cooled to RT under evacuation before their TPR profiles were determined. The TPR profile of used 5.4wt.% (7C) iron oxide doped MgO (curve i) and 6.0wt.% (3C) iron oxide doped Li_2CO_3/MgO (curve ii) are given in figure 6.4.2.h. The profiles of the 5.4% catalyst shows that under the condition of oxidative reaction of methane, the steady state composition of iron oxide phases are low compared to that in fresh catalysts (see curve ii of figure 6.4.2.e). This suggests that most of the iron oxide phase were reduced under reaction condition.

In the case of the used iron oxide doped Li_2CO_3/MgO catalysts (curve i), no reduction peak that can be assigned to the iron oxide phase are present. However, the peak of Li_2CO_3 decomposition was much larger than that on fresh catalysts (see curve ii of figure 6.4.2.h). The increases in the Li_2CO_3 decomposition peaks and the absence of the iron oxide reduction peak further suggests that the enrichment of Li_2CO_3 on the surface of the iron oxide doped Li_2CO_3/MgO catalysts occurs under reaction condition.

The TPR of doped MgO show that the iron oxide phase of the doped MgO catalysts are available to be reduced. On the doped Li_2CO_3/MgO catalysts the iron oxide is not available to be reduced even for loading of 28.6% (4C). This suggests that the surface nature of the doped Li_2CO_3/MgO catalysts are similar to that of undoped Li_2CO_3/MgO. Direct correlation between these observations and the catalytic

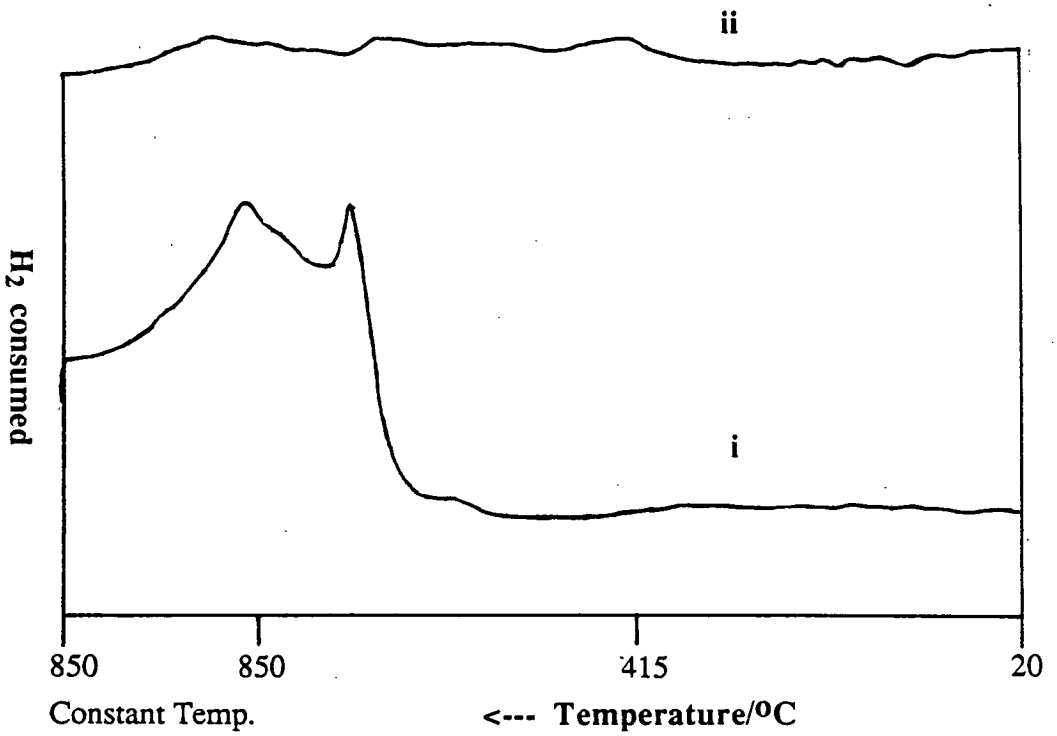

Figure 6.4.2.h TPR profiles of i) 3C and ii) 7C catalytic materials after 2 hours on-stream under the condition of oxidative reaction of methane at 800°C.

activity of these catalysts can be drawn. The presence of iron oxide on MgO facilitate the exhaustive oxidation of methane to carbon dioxide. On the other hand, the catalytic activity of the doped Li_2CO_3/MgO are similar to that of Li_2CO_3/MgO because the iron oxide present are not available for reaction. The stabilisation of the Li_2CO_3 layer on the doped catalysts is likely to be promoted by the similarity in the ionic radii of iron ions with that of Mg^{2+} and Li^+.

6.4.3 Zinc oxide doped on MgO and Li_2CO_3/MgO system

The formation of the surface layer coating samples which were precalcined at 900°C for 10 hours was also observed on zinc oxide doped Li_2CO_3/MgO system. As in the case of iron oxide doped catalysts the extent of surface layer formation decreases with the increase of loading (figure 6.4.3.a) but the effect of zinc oxide loading on the layer formation is less severe than that of iron oxide. It was also observed that on the 32.1wt% (12C) catalysts (micrograph iv) some surface layer were still present. As in Li_2CO_3/MgO, the composition of the layer structure seems to be different from the bulk. This is highlighted in figure 6.4.3.b which contains SEM micrographs of the calcined 32.1wt.% catalyst at lower magnification. A question that arises here is whether the layer structure is formed from Li_2CO_3 and MgO or Li_2CO_3 with zinc oxide. This is because Zn^{2+} has ionic radii similar to Li^+ (74pm, see table 6.5.a) while Mg^{2+} is smaller by 2pm.

The SEM micrographs of powdered zinc oxide doped Li_2CO_3/MgO catalyst are given in figure 6.4.3.c. The catalysts particles do not have any regular shapes and and seem to have sharp edges. The average cluster size was about 3 μ-metre. The cluster size of the zinc oxide doped catalysts is much larger than that of iron oxide doped catalysts. The larger cluster size of zinc oxide doped Li_2CO_3/MgO catalysts suggested that the calcined sample of these catalysts are harder and hence more difficult to grind than that of the iron oxide catalysts.

In order to further characterise the zinc oxide doped Li_2CO_3/MgO catalysts, some X-ray microprobe analysis of the various forms of these materials have been

i) ii)

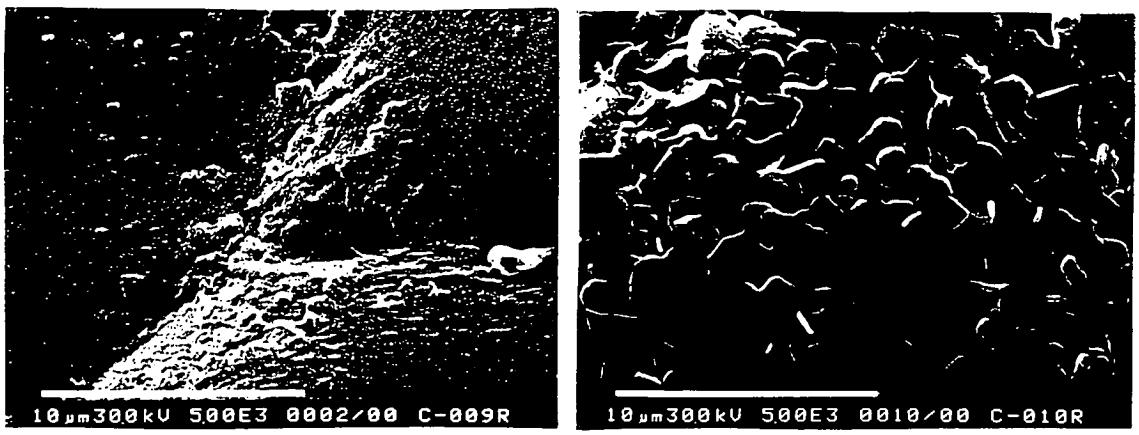

iii) iv)

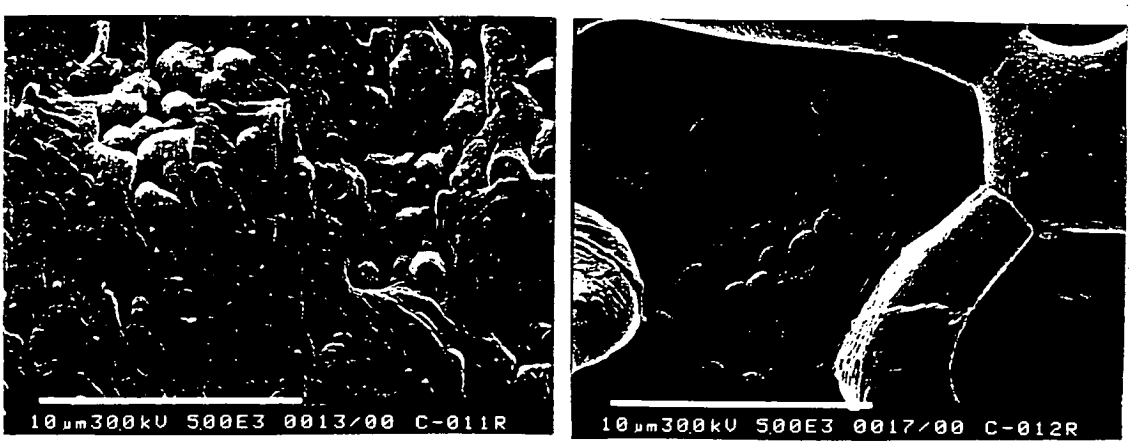

Figure 6.4.3.a SEM micrographs of Li_2CO_3/MgO doped with different loading of zinc oxide, after precalcination at 900°C for 10 hours (magnification of $5x10^3$). Micrographs i), ii), ii) and iv) correspond to catalytic sample 9C, 10C, 11C and 12C respectively whose composition are given in table 6.2.3.1.a.

i) ii)

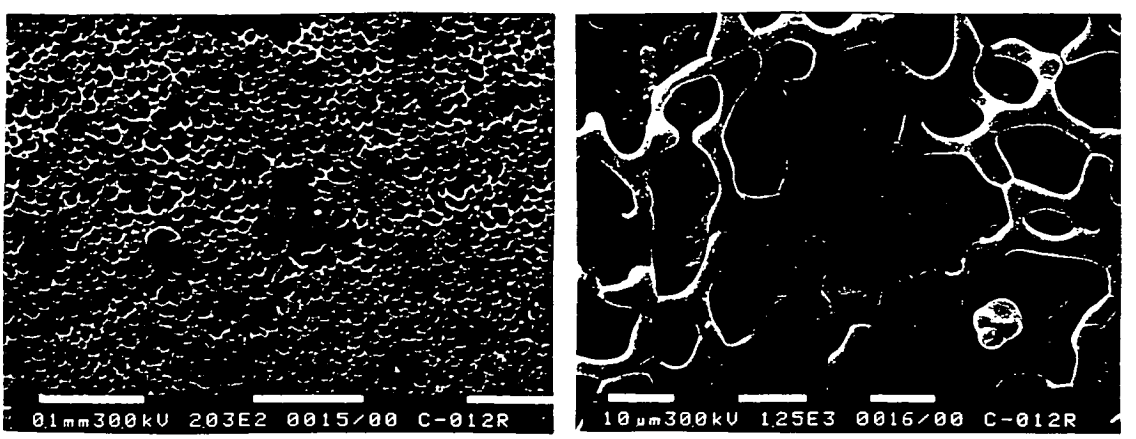

Figure 6.4.3.b More SEM micrographs of 12C catalytic material at magnification of i) $2x10^2$ and ii)$1.25x10^3$.

i)

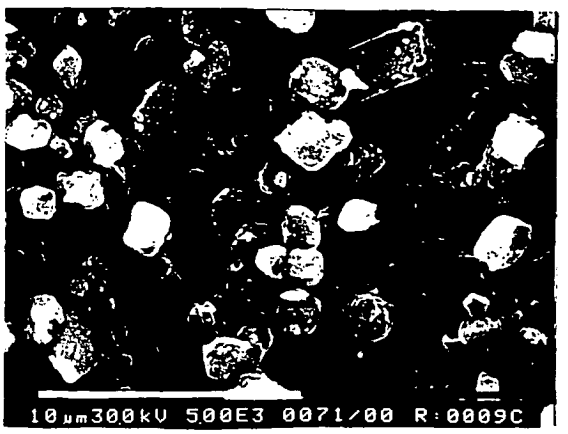

ii)

iii)

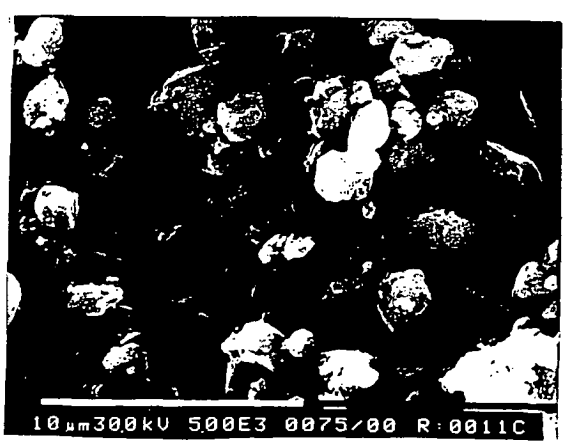

iv)

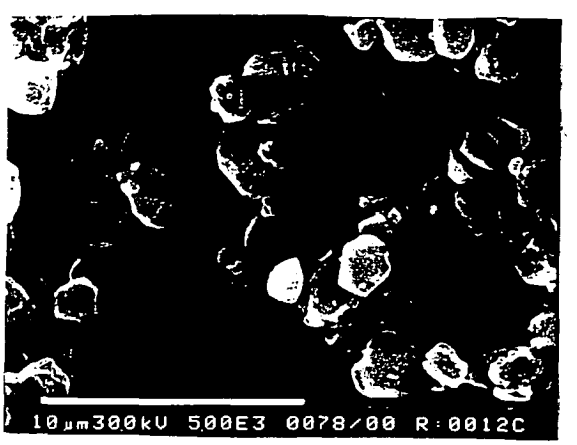

Figure 6.4.3.c SEM micrographs of calcined, ground and sieved Li_2CO_3/MgO catalysts doped with different loadings of zinc oxide (magnification of $5x10^3$). Micrographs i), ii), iii) and iv) correspond to catalytic sample 9C, 10C, 11C, and 12C respectively, whose composition are given in Table 6.2.3.1.a.

studied. Table 6.4.3.a shows the x-ray microprobe analysis of calcined samples of zinc oxide doped Li_2CO_3/MgO and the powdered samples. The analysis of the powdered form of the calcined sample should represent the composition of the bulk and the difference between the calcined and powdered calcined samples should indicate the changes that happened on the catalysts as a result of precalcination. As a comparison, the analysis for some manganese oxide doped Li_2CO_3/MgO catalysts were also presented.

Table 6.4.3.a Composition of calcined and powdered Li_2CO_3/MgO catalysts doped with zinc and manganese oxides as determined by microprobe analysis

Catalyst label	Wt% (microprobe)		
see table 6.2.3.1.a	MgO	ZnO	Total
9C	26.0(2.0*)	3.26(0.02)	29.26
9C(powder)	81.4(1.0)	0.35(0.02)	81.75
10C	45.5(3.6)	5.80(0.03)	51.30
10C(powder)	77.8(1.2)	0.92(0.02)	78.72
11C	23.1(5.5)	21.73(1.0)	44.83
11C(powder)	70.9(1.6)	4.55(0.2)	75.45
see table 6.2.4.1.a	MgO	MnO	Total
18C	36.5(4.5)	0.42(0.03)	36.92
18C(powder)	81.3(1.3)	0.68(0.02)	81.98
19C	58.0(5.3)	4.14(0.17)	62.14
19C(powder)	66.4(0.8)	3.52(0.10)	69.92

*average deviation from three analysis

On the Li_2CO_3/MgO catalyst doped with zinc oxide the micro probe analysis performed were for the determination of MgO and ZnO content while on the

manganese oxide doped catalysts the analysis were for MgO and manganese as MnO. As in ealier studies the value of (100-total) can be taken to be proportional to the amount of Li_2CO_3 present on the samples. Table 6.4.3.a show that on both of the zinc and manganese oxide doped catalysts, the total weight percent of the chemical components detected increases with the load of the transition metal oxides.

An interesting observation made on the basis of the information in table 6.4.3.a is that, the calcined zinc oxide doped catalysts showed a higher content of zinc oxide than their powdered counterpart while no such observation was made on the manganese oxide doped catalysts. This indicates the enrichment of the surface with zinc oxide occurs during the precalcination stage. The higher average deviation in the weight percentage of MgO on calcined sample relative to the powdered form suggested the uneven distribution of Li_2CO_3 phase on the sample surface. On manganese oxide doped Li_2CO_3/MgO catalysts however no significant enrichment with manganese oxide was observed. This further indicates the significance of ionic radii factor in determining the physical and hence chemical nature of the doped Li_2CO_3/MgO catalysts. Due to the similarity between the ionic radii of Li^+ and Zn^{2+}, Li_2CO_3 and ZnO form a better solid matrix than that between MgO and Li_2CO_3. Under reaction condition, significant migration of Li_2CO_3 from the Li_2CO_3/MgO matrix to the ZnO phase would occur. This could probably be the reason for the variation in tha activity of zinc oxide doped Li_2CO_3/MgO catalysts.

The XRD patterns for different loading of ZnO on MgO and Li_2CO_3/MgO have also been determined and are given in figure 6.4.3.d and 6.4.3.e. No XRD pattern of ZnO was observed in that of doped MgO (figure 6.4.3.d) suggesting that the ZnO exists as very small crystallites or in amorphous form.

On the doped Li_2CO_3/MgO catalysts, at low loading of zinc oxide the major XRD features indicate the presence of MgO and Li_2CO_3 (curve i of figure 6.4.3.e). At higher ZnO loading, the XRD pattern changes considerably. Initially the peaks associated with Li_2CO_3 were enhanced at 6.9 wt % loading (curve ii). These peaks were actually present at low zinc oxide loading but were enhanced at the higher

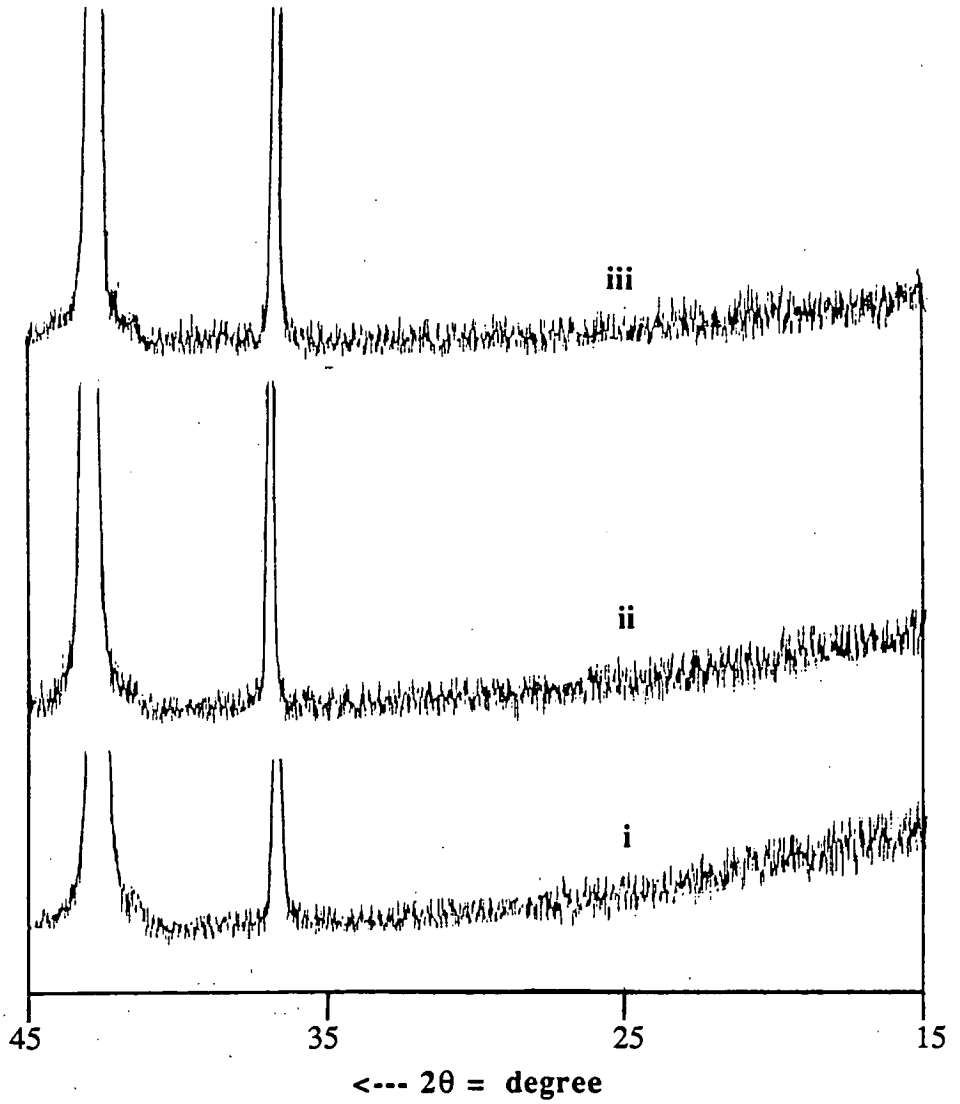

Figure 6.4.3.d XRD patterns of calcined, ground and sieved MgO catalysts doped with different loadings of zinc oxide. Patterns i), ii) and iii) correspond to catalytic sample 14C), 15C, and 16C respectively, whose composition are given in Table 6.2.3.1.b.

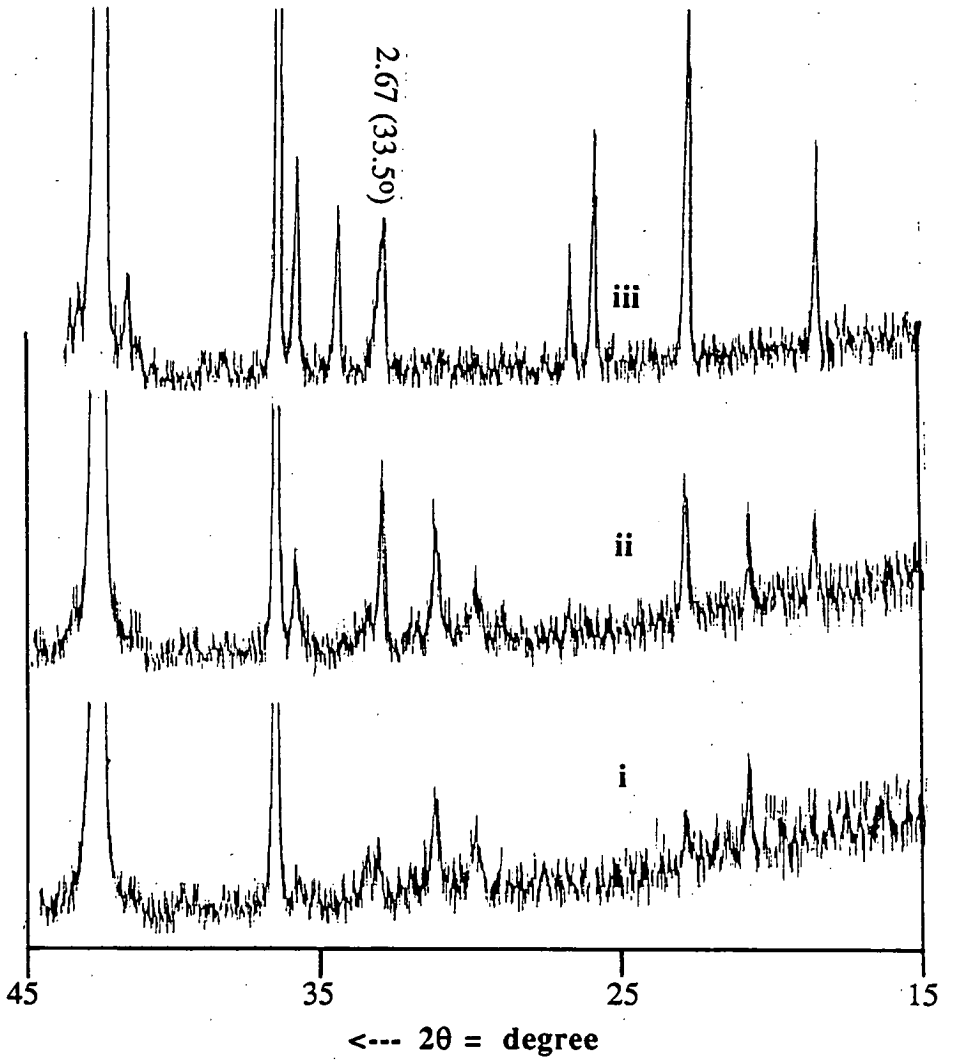

Figure 6.4.3.e XRD patterns of calcined, ground and sieved Li_2CO_3/MgO catalysts doped with different loadings of zinc oxide. Patterns i), ii) and iii) correspond to catalytic sample 10C, 11C and 12C respectively, whose composition are given in Table 6.2.3.1.a. The value presented at any particular peak correspond its d-spacing.

loading. It was also observed that the XRD peaks of MgO on the doped Li_2CO_3/MgO catalysts does not change significantly with loading as on the iron oxide doped Li_2CO_3/MgO catalysts. The detail assignments of these peak were not attempted but the presence of the peak at 2θ of 33.5° (d-spacing of 2.67) suggests that zinc oxide phase (2.66_x,1.57_9,1.48_6) is present.

In the activity studies it was observed that zinc oxide doped on MgO also promoted the exhaustive oxidation of methane to carbon dioxide. The presence of zinc oxide on MgO is not likely to result in a major increase in the redox ability of the doped catalysts. However, it is more likely that the dispersion of ZnO on MgO must have contributed to the higher catalytic activity of the doped catalysts. In order to confirm the absence of reducible sites on the zinc oxide doped MgO and Li_2CO_3/MgO catalysts, their TPR natures were also determined.

The TPR profiles of different loading of zinc oxide on MgO and Li_2CO_3/MgO are presented in figure 6.4.3.f and 6.4.3.g respectively. On the zinc oxide doped MgO (figure 6.4.3.f), a peak at around 700°C was observed for all samples. Since the reduction of zinc oxide are not considered feasible at this condition, this peak is probably be due to the decomposition of Li_2CO_3 phase left on the reactor wall. The TPR of zinc oxide doped Li_2CO_3/MgO catalysts (figure 6.4.3.g) are typical of Li_2CO_3 decomposition profiles as was observed on undoped Li_2CO_3/MgO catalysts. The TPR profiles of used 5.9wt.% zinc oxide doped MgO and 6.9wt.% zinc oxide doped Li_2CO_3/MgO catalysts after reaction at 800°C for 2 hours have also been determined. The profiles of the used 5.9wt.% catalysts (curve i) indicate the absence of any reducible sites. An increase in size of the Li_2CO_3 decomposition profiles of the used 6.9wt.% catalysts (curve ii) further confirmed the enrichment of the surface with Li_2CO_3 under reaction condition.

The TPR results shows that no reducible phase is present on zinc oxide doped MgO. On the doped Li_2CO_3/MgO similar profiles to that of Li_2CO_3MgO (compare figure 6.4.3.g with figure 6.4.2.f) were observed indicating the similarity in their physical and chemical characteristics.

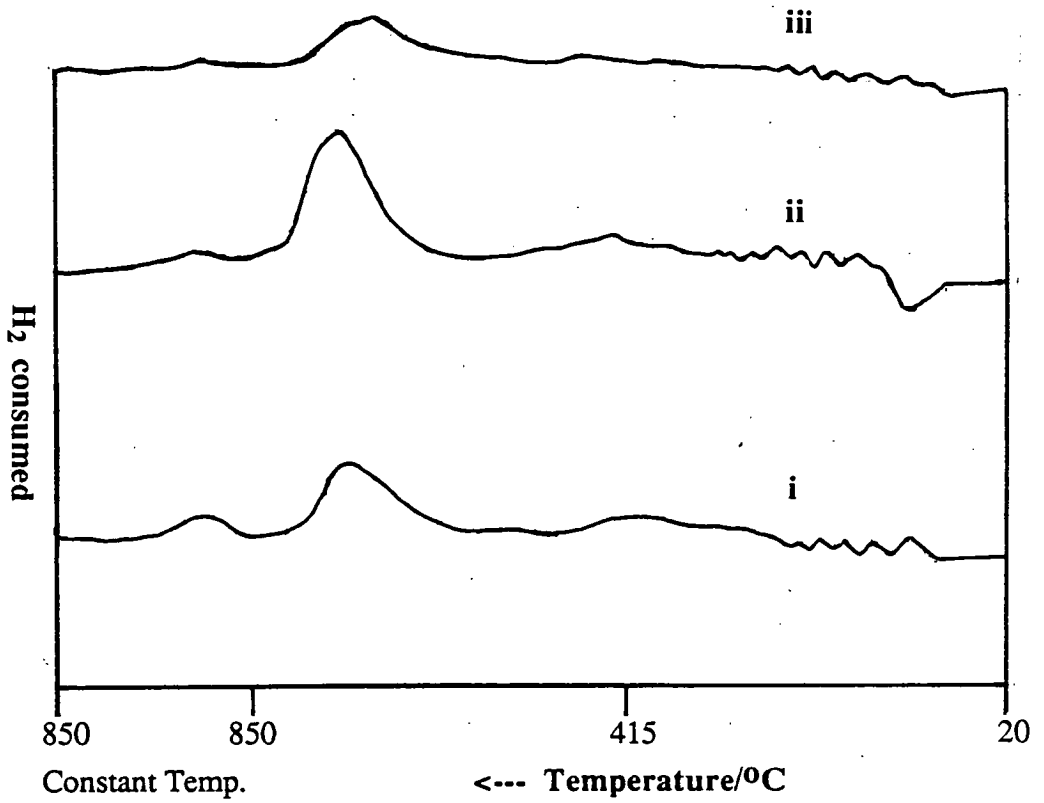

Figure 6.4.3.f TPR profiles of calcined, ground and sieved MgO catalysts doped with different loading of zinc oxide. Profiles i), ii) and ii) correspond to catalytic sample 14C, 15C and 16C respectively, whose composition are given in Table 6.2.3.1.b.

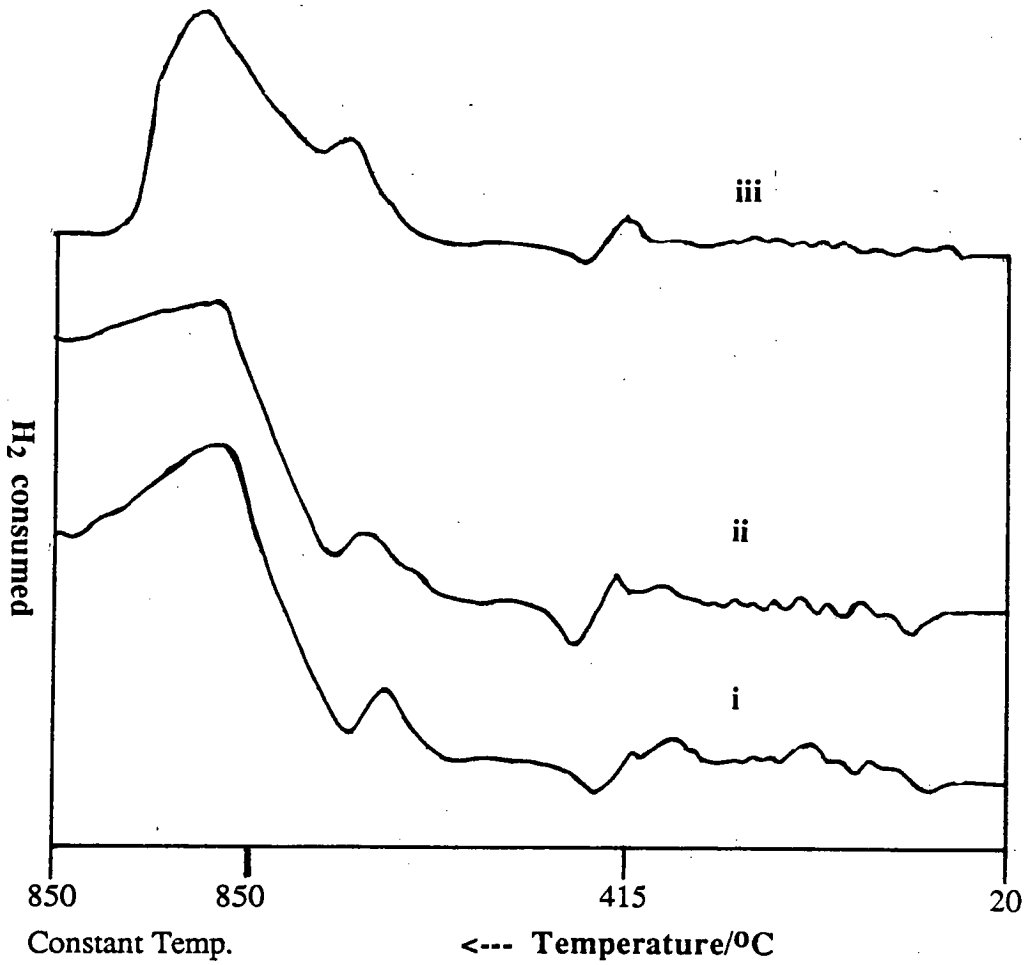

Figure 6.4.3.g TPR profiles of calcined, ground and sieved Li_2CO_3/MgO catalysts doped with different loadings of zinc oxide. Profiles i), ii) and iii) correspond to catalytic sample 10C, 11C and 12C respectively, whoese composition are given in Table 6.3.2.1.a.

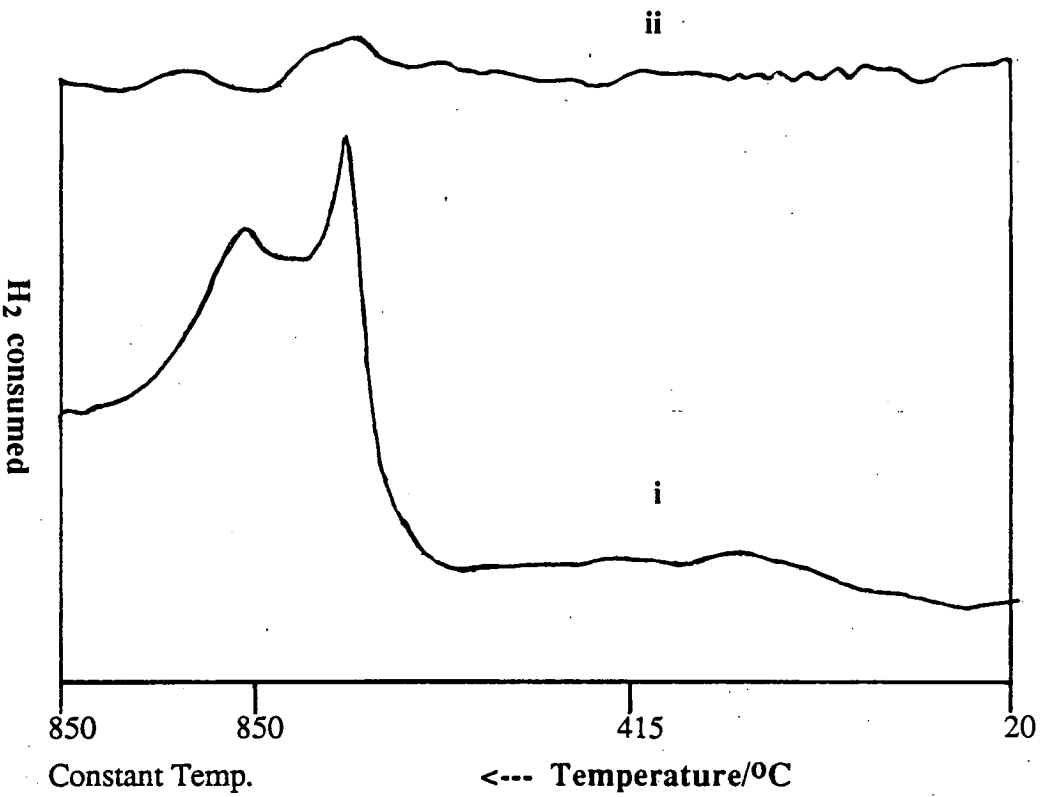

Figure 6.4.3.h TPR profiles of i) 11C and ii) 15C catalytic materials after 2 hours on-stream under the condition of oxidative reaction of methane at 800°C.

The role of ionic radii factor in affecting the physical and chemical nature of the doped Li_2CO_3/MgO catalysts was further highlighted here. Enrichment of the surface with zinc oxide and Li_2CO_3 phase occurs due to the similarity of the ionic radii between Zn^{2+} and Li^+. The Li_2CO_3/ZnO systems have been found to have good oxidative coupling activity by Matsuura et. al.,1986, Zhang, et al.,1988 and Roos et al.,1988. It is likely that as in the Li_2CO_3/MgO system the stabilisation of Li_2CO_3 on ZnO contribute to the catalytic activity of this material.

6.4.4 Manganese oxide doped MgO and Li_2CO_3/MgO system

The presence of manganese oxide on Li_2CO_3/MgO seems to have a detrimental effect on the layer formation of the catalysts samples after the precalcination (figure 6.4.4.a). On the 0.2 wt % catalysts some surface layer was still present (micrograph i) but on the 0.6 wt % (micrograph ii) no such structure was observed. On the latter sample the material seem to be composed of fine particles which agglomerate to form clusters. At a higher manganese oxide loading the particles size increases significantly while the cluster size decreases (micrograph iii and iv). The presence of manganese oxide does not seem to stabilise the bulk surface layer which normally coat the catalysts samples after the 10 hours precalcination at 900°C.

The SEM micrograph of grinded manganese oxide doped catalysts which were precalcined are given in figure 6.4.4.b. The average cluster size on the powdered 0.2, 0.6 and 4.6 wt.% catalyst loading was about 0.2 μ-metre (micrographs i, ii, and iii). On the 19.8wt.% catalysts however the average cluster size was about 0.5 μ-metre (micrograph iv). The average cluster size of these catalysts is much smaller than that of the zinc oxide doped Li_2CO_3/MgO catalysts. It was also observed that on the 19.8wt.% manganese oxide doped catalysts shapes of the particles of these catalysts become more spherical.

The XRD patterns for manganese oxide doped MgO and Li_2CO_3/MgO catalysts are given in figure 6.4.4.c and 6.5.3.d respectively. The XRD pattern (patterns i and ii) on the 0.3 and 1.0wt.% manganese oxide doped MgO catalysts

i)

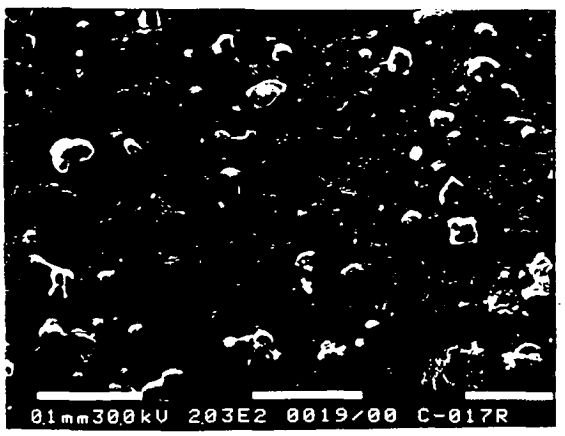

ii)

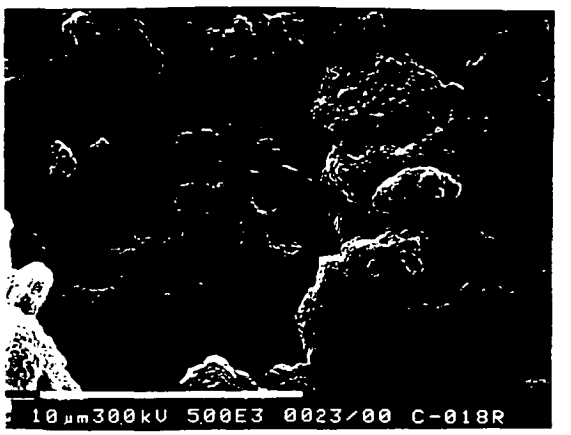

iii)

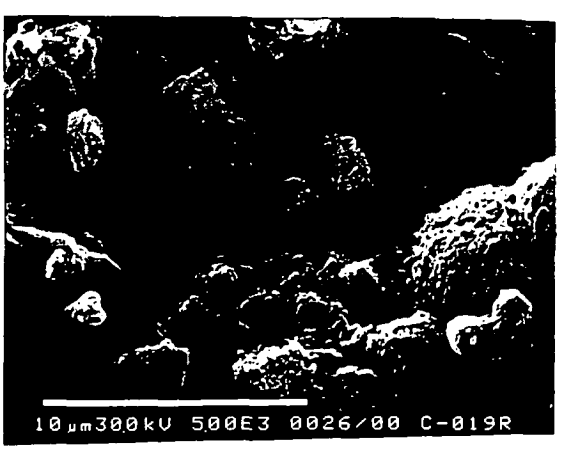

iv)

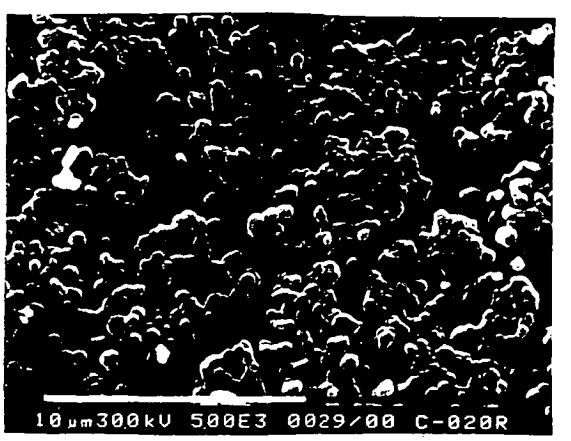

Figure 6.4.4.a SEM micrographs of the Li_2CO_3/MgO doped with different loadings of manganese oxide after precalcination at 900°C for 10 hours. Micrograph i) correspond to catalytic sample 17C at a magnification of $2x10^3$, while ii), iii) and iv) are micrographs of 18C, 19C and 20C respectively at a magnification of $5x10^3$. The composition of these catalytic sample are given in Table 6.2.4.1.a

i)

ii)

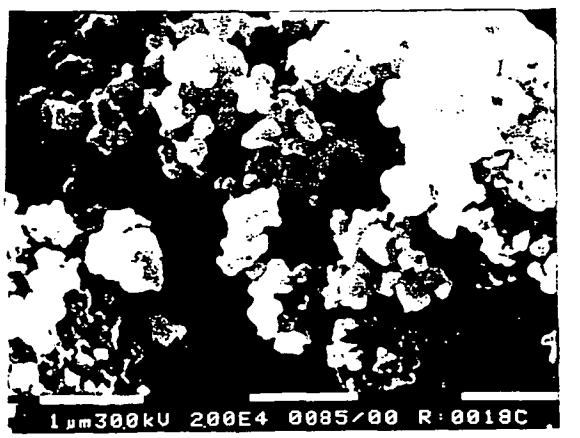

iii)

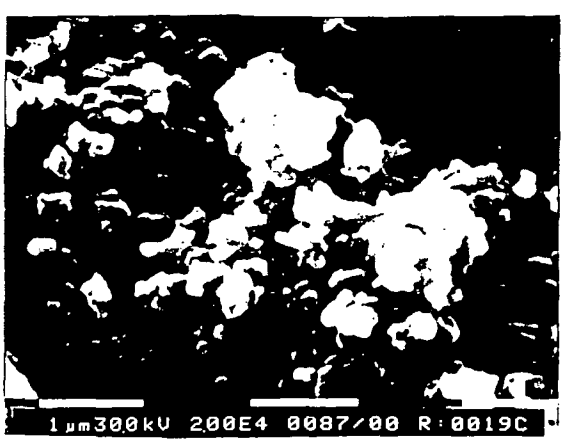

iv)

Figure 6.4.4.b SEM micrographs of calcined, ground and sieved Li_2CO_3/MgO catalysts doped with different loadings of manganese oxide (magnification of $2x10^4$). Micrographs i), ii), iii) and iv) correspond to catalytic sample 17C, 18C, 19C, and 20C respectively, whose composition are given in Table 6.2.4.1.a.

shows only the presence of MgO. On the 4.5wt.% catalysts (pattern iii), two new peak was observed at 2θ of 18.3 and 35.5° corresponding to the d-spacing value of 4.84 and 2.53 respectively. These peaks could represent that of Mn_3O_4 phase (2.54_x,1.49_6,4.86_5)

The XRD pattern of the 0.2 and 0.6wt.% (pattern i and ii of figure 6.4.4.d) manganese oxide on Li_2CO_3/MgO indicates that the catalysts consists mainly of MgO and Li_2CO_3. In the XRD patterns of 4.6wt.% catalysts (pattern iv) a new peak at 2θ of 33.6° was present corresponding to a d-spacing of 2.69 suggesting the presence of $MgMnO_3$ phase on the catalyst (1.68_x,2.68_8,2.47_8). Two new XRD peaks at 18.7 and 44.6° corresponding to d-spacing of 4.85 and 2.02 respectively, were observed on the 19.8wt.% catalysts. These peaks suggest the presence of Li_2MnO_3 (2.02_x,4.79_5,2.42_5).

The TPR profiles of manganese oxide doped MgO catalysts are presented in figure 6.4.4.e. At low loading of manganese oxide broad reduction peak was observed between 300-600°C. In the TPR pattern of 4.5 wt % catalysts a sharp reduction peak between 600-700°C together with the broad reduction peak at lower temperature were. The possible conversion involving the independent manganese oxide phase happening under the TPR condition are listed in equation 6.4.4.a-6.4.4.c.

Equation 6.4.4.a $H_2 + 3Mn_2O_3 \rightarrow 2Mn_3O_4 + H_2O$

Equation 6.4.4.b $H_2 + 2MnO_2 \rightarrow Mn_2O_3 + H_2O$

Equation 6.4.4.c $H_2 + Mn_3O_4 \rightarrow 3MnO + H_2O$

At any particular temperature the standard free energy change for the reduction of the manganese oxide phases are in the order of Eq.6.4.4.a< Eq. 6.4.4.b < Eq. 6.4.4.c (Bhasin 1988). In this respect the broad peak at 300-500°C in TPR profiles of the 4.5wt.% can be assign to the reduction of Mn_2O_3 phase to form Mn_3O_4 while the sharp peak at about 600°C is due to the reduction process of Mn_3O_4 to form MnO. The shoulder peak at about 730°C can be assign to the reduction of Mn_3O_4 to MnO.

The TPR patterns of the manganese oxide doped Li_2CO_3/MgO show the presence of reduction peaks together with that due to Li_2CO_3 decomposition (figure

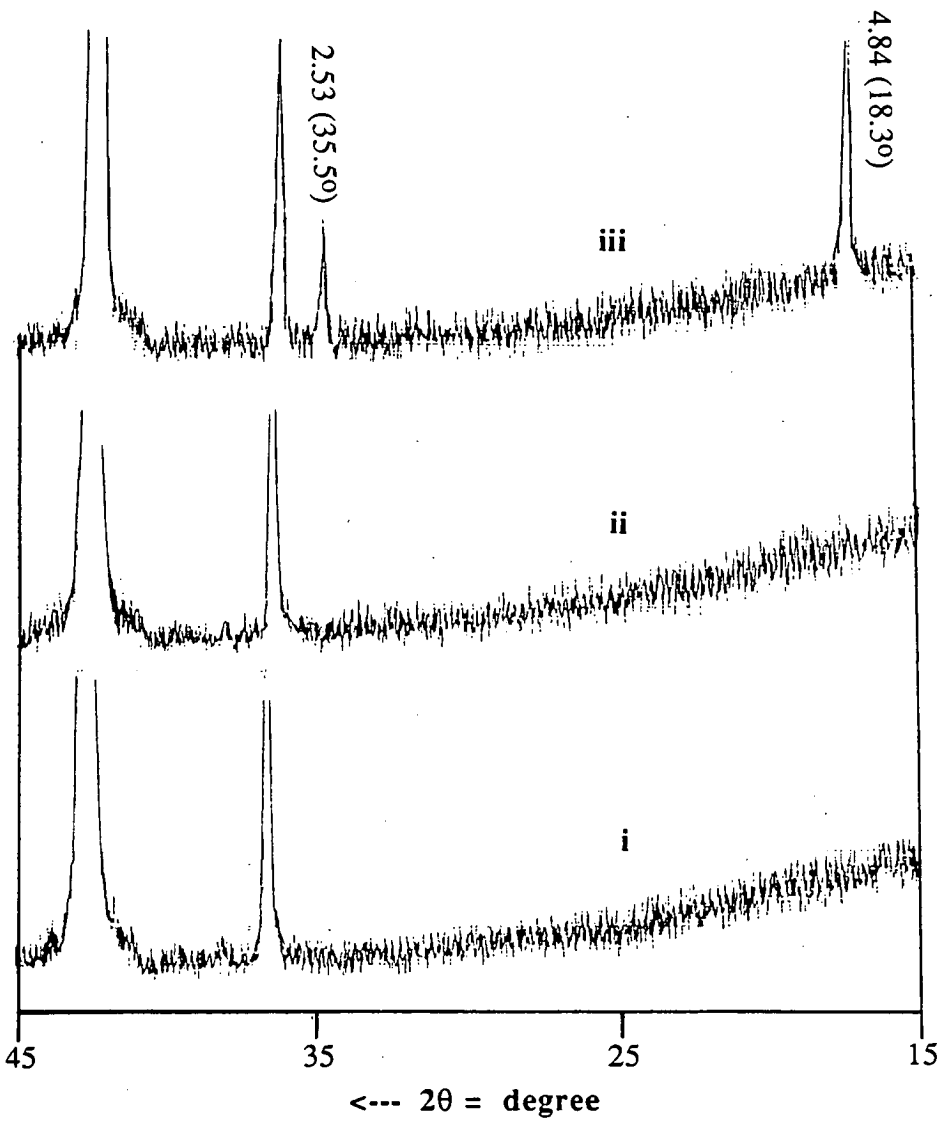

Figure 6.4.4.c XRD patterns of calcined, ground and sieved MgO catalysts doped with different loadings of manganese oxide. Patterns i), ii) and iii) correspond to catalytic sample 21C, 22C, and 23C respectively, whose composition are given in Table 6.2.4.1.b. The value presented at any particular peak correspond its d-spacing.

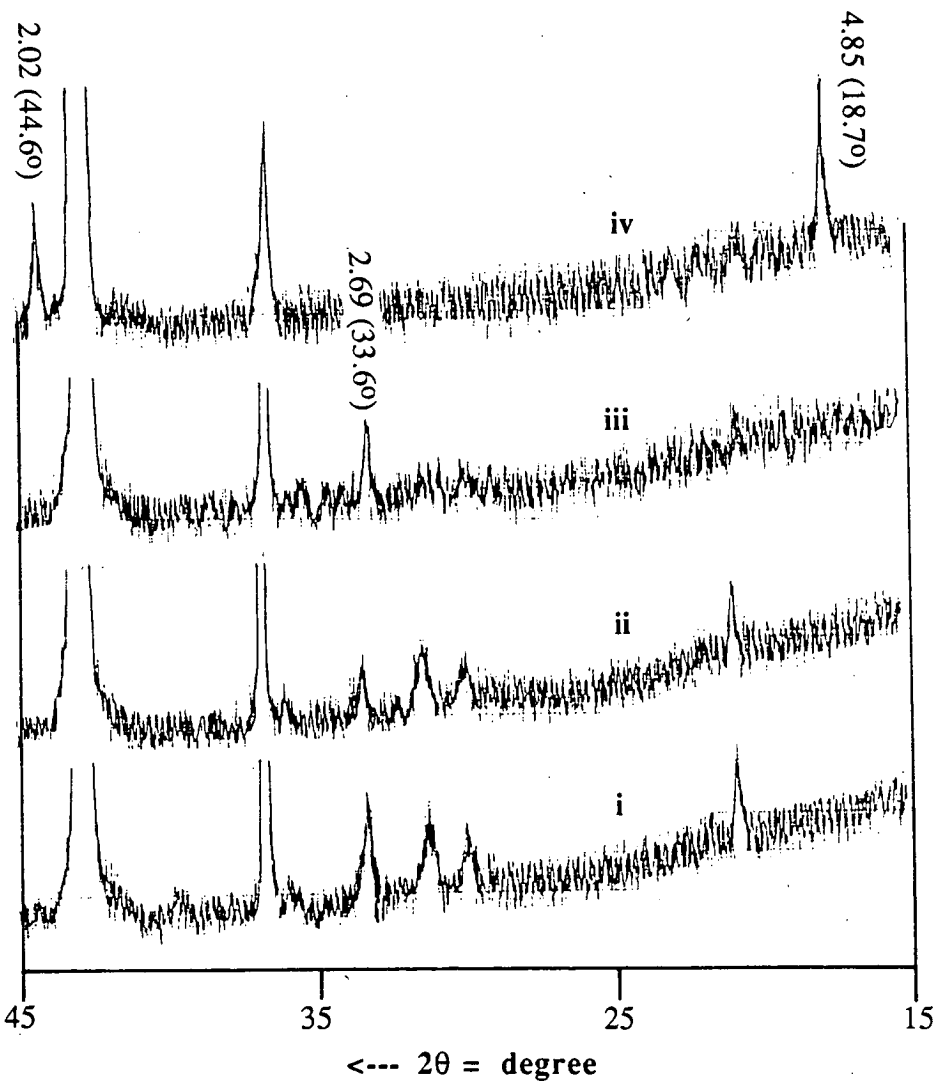

Figure 6.4.4.d XRD patterns of calcined, ground and sieved Li_2CO_3/MgO catalysts doped with different loadings of manganese oxide. Patterns i), ii), iii) and iv) correspond to catalytic sample 17C, 18C, 19C, and 20C respectively, whose composition are given in Table 6.2.4.1.a. The value presented at any particular peak correspond its d-spacing.

6.4.4.f). On 0.2wt % catalyst, reduction peaks at 430 and 690°C were present. The intensity of these peaks increased at higher manganese loading (profiles ii & iii). At the loading of 19.8wt.% the peak at 690°C becomes much more dominant while the peak at lower temperature decreases in intensity. It was also observed that the lower temperature reduction peak increases towards higher temperature with the increase in manganese oxide loadings.

In term of TPR peaks assignment, as in the manganese oxide doped MgO, the lower temperature reduction peak is likely be due to the reduction of Mn_2O_3 to form MnO, and possibly Li_2MnO_3 to form Li_2MnO_2, while the main peak (at about 700°C) is due to the reduction of MnO_2 to Mn_2O_3. The higher temperature shoulder of the main peak can similarly be assigned to the reduction of Mn_2O_3 to Mn_3O_4. On the manganese oxide doped Li_2CO_3/MgO catalysts the presence of distinct reduction peak at 400°C could possibly suggest the presence of Li_2MnO_3 phase.

The TPR profiles of used 4.5wt.% manganese oxide doped MgO (23C) and 4.6wt.% manganese oxide doped Li_2CO_3/MgO (19C) catalysts have also been determined and are presented in figure 6.4.4.g. Unlike the comparable iron oxide doped Li_2CO_3/MgO catalysts the used 4.6wt% (19C) manganese oxide doped Li_2CO_3/MgO (profile i) showed the presence of reducible manganese oxide phase.However under the condition of oxidative reaction of methane, the steady state composition of reducible manganese oxide species on the catalysts is much lower than that on fresh catalysts. The peak due to Li_2CO_3 decomposition on the used catalyst was observed to increase significantly in agreement with the enrichment of catalysts surface with Li_2CO_3 during reaction condition also occurs. This indicates that in all Li_2CO_3/MgO catalytic system, migration of Li_2CO_3 phase to the surface occurs under reaction condition.

In this study, the physical and chemical nature of the doped Li_2CO_3/MgO catalysts were observed to be significantly affected by manganese oxide loading. The SEM micrographs of the catalytic sample indicate that manganese oxide doping prevented formation of surface layer on the calcined samples. The presence of

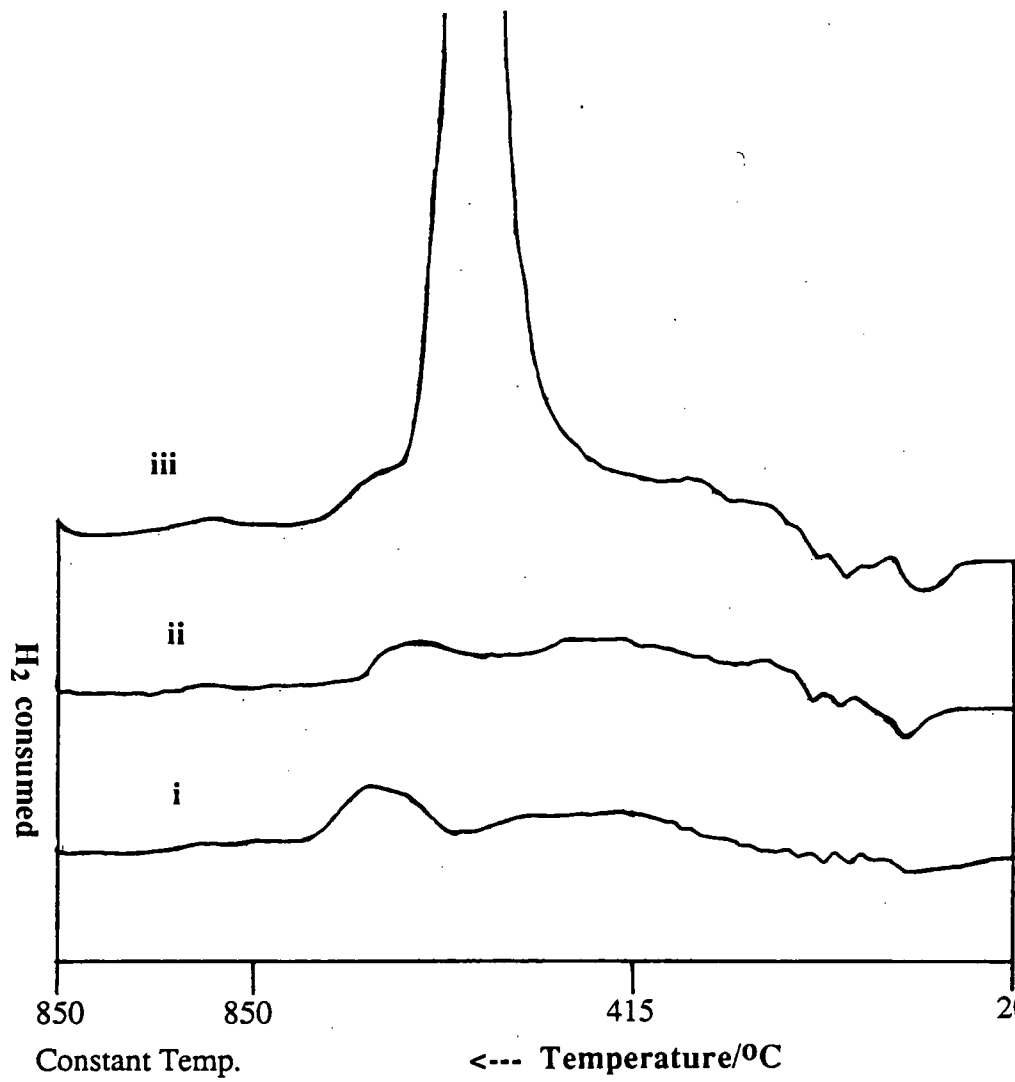

Figure 6.4.4.e TPR profiles of calcined, ground and sieved MgO catalysts doped with different loading of manganese oxide. Profiles i), ii) and ii) correspond to catalytic sample 21C, 22C and 23C respectively, whose composition are given in Table 6.2.4.1.b.

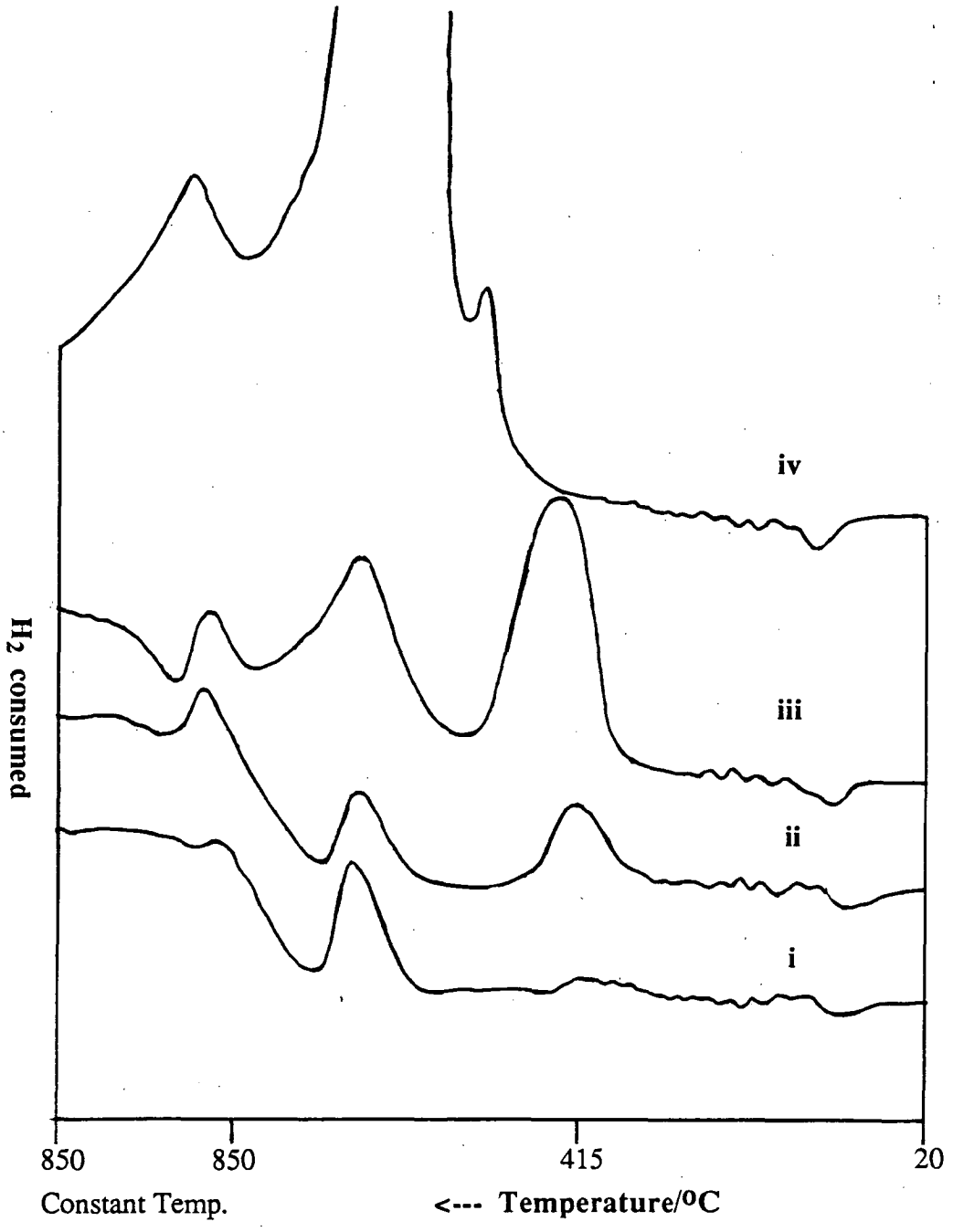

Figure 6.4.4.f TPR profiles of calcined, ground and sieved Li_2CO_3/MgO catalysts doped with different loadings of manganese oxide. Profiles i), ii), iii) and iv) correspond to catalytic sample 17C, 18C, 19C and 20C respectively, whoese composition are given in Table 6.2.4.1.a.

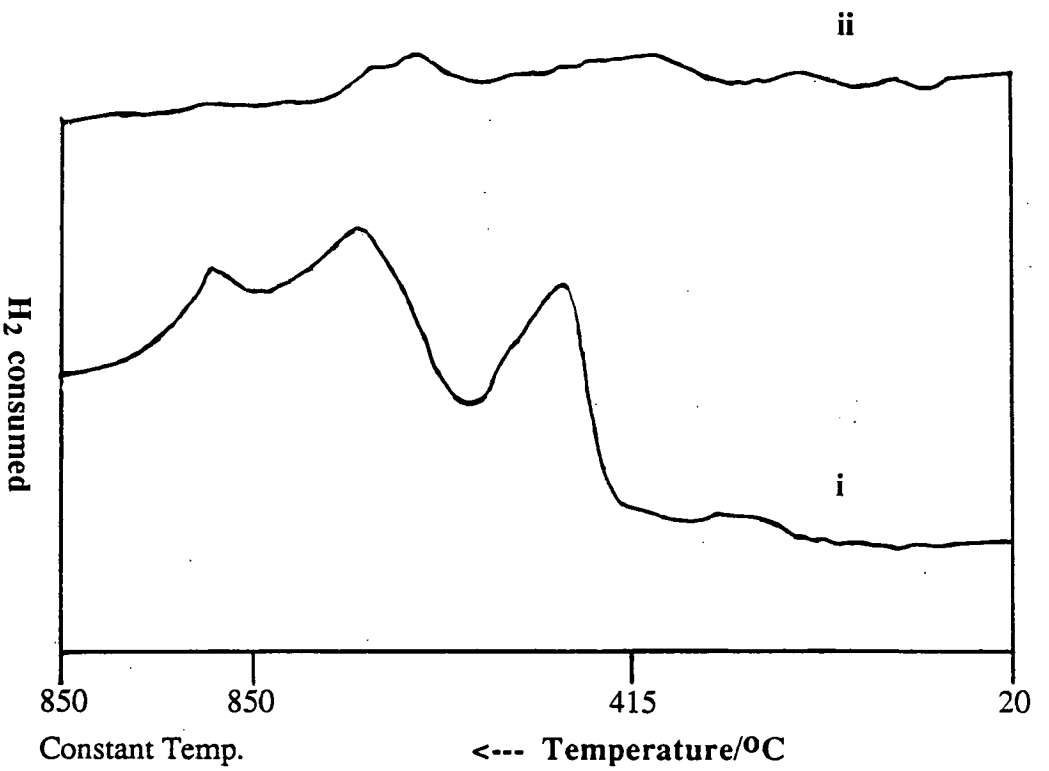

Figure 6.4.4.g TPR profiles of i) 18C and ii) 23C catalytic materials after 2 hours on-stream under the condition of oxidative reaction of methane at 800°C.

manganese oxide also disrupts the formation of solid matrix between Li_2CO_3 and MgO making the resulting material easier to grind. it has been observed that the particles of manganese oxide doped catalysts are finer and more spherical in shape compared to that of undoped Li_2CO_3/MgO catalyst. In turn the finer particle size of these catalysts could partly explained their higher activity relative to the undoped Li_2CO_3/MgO catalyst.

It was also observed from TPR experiments that the manganese oxide phase of doped Li_2CO_3/MgO catalysts are available for reduction. This indicates that the reducible manganese oxide sites are available on the catalysts surfaces during the oxidative reaction of methane. The presence of these redox sites will facilitate the oxygen transfer resulting in higher oxidative reaction activity of the manganese oxide doped Li_2CO_3/MgO catalysts. However, the presence of these sites would result in the decrease of selectivity to C_2 hydrocarbon.

In the catalytic study it was observed that the presence of manganese oxide at loading less than 4.6% resulted in methane conversion higher than that of Li_2CO_3/MgO. Moreover the C_2 selectivity was observed to be retained. At higher manganese loading however, an increase in the exhaustive reaction of methane occur resulting in the loss of C_2 selectivity. These suggest that at low loading, the change in the physical nature of the catalysts as a result of manganese oxide presence caused the increase in methane conversion. At higher loading however, the increase of reducible manganese oxide phase on the surface leads to the increase of exhaustive reaction of methane.

The doping of manganese oxide on MgO have been observed to result in exhaustive oxidation of methane to carbon dioxide. The TPR of the manganese oxide doped catalysts shows that reducible manganese oxide species are present on these catalysts The presence of manganese oxide on MgO increases the redox capability of the catalysts and this should facilitate the exhaustive reaction to occur.

In terms of 'ionic radii factor' , the ionic radii of manganese ions are very different (example Mn2+ 83pm, see table 6.5.a) from that of Mg^{2+} (72pm) and Li^{+}

(74pm). This could explain the disruption of surface layer formation on the calcined samples of these catalytic materials. Moreover, because the Li_2CO_3 layer was not stabilised on the catalysts surface, the manganese oxide phases will be exposed and are accesible to the reactant gas. This enable the manganese oxide to be involved in the oxidative reaction of methane especially in facilitating the oxygen transfer.

6.4.5 Chromium oxide doped on MgO and Li_2CO_3/MgO system

The SEM micrographs of chromium oxide doped Li_2CO_3/MgO samples after precalcination are shown in figure 6.4.5.a. The micrograph of 0.1wt.% catalyst (25C, micrograph i) indicate that no significant surface layer formation takes place on this sample. This lack of any surface layer formation also occur on the 0.4 (26C, micrograph ii) and 1.6wt.% (27C, micrograph iii) catalysts. However it was observed that the cluster size on these materials increases with chromium oxide loading. The nature of the powdered form of the calcined chromium oxide doped Li_2CO_3/MgO catalysts have also been studied by SEM (figure 6.4.5.b). The micrographs of these catalysts show that the average cluster size on these sample was about 0.5 μ-metre.

The XRD patterns for calcined chromium oxide doped on MgO and Li_2CO_3/MgO are given in figure 6.4.5.c and figure 6.4.5.d respectively. The XRD pattern for 0.1 and 0.4 wt % chromium oxide doped MgO (patterns i and ii) shows only the presence of MgO. On the 1.6wt.% catalyst (30C) (pattern iii) three new peaks were observed at 2θ of 18.5, 30.4 and 35.8° which correspond to d-spacing of 4.79, 2.94 and 2.51 respectively. These new XRD peaks suggest the presence of $MgCr_2O_4$ (2.52_x,4.81_7,2.08_6) and/or the $Mg_{1.92}Cr_{1.08}$) $Cr_{16}O_{32}$ (2.51_x,4.79_8,2.08_8) species where most of the chromium ion existed in the oxidation state of +3. However, chromium oxide phase like Cr_2O_3 (2.67_x,2.48_x,1.67_9), CrO_2 (3.11_x,1.63_8,2.42_6) and CrO_3 (4.16_x, 3.42_x, 3.36_x) could also be present even though their XRD pattern are absent.

Generally the XRD patterns of chromium oxide doped Li_2CO_3/MgO catalysts (figure 6.4.5.d) show the prominence of MgO and Li_2CO_3 phase. However, the XRD

i)

ii)

iii)

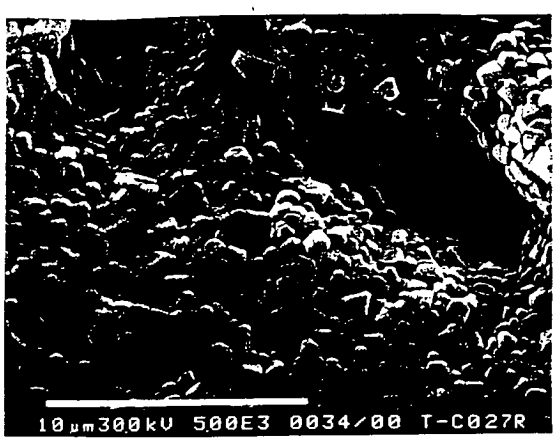

Figure 6.4.5.a SEM micrographs of the Li_2CO_3/MgO doped with different loadings of chromium oxide after precalcination at 900°C for 10 hours (magnification of $5x10^3$). Micrographs i), ii) and iii) correspond to catalytic sample 25C, 26C and 27C respectively, whose composition are given in Table 6.2.5.1.a.

i) ii)

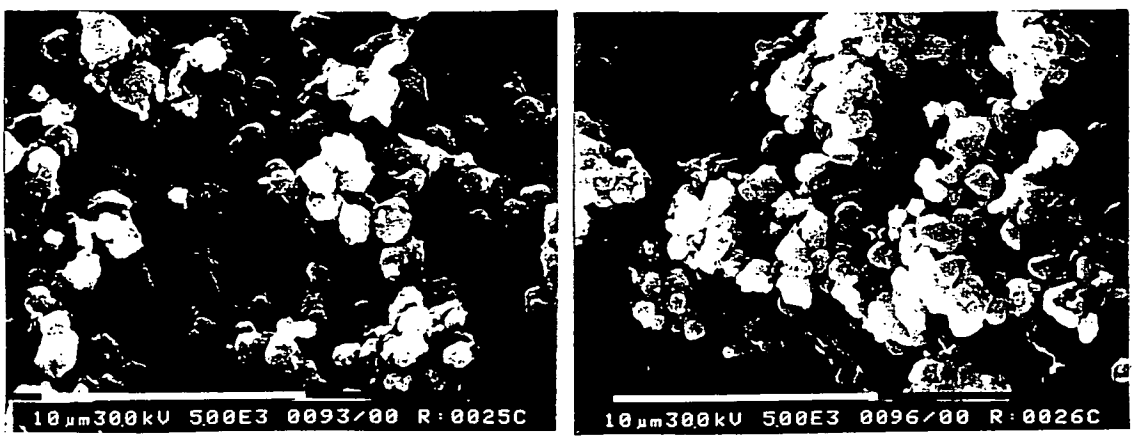

iii)

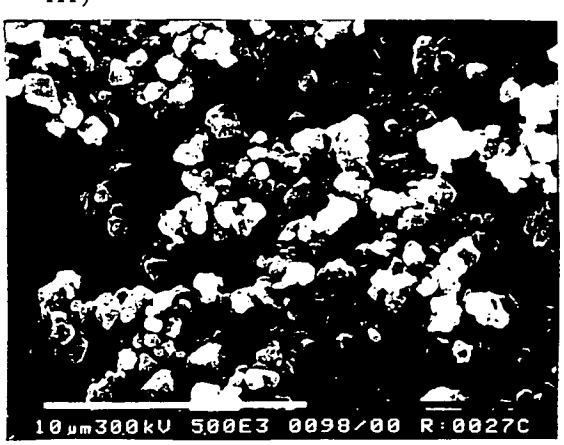

Figure 6.4.5.b SEM micrographs of calcined, ground and sieved Li_2CO_3/MgO catalysts doped with different loadings of chromium oxide (magnification of $5x10^3$). Micrographs i), ii) and iii) correspond to catalytic sample 25C, 26C and 27C respectively, whose composition are given in Table 6.2.5.1.a.

pattern of 0.4wt.% catalyst (26C, pattern ii) also show the presence of chromiun oxide phase. The XRD peak at 2θ of 18.2 and 21.7° which correspond to d-spacing of 4.87 and 4.09 suggested the presence of at least the $MgCr_2O_4$ (2.52x,4.87,2.08) and Li_2CrO_4 (4.10_x,4.39_3,3.50_3) phases on this catalysts. As in the doped Li_2CO_3/MgO catalysts, other chromium oxide phase can also be present on these catalysts. The increase in the intensity of these peaks in the pattern of the 1.6wt.% catalysts is agreement with the increase in the amount of the chromium oxide phases on the catalyst.

The TPR profile of chromium oxide doped MgO catalysts are given in figure 6.4.5.e. It is possible to identify at least three reduction peaks at about 200, 350 and 450°C respectively. The oxide phase related to the reduction peak at 450°C is likely to be the major component of the chromium oxide. In the case of the TPR of chromium oxide doped Li_2CO_3/MgO catalysts (figure 6.4.5.f), the major reduction peak occurs at about 380°C and it increases to about 500°C for the 2.2% catalysts. The reduction peak at about 200°C can be tentatively assigned to the reduction of CrO_3 species to form CrO_2 while the one at 350°C due to the reduction of CrO_2 to Cr_2O_3. Moreover the CrO_3 and CrO_2 phase are known to decompose at 200 and 300°C respectively (Aylward and Findlay,1971). In the case of the major reduction peak, at 450°C, it can be assigned to the reduction of Cr_2O_3 as describe by equation 6.4.5.a.

Equation 6.4.5.a $3H_2 + Cr_2O_3 \rightarrow 2Cr(OH)_2 + H_2O$

In the catalysts screening, it has been observed that the colour of used chromium oxide doped Li_2CO_3/MgO catalysts is yellow while the unused catalyst is green. Recalcination of the used catalyst in air at 800°C changes the colour of the used catalysts back to green. These observation suggests that the major chromium oxide phase present on the calcined catalyst is the Cr_2O_3 phase which is green in colour while the used catalysts contains the yellowish chromium hydroxide. Calcination of the used catalyst will convert $Cr(OH)_2$ back to Cr_2O_3. Moreover, these observation also suggest that the redox process involving these two phase are likely to facilitate the exhaustive reaction of methane.

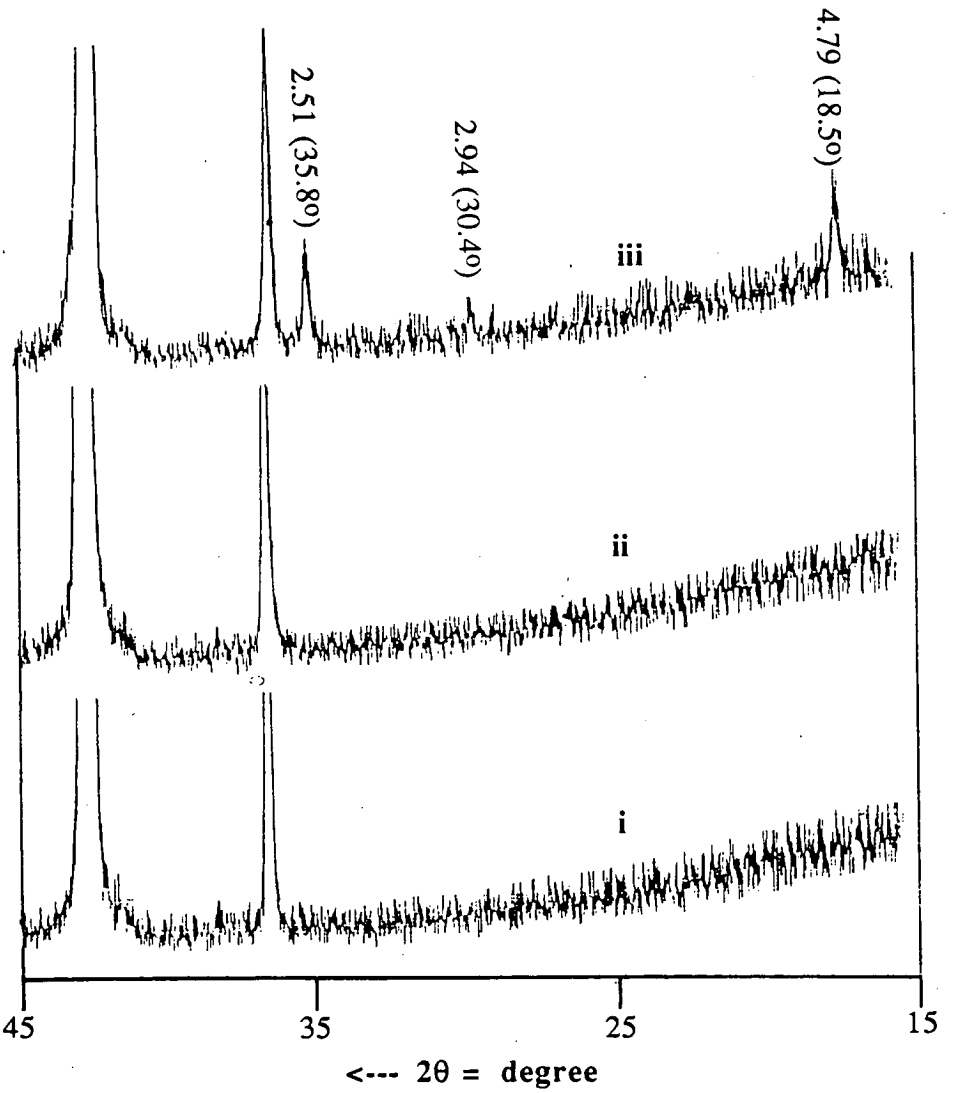

Figure 6.4.5.c XRD patterns of calcined, ground and sieved MgO catalysts doped with different loadings of chromium oxide. Patterns i), ii) and iii) correspond to catalytic sample 28C, 29C, and 30C respectively, whose composition are given in Table 6.2.5.1.b. The value presented at any particular peak correspond its d-spacing.

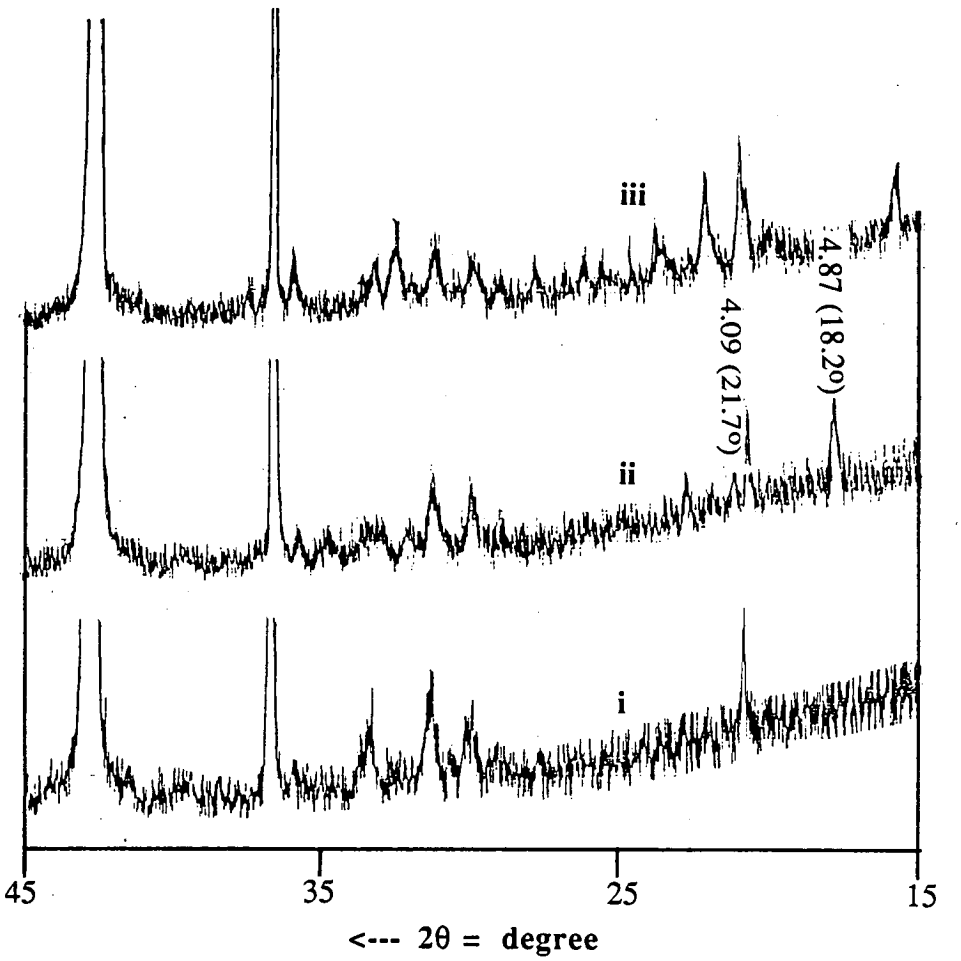

Figure 6.4.5.d XRD patterns of calcined, ground and sieved Li_2CO_3/MgO catalysts doped with different loadings of chromium oxide. Patterns i), ii) and iii) correspond to catalytic sample 25C, 26C and 27C respectively, whose composition are given in Table 6.2.5.1.a. The value presented at any particular peak correspond its d-spacing.

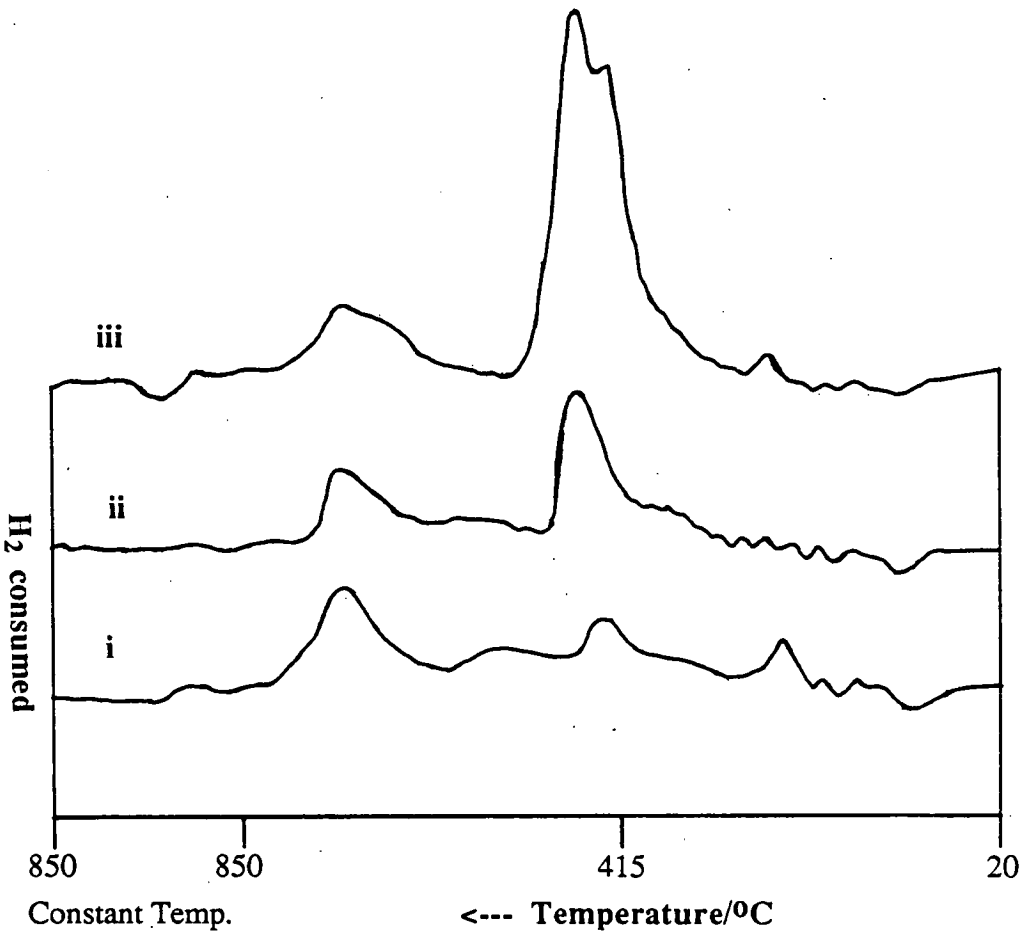

Figure 6.4.5.e TPR profiles of calcined, ground and sieved MgO catalysts doped with different loading of chromium oxide. Profiles i), ii) and ii) correspond to catalytic sample 28C, 29C and 30C respectively, whose composition are given in Table 6.2.5.1.b.

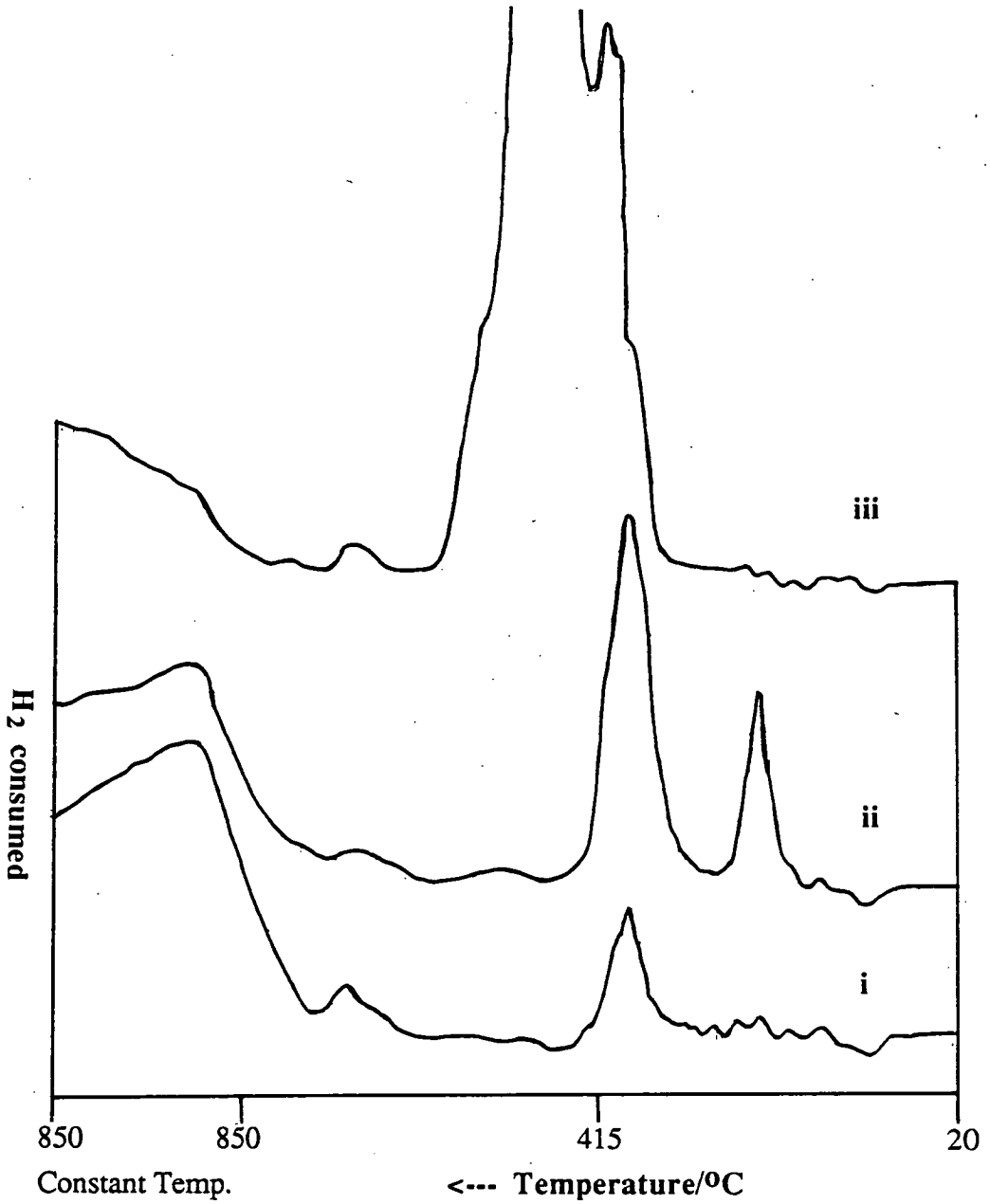

Figure 6.4.5.f TPR profiles of calcined, ground and sieved Li_2CO_3/MgO catalysts doped with different loadings of chromium oxide. Profiles i), ii) and iii) correspond to catalytic sample 25C, 26C and 27C respectively, whoese composition are given in Table 6.2.5.1.a.

The TPR profiles of used 0.4wt.% chromium oxide doped MgO (29C) and chromium oxide doped Li_2CO_3/MgO (26C) catalysts are presented in figure 6.4.5.g. The profile of the doped MgO catalysts (profile i) indicate a significant steady state concentration of the reducible chromium oxide species during the oxidative reaction of methane. A similar observation was also made for the doped Li_2CO_3/MgO catalysts (profile ii).

These results clearly show that when chromium oxide was doped on Li_2CO_3/MgO it resulted in severe physical and chemical changes. The SEM results show that the presence of chromium oxide on Li_2CO_3/MgO prevented the formation of a Li_2CO_3 rich surface layer on the calcined samples. It was observed from the XRD experiment that the chromium oxide of the doped Li_2CO_3/MgO catalysts also existed as mixed oxide or independent chromium oxide phases. The formation of solid matrix between Li_2CO_3 and MgO was totally disrupted by the presence of chromium oxide and this enabled the chromium oxide phase to be exposed on the catalysts surface.

The chromium oxide on the doped Li_2CO_3/MgO catalysts are available for reduction, even in the case of 0.1wt% catalysts. This indicates that during the oxidative reaction of methane, the chromium oxide phase on the doped Li_2CO_3/MgO catalysts are accesible to the reactants. Therefore, under oxidative reaction conditions chromium oxide will serve as an efficient redox site and this explains why the chromium oxide doped Li_2CO_3/MgO catalyst favours the exhaustive oxidation of methane.

6.5 The effect of ionic radii factor on the physical and chemical properties of catalysts and also on the catalytic activity

The results obtained in this chapter shows that different transition metal oxides affect the physical and chemical nature on the doped MgO and Li_2CO_3/MgO catalysts differently. In order to elucidate the possible role of the 'ionic radii factor' on these changes, the ionic radii of the various transition metal ions listed by Aylward and Findlay, 1971 are reproduced in table 6.5.a.

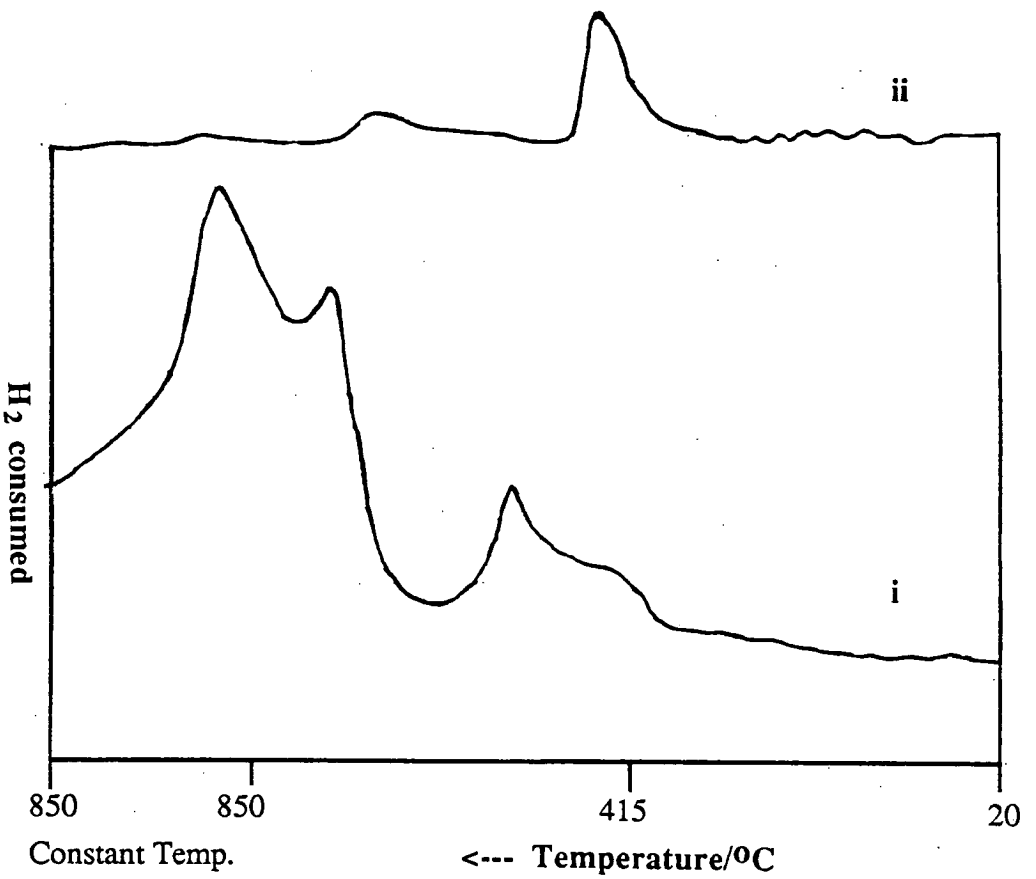

Figure 6.4.5.g TPR profiles of i) 26C and ii) 29C catalytic materials after 2 hours on-stream under the condition of oxidative reaction of methane at 800°C.

The effect of the various transition metal oxides on MgO are not distinctly different from each other. SEM studies of the precalcined transition metal oxide doped MgO samples, unlike the doped Li_2CO_3/MgO, shows no layer formation . To illustrate this point the photomicrograph of zinc oxide doped MgO samples are given in figure 6.5.a. These micrographs indicate that the calcined zinc oxide doped MgO samples are made of clusters which are spherical in shape. No significant variation due to the loading of zinc oxide was observed. Moreover, on the doped MgO catalysts, the presence of the transition metal oxide always increase the redox capability of the catalysts as was observed in their TPR profiles. This properties promoted the predominance of exhaustive oxidation of methane to carbon dioxide over these catalysts.

Table 6.5.a The ionic radii of various transition metal ions

Element	ionic radii (pm)*
Chromium	63(3+), 52(6+)
Iron	*78* (+2), 74, 64(3+)
Lithium	*74* (1+), 68
Magnesium	*72* (+2), 66
Manganese	*83* (2+), 80, 46(7+)
Zinc	74(2+)

* Values given in plain text are taken from Ahrens,1952, while the one in italics are that of Shannon and Previtt, 1969. In this work the values given by Shannon and Previtt,1969,1970 are preferred. If the absolute value of the difference between ionic radii of the ions and Li^+ were compared, the order with increasing difference will be Zn^{2+}(0pm),Mg^{2+}(2pm),Fe^{2+}(4pm),Mn^{2+}(9pm),Cr^{3+}(11pm).

The different effect of the various transition metal oxide are more distinct on the doped Li_2CO_3/MgO catalysts. It has been observed on the undoped Li_2CO_3/MgO sample that precalcination at 900°C for 10 hours resulted in the formation of surface layer coating the calcined sample (figure 5.2.1.a). This surface layer has been shown to be mainly composed of the Li_2CO_3 phase. The doping of transition metal oxides

i)

ii)

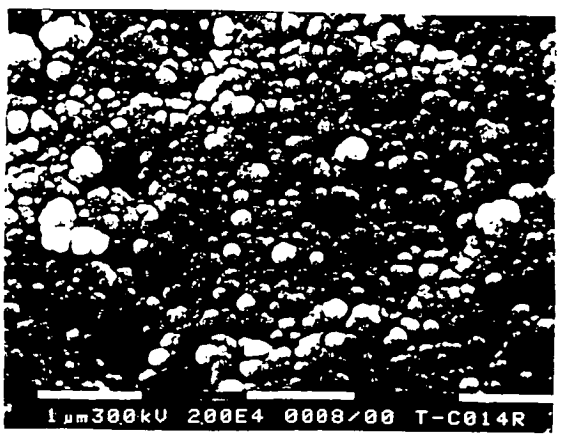

iii)

iv)

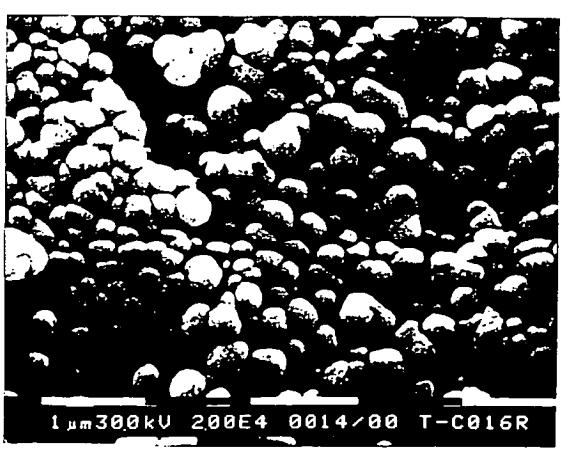

Figure 6.5.a SEM micrographs of MgO doped with different loadings of zinc oxide after precalcination at 900°C for 10 hours (magnification of $2x10^4$). Micrographs i), ii), iii) and iv) correspond to catalytic sample 13C, 14C, 15C and 16C respectively, whose composition are given in Table 6.2.3.1.a.

generally resulted in the decrease of the extent of the surface layer formed. Judging from the SEM micrograph of the Li_2CO_3/MgO catalysts doped to a similar extent, the destruction of the surface layer increases in the order Zn < Fe < Mn < Cr. Moreover, it was observed that on the zinc oxide doped Li_2CO_3/MgO catalysts enrichment of Li_2CO_3 with ZnO occurs. These behaviours of the calcined catalysts correlate with the difference in ionic radii of the transition metal ion to that of Li^+ and Mg^{2+}.

The TPR profiles of fresh and used Li_2CO_3/MgO catalysts doped with transitional metal oxide doped indicates the significance of the ionic radii factor. No reducible phases were observed on the Li_2CO_3/MgO catalysts doped with iron oxide and zinc oxide. In the case of catalysts doped with manganese oxide and chromium oxide the presence of the reducible phases are evident even on low loading catalysts. The ionic radii of the zinc and iron ions are quite similar to that of lithium and magnesium, while the ionic radii of manganese and chromium ion are significantly different.

In the activity studies of the Li_2CO_3/MgO catalysts doped with zinc and iron oxides, the oxidative coupling activities were retained. In the case of manganese oxide doped catalysts, the activity of the catalysts was generally increased except at the highest loading when the exhaustive reaction become more dominant. On chromium oxide doped catalysts however the exhaustive reaction was more favoured. Chromium oxide is a good oxidation catalyst.

The effect of transition metal oxide doping on the physical and chemical characteristics and the catalytic activity of Li_2CO_3/MgO catalysts does seem to correlate with the differences between the ionic radii of the transition metal ions and the Li^+ and Mg^{2+} ions. Transition metal oxide whose ions have similar ionic radii to those of Mg^{+2} and Li^+ resulted in some changes in the physical properties of the catalyst but do not change the chemical nature of the catalysts significantly. The oxidative coupling activity of the doped catalysts was retained. On the other hand the transition metal oxides whose ions have very different ionic radii to those of the Li^+ and Mg^{2+} resulted in significant changes in the physical and chemical properties of the catalysts.

Disruption of surface layer formation on calcined samples occurs with the reducible transition metal oxide phases being exposed on the catalysts surface during reaction condition. The catalytic activity of these catalysts was also affected due to these changes.

6.6 Summary of findings

1. The presence of about 3wt.% (1mole%) of transition metal oxide on Li_2CO_3/MgO affects its catalytic activity. Manganese oxide promotes the oxidative coupling activity while chromium oxide resulted in the exhaustive oxidation reaction of methane to carbon oxide (section 6.2.1).

2. Different loadings of iron oxide on MgO resulted in exhaustive oxidation while the same loading on Li_2CO_3/MgO did not affect the oxidative coupling properties (section 6.2.2). A similar observation was made for zinc oxide doped catalysts (section 6.2.3).

3. On the manganese oxide doped Li_2CO_3/MgO catalyst, low loading of metal oxide was observed to promote methane conversion while retaining the C_2 selectivity. At higher loading the exhaustive oxidation of methane become more favoured (section 6.2.4). In the case of chromium oxide doped MgO and Li_2CO_3/MgO catalysts, the exhaustive oxidation was favoured even with low loadings of chromium oxide (section 6.2.5).

4. The presence of the various transition metal oxide on Li_2CO_3/MgO causes significant physical and chemical changes relative to the undoped Li_2CO_3/MgO catalysts. Generally the formation of Li_2CO_3/MgO rich surface layer as studied by SEM, was reduced at higher loading of transition metal oxide. The effect is most severe with chromium oxide (section 6.4.5) and least severe with zinc oxide (section 6.4.3). Iron (section 6.4.2) and manganese (section 6.4.4) have effects of intermediate severity.

5. On the iron oxide (section 6.4.2) and zinc oxide (section 6.4.3) doped Li_2CO_3/MgO catalysts, no reducible phase was present. The TPR of the Li_2CO_3/MgO catalysts doped with manganese (section 6.4.4) and chromium (section 6.4.5) oxides show the presence of reducible phases.

6. The physico-chemical changes occurring on the doped Li_2CO_3/MgO catalysts were observed to be related to the difference in the ionic radii of the transition metal ions to those of Li^+ and Mg^{+2}. The larger the ionic radii differences, the more severe the physico-chemical changes. Similar trends were observed with respect to the catalytic activity of these catalysts with the difference in the ionic radii. Li_2CO_3/MgO catalysts doped with transition metal oxides whose ionic radii are similar to that of Li^+ retained the oxidative coupling activity. The results obtained in this work are consistent with the ionic radii parameter being an important factor which influence the physico-chemical and catalytic properties of the metal oxide doped Li_2CO_3/MgO catalysts (section 6.5).

CHAPTER 7

CATALYSTS NATURE UNDER REACTION CONDITIONS AND THE EXTENT OF CATALYTIC REACTION; RESULTS AND DISCUSSION

7.1 Introduction

Driscoll and Lunsford,1985 observed the formation of methyl radicals when a methane and oxygen gas mixture was passed over MgO and Li_2CO_3/MgO catalysts. Up to 19% yield to C_2 hydrocarbons was observed when the catalytic oxidative reaction was performed over Li_2CO_3/MgO (Ito and Lunsford,1985). The active site on Li_2CO_3/MgO was proposed to be a Li^+O^- centre (Driscoll et al.,1985a, 1985b). O_2 was found to be a better oxidant while N_2O resulted in significant loss of activity with time on stream (Driscoll et al.,,1985a). A mechanism for the catalytic oxidative reaction of methane over the Li_2CO_3/MgO catalyst was proposed to involved methyl radicals as the primary reaction intermediate (Ito et al.,1985). The amount of methyl radicals trapped from the outlet gas increases as the distance from the catalyst bed and the trap was decreased (Campbell et al.,1987). This further support the proposal of methyl radicals being the primary intermediate of the reaction.

The hydrocarbon product distribution from the catalytic oxidative coupling reaction and the homogeneous reaction have been compared by many workers (Asami et. al, 1987, 1988; Hutchings et. al, 1988, Lane and Wolfe 1988a, 1988b). A general conclusion seem to be that the hydrocarbon product distribution of the catalytic reaction are broadly similar to that of the homogeneous reaction. Various modelling and reaction rate calculations have shown that a series of gaseous phase reaction can reproduce the hydrocarbon product distribution of the catalysed reaction (Kimble and Kolts, 1987, Labinger and Ott, 1987, Lee and Oyama, 1988).

In order to gain further understanding on the role of the catalyst and the extent of catalytic reaction, a series of mechanistic experiments were performed. *In-situ* FTIR experiments on the catalytic oxidative reaction of methane were carried out to investigate the presence of reaction intermediate and the nature of the catalysts under reaction condition. The routes for the formation of carbon oxide was also investigated by studying the effect of carbon monoxide partial pressure on the oxidative reaction of methane over the various catalysts. Using azomethane as a source of methyl radicals, the gaseous phase reactions of methyl radicals have been studied. The product distribution from the gaseous phase reaction of methyl radicals have been compared to that of the catalysed reactions. In order to evaluate the mechanisms proposed for the catalytic oxidative reaction of methane, the reaction of methyl radical under an oxidative environment was also performed.

7.2 *In-situ* FTIR experiment

7.2.1 Probing the reaction intermediate

The initial focus of the *in-situ* FTIR experiments was to detect any reaction intermediates that might be present during the catalytic oxidative reaction of methane. To achieve this, the reaction was conducted in the infra red cell, over 0.02gm of catalyst in the form of a self supporting disc. The flow rate of $Ar/CH_4/O_2$ during these experiment were normally 5, 3, and 2 ml/min respectively. The transmission IR spectra were accumulated *in-situ* with a resolution of $4cm^{-1}$ and with a total number of scan around 200-500 depending on the catalyst studied.

Among the effects of the oxidative reaction of methane at temperature up to 750°C on the the transmission IR spectra of the catalyst are the significant changes in the hydroxyl (O-H stretching, 3500-3800 cm^{-1}) and the region associated with H_2O and CO_2 bending mode at 1200-1800 cm^{-1}. In the spectra of various catalyst under *in-situ* condition, the extent of this changes differ from from one type of catalyst to another. This changes will be discussed further in this chapter. In all of these spectra

however, no IR assignment can be made to that of adsorbed hydrocarbon or oxygenates species.

The failure in detecting the adsorbed hydrocarbon or oxygenates species can be attributed to the transient nature of these species. Under the condition necessary for these experiments, an oxidising environment at high temperature, these species will be at low concentration. Moreover under these condition their half life will be very short making them undetectable by the *in-situ* high temperature FTIR technique.

7.2.2 Changes to metal oxide catalyst during oxidative reaction of methane at 750°C

In this work the FTIR spectrum of the catalyst at 750°C (after 2 hours pretreatment at this temperature in air)-spectrum i, were compared to the spectrum of catalyst after 1 hour on stream-spectrum ii. The difference spectrum-spectrum iii, was plotted by subtracting spectrum i from spectrum ii. An automatic subtraction procedure was performed to remove most of the gaseous phase component of the spectrum iii. However some of the gaseous phase component are still present in spectrum iii. Spectrum iii should illustrate any changes occurring on the catalyst as a result of oxidative reaction of methane under the condition studied.

The spectra for MgO are given in figure 7.2.2.a. After pretreatment , the FTIR spectra of MgO (spectrum i) does not shows any presence of carbonate phase but shows the presence of some water vapour. After 1 hour on stream, the catalyst shows a significant increase of absorption at 1200-1800cm^{-1} and a small absorption band at 2100-2200cm^{-1} (spectrum ii). The difference spectrum (spectrum iii) clearly indicate the changes occurring on MgO catalysts during the oxidative reaction of methane. The presence of the large absorption band at 1200-1800cm^{-1} region in spectra iii is indicative of the formation of carbonates and other adsorbed CO_2 species while the small peak at 2100-2200cm^{-1} indicate the presence of carbonyl

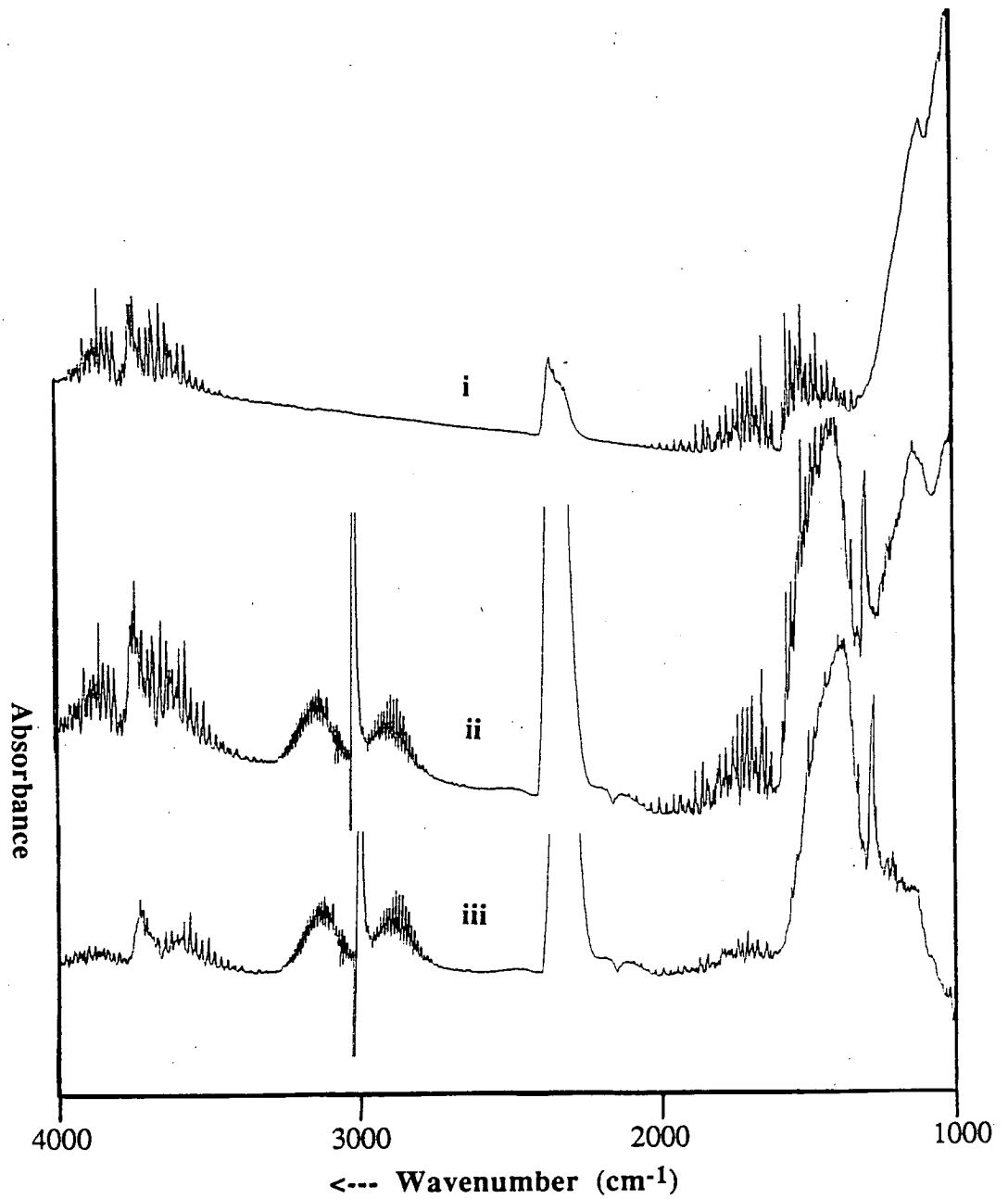

Figure 7.2.2.a *In-situ* FTIR spectra of MgO catalyst during the oxidative reaction of methane at 750°C. Spectrum i was accumulated after 2 hours of equilibration time in air while spectrum ii was accumulated after 1 hour of exposure to the reactant gases. These spectra were accumulated with 200 scans and a resolution of $4cm^{-1}$. Spectrum iii was derived by substracting spectrum i from spectrum ii.

species on MgO catalysts (Rethwisch and Dumesic,1986), and possibly some gaseous phase CO during the oxidative reaction of methane at 750°C. The absorption peak at 2250-2400cm-1 correspond to gaseous phase CO_2.

As in the case of MgO the spectra of CaO at 750°C also indicate the absence of carbonate phase but the presence of some H_2O (spectrum i of figure 7.2.2.b). Under reaction condition the FTIR properties of CaO catalysts changes significantly (spectrum ii and iii) with the formation of new absorption bands in the 1200-1800cm^{-1}, 2100-2200cm^{-1} and 2400-2700cm^{-1} regions. The band at 2100-2200cm^{-1} is the carbonyl species while that at 1200-1800cm^{-1} and 2400-2700cm^{-1} are typical of the carbonate and other adsorbed CO_2 species. The area of the carbonates bands of CaO spectra is larger than that of MgO and this indicate that significantly more carbonate phase form on CaO catalyst during oxidative reaction of methane than that on MgO. It is known that $CaCO_3$ are more stable than $MgCO_3$ (Aylward and Findlay,1971) and hence this observation parallels the relative stability of the carbonate phase.

The various spectra for SiO_2 are given in figure 7.2.2.c. SiO_2 have an IR absorption band in the 1200-2000cm^{-1} region (spectrum i). It can also be seen that the spectra of SiO_2 are noisier than that of MgO and CaO because the SiO_2 disk is less transparent than the others. Under the condition of the oxidative reaction of methane no significant changes on the FTIR spectra of SiO_2 was observed (spectum iii). This indicates that during the oxidative reaction of methane over SiO_2 no significant adsorbed species form on the catalysts.

As in the case of MgO and CaO the spectra of γ-Al_2O_3 at 750°C shows the absence of any carbonate species (spectrum i of figure 7.2.2.d). The spectra of the catalysts under oxidative reaction of methane (spectra ii and iii) suggest the presence of some carbonyl species (2100-2200cm^{-1}). The absence of absorption band in the 1200-1800cm^{-1} region of spectrum ii indicated that as on SiO_2 the formation of

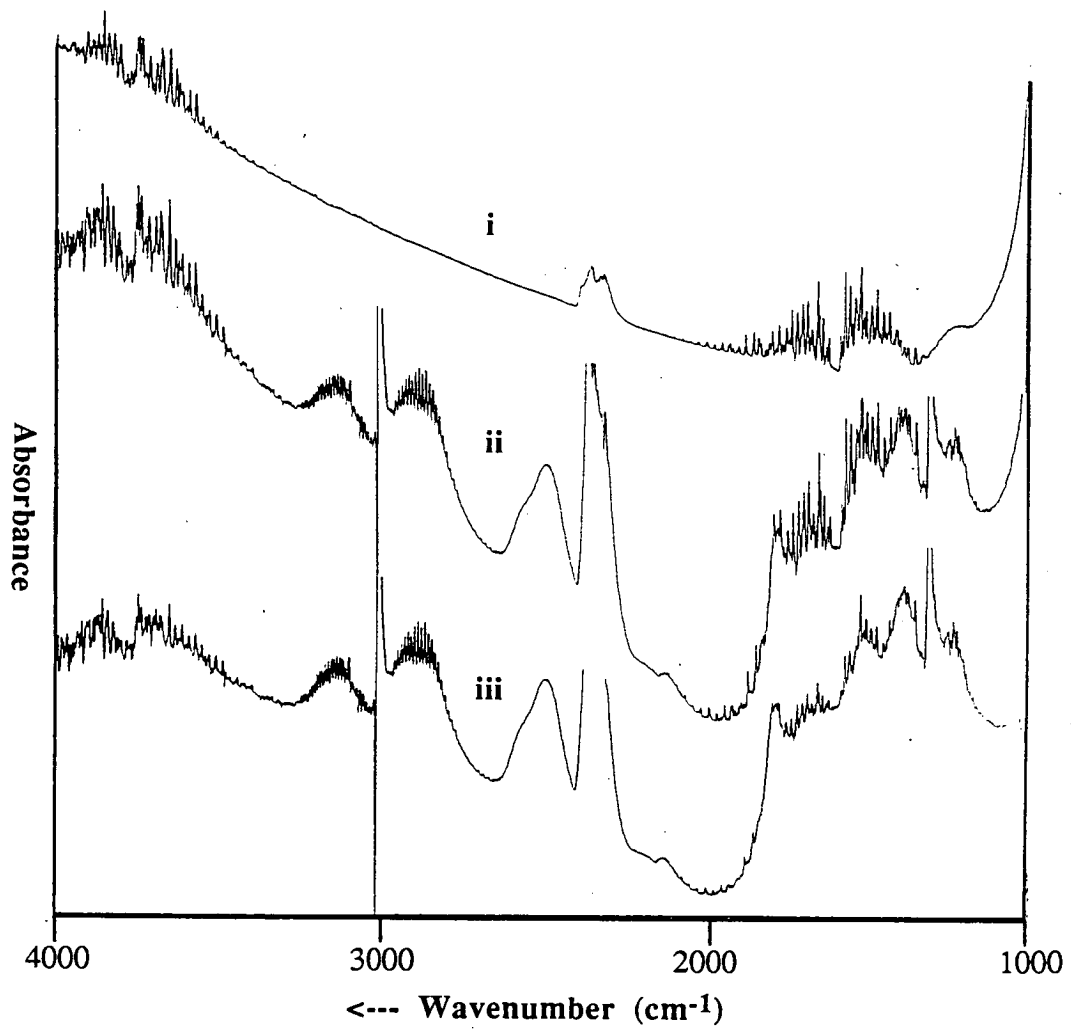

Figure 7.2.2.b *In-situ* FTIR spectra of CaO during the oxidative reaction of methane at 750°C. Spectrum i was accumulated after 2 hours of equilibration time in air while spectrum ii was accumulated after 1 hour of exposure to the reactant gases. These spectra were accumulated with 500 scans and a resolution of $4cm^{-1}$. Spectrum iii was derived by substracting spectrum i from spectrum ii.

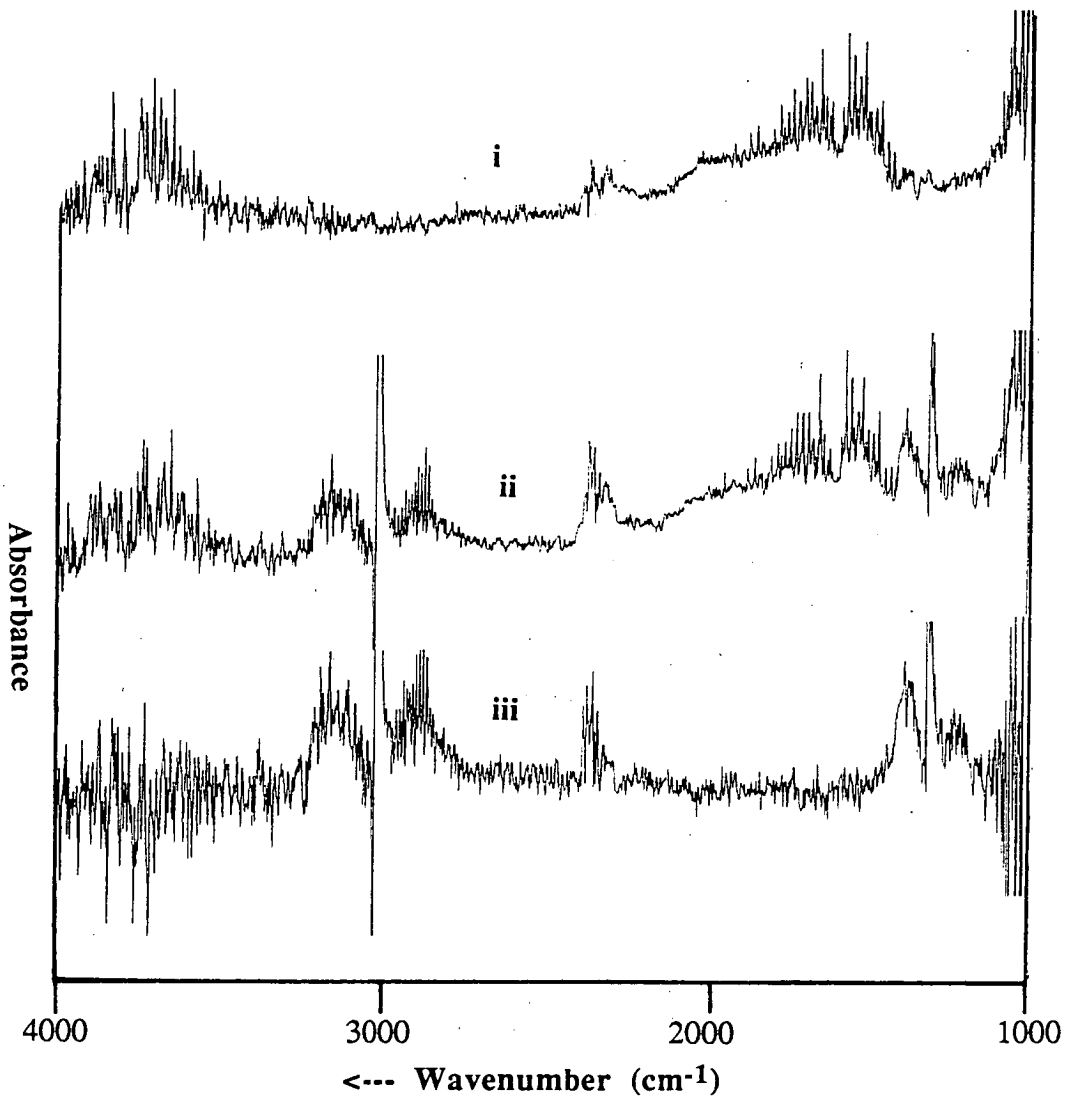

Figure 7.2.2.c *In-situ* FTIR spectra of SiO_2 during the oxidative reaction of methane at 750°C. Spectrum i was accumulated after 2 hours of equilibration time in air while spectrum ii was accumulated after 1 hour of exposure to the reactant gases. These spectra were accumulated with 500 scans and a resolution of $4cm^{-1}$. Spectrum iii was derived by substracting spectrum i from spectrum ii.

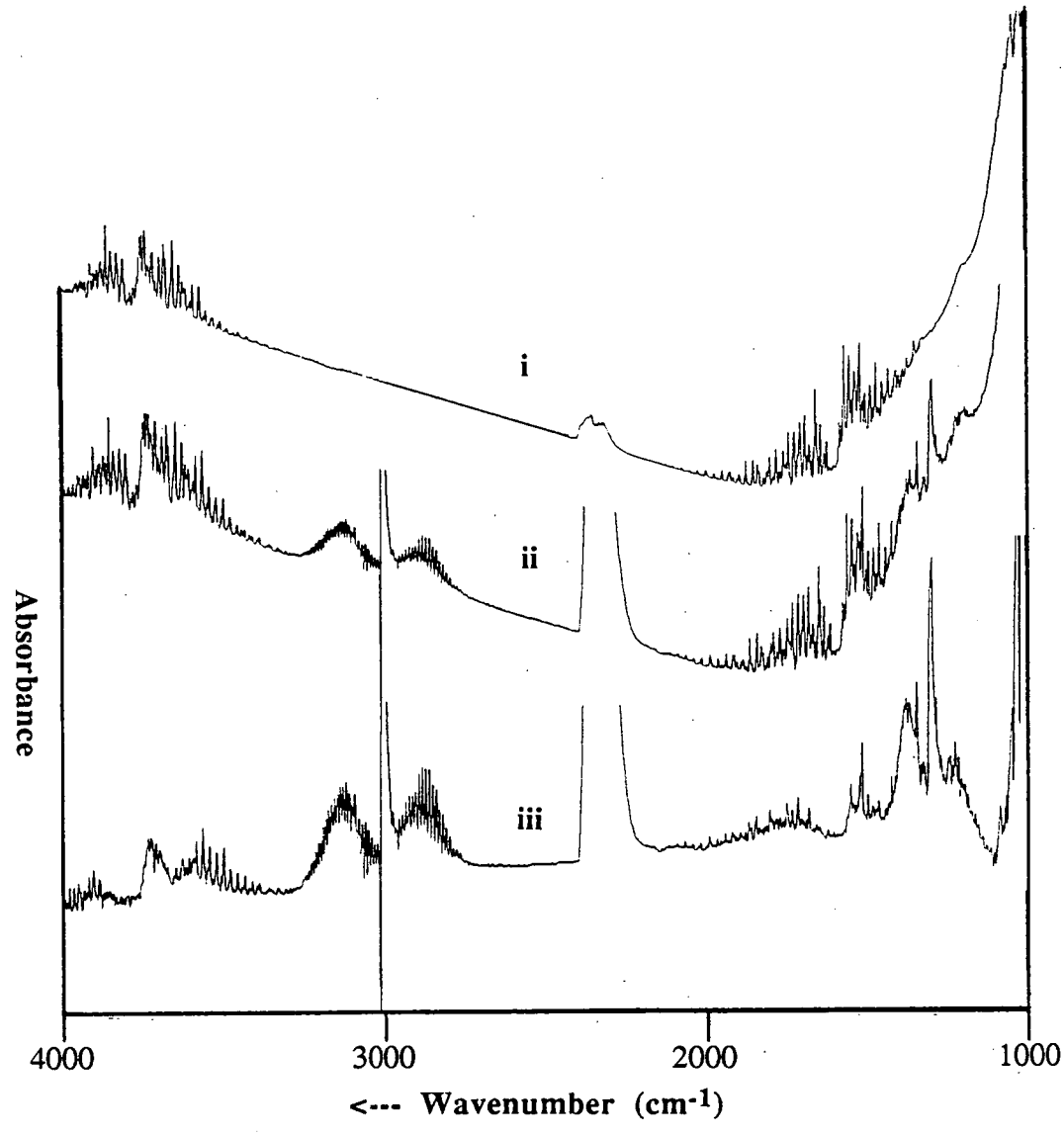

Figure 7.2.2.d *In-situ* FTIR spectra of γ-Al_2O_3 during the oxidative reaction of methane at 750°C. Spectrum i was accumulated after 2 hours of equilibration time in air while spectrum ii was accumulated after 1 hour of exposure to the reactant gases. These spectra were accumulated with 500 scans and a resolution of $4cm^{-1}$. Spectrum iii was derived by substracting spectrum i from spectrum ii.

stable adsorbed CO_2 species on γ-Al_2O_3 under oxidative reaction of methane does not occur.

The spectra for Sm_2O_3 are given in figure 7.2.2.e. The spectrum of fresh Sm_2O_3 (not given) indicate that absorbed H_2O, CO_2 and carbonate species were present on the material. By heating the sample at 750°C for 0.5 hours, most of these species desorbed and decomposition of the carbonate also occurs as evident in the absorption band of gaseous CO_2 in spectrum i. When the catalyst was exposed to the condition of oxidative reaction of methane no net increase of absorption peak in its FTIR spectrum was observed (spectrum ii). Instead the difference spectrum, spectrum iii, show that a net loss of absorption occurs in the 1200-1800cm^{-1} regions and at above 3300cm^{-1}. This indicate that during the oxidative reaction of methane the formation of stable adsorbed species of CO and CO_2 does not occur.

The overall finding therefore is that the formation of stable adsorbed CO_2 and carbonate species under the conditions of oxidative reaction of methane occurred on MgO and CaO but not on SiO_2, γ-Al_2O_3 and SiO_2. The extent of carbonate formation seem to be dependent on the basicity of the metal oxide. Moreover it was observed that more carbonate phase was formed on CaO than on MgO and this is consistent with the relative stability of $CaCO_3$ and $MgCO_3$. It was also observed that the surface carbonyls species are also present under the condition of oxidative reaction of methane over MgO, CaO and γ-Al_2O_3.

In the activity studies it has been observed that the MgO, CaO Sm_2O_3 resulted in high methane conversion with the carbon oxide selectivity predominantly to CO_2. In the case of γ-Al_2O_3 high conversion was also observed but the main carbon oxide product is CO. As has been discussed above the basicity of the metal oxides influence the extent of surface carbonate formation. From this result it is possible that the favoured formation of CO_2 in the reaction over the basic oxide is associated to the stronger interaction between the surface of this materials with CO and oxygenates. The stronger interaction would enable the surface oxidation of these

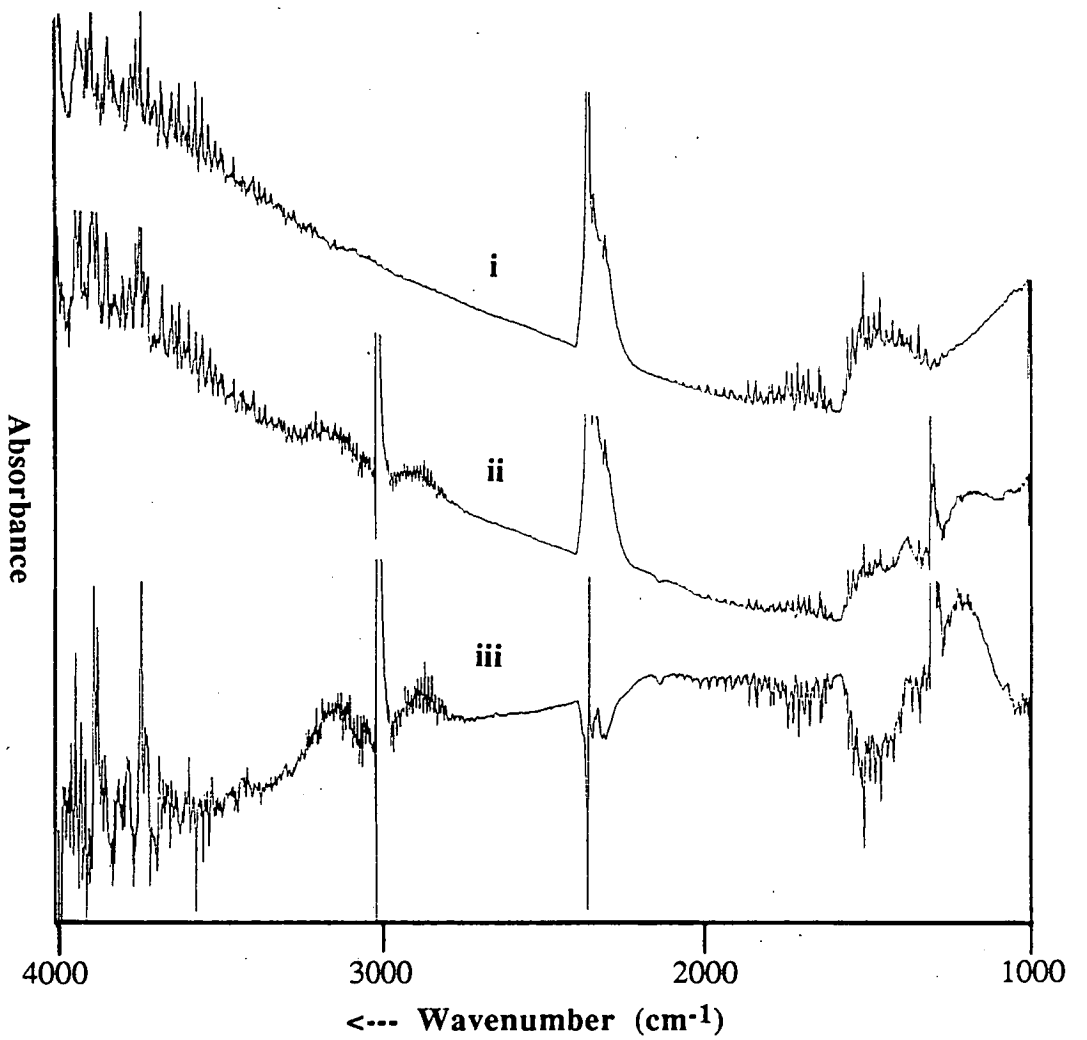

Figure 7.2.2.e *In-situ* FTIR spectra of Sm_2O_3 during the oxidative reaction of methane at 750°C. Spectrum i was accumulated after 2 hours of equilibration time in air while spectrum ii was accumulated after 1 hour of exposure to the reactant gases.These spectra were accumulated with 500 scans and a resolution of $4cm^{-1}$. Spectrum iii was derived by substracting spectrum i from spectrum ii.

intermediate to form CO_2. Most of the CO_2 produced would desorbed from the surface into the product stream and depending on the basicity of the oxide some formation of the surface carbonate species will occur.

7.2.3 Changes on Li_2CO_3/MgO and LiCl/MgO catalysts during the oxidative reaction of methane at 750°C

The various spectra of Li_2CO_3/MgO and LiCl/MgO catalysts under condition used in section 7.2.2 are given in figure 7.2.3.a and figure 7.2.3.b respectively.

As was observed earlier the spectra of 7.8wt.% Li_2CO_3/MgO catalysts showed the prominent presence of Li_2CO_3 phase (figure 7.2.3.a). Spectrum iii shows that under the conditions of oxidative reaction of methane no net formation of any carbonate or carbonyl species was detectable on these catalysts. Instead some loss of carbonate phase from the catalysts was observed to occur. The net loss of Li_2CO_3 under reaction condition is consistent with the observation made earlier in section 4.3.3.

The *in-situ* spectrum of LiCl/MgO catalysts at 750°C (spectrum i of figure 7.2.3.b) shows the absence of any carbonate species on the catalysts. When the catalyst was exposed to the reactant gas, an increase in the absorbance band was observed in the region of 1300-1600 cm^{-1}. The changes observed on LiCl/MgO under reaction conditions is to a smaller extent similar to that on MgO. This would indicate that on LiCl/MgO, a significant amount of MgO support was available to serve as a site for carbonyl and carbonate species formation.

These results indicate that a significant phase transformation occurs on Li_2CO_3/MgO and LiCl/MgO catalyst under reaction conditions. From the activity studies it was known that carbonate decomposition and lithium losses occurred on Li_2CO_3/MgO catalyst. Under the condition of these experiment it was observed that no net formation of carbonate or carbonyl species occurs on Li_2CO_3/MgO. Instead it

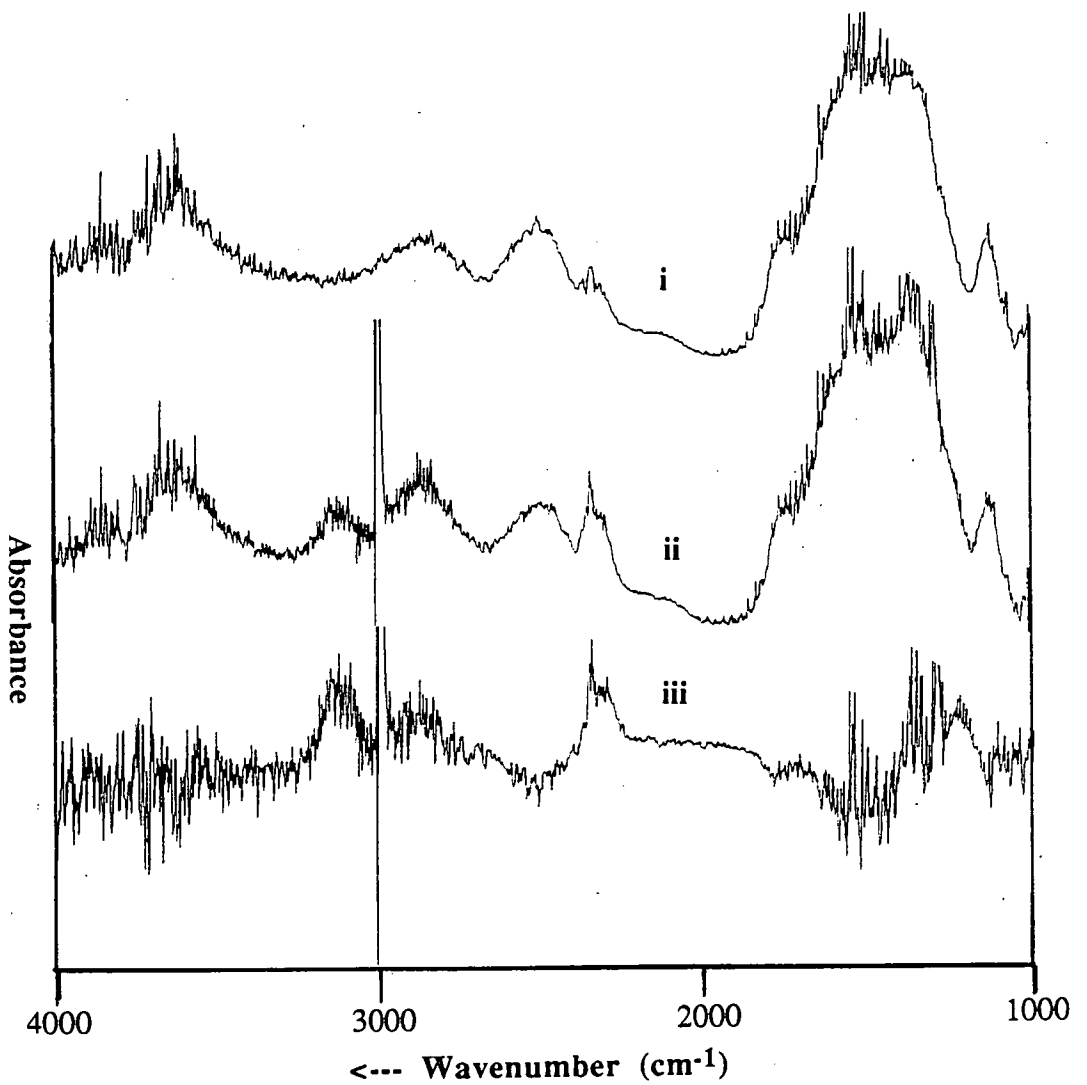

Figure 7.2.3.a *In-situ* FTIR spectra of Li_2CO_3/MgO during the oxidative reaction of methane at 750°C. Spectrum i was accumulated after 2 hours of equilibration time in air while spectrum ii was accumulated after 1 hour of exposure to the reactant gases. These spectra were accumulated with 500 scans and a resolution of $4cm^{-1}$. Spectrum iii was derived by substracting spectrum i from spectrum ii.

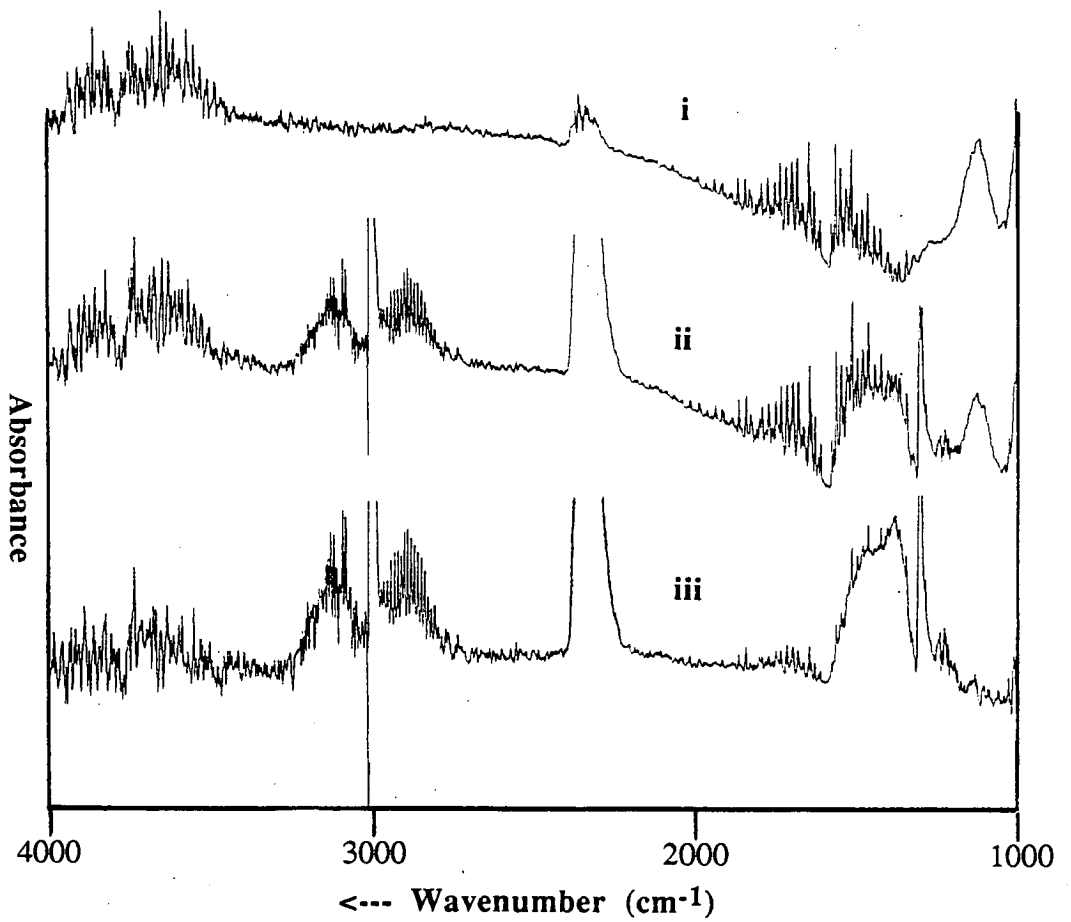

Figure 7.2.3.b *In-situ* FTIR spectra of LiCl/MgO during the oxidative reaction of methane at 750°C. Spectrum i was accumulated after 2 hours of equilibration time in air while spectrum ii was accumulated after 1 hour of exposure to the reactant gases. These spectra were accumulated with 500 scans and a resolution of $4cm^{-1}$. Spectrum iii was derived by substracting spectrum i from spectrum ii.

was observed that the carbonate decomposition occurs and this further highlighted the instability of Li_2CO_3/MgO catalyst. The decomposition of the carbonate phase is indicative that the amount of Li_2CO_3 present on the catalyst prior the reaction are not the equilibrium amount under reaction condition causing decomposition to occurs. On the contrary, over basic metal oxides and to some extent on LiCl/MgO the oxidative reaction of methane facilitate the formation of surface carbonyl and carbonate species.

7.2.4 Changes to Li_2CO_3/SiO_2, Li_2CO_3/γ-Al_2O_3 and Li_2CO_3/CaO catalyst during the oxidative reaction of methane at 750°C

The various spectra for Li_2CO_3/SiO_2 catalyst accumulated under the condition of section 7.2.2 are given in figure 7.2.4.a. No formation of any carbonyl or carbonate phase was observed on the catalyst under the condition of oxidative reaction of methane. Similar observation were also made for Li_2CO_3/γ-Al_2O_3 (figure 7.2.4.b) and Li_2CO_3/CaO catalyst (figure 7.2.4.c). As was discussed in section 5.4.2 the absence of absorption band of Li_2CO_3 phase in the spectra of Li_2CO_3/SiO_2 and Li_2CO_3/γ-Al_2O_3 indicate that the Li_2CO_3 phase are not stabilised over these metal oxide under the high temperature condition. Most of the Li_2CO_3 phase which was present during the catalyst preparation decomposed during precalcination and during the high temperature treatment in the IR cell. On Li_2CO_3/CaO catalysts however the carbonate species present are predominantly $CaCO_3$.

The fact that no carbonyl or carbonate species was present on these catalyst under reaction condition does not mean that they are totally absent during the reaction. In the activity studies it has been observed that the doping of Li_2CO_3 on γ-Al_2O_3 favour the formation of CO_2. It is likely that this reaction involved the formation of surface intermediate but the steady state concentration was below the detectable level of the FTIR instrument.

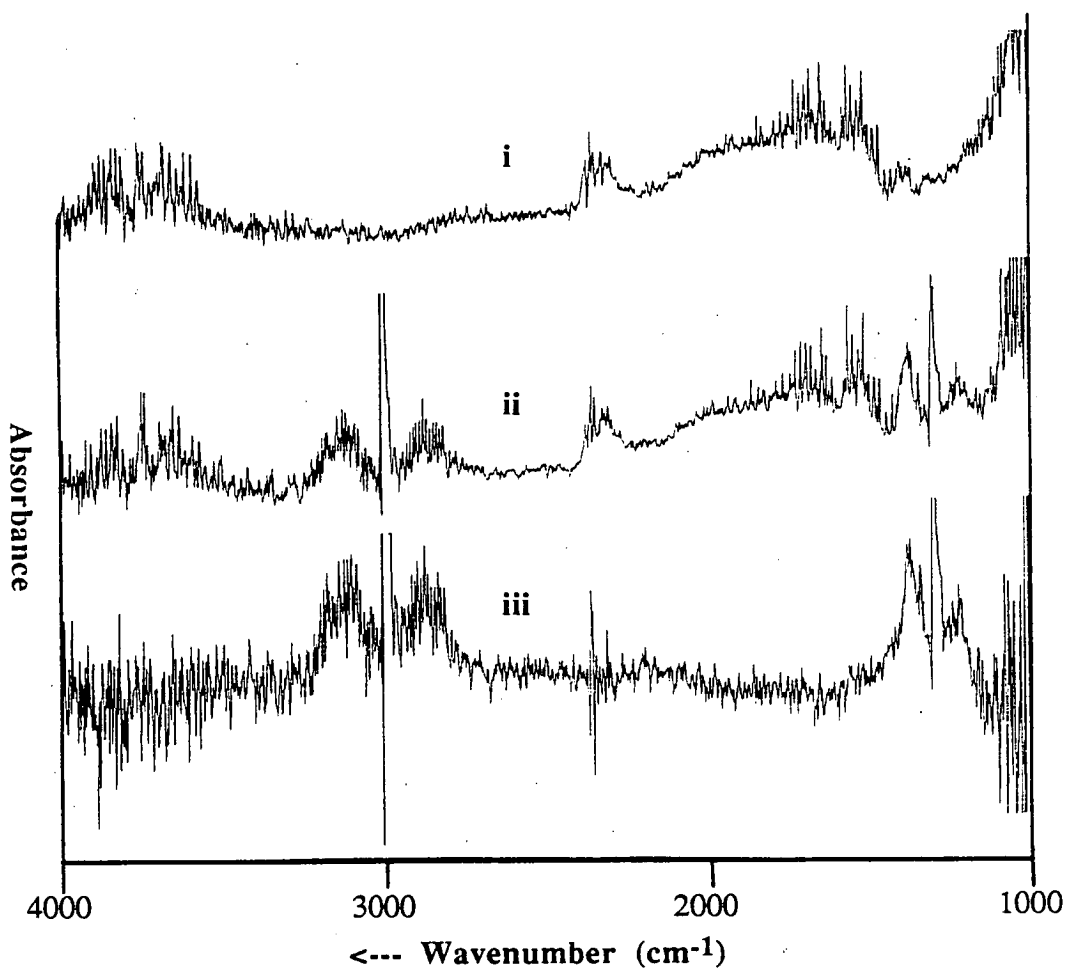

Figure 7.2.4.a *In-situ* FTIR spectra of Li_2CO_3/SiO_2 during the oxidative reaction of methane at 750°C. Spectrum i was accumulated after 2 hours of equilibration time in air while spectrum ii was accumulated after 1 hour of exposure to the reactant gases. These spectra were accumulated with 500 scans and a resolution of $4cm^{-1}$. Spectrum iii was derived by substracting spectrum i from spectrum ii.

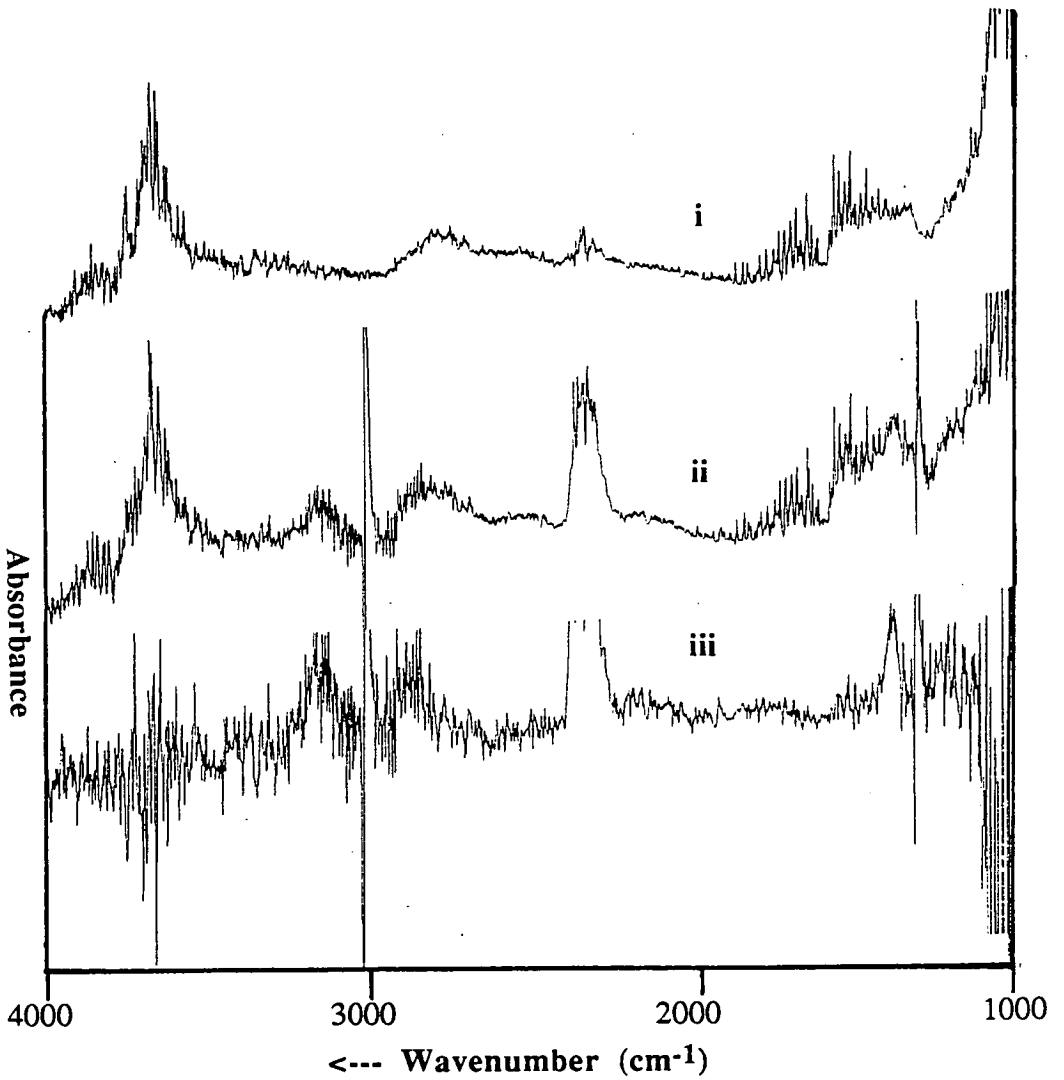

Figure 7.2.4.b *In-situ* FTIR spectra of Li_2CO_3/γ-Al_2O_3 during the oxidative reaction of methane at 750°C. Spectrum i was accumulated after 2 hours of equilibration time in air while spectrum ii was accumulated after 1 hour of exposure to the reactant gases. These spectra were accumulated with 500 scans and a resolution of $4cm^{-1}$. Spectrum iii was derived by substracting spectrum i from spectrum ii.

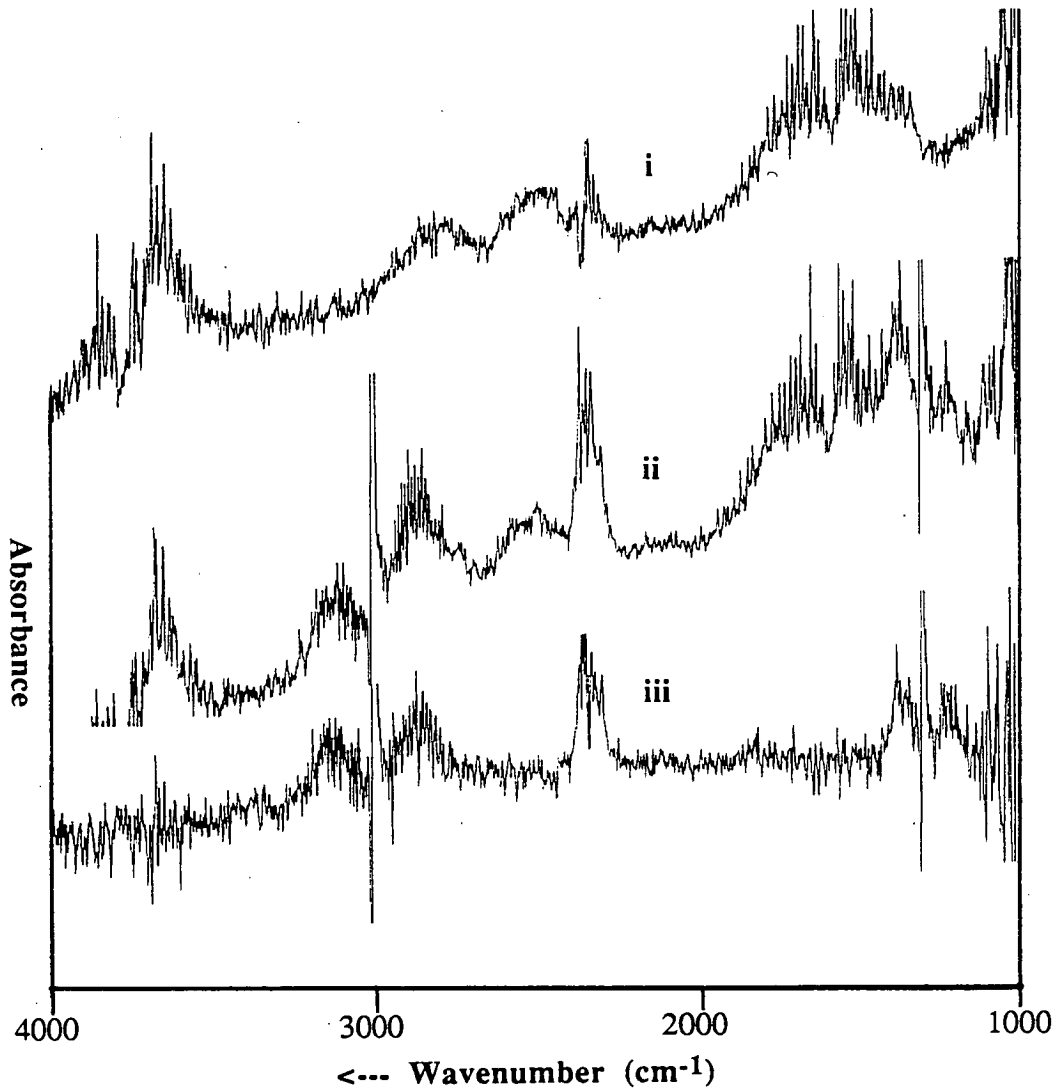

Figure 7.2.4.c *In-situ* FTIR spectra of Li_2CO_3/CaO during the oxidative reaction of methane at 750°C. Spectrum i was accumulated after 2 hours of equilibration time in air while spectrum ii was accumulated after 1 hour of exposure to the reactant gases. These spectra were accumulated with 500 scans and a resolution of $4cm^{-1}$. Spectrum iii was derived by substracting spectrum i from spectrum ii.

Another observation that was made in these studies is the presence of intense absorption band in the 3500-3800 cm^{-1} region especially in the high temperature spectrum of Li_2CO_3/MgO, Li_2CO_3/γ-Al_2O_3 and Li_2CO_3/CaO. This absorption band can be assigned to that of gaseous H_2O and surface hydroxyl species. It have been observed that the doping of the metal oxide with Li_2CO_3 resulted in higher selectivity to C_2 hydrocarbon relative to the bare oxide. On the contrary the IR spectra of Li_2CO_3/SiO_2 and Li_2CO_3/TiO_2 at high temperature are similar to that of the oxide. It has also been observed that catalytic activity of doped SiO_2 and TiO_2 are similar to that of the bare oxide.

The increase in the absorption band in the 3500-3800cm^{-1} region of the FTIR spectrum of doped MgO, CaO and γ-Al_2O_3 relative to that of undoped oxide is likely to be related to the catalytic activity of these materials. It is possible that under the high temperature condition of the oxidative reaction of methane, the surface of the metal oxide does not contained any adsorbed H_2O or hydroxyl species while on the surface of doped catalysts significant amount of hydroxyls species are presence. Less oxygen sites will be available on the doped catalysts reducing the extent of secondary reaction and hence causing the higher selectivity to C_2 products.

7.2.5 Probing the hydroxyl formation during the oxidative reaction of methane on Li_2CO_3/MgO

The previous procedure for *in-situ* work only enable the gross changes on the catalyst during the catalytic reaction to be observed. In order to probe in-detail the changes occurring on the catalyst with respect to its active site, the formation of hydroxyls species during the reaction was investigated. In this experiment the catalyst was evacuated *in-situ* at 750°C for 1 hour in an attempt to completely removed adsorbed H_2O on the catalysts and gaseous H_2O from the cell before exposing the catalyst to the reactant gas.

The various spectra accumulated in this experiment are given in figure 7.2.5.a. The spectrum of the catalyst after 10 min at 750°C (spectrum i) shows the presence of gaseous H_2O accumulated in the cell. Evacuation of the cell at 750°C for 1 hour removed most of the gaseous H_2O (spectrum ii). When the catalyst was exposed to the reactant gas new absorption peaks in the hydroxyl stretching region were formed. After 20 minutes on stream three major peaks at 3674, 3669 and 3647 cm-1 were observed (spectrum iii). After 30 minutes on stream the 3674 peak increases in size while a new peaks at 3690 cm-1 and 3626 were observed (spectrum iv). At longer time on stream all of these absorption peaks diminished and the spectra provided mainly evidence of gaseous H_2O (spectrums v, vi and vii).

This result indicate that surface free hydroxyl species were formed during the course of the oxidative reaction of methane over Li_2CO_3/MgO. The hydroxyl species associated with absorption peak at 3674 cm^{-1} can be assigned to LiOH species (Smyrl et al.,1983). The presence of the other peaks suggested the presence of other oxygen sites on the catalysts which form the free hydroxyl species under reaction condition. This illustrate the complex nature of the catalysts surface under reaction condition. The disappearence of these peaks at longer time on stream is likely to be associated with surface hydrogen bonding of the OH species and the increase of gaseous H_2O in the cell produced by the oxidative reaction of methane; it also illustrate the difficulty of using *in-situ* FTIR technique for studying the presence of adsorbed species or reaction intermediate in the catalytic oxidative reaction of methane. However the formation of the free hydroxyls species observed above indicate that various type of oxygen species are present on Li_2CO_3/MgO catalyst under the reaction condition.

In order to probe further the nature of oxygen sites on the various catalysts used for catalytic screening, the formation of free hydroxyl species on these catalyst after high temperature pretreatment was determined. Figure 7.2.5.b give the IR spectra of the various oxidative coupling catalyst at RT after the high temperature

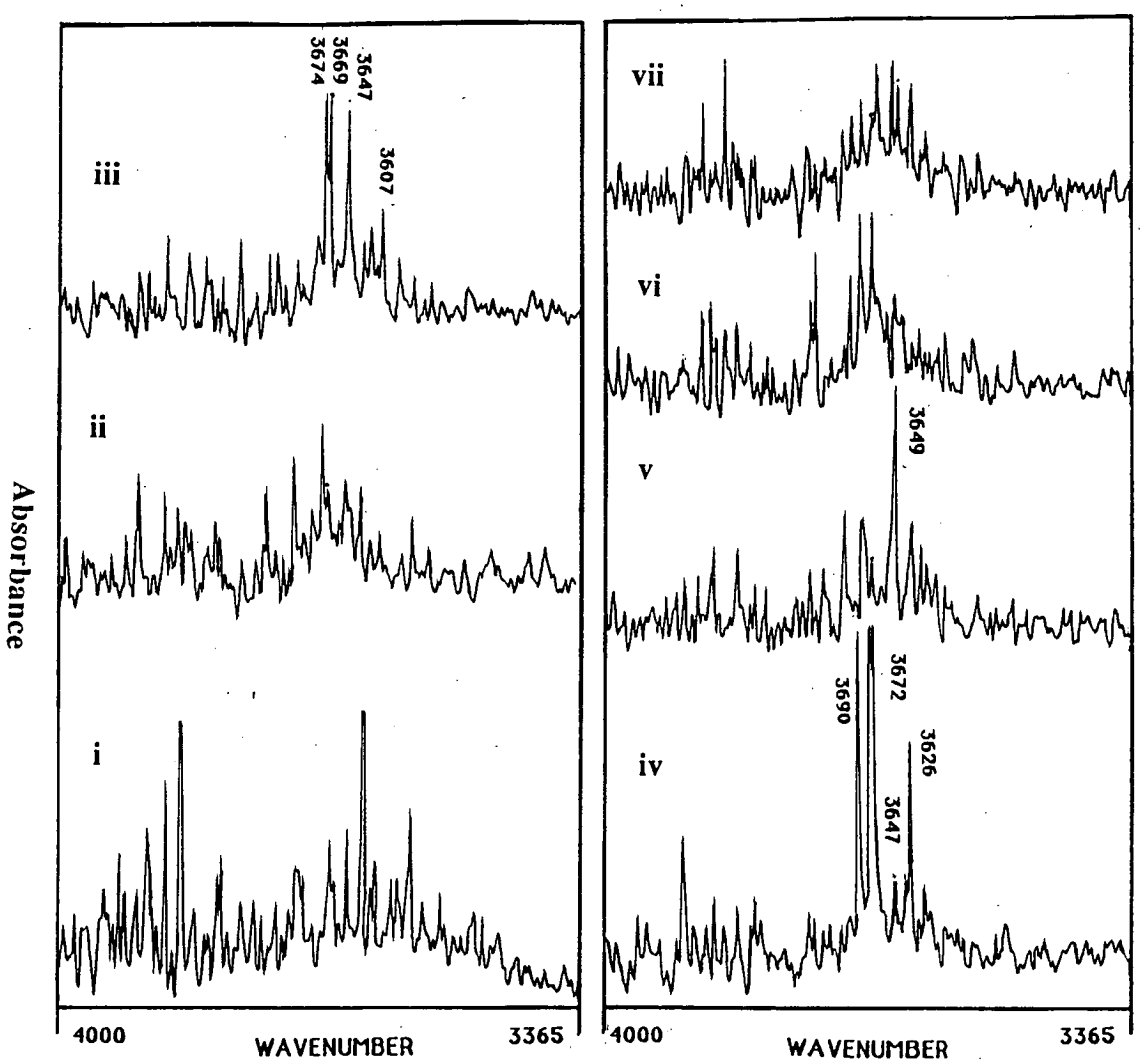

Figure 7.2.5.a The formation of hydroxyl species on Li_2CO_3/MgO catalyst during the oxidative reaction of methane. Spectrum i was accumulated after 10 minutes of equilibration time at 750°C while spectrum ii after 1 hour of evacuation at 750°C. Spectra iii, iv, v, vi, and vii were accumulated at 750°C after 20, 30, 50 70 and 90 minutes of exposure to the reactant gas, respectively. These spectra were accumulated with 300 scans and a resolution of $4cm^{-1}$.

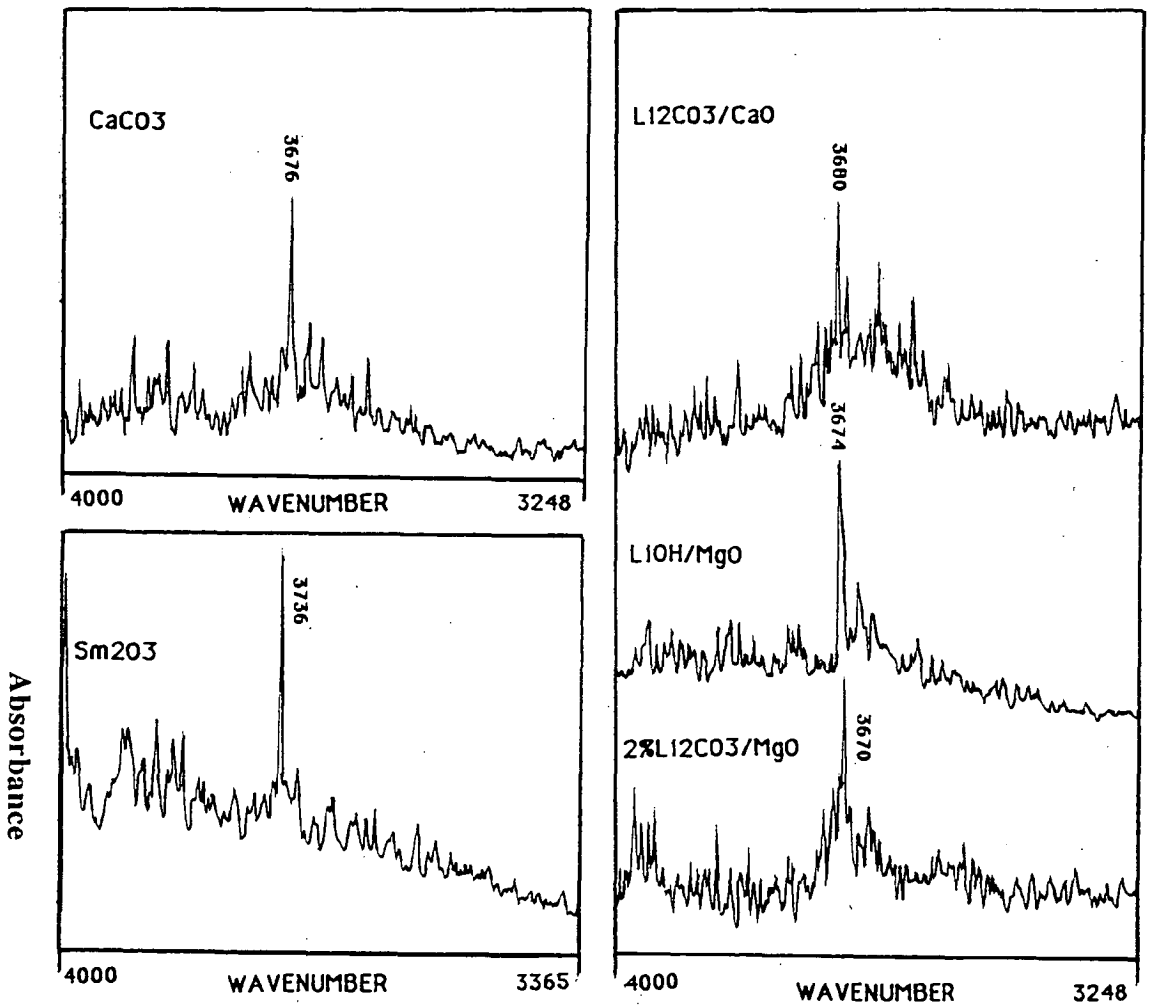

Figure 7.2.5.b The presence of hydroxyl species on thermal pretreated catalysts. These catalysts have also been observed to show significant activity for the oxidative coupling of methane. The spectra were accumulated with a resolution of $4cm^{-1}$.

pretreatment. The presence of free hydroxyl species were observed on Sm_2O_3, $CaCO_3$, Li_2CO_3/CaO, LiOH/MgO and Li_2CO_3/MgO (spectra i to v respectively) catalysts. These materials have been determined to show significant activity for oxidative coupling reaction of methane (chapter 5).

The presence of Li_2CO_3 on certain metal oxide has been found to result in higher C_2 selectivity. These materials also favour the formation of carbon dioxide. In the *in-situ* FTIR work, the presence of Li_2CO_3 on these oxide was also found to cause an increase in the presence of free hydroxyl species at the high temperature. This suggest that the doping of Li_2CO_3 on these oxide favours the formation of O^- type oxygen sites.

It has also been observed that in the IR spectra, less adsorbed H_2O are present on the calcined Li_2CO_3 doped catalyst relative to the undoped metal oxide. This is consistent with the decrease in surface area of the calcined catalysts and also resulted in a decreased of the total number of oxygen sites available for the oxidative reaction of methane. It is possible that the presence of O^- type sites and the decrease in the overall number of sites as a result of Li_2CO_3 presence possibly explained the higher C_2 selectivity of the doped catalysts.

This results is consistent with the proposal of Driscoll et al.,1985a with regard to the presence of Li^+O^- type sites on Li_2CO_3/MgO catalysts which they suggest to be responsible for the oxidative reaction of methane. Moreover in this work it was also that the formation O^- type sites are not unique to the Li_2CO_3/MgO type system. The formation of free hydroxyl species on other catalysts have also been observed; suggesting the presence of similar oxygen sites on these catalysts. These catalysts have also been found to show good oxidative coupling activity.

7.3 Probing the extent of gaseous and surface reactions

7.3.1 Gaseous phase and catalysed oxidative reaction of the hydrocarbon mixture

In order to probe the possible significance of oxidative reaction of hydrocarbon products in the oxidative reaction of methane, the reaction of hydrocarbon mixtures under condition similar to catalyst screening was performed. The gas mixture comprised about 120 torr of O_2, 175torr of CH_4, 18 torr of C_2H_4, 19 torr of C_2H_6, 5.9 torr of C_3H_6 and 5.9 torr C_3H_8. This gas mixture was passed at 25ml/min through a blank reactor or over a catalyst bed containing 0.2gm of catalyst at 805°C. The composition of the product gas was determined and changes to the reactant gas as a result of the oxidative reaction were then calculated. A carbon balance of about 90% was normally achieved in these experiments.

Table 7.3.1.a The percentage of changes occurring to the reactant gases containing C_1-C_3 hydrocarbons and oxygen after they were flowed through the reactor at 805°C

Catalyst	% Changes						%Selectivity	
	O_2	CH_4	C_2H_4	C_2H_6	C_3H_6	$C3H_8$	CO	CO_2
Blank	-50	-2	50	-66	-74	-100	69	31
LiF/MgO	-23	-2	49	-49	-50	-19	95	5
γ-Al_2O_2	-100	-3	-9	-65	-100	-100	69	31
MgO	-93	-15	31	-63	-71	-100	37	63
$AlPO_4$-5	-100	-7	-29	-70	-100	-100	61	39
$CaCO_3$	-98	-9	1	-58	-74	-95	18	82
Li_2CO_3/MgO	-84	-11	35	-48	-73	-93	12	88
Li_2CO_3/γ-Al_2O_3	-100	-1	-32	-76	-100	-100	40	60
LiCl/MgO	-100	-18	91	-87	-58	-100	0	100
Cr/Li_2CO_3/MgO	-100	-19	12	-43	-66	-72	0	100
Sm_2O_3	-100	-18	26	-50	-66	-90	23	77

Table 7.3.1.a shows the changes in the reactant gas composition as a result of the reaction occurring over the various catalysts. Positive values in the table

indicate the percentage of net formation with respect of any particular component while negative values indicate the percentage of the components which have reacted. The value for CO ,and CO_2 will always be between 0 and 100 since it was defined as the moles of carbon in CO, and CO2 over the total mole of carbon from hydrocarbon which was oxidised to carbon oxide.

The result for the blank reactor shows that significant oxidative reaction of higher hydrocarbons occurs in gaseous phase. A net formation of 50% for C_2H_4 was observed and carbon monoxide is the major carbon oxide products (69%). Only 50% of oxygen was consumed during the reaction. This illustrate the problem in the oxidative reaction of methane where the desired hydrocarbon products are more likely to undergoes further oxidation to carbon oxide. The presence of LiF/MgO reduces the oxygen consumption to 22% compared to the 50% of the reaction occurring in the blank reactor tube, and change the product distribution significantly. A net formation of C_2H_4 still occurs while the selectivity to carbon monoxide increased to 95%.

Full consumption of oxygen occurs over γ–Al_2O_3 resulting in the oxidative reaction of the hydrocarbon with net formation of C_2H_4 being observed. A high selectivity to CO, 69%, was also observed. $AlPO_4$-5 also have similar effect as γ–Al_2O_3 while MgO, Li_2CO_3/MgO and Sm_2O_3 resulted in a net formation of C_2H_4 beside the net formation to CO. The doping of Li_2CO_3 on MgO and γ-Al_2O_3 reduces the amount of net formation to CO relative to that of the undoped oxide. The low net formation to CO was also observed in the oxidative reaction of the hydrocarbon mixture on $CaCO_3$.

In the case of the oxidation of the hydrocarbon over LiCl/MgO and chromium oxide doped Li_2CO_3/MgO catalysts only carbon dioxide was observed as the carbon oxide product. The net formation to C_2H_4 over the LiCl/MgO and the chromium oxide doped Li_2CO_3/MgO catalysts were about 91 and 12% respectively.

The result of the blank reactor indicate that under the condition of catalytic oxidative reaction of methane significant gaseous phase oxidation of the products will occurs. It has been observed earlier in the catalytic screening work that LiF/MgO does not have significant catalytic activity for the oxidative reaction of methane. In this experiment the result of the reaction over LiF/MgO is basically the effect of a reduction in residence time of the hydrocarbon mixture due to the presence of a catalysts bed. As was expected, based on the amount of oxygen consumed, the gaseous oxidative reaction of the hydrocarbon was reduced by about 50% when LiF/MgO was present. Moreover the net formation to C_2H_4 and CO was observed with a higher net formation to CO consistent with the decrease in residence time of the hydrocarbon gas in the reactor because of the presence of LiF/MgO in the reactor.

The presence of catalysts which show high activity to the oxidative reaction of methane influenced the reactions of the hydrocarbon mixtures. Generally the effect of the catalysts on the oxidative reaction of the hydrocarbon mixture parallel the effects of these catalysts for the oxidative reaction of methane. In both reaction γ–Al_2O_3 and $AlPO_4$-5 resulted in high selectivity to CO. Moreover the doping of Li_2CO_3 on MgO and γ–Al_2O_3 resulted in lower CO formation in both of the reaction relative to the undoped catalysts. The high selectivity to C_2H_4 of the LiCl/MgO catalyst was observed in the oxidative reaction of the hydrocarbon mixtures as in the oxidative reaction of methane only. The high activity for exhaustive by chromium oxide doped Li_2CO_3/MgO also occurs in the oxidative reaction of the hydrocarbon mixture.

The results of this section basically emphasized two particular points. Firstly, that significant gaseous phase oxidative reaction of the product from oxidative reaction of methane can occur. The extent of which this reaction will occur is certainly dependent on the partial pressure of oxygen present and the reaction temperature. Secondly the catalytic effects observed in the earlier chapter are certainly

true. Moreover under the condition of the reaction the desired hydrocarbon products is more susceptible than methane of being oxidised to form carbon oxide.

7.3.2 Effect of carbon monoxide partial pressure on the oxidative reaction of methane over various catalysts at 805°C

The effects of CO partial pressure in the reactant stream on the oxidative reaction of methane over various catalysts at 805°C have been investigated. The major objectives of this work were to probe the route for carbon oxide formation and to investigate the role of different catalytic materials in determining the product selectivity in the reaction. In this experiment the total flow rate of reactant used was 25ml/min with the partial pressure of CH_4 and O_2 of 220 torr and 110 torr respectively. The effect of CO partial pressure in the reactant stream was studied by increasing the partial pressure of CO and reducing that of helium while the partial pressure of CH_4 and O_2 were kept constant. The oxidative reaction of methane in the presence of CO at various partial pressures over 8 different catalysts are summarised in table 7.3.2.a.

Over Li_2CO_3/MgO catalysts the oxidative reaction of methane at 805°C in the absence of input CO resulted in 26.8% and 49.8% conversion of CH_4 and O_2 respectively. The selectivity to CO, CO_2 and C_2 hydrocarbons was 0.0, 35.9 and 64.1% respectively with 52.7% of the C_2 present as C_2H_4. As the partial pressure of CO in the reactant stream was increased, methane conversion decreases, C_2 selectivity increases and the percentage of C_2H_4 in the C_2 product decreases. About 90% of the input CO was oxidised to CO_2. When 118 torr of CO was presence in the reactant stream 10.3 and 59.4% of CH_4 and O_2 was converted respectively. The selectivity to CO, CO_2 and C_2 hydrocarbons was 0.0, 20.6 and 79.4% respectively with only 29.8% of the C_2 in the form of C_2H_4.

Table 7.3.2.a The effect of CO partial pressure in the reactant flow on the activity of various catalytic systems at 805°C

Reactant*			%Conversion			%Selectivity			
P_{CH_4}	P_{O_2}	P_{CO}	CH_4	O_2	CO	CO#	CO_2	C_2	$C_2^=/C_2tot$
Catalyst:		7.8wt.% Li_2CO_3/MgO							
219	113	0	26.8	49.8	-	0.0	35.9	64.1	52.7
225	114	35	23.2	56.4	90.5	0.0	33.7	66.3	50.6
219	109	69	15.5	50.7	87.5	0.0	23.4	76.6	39.2
219	107	118	10.3	59.4	81.9	0.0	20.6	79.4	29.8
Catalysts:		6.9wt.% LiF/MgO							
200	103	0	3.1	5.1	-	0.0	33.1	66.9	36.7
206	112	36	4.0	9.6	16.1	0.0	38.5	61.5	19.8
211	111	70	4.2	13.5	26.1	0.0	20.1	79.9	23.3
211	113	138	1.6	27.3	40.2	0.0	14.5	85.5	34.0
Catalysts:		2.9wt.% LiCl/MgO							
210	104	0	37.2	0.0	-	0.0	56.9	43.1	53.2
237	113	33	33.7	100	100	0.0	44.1	56.0	85.8
225	113	71	30.3	100	100	0.0	43.8	56.2	81.3
234	103	119	23.3	100	100	0.0	23.5	76.5	81.5
Catalysts:		2.6wt.% Li_2CO_3/CaO							
224	104	0	37.2	0.0	-	3.3	38.2	58.5	62.8
217	107	31	26.1	65.3	87.4	0.0	37.5	62.5	54.1
210	107	66	18.1	65.8	83.2	0.0	30.7	69.3	45.9
218	111	127	14.3	74.3	88.8	0.0	28.4	71.7	42.5
Catalysts:		$Mn^@/Li_2CO_3$/MgO (18C, see table 6.2.4.1.a)							
228	108	0	39.1	94.5	-	0.0	47.0	53.0	58.4
242	114	33	34.2	100	100	0.0	48.5	51.5	53.9
237	113	72	29.6	100	100	0.0	43.9	56.1	50.7
237	111	127	21.8	93.3	100	0.0	36.1	63.9	43.1
Catalyst:		$Cr^@/Li_2CO_3$/MgO (28C, see table 6.2.5.1.a)							
231	106	0	25.5	100	-	0.0	94.5	5.5	38.6
234	110	33	21.4	100	100	0.0	92.8	7.2	36.1
229	105	67	17.1	100	100	0.0	90.8	9.2	33.3
236	111	127	11.6	100	95.5	0.0	89.8	11.6	31.5
Catalyst:		Sm_2O_3							
220	106	0	35.0	100	0	6.5	57.6	35.9	50.7
229	112	36	31.2	100	76.6	0.0	63.8	36.2	52.0
225	107	68	28.1	100	69.2	0.0	59.1	40.9	46.4
234	113	127	24.5	100	68.3	0.0	51.8	48.2	47.2
Catalysts:		$\gamma-Al_2O_3$							
209	106	0	27.8	88.1	-	58.4	35.9	5.7	54.7
222	107	34	27.7	100	0.0	24.1	66.8	9.1	53.9
226	110	68	20.9	100	54.2	0.0	92.5	7.5	35.1
213	103	118	19.0	100	42.1	0.0	90.4	9.5	52.0

* total flow rate of 25ml/min and partial pressure is in unit torr;
# defined as mole of CO from CH_4/ mole of CH_4 reacted
@ of transition metal M_xO_y

The slight variation of O_2 conversion and the decrease in CH_4 conversion with the increased in CO partial pressure in the reactant stream indicate that the oxidative reaction of methane over Li_2CO_3/MgO catalysts are surface phenomena. The results also suggest that that the sites responsible for methane activation are also responsible for oxidising CO to CO_2. Since the O_2 consumed do not vary significantly in the presence of higher partial pressure of CO in the reactant stream this further indicate that minimal gaseous phase oxidation of CO occurs under the reaction condition and that CO oxidation compete successfully for the active site against methane activation causing lower methane conversion to occur. The increase in C_2 selectivity and the decrease in the percentage of C_2H_4 in the C_2 product is consistent with the decrease in number of sites available for hydrocarbon activation.

LiF/MgO has been shown in section 4.6 to have low activity for oxidative reaction of methane. In the presence of various partial pressure of CO, the low methane conversion (<5%) over this material remained while the percentage of CO converted to CO_2 increases. However the low percentage of CO conversion relative to that over Li_2CO_3/MgO catalysts further indicate the inactivity of this material. Moreover the lower conversion of methane compared to CO further indicate that under the condition of the oxidative reaction of methane, oxidation of CO to CO_2 is more favoured than methane activation. It was also observed that on this catalyst the selectivity to C_2 hydrocarbon increases at higher partial pressure of CO in the reactant stream.

On LiCl/MgO catalysts all of the CO present in the reactant stream was converted to CO and full oxygen consumption occurs under all conditions. The presence of 33 torr of CO in the reactant stream increases the percentage of C_2H_4 in C_2 product from 53.2 to 85.8%. As on the Li_2CO_3/MgO catalyst the increase of CO partial pressure in the reactant stream resulted in the increase in C_2 selectivity and a decrease of methane conversion.

The trends associated with the effects of different partial pressure of CO in the reactant stream on the oxidative reaction of methane over Li_2CO_3/CaO are also similar to that over Li_2CO_3/MgO catalyst. The presence of only a slight variation in the amount of O_2 consumed even at the highest CO partial pressure and the decrease in CH_4 conversion further suggest that on this catalyst CH_4 and CO compete for the same surface sites under the condition of oxidative reaction of methane.

In the activity studies of transition metal oxide doped Li_2CO_3/MgO catalysts the doping with manganese and chromium oxides have been observed to caused the most prominent effects on the catalytic activity of the doped catalysts (section 6.2). However similar effect of CO partial pressure in the reactant stream were observed on these catalysts as in the undoped Li_2CO_3/MgO. Moreover the higher percentage of O_2 consumed and the higher conversion of CO to CO_2 observed on the doped catalysts is consistent with their higher activity for the oxidative reaction of methane.

Full oxygen consumption over Sm_2O_3 were observed in the oxidative reaction of methane in the presence of CO up to 127 torr. The decrease in methane conversion and increase in C_2 selectivity was also observed over this catalyst as higher partial pressure of CO was present. However it was observed that the percentage of CO converted to CO_2 over Sm_2O_3 catalyst is lower than that over Li_2CO_3/MgO catalyst.

In the absence of input CO, the oxidative reaction of 209 torr of CH_4 and 106 torr of O_2 on γ-Al_2O_3 resulted in 27.8 and 88.1% conversion of CH_4 and O_2 respectively. Carbon oxide is the favoured product with the selectivity to CO and CO_2 of 58.4 and 35.9% respectively. In the presence of 34 torr of CO in the reactant stream, a 24.1% net selectivity to CO was still observed while at higher partial pressure of CO the conversion of CO to CO_2 occurs. However the percentage of CO converted to CO_2 when 118 torr of CO is presence in the reactant stream is lower (42.1%) than that over Li_2CO_3/MgO catalyst (81.9%). Moreover it was also

observed that the reduction in methane conversion as a result of CO present in the reactant stream is less than that over Li_2CO_3/MgO catalysts.

The observation made in the effect of CO partial pressure in the reactant stream on the catalytic activity of various catalysts suggest that the the activation of methane is certainly a surface effect. Moreover the sites responsible for methane activation are also capable for converting CO to CO_2. On chemically basic catalysts the conversion of CO to CO_2 is more favoured than methane activation. In the catalyst screening it has been observed that the increase in oxidative coupling properties of Li_2CO_3 doped catalysts was normally followed by the increase in selectivity to CO_2 relative to CO in the carbon oxide products. The trend observed here is certainly consistent with that made in the catalysts screening. Moreover on acidic γ–Al_2O_3 the net formation of CO when 34 torr of CO are present in the reactant stream and the low conversion of CO to CO_2 suggest that the acidic materials favours the partial oxidation of methane to CO while on more basic catalysts the complete oxidation of CO and oxygenate intermediate to CO_2 are more favoured.

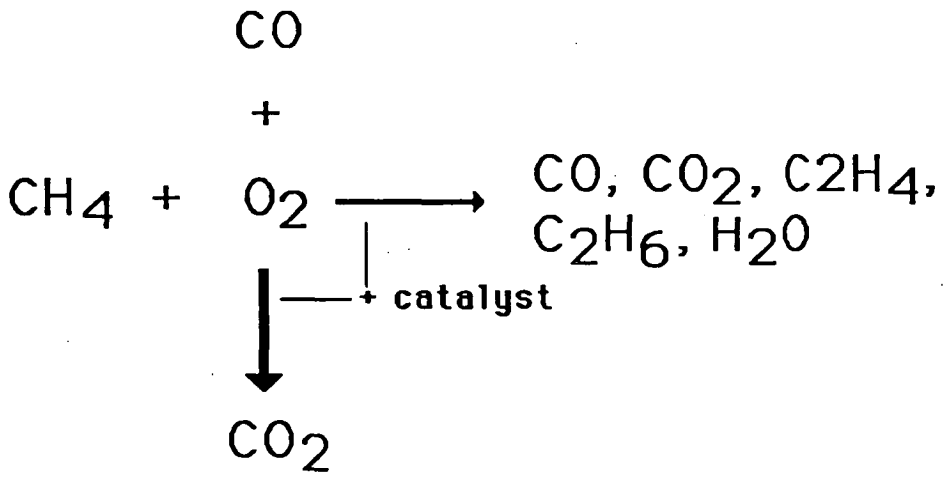

Figure 7.3.2.a. The preferential oxidation of CO to CO_2 relative to methane activation under the condition of catalytic oxidative reaction of methane in the presence of different partial pressures of CO in the reactant gas.

The preference of CO oxidation to form CO_2 over methane activation as observed in this section is illustrated in figure 7.3.2.a. The presence of CO in the reactant stream generally reduces the availability of active site for oxidative reaction of methane. CO was oxidised in preference to CH_4 activation resulting in the loss of methane conversion and the increase in selectivity to total C_2 hydrocarbon. In terms of the distribution to the various C_2 products, the percentage of C_2H_4 in C_2 product is more dependent on the percentage of methane conversion than on the nature of the various catalysts used.

7.4 Overall analysis of activity results

In order to obtain an overview of the oxidative reaction of methane, all of the activity data obtained in this study have been collected and represented as scatter plots. These activity data were of different catalysts, at different reaction temperatures and under different reactant compositions.

Figure 7.4.a is a scatter plots of the percentage of total selectivity, and yield to C_2 hydrocarbon against percentage of methane conversion. At lower methane conversion, high selectivity to C_2 hydrocarbon (>90%)was shown to be achievable. As methane conversion increases however the total achieveable C_2 selectivity decreases. In terms of the percentage of yield to C_2 hydrocarbon, the maximum achievable yield to C_2 hydrocarbons initially increased with methane conversion but then converged to a value of about 20% at the higher methane conversion. Further increase in methane conversion at above 40% does not seem to result in any significant increase in the maximum achievable yield to C_2 hydrocarbons. The barrier for the maximum achievable selectivity to C_2 hydrocarbon and hence C_2 yield, at any percentage of methane conversion, as in figure 2.12.a , can also be drawn in figure 7.4.a. These scatter plots clearly suggest that there seem to be a limit to which the oxidative coupling reaction will occur under the condition of catalytic oxidative reaction of methane. Increasing methane conversion by

increasing reaction severity, will always result in an increase of the exhaustive oxidation of methane, through the oxidation of reaction intermediates and the hydrocarbon products to form carbon oxide.

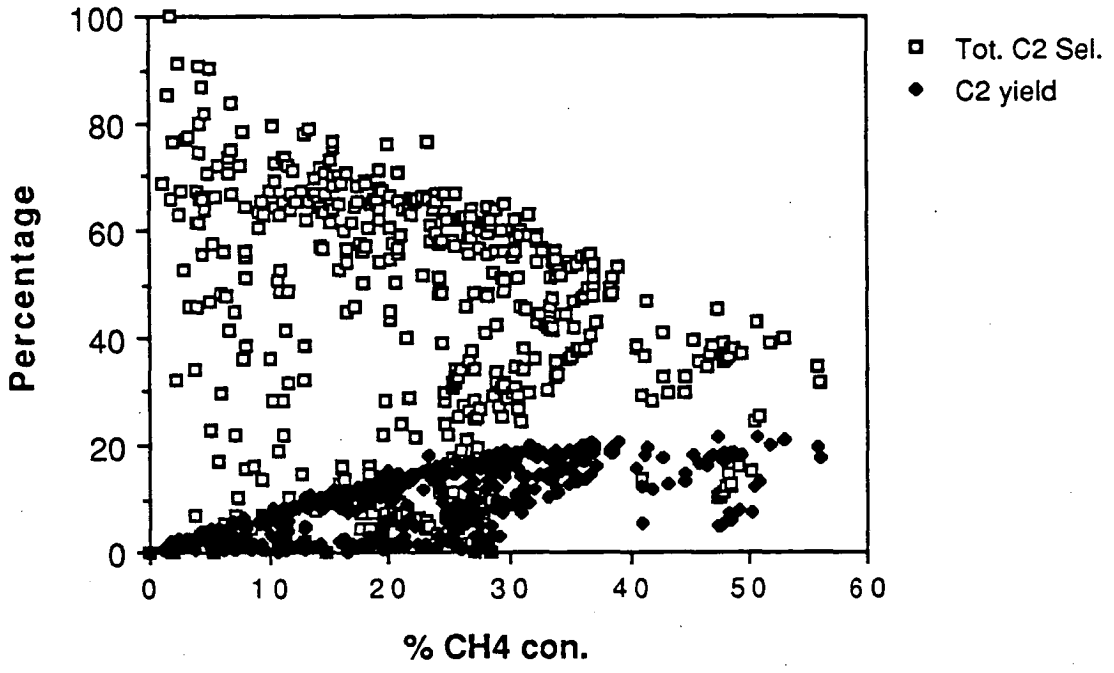

Figure 7.4.a The scatter plots of percentage of selectivity, and yield to total C_2 hydrocarbon against percentage of methane conversion from activity data obtained in this work.

In terms of the distribution to the various C_2, C_2H_6 is the favoured C_2 product at low methane conversion. The percentage of C_2H_4 in the C_2 product was plotted against percentage of methane conversion in figure 7.4.b. At higher methane conversion, the percentage of C_2H_4 in C_2 product increases. The few exceptional points where high C_2H_4 selectivity was observed even at low methane conversion are that of LiCl/MgO catalyst. The high selectivity to C_2H_6 at low methane conversion and the decrease in selectivity to C_2H_6 and the increase in selectivity to C_2H_4 at higher methane conversion clearly indicate that C_2H_6 is the primary product

of the catalytic oxidative reaction of methane. Moreover the C_2H_4 is a secondary product of reactions involving C_2H_6. The trends of decrease in total selectivity to C_2 hydrocarbon have also been made in section 2.12. and by Lee and Oyama,1988. For any particular catalytic system the increase in methane conversion as a result in the increase in reaction severity will always result in the decrease in total selectivity to C_2 hydrocarbons but an increase in the percentage of C_2H_4 in the C_2 products.

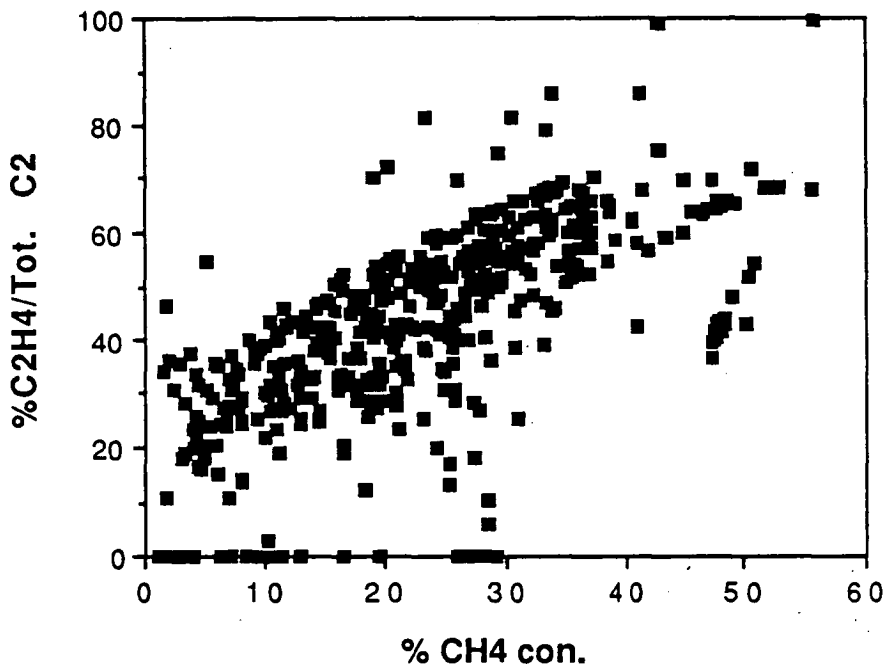

Figure 7.4.b. The scatter plot percentage of C_2H_4/Total C_2 product against percentage of methane conversion from activity data obtained in this work.

The overall catalytic activity scatter plots of figures 7.4.a and 7.4.b (also figures 2.12.a and 2.12.b), to a certain extent indicate the nature of reaction occurring in the catalytic oxidative reaction of methane. As was proposed by Keller and Bhasin,1982, Ito. et al.,1985, Otsuka et al.,1986 and many others, the catalytic oxidative reaction of methane to form C_2 hydrocarbons involved the formation of

C_2H_6 as the primary hydrocarbon product. Methyl radicals has been proposed to be the primary reaction intermediate (Ito et al.,1985) and the finding of Campbell et al.,1987 that the amount of methyl radicals trapped increases with the decrease in the distance between the trap and the catalysts bed further supported this proposal. In line with the mechanism C_2H_4 was formed from the secondary reaction of C_2H_6.

The proposal about the significant of carbene species as reaction intermediate has also been made (Martin and Miradatos,1987). Under this circumstances however C_2H_4 should form as a primary product. Such observation has not been reported as yet. The nature of the catalytic oxidative reaction of methane to form C_2 hydrocarbons as observed fron the overall catalytic activity patterns from this work (figure 7.4.a) and from that reported in the literature (figure 2.12.a) indicate C_2H_6 and not C_2H_4 being the primary product of the reaction.

7.5 Using azomethane to model the catalytic oxidative reaction of methane

Methyl radicals have been proposed as the primary reaction intermediate in the catalytic oxidative coupling reaction of methane (Keller ans Bhasin, 1983; Ito et al.,1985; Otsuka et al.,1986a). In order to investigate the hydrocarbon formation route and to simulate the gaseous phase reaction of methyl radicals, the reaction of methyl radicals from azomethane decomposition under various condition have been studied.

Azomethane was prepared from 1,2-dimethylhydrazine dihydrochloride (Aldrich,99% purity) according to the procedure as described by (Renaud and Leitch,1954). The azomethane was then transferred to a trap cum bubbler for storage and introduction into the reaction stream. When not in use the azomethane container was kept at ice/salt bath temperature and placed away from light. The azomethane was analysed with gcms (H.P. 5890A GC with H.P. 5970 Mass Selective Detector) and only two components, azomethane and methyl chloride was present at a ratio of

1000:1. No further attempt was made to remove the methyl chloride. The one atmosphere flow system used in this studies has been illustrated in figure 3.1.a. The azomethane bubbler was connected to the rest of the flow system by means of B10 quick fit glass joint and Ultra-Torr Cajon fittings. The bubbler was immersed in 2-methyl propanoic acid slush at -46°C. At this temperature the partial pressure of azomethane should be about 72 torr (Taylor and Flowers,1982). The introduction of azomethane into the gas stream was facilitated by flowing helium through the bubbler. A second helium stream was also added in order to increase the flexibility in setting the partial pressure of azomethane in the final reactant stream. As in the catalytic screening work, a total flow rate of 25ml/min was used in most of the experiment. The reactor set-up used was also the one used in the catalysts screening work. The reactor body was made of 9mm o.d. (6mm i.d.) Alsint tubing of which 11cm of its length was heated with a resistive microfurnace. When a total flow rate of 25ml/min was used, the residence time of which the gas was in the reactor is about 7 seconds. Under the condition of this experiments the decomposition of azomethane will be rapid ($t_{1/2} < 10^{-3}$s; Marshall and Sharkar,1983) and hence the reaction that will arise are predominantly from the reaction of the methyl radicals.

In the azomethane experiments the sample gas for analysis was taken 5 minutes after the reactant gas was introduced into the reactor. The exact amount of azomethane used during the reaction was determined by monitoring the amount of nitrogen present in the reactant effluent. A carbon balance of about 95% was normally achieved in most of the experiments. As was observed by Chen et al.,1975 in the pyrolytic reaction of methane, some carbon was deposited on the reactor wall when azomethane was pyrolysed in the absence of oxygen. In order to have a consistent experimental conditions the reactor was normally heated in air at the reaction temperature for two hours after each run to remove the carbon deposit.

7.5.1 Decomposition of azomethane at different temperature

The decomposition reaction of azomethane at different temperature have been studied. Azomethane/helium gas mixture containing about 50 torr of azomethane was flowed at 25ml/min through a blank reactor tube at various temperature. The result from the reactions are presented in Table 7.5.1.a.

Table 7.5.1.a The decomposition of azomethane at different temperature

$PCH_3N_2CH_3$ (Torr)	Temp (°C)	%Selectivity*				
		CH_4	C_2H_4	C_2H_6	C_3H_6	C_3H_8
53	680	14	10	65	0	11
47	720	14	19	59	0	8
58	760	16	24	53	0	7
53	800	17	35	42	1	5
44	840	19	52	28	0	1
47	880	23	66	11	0	0

*selectivity is defined as the number of moles of carbon in a product per mole of carbon present in azomethane

At 680°C, the selectivity to methane, ethene, ethane, propene and propane was 14, 10, 65, 0 and 11% respectively. In terms of the correlation between temperature and selectivity to the various products, the selectivity to methane and ethene increases with temperature while that to propene initially increase but at above 800°C it decreases. The selectivity to ethane and propane decreases continously with the increase in reaction temperature. At 880°C the decomposition of azomethane resulted in 23% selectivity to methane with 66% and 11% selectivity to ethene and ethane respectively.

The preference of ethane selectivity in lower temperature decomposition of azomethane and the decrease in selectivity of ethane but increases in selectivity to ethene with increase in reaction temperature are similar to the trends observed in the catalytic oxidative reaction of methane. In other word the trends observed with

temperature of the hydrocarbon product distribution of azomethane decomposition and the catalytic oxidative reaction of methane are similar. This similarity should imply that a similar series of reaction step occurs for the two processes.

The nature of the decomposition of azomethane at moderate temperature (Temp < 650°C) have been studied by Forst and Rice,1963; Paquin and Forst,1973; Back,1983 and Marshall and Sharkar,1983. The overall mechanism for the decomposition reaction of azomethane may be written as follows:

Equation 7.5.1.a	$CH_3N_2CH_3$	---- $CH_3 + CH_3 + N_2$
Equation 7.5.1.b	$M + CH_3 + CH_3$	---- $C_2H_6 + M$
Equation 7.5.1.c	C_2H_6	---- $CH_3 + CH_3$
Equation 7.5.1.d	$CH_3 + C_2H_6$	---- $CH_4 + C_2H_5$
Equation 7.5.1.e	C_2H_5	---- $C_2H_4 + H$
Equation 7.5.1.f	$H + C_2H_6$	---- $C_2H_5 + H2$
Equation 7.5.1.g	$CH_3 + C_2H_5$	---- C_3H_8

Back,1983 have proposed that in pure azomethane at temperature up to 630°C, the reaction of methyl radicals with azomethane resulted in the formation of methane (Equation 7.5.1.g) and radicals species $CH_3N_2CH_2$. Subsequent reactions of $CH_3N_2CH_2$ with other radicals lead to a short chain reaction with a chain length of 2 or 3 yielding N_2, CH_4, C_2H_6 and other products (Paquin and Forst,1973). In fact at 290°C, methane is the major product from the decomposition of azomethane.

Under the high temperature condition, the nature of the decomposition of azomethane are likely to be different. The rate of azomethane decomposition to form methyl radicals (equation 7.5.1.a) will be much faster that the amount of reactions involving methyl radicals with the azomethane will be minimal. The decrease in the selectivity to C_3 hydrocarbons at the higher reaction temperature is consistent with the above proposal. Moreover the increase in selectivity to methane is also indicative of the increase in the concentration of methyl radical due to the rapid decomposition of azomethane.

In the decomposition of azomethane under the condition of this work, the reaction of methyl radicals play a major role in determining the hydrocarbon product distribution. Since a similar trend in the hydrocarbon product distribution with changes in reaction temperature was observed in the decomposition of azomethane and in the catalytic oxidative reaction of methane this suggest that the reaction involving methyl radicals also plays a significant role in the catalytic oxidative reaction of methane. This is consistent with the proposal made by others regarding methyl radicals being the primary reaction intermediate of the catalytic oxidative reaction of methane. Moreover Kimble and Kolts, 1989; Larbinger and Ott,1987; and Lee and Oyama, 1988 have shown through kinetic computation that a series of gaseous phase reaction, involving methyl radicals and others can produce the hydrocarbon product distribution observed for the catalysed oxidative reaction of methane.

7.5.2 Effect of azomethane partial pressure on the product distribution at 800°C

In order to simulate the catalytic reaction where the amount of methane conversion is higher, an experiment where the azomethane partial pressure in the reactant stream was varied has been performed. As illustrated in table 7.5.2.a the selectivity to the various products from the decomposition of azomethane at 800°C is significantly affected by the partial pressure of azomethane. When the partial pressure of azomethane was 8 torr, the selectivity to methane ethene, ethane and C_3 hydrocarbons were 9, 23, 55 and 13% respectively. When the partial pressure of azomethane was increased to 55 torr, the selectivity to methane, ethene, ethane and C_3 hydrocarbons was 17, 35, 42 and 6% respectively. As evidenced from table 7.5.2.a, the percentage of selectivity to methane and ethene increases slightly as the partial pressure of azomethane was increased while the selectivity to ethene and C_3 hydrocarbons decreases slightly.

Table 7.5.2.a The effect of different partial pressure of azomethane on the product distribution at 800°C

$P_{CH_3N_2CH_3}$ (torr)	%Selectivity			
	CH_4	C_2H_4	C_2H_6	C_3
8	9	23	55	13
11	10	28	52	10
25	12	30	48	10
33	13	31	47	9
41	13	32	46	9
52	17	35	42	6

Increasing the partial pressure of azomethane at fixed total flow rate of the reactant gas does not change the time of which the reactant dwelled in the reactor. In other word the effect studied here is solely the effect of increase in the presence of methyl radicals on the product distribution. The increase in the partial pressure of azomethane, and hence the methyl radicals would be analogous to the increase in methane conversion in the catalytic reaction of methane. It has been observed in the catalytic oxidative reaction of methane that the selectivity to ethene increases while that to ethane decreases as methane conversion increases. In the decomposition of azomethane, the selectivity to ethene also increases while that to ethane decreases as the partial pressure of azomethane increases. This further indicate the similarity in the nature of the reaction involved in the hydrocarbon formation of the decomposition of azomethane and that in the catalytic oxidative reaction of methane. Moreover this also lend some support to the proposal that methyl radicals is the primary reaction intermediate of the catalytic oxidative reaction of methane.

7.5.3 The reaction of azomethane in different partial pressure of oxygen

The effect of oxygen partial pressure (0-117 torr) on the decomposition of azomethane have been studied. When O_2 was present in the azomethane/helium flow and reacted at 800°C, losses of hydrocarbons products occurs in the form of CO

and CO_2. As evidenced in Table 7.5.3.a, the selectivity to the carbon oxides increases as the ratio of the oxygen to azomethane in the reactant gas was raised.

Table 7.5.3.a The reaction of azomethane at 800°C in different partial pressure of oxygen

$P_{CH_3N_2CH_3}$ (Torr)	P_{O_2} (Torr)	%Selectivity CO	CO_2	CH_4	C_2H_4	C_2H_6	C_3
33	0	0	0	13	31	47	9
31	21	9	12	14	18	47	0
33	47	16	15	16	19	34	0
43	77	48	34	11	1	6	0
40	117	48	48	4	0	0	0

One notable observation that can be made in the results is the near equivalent amount of CO and CO_2 being formed in the carbon oxide products. Similar observation has been made for the homogeneous oxidative reaction of hydrocarbon mixtures. On the other hand the catalytic oxidative reaction of methane normally favours the formation of carbon dioxide as the preferred carbon oxide products.

The results observed here clearly indicate that the presence of oxygen in the decomposition of azomethane resulted in the oxidation of methyl radicals and the hydrocarbon products to form carbon oxides.

7.5.5 The oxidative reaction of azomethane under various conditions

In order to probe further the nature of the oxidative reaction of azomethane, the effect of temperature have been studied. Azomethane/helium/O_2 gas mixture was reacted in a blank reactor, over 0.2g of LiF/MgO and Li_2CO_3/MgO catalysts. In these experiments the total flow rate used was 25ml/min and the ratio of azomethane to oxygen remained about constant . About 50% selectivity to

hydrocarbon products resulted. The finding of these experiments are summarised in table 7.5.4.a.

Table 7.5.4.a The product distribution from oxidative reaction of azomethane under various condition

Temp. (°C)	$P_{CH_3N_2CH_3}$ (Torr)	P_{O_2} (Torr)	%Selectivity CO	CO_2	CH_4	C_2H_4	C_2H_6
i) over empty reactor tubing							
720	38	46	17	24	18	9	32
760	38	38	20	15	19	15	31
800	41	43	21	15	20	19	25
840	34	36	27	9	21	28	15
880	38	37	27	6	22	36	9
ii) over 0.2g of LiF/MgO catalyst							
720	26	38	26	25	18	5	26
760	26	36	27	23	20	7	23
800	27	35	27	21	20	9	23
840	28	31	26	15	22	17	20
880	29	32	27	12	23	23	15
iii) over 0.2 g of Li_2CO_3/MgO catalyst							
720	22	38	27	23	15	5	30
760	30	36	26	16	19	8	31
800	28	32	29	13	19	13	26
840	36	34	23	11	20	21	25
880	37	36	24	9	21	29	17

Generally the effect of increasing reaction temperature was to result in a slight increase in selectivity to methane and ethene and a decrease in the selectivity to ethane. The presence of different catalysts does not seems to have major effects in the product distribution of the reaction. Any difference observed in the total hydrocarbon selectivity at any particular temperature under the different condition can be explained in terms of the variation in the slight variation of the ratio of oxygen to azomethane in the reactant stream. This observation suggest that the oxidative

reaction of azomethane achieved completion long before the reactant gas passed through the catalyst bed. This is likely since it would take about 15 seconds for the gas mixture front to travelled from the reactor inlet to the catalyst bed. In this respect the presence of the different catalysts will not have have any significance in the oxidative reaction of azomethane.

The results of these experiments further highlighted the detrimental role of oxygen towards the hydrocarbons building reactions. In the presence of oxygen, methyl radicals may be removed by direct reaction with oxygen molecule (Equation 7.5.4.a) and with oxygen atoms (Equation 7.5.4.b). The latter route is favoured in the rich methane flame. It is possible that due to the high concentration of methyl radicals and oxygen under the conditions of this experiments the methyl peroxyl route can be the major route for the production of carbon oxides eventhough it is established that this reaction (reaction 7.5.4.a) is an equilibrium reaction and favours the reverse reaction at higher temperature. An observation made in this work which could support the significance of the methyl peroxyl route in the oxidative reaction of azomethane is that at higher reaction temperature the selectivity to CO increases possibly as a result of the decrease rate of reaction 7.5.4.a.

Equation 7.5.4.a $\quad CH_3 + O_2 \text{ ===== } CH_3O_2$

Equation 7.5.4.b $\quad CH_3 + O \text{ ------- } CH_2O + H$

In the catalytic reaction however, a different mechanism for the carbon oxide formation is likely to occur. Carbon dioxide is the major carbon oxide product in the catalytic oxidative reaction of methane to C_2 hydrocarbons. The full oxidation of oxygenates and carbon oxide intermediates was facilitated by the catalysts through surface reactions. It has been observed in the catalytic screening that chemically basic catalysts favours the formation of carbon dioxide over carbon monoxide in the carbon oxide products. The formation of carbon dioxide over this catalysts could possibly involved the formation of carbonyl and carbonate species as was observed in the *in-situ* FTIR work.

7.6 Contribution of this work toward understanding the mechanism of the catalytic oxidative reaction of methane

The catalyst screening activity performed in this study has basically confirmed that ethane is a primary hydrocarbon product of the catalytic oxidative reaction of methane, while ethene was formed through the secondary reactions involving ethane. The carbon dioxide was observed to be the favoured carbon oxide products over most catalysts which shows significant oxidative coupling properties. The preference towards higher C_2 hydrocarbon selectivity and CO, among the carbon oxide products increases with basicity of the catalysts. It was also observed that good oxidative coupling properties under the condition of these experiments is associated with catalysts which have monovalent oxidation state. Catalysts which contain easily reducible component favours the exhaustive oxidation of methane to carbon dioxide.

Various type of chemical compounds have been observed to be active for the oxidative reaction of methane to form C_2 hydrocarbons. Because of this the exact neture of active sites on these materials are difficult to be identified. However in this work it was observed that most of the materials shown to have good oxidative coupling properties gave rise to hydroxyl species formation after high temperature pretreatments. This might indicate the presence of O^- type species on the surface of these catalysts under the conditions associated with the reaction. In turn this oxygen sites could be responsible for the oxidative reaction of methane to higher hydrocarbons.

The activation of methane on the active sites of the catalysts resulted in the formation of methyl radicals. The methyl radicals may couple on the catalysts surface or in the gaseous phase to form ethane. In this work it has been observed that the gaseous phase reaction of methyl radicals could give rise to the hydrocarbon product distribution similar to that in the catalytic reaction of methane. In both processes the

trends on the product distribution due to the effect of temperature and conversion are also similar. This result lends some support the proposal of methyl radicals being the primary reaction intermediate in the catalytic oxidative reaction of methane.

It has also been demonstrated in this work that in the presence of excess oxygen the hydrocarbon products from oxidative reaction of methane can undergo homogeneous oxidative reaction. The homogeneous reaction resulted in near equivalent selectivity to CO and CO_2 among the carbon oxides products. Similar observation was made in the oxidative reaction of azomethane. In the catalytic oxidative reaction carbon dioxide normally formed as a major carbon oxide products. This suggest that the exhaustive reaction involved the surface reactions. The oxidation of CO to CO_2 was observed to compete successfully against methane activation over most oxidative coupling catalysts. This indicate that similar sites were involved in for methane activation and for the exhaustive oxidation and is consistent with the observation made regarding the increase C_2 selectivity together with increase in the selectivity to CO_2 in the carbon oxide products as the catalyst become more basic.

It has also been observed that the nature of the oxidative reaction of methane put a limit on the performance of any catalysts in the catalytic reaction. This is because under the severe reaction condition necessary for higher conversion, the gaseous phase exhaustive reaction as well as the surface reaction will become more dominant and will tend to limit the hydrocarbon yield.

CHAPTER 8

CONCLUSION AND FUTURE WORK

8.1 Conclusion

8.1.1 Catalyst screening

About 110 solid catalytic material have been prepared and their catalytic activity for the oxidative coupling reaction of methane to form C_2 hydrocarbon, together with that of about 20 standard chemical compounds, have been determined. A variety of materials showed significant activity for the oxidative reaction of methane. Generally materials which are chemically basic in nature resulted in higher C_2 hydrocarbon yield.

Fresh MgO was observed to have good oxidative coupling activity. At 800°C methane conversion of greater than 30% and total C_2 yield of about 15% can be achieved over fresh MgO. Other alkaline earth compounds were also found to have significant catalytic activity. SiO_2 and TiO_2 resulted in lower activity while $AlPO_4$-5 is active but mainly favours the exhaustive reaction of methane to carbon oxide. Sm_2O_3 was shown to have high activity for oxidative conversion of methane. However, it was also found that it resulted in lower selectivity to C_2 hydrocarbons compared to that of Li_2CO_3/MgO catalyst. The presence of Li_2CO_3 on MgO resulted in a significant increase of selectivity to C_2 hydrocarbon but a slight decrease in methane conversion. Generally, the presence of Li_2CO_3 on other metal oxide also increase their selectivity to C_2 hydrocarbons (section 4.5). Among the catalytic materials formed by supporting Li_2CO_3 on various metal oxides, the Li_2CO_3/MgO system was found to have the most optimum catalytic activity (section 4.7).

The activity of various lithium salts supported on MgO varies from each other. Li_2CO_3 and LiOH on MgO resulted in material with good catalytic activity while LiF and Li_2SO_4 destroyed the activity of MgO. LiCl/MgO as in $LiCl/Sm_2O_3$ (Otsuka et al.,1986a) showed good conversion and high selectivity to C_2H_4. However, the high selectivity to C_2H_4 over the LiCl/MgO catalyst decreases rapidly with time-on-stream (section 4.6).

The presence of different loadings of transition metal oxides on MgO resulted in the exhaustive oxidation of methane to form carbon oxide products. However in the presence of a low loading of the transition metal oxide on Li_2CO_3/MgO, a slight increase in methane conversion was observed relative to that of undoped catalysts, with the high C_2 selectivity being retained. The extent to which the transition metal oxides effect the activity of Li_2CO_3/MgO increases in the order of Zn<Fe<Mn<Cr. This order parallels the differences between the ionic radii of the transition metal ions and lithium. The presence of a low loading of manganese oxide on Li_2CO_3/MgO was found to promote methane conversion significantly and yet the high selectivity to C_2 hydrocarbon was retained. The activity of 2.3wt% manganese oxide doped Li_2CO_3/MgO at 760°C was found to be similar to that of Li_2CO_3/MgO at 800°C. The presence of chromium oxide on Li_2CO_3/MgO however has a detrimental effect on the oxidative reaction of methane. Even at low chromium oxide loadings, the catalysts resulted in the exhaustive oxidation of methane to carbon oxides (section 6.2.5).

At lower reaction temperatures (600°C to 700°C) C_2H_6 was mainly observed as the major component of the C_2 products but at higher temperatures selectivity to C_2H_4 increases while selectivity to C_2H_6 decreases. The increase in methane conversion with the increase in reaction temperature or reaction severity in general, on any particular catalyst is generally followed by an increase in C_2H_4 selectivity. This indicates that ethene is a secondary product of the oxidative

coupling reaction. It has also been demonstrated that there exists a limit for the maximum achievable selectivity to C_2 hydrocarbons at any particular methane conversion. Over any particular catalyst an increase in methane conversion by changing the reaction condition, (increase in temperature, residence time, O_2 partial pressure and the amount of catalyst used), will result in a decrease in C_2 selectivity. This relationship highlighted the main problem in any process involving oxidative reaction. Severe reaction conditions are necessary for higher conversion. However, this would always results in a higher proportion of the desired product undergoing further oxidation causing lower hydrocarbon product selectivity (sections 2.12 and 7.3).

Chemically basic materials show good oxidative coupling properties and favours the formation of carbon dioxides as the the major carbon oxide product. Acidic materials like Al_2O_3/SiO_2 and γ-Al_2O_3 favours the formation of carbon monoxide and poorer hydrocarbon yields. The homogeneous (non-catalytic) oxidation of methane also favours the formation of carbon monoxide. In order to elucidate this phenomena, the effect of different partial pressures of carbon monoxide on the oxidative coupling reaction at 800°C has been determined (section 7.3.2). In the presence of low partial pressure of CO in the reactant it was observed that over chemically basic materials CO was preferentially oxidised to CO_2 while over γ-Al_2O_3 a net formation of CO occurred. This indicated that over γ-Al_2O_3 as in the case of the homogeneous oxidative reaction of methane complete oxidation to form carbon dioxide are not facilitated (section 7.2.2). This also highlights the different nature of reaction sites on basic and acidic samples.

8.1.2 Physico-Chemical Properties and Catalytic Activity

Some relationship can be drawn between the catalytic activity and the physico-chemical properties of the materials studied.

Generally materials with low surface area resulted in higher yield of C_2 hydrocarbons. Surface area is not a sufficient condition for the catalytic activity. For an active material the selectivity to C_2 product increases with a decrease in surface area (section 5.6.1).

Most of the catalytic materials prepared have been found to undergo significant physical and chemical transformation at reaction temperature. Using *in-situ* FTIR it was observed that the Li_2CO_3 phase of Li_2CO_3/MgO catalyst was in a molten state at 750°C (section 5.2.3). It has been observed that the carbonate phase undergoes decomposition at high temperature and this contributes to the loss of lithium. From atomic absorption spectroscopy of calcined Li_2CO_3/MgO catalysts with different lithium loadings, it was found that the precalcination process (at 900°C for 10hrs) resulted in significant loss of lithium for initial loading less than 2wt.%. No significant loss occurs for lithium loadings greater than 2wt.% (section 5.2.4). In the activity studies it was observed that the calcined catalysts with lithium loading less than 2wt.%, have much lower activity than MgO or the higher lithium loading catalysts (section 4.3.1) This indicates that significant physical and chemical changes occurred on the catalysts during calcination. The loss of lithium during the precalcination of lower loading catalysts must have permanently deactivated these catalysts. On the higher loading catalysts, however, most of the Li_2CO_3 phase was still present after precalcination. The retention of the Li_2CO_3 phase in the higher loading Li_2CO_3/MgO catalysts is likely to contribute to the catalytic activity of these materials.

Li_2CO_3 phase was found to be stabilised on MgO through the formation of a good solid matrix. On other supports however it was found that the Li_2CO_3 phase was decomposed to Li_2O. This phenomena is related to the differences between the ionic radii of lithium and that of the support metal ions. If the ionic radii are similar then formation of solid matrix occurs and the carbonate phase is

stabilised. On the other hand, if the ionic radii of the metal ions of the support are different from that of Li^+, the Li_2CO_3 phase undergoes decomposition to Li_2O. The presence of Li_2CO_3 on MgO caused significant changes in the catalytic activity since Li_2CO_3 was stabilised. On γ-Al_2O_3, the presence of Li_2CO_3 does not influence methane conversion but changes the product distribution significantly. The presence of Li_2CO_3 on TiO_2 and SiO_2 causes only a slight changes in activity. It has been observed that Li_2CO_3 was not stabilised on these oxides (section 5.4).

Using SEM, it was observed that Li_2CO_3 rich layers were formed on the surface of Li_2CO_3/MgO sample which were precalcined at 900°C for 10 hours (section 5.2.1). The presence of iron and zinc oxides on Li_2CO_3/MgO does not disrupt the formation of this layer as much as that by Cr and Mn oxides. Low loading of manganese and chromium oxide not only disrupted the formation of lithium rich layers and but also make the composition of the calcined samples more homogeneous (section 6.4). In the catalysts screening low loadings of zinc and iron oxides on Li_2CO_3/MgO resulted in catalytic activity similar to the undoped Li_2CO_3/MgO catalyst while manganese and chromium oxides doped Li_2CO_3/MgO catalysts have significantly different activity from that of the undoped catalysts (section 6.2).

The TPR results shows that less reducible metal oxide phases were present on the transition metal oxide doped Li_2CO_3/MgO catalysts ralative to the doped MgO. TPR reducible phases were not observed on the iron oxide doped Li_2CO_3/MgO catalysts. This can be explained in-terms of the formation of Li_2CO_3 rich layer on the catalysts surface, preventing the exposure of iron oxide phase for reduction. In the TPR of manganese and chromium oxides doped Li_2CO_3/MgO systems, reducible oxide phases were observed to be present (section 6.4). This suggest that when Li_2CO_3/MgO was doped with manganese and chromium oxides the formation of the Li_2CO_3 rich layer was disrupted facilitating the exposure of

transition metal oxide phases on the surface. The exposed manganese and chromium oxide phases of the doped Li_2CO_3/MgO catalysts served as the redox site during the oxidative reaction of methane.

8.1.3 Active Sites

The Li^+O^- species has been proposed to be the active site on Li_2CO_3/MgO catalyst (Wang and Lunsford, 1986a). Since a variety of materials shows significant catalytic activity, this indicates that no particular site is responsible for the reaction on every single material. In this work it was observed by *in-situ* FTIR that most of the active material gave rise to free hydroxyl species after pretreatment at 750°C. It was also observed that during the course of oxidative reaction on Li_2CO_3/MgO surfaces which was evacuated prior to exposure to the reactant gas, surface hydroxyl was formed indicating that the O^- type species were present on the active catalyst. This also suggests that it is the O^- type sites which are responsible for oxidative coupling reaction. On materials with non variable oxidation state, such as the alkali earth metal oxides, the different O^- type site can consist of the M^+O^- sites, the coordinatively unsaturated O^{2-}, and the O^- species produced by surface defects and hydroxyl species of the [111] micro plane (Che and Tench,1982).

On material with variable oxidation states, such as the transition metal oxides, a different situation existed. The labile oxygen species associated with the transition metal ions plays a major role. These sites form a part of the redox cycle in the oxidative reaction of methane over the catalyst doped with transition metal oxide. In this work it was found that the presence of Li_2CO_3 reduced the availability of such sites and hence this reduced the exhaustive oxidation reaction of methane causing higher selectivity to C_2 hydrocarbons to be realised.

8.1.4 On Reaction Mechanism

Methane reacts with the active site on the catalyst surface to form methyl radical and hydroxyl species. Methyl radicals has been trapped from the effluent of oxidative reaction of methane and since then it was considered to be the primary reaction intermediate (Ito et al.,1985). The coupling of methyl radicals on the catalyst surface and/or in the gaseous phase resulted in the formation of ethane. The further reaction of ethane with the surface and in the gaseous phase resulted in the formation of ethene.

The oxidation of methyl radicals in the catalysed reaction mainly occur on the catalyst surface and carbon dioxide was formed as the major carbon oxide products. The oxidation of methyl radicals can also occur in the gaseous phase and is likely to favour the formation of carbon monoxide instead. Most of the carbon oxide product in the catalysed reaction is derived from the oxidation of methyl radicals and not from C_2 hydrocarbons.

The catalytic oxidative reaction of methane have been modelled by the reaction of methyl radicals under condition similar to catalytic studies (section 7.5). It was found that the hydrocarbon product distribution from the gaseous phase reaction of methyl radicals are similar to the hydrocarbon product distribution from the catalysed reaction. The presence of oxygen with gaseous phase methyl radicals caused the loss of hydrocarbon products. These result lend some support to the proposal that methyl radicals are the primary intermediate of the catalytic reaction. It also suggests that the gaseous phase reaction of methyl radicals can account for the hydrocarbon product formation in the catalysed reaction.

8.2 Future Work

The nature of the catalytic oxidative coupling reaction of methane to C_2 hydrocarbons have been understood to a certain extent. The question that is of

interest to every researcher is the potentiality of this route for producing chemical feedstocks and liquid fuels under current economic climate. Gray et al.,1988 have proposed that this route can become competitive with established technologies if about 25% of methane conversion per single pass and about 75% selectivity to C_2 hydrocarbons were achieved together. Another requirement is for the catalysts to have long performance life, e.g.in the order of 1000 hours (see Pierrot et al.,1988). Several catalytic systems (such as Li/MgO and $K/BaCO_3$) were shown to have the potential of fulfil the first two requirements (sections 2.12 and 7.3) but to the best of the author knowledge none has been demonstrated to possess the lifetime required. Clearly there is a need to focus future work in achieving catalytic stability and reaction conditions which fullfil all the three requirements above.

Most of the current catalysts which show promising activity contain alkali metal as one of its components. It has been demonstrated in this work that the loss of catalytic activity of these catalyst is associated with the loss of the alkali metal through decomposition and volatilization. An improvement in the lifetime of these catalyst could possibly be made by changing the physical nature and the composition of these catalyst slightly. By making the catalyst particles larger the rate of alkali losses can be slowed down through the formation of protective layer as it was observed in this work. Changing the reaction condition could also prolong the catalyst lifetime even though it might affect its activity. In terms of catalyst development, it is possible that new catalysts can be synthesised from mixed mono oxidation state metal oxides.

REFERENCES

Ahmed, S., Kasztelan, S., and Moffat, J.B., Am. Chem. Soc., Div. Fuel Chem., 1988, 33, p. 437.

Ahren, L. H., Geochim. Cosmochim. Acta, 1952, 2, p.155.

Aika, K., and Nishiyama, T., Int. Congr. Catal. [Proc.], 9th 1988b, 2, p. II 907.

Aika, K., Moriyama, T., Takasaki, N., and Iwamatsu,E., 1986a, J. Chem. Soc., Chem. Commun., p. 1210.

Aika, K., Liu, Q., and Morikawa, A., Inorganica Chimica Acta, 1986b, 118, L 23.

Aika, K., Moriyama, T., Fujimoto, N., Takasaki, N., and Iwamatsu, E., VI th Int. Symp. Heterogeneous Catalysis, Sofia, , 1987, 1, p. 418.

Aika, K., and Nishiyama, T., J. Chem. Soc., Chem. Commun., 1988a, p. 70.

Amesh, I. T.A., and Amenomiya, Y., J. Phys. Chem., 1986, 90, p. 4785.

Arakawa, H., Fukushima, T., and Ichikawa, M., Applied Spectroscopy, 1986, 40, p. 884.

Anderson, J. R., and Tsai, P., Applied Catalysis, 1985, 19, p. 141.

Anderson, J. R., Appl. Catal., 47(2), p.177.

Amorebieta, V. T., and Colussi, A. J., J. Phys. Chem., 1988, 92, p. 4576.

Asami, K., Shikada, T., Fujimoto, K., and Tominaga, H., Ind. Eng. Chem. Res., 1987a, 26, p. 2348.

Asami, K., Hashimoto, S., Shikada, T., Fujimoto, K., and Tominaga, H., Ind. Eng. Chem. Res., 1987b, 26, p. 1485.

Asami, K., Omata, K., Fujimoto, K., and Tominaga, H., J. Chem. Soc., Chem. Commun., 1987c, p. 1287.

Asami, K., Hashimoto, S., Fujimoto, K., and Tominaga, H., Stud. Surf. Sci. Catal., 1988a, 36, p. 403.

Asami, K., Omata, K., Fujimoto, K., and Tominaga, H., Energy & Fuels, 1988b, 2, p. 574.

Aylward, G. H., and Findlay, T.J.V., SI Chemical data, John Wiley and Son Inc., 1971, p.72.

Back, R.A., Can. J. Chem., 1983, 61, p.916.

Baghal, M.H.V., Colussi, A.J., and Benson, S.W., J. Am. Chem. Soc., 1978, 100(10), p. 3215.

Baghal, M.H.V., Colussi, A.J., and Benson, S.W., Int. J. Chem. Kin., 1979, 11, p. 147.

Benson, S.W., Patent US 4199533 (1980).

Bhasin, M. M., Stud. Surf. Sci. Catal., 1988, 36, p. 343.

Bohme and Fehsenfeld, Can. J. Chem., 1969, 47, p.2717.

Brown, R. S., Cooper, J. R., and Wilkins, C. L., Annal. Chem., 1985, 57, p. 2275.

Buevskaya, O. V., Suleimanov, A. I., Aliev, S. M., and Sokolovskii, V. D., React. Kinet. Catal. Lett., 1987, 33, p. 223.

Bytyn, W., and Baerns, M., 1986, App. Catal., 28, p.199.

Burgt, M.J.v.d., van Leeuwen, C.J., del 'Amico, J.J., and Sie, S.T., Stud. Surf. Sci. Catal., 1988, 36, p.473.

Campbell, K. D., Morales, E., and Lunsfords, J. H., J. Am. Chem. Soc., 1987, 109, p. 7900.

Campbell, K. D., Zhang, H., and Lunsford, J. H., J. Phys. Chem., 1988, 92, p. 750.

Cant, N. W., Lukey, C. A., Nelson., P. F., and Tyler, R. J., J. Chem. Soc., Chem. Commun., 1988, p. 766.

Carreiro, J. A.S. P., Follmer, G., Lehmann, L., Baerns, M., Int. Congr. Catal. [Proc.], 9th. 1988, 2, p. II 891.

Carreiro, J.A.S.P., and Baerns, M., 1989, J. of Catal., 117, p. 258.

Che, M., and Tench, A. J., J. Catal., 1982, 32, p.77.

Chen, C.J., Back, M.H., and Back, R.A., Can. J. Chem., 1975, 53, p.3580.

Cullis, C.F., and Willat, B.M., 1983, J. Catal., 1983, 83, p. 267.

DeBoy, J. M., and Hicks, R. F., J. Chem. Soc., Chem. Commun., 1988a, p. 982.

DeBoy, J. M., and Hicks, R. F., I & EC Research, 1988b, 27, p. 1577.

DeBoy, J. M., and Hicks, R. F., Journal of Catalysis, 1988c, 113, p. 517.

Doi, T., Utsumi, Y., and Matsuura, Int. Congr. Catal. [Proc.], 9th. 1988, 2, p. II 937.

Driscoll, D. J., Martir, W., Wang, J. X., and Lunsford, J. H., J. Am. Chem. Soc., 1985, 107, p. 58.

Driscoll, D. J., Martir, W., Wang, J. X., and Lunsford, J. H., J. Am. Chem. Soc., 1985, 107, p. 2682.

Driscoll, D. J., and Lunsford, J. H., J. Phys. Chem., 1985, 89, p. 4415.

Ekstrom, A., and Lapszewicz, J. A., J. Chem. Soc., Chem. Commun., 1988, p. 797.

Ekstrom, A., and Lapszewicz, J. Am. Chem. Soc., 1988b, 110, p.5226.

Ekstrom, A., and Lapszewicz, J. Phys. Chem., J. Phys. Chem., 1989, 93(13), p.5230.

Edwards, J. H., and Tyler, R. J., Stud. Surf. Sci. Catal., 1988, 36, p. 359.

Fang, T., and Yeh, C. T., Journal of Catalysis, 1981, 69, p. 227.

Forst, W., and Rice, O.K., Can. J. Chem., 1963, 41, p.562.

Follmer, G., Lehmann, L., and Baerns, M., Am. Chem. Soc., Div. Fuel Chem., 1988, 33, p. 453.

Foster, N.R., Appl. Catal., 1985, 19, p.1.

France, J. E., Shamsi, A., and Ahsan, M. Q., Energy and Fuels, 1988, 2, p. 235.

Freund, F., Wengeler, H., Kathrein, H., Knobel, R., Oberheuser, G., Maiti, G.C., Reil, D., Knipping, and Kotz, J., Bull. Mineral, 1983, 106, p.105.

Gaffney, A. M., Jones, C. A., Leonard, J. J., and Sofranko, J. A., Am. Chem. Soc., Div. Pet. Chem., 1988a, 33, p. 445.

Gaffney, A. M., Jones, C. A., Leonard, J. J., and Sofranko, J. A., J. Catal, 1988b, 114, p. 422.

Gardiner Jr., W. C., and Olson, D. B., Ann. Rev. Phys. Chem., 1980, 31, p. 377.

Garnett, J. L., Kennedy, E. M., Long, M. A., Than, C., and Watson, A. J., Stud. Surf. Sci. Catal., 1988, 36, p. 389.

Gavalas, G.R., Phichitkul, C., and Voecks, G.E., J. of Catal., 1984, 88, p. 65.

Gesser, H. D., Hunter, N. R., and Prakash, C. B., Chemical Reviews, 1985, 85, p. 235.

Gesser, H. D., Hunter, N. R., Morton, L. A., Yarlagadda, P. S., and Fung, D. P. C., Am.Chem. Soc., Div. Fuel Chem., 1987a, 32, p. 255.

Gesser, H. D., Hunter, N. R., Morton, L. A., and Yarlagadda, P. S., Am. Chem. Soc., Div. Pet. Chem. 1987b, 32, p. 779.

Gray, D., Tomlinson, G., and Shen, J., Am. Chem. Soc., Div. Fuel Chem., 1988, 33, p. 432.

Haggin, J., Chem. Eng. News, 1988, July 4, p. 22.

Hinsen, W., Bytyn, W., and Baerns, M., Proc. 8th. Int. Cong. Catal.,1984, 3, p. 581, Verlag Chemie, Weinheim.

Hutchings, G. J., Scurrell, M. S., and Woodhouse, J., J. Chem. Soc., Chem. Commun., 1987a, p. 1862.

Hutchings, G. J., Scurrell, M. S., and Woodhouse, J., J. Chem. Soc., Chem. Commun., 1987b, p. 1388.

Hutchings, G. J., Scurrell, M. S., and Woodhouse, J., J. Chem. Soc., Chem. Commun., 1988a, p. 253.

Hutchings, G. J., Scurrell, M. S., and Woodhouse, J., Stud. Surf. Sci. Catal., 1988b, 36, p. 415.

Hutchings, G. J., Scurrell, M. S., and Woodhouse, J. R., Applied Catalysis, 1988c, 38, p. 157.

Hutchings, G. J., Woodhouse, J. R., and Scurrel, M.S., Int. Congr. Catal [Proc], 1988d, p. 923.

Ito, T., Wang, J. X., Lin, C. H., and Lunsford, J. H., J. Am. Chem. Soc., 1985, 107, p. 5062.

Ito, T., and Lunsford, J. H., Nature, 1985, 314, p. 721.

Imai, H., and Tagawa, T., J. Chem. Soc., Chem. Commun., 1986, p. 52.

Imai, H., Tagawa, T., and Kamide, N., Journal of Catalysis, 1987, 106, p. 394.

Imai, H., Tagawa, T., Kamide, N., and Wada, S., Int. Congr. Catal. [Proc.], 9th 1988, 2, p. II 952.

Inque, Y., and Yasumori, I., Bull. Chem., Soc. Jpn., 1981, 54, p. 1505.

Iwamatsu, E., Moriyama, T., Takasaki, N., and Aika, K., J. Chem. Soc., Chem. Commun., 1987, p. 19.

Iwamatsu, E., Moriyama, T., Takasaki, N., and Aika, K., Journal of Catalysis, 1988a, 113, p. 25.

Iwamatsu, E., Moriyama, T., Takasaki, N., and Aika, K., Stud. Surf. Sci. Catal., 1988b, 36, p. 373.

Jens, K. J., Halvorsen, S., and Ofstad, E. B., Stud. Surf. Sci. Catal., 1988, 36, p. 483.

Jones, C. A., Leonard, J. J., and Sofranko, J. A., Energy and Fuels, 1987a, 1, p. 12.

Jones, C. A., Leonard, J. J., and Sofranko, J. A., Journal of Catalysis, 1987b, 103, p. 311.

Jones, A., and McNicol, B.D., Temperature Programmed Reduction for Solid Material Characterisation, Chemical Industries Series vol. 24, Ed. Heinemann H., Marcel Decker, New York, Basel, 1986.

Kastanas, G. N., Tsigdinos, G. A., and Schwark, J., Am. Chem. Soc., Div. Fuel Chem., 1988a, 33, p. 393.

Kastanas, G. N., Tsiddinos, G. A., and Schwank, J., J. Chem. Soc., Chem. Commun., 1988b, p. 1298.

Kasztelan, S., and Moffat, J. B., J. Chem. Soc., Chem. Commun., 1987a, p. 1663.

Kasztelan, S., and Moffat, J. B., Journal of Catalysis, 1987b, 106, p. 512.

Kasztelan, S., and Moffat, J. B., Journal of Catalysis, 1988a, 109, p. 206.

Kasztelan, S., and Moffat, J. B., Int. Congr. Catal. [Proc.], 9th., 1988b, 2, p. II 883.

Kazansky, V.B., Kinet. Katal., 1977, 88, p. 43.

Kasteren, H. M. N., Geerts, J. W. M. H., and Wiele, K. V. D., Int. Congr. Catal. [Proc.], 9th. 1988,2, p. II 931.

Keller, G. E., and Bhasin, M. M., Journal of Catalysis, 1982, 73 , p. 9.

Khan, M. M., and Somarjai, G. A., Journal of Catalysis, 1985, 91, p. 263.

Khan, M. S., and Crynes, B. L., Ind. Eng. Chem., 1980, 10, p. 54.

Kimble, J. B., and Kolts, J. H., Chemtech, 1987, August, p. 501.

Kirk Othmer, Encyclopedia of Chemical Technology, Third Edition, 1980, Vol. 11, p. 630, John Wiley and Sons. Inc.

Korf, S. J., Roos, J. A., de Bruijn, N. A., van Ommen, J. G., and Roos, R. H., J. Chem. Soc., Chem. Chemm., 1987, p. 1433.
ommun.

Korf, S. J., Roos, J. A., Diphoorn, J. M., Veehof, R. H. J., van Ommen, J. G., and Roos, J. R. H., Am. Chem. Soc., Dic. Pet. Chem., 1988, 33, p. 437.

Kowalak, S., and Moffat, J. B., Applied Catalysis, 1988, 36, p. 139.

Kuijpers, E.G.M., Breedijk A.K., Van Der Wal, w.J.J and Gens, J. W., J. Catal., 1981, 72, p.210.

Labinger, J. A., and Ott, K. C., J. Phys. Chem, 1987, 91, p. 2682.

Lane, G. S., and Wolf, E. E., Int. Congr. Catal. [Proc.], 9th 1988a, 2, p. II 944.

Lane, G. S., and Wolf, E. E., Journal of Catalysis, 1988b, 113, p. 144.

Lane, G. S., and Wolf, E. E., Am. Chem. Soc., Div. Fuel Chem., 1988c, 33, p. 373.

Larkins, F. P., and Nordin, M. R., Stud. Surf. Sci. Catal., 1988a, 36, p. 409.

Larkins, F. P., and Nordin, M. R., Applied Spectroscopy, 1988b, 42, 906.

Lee, J. S., and Oyama, S. T., Catal. Rev. Sci. Eng., 1988, 30, p. 249.

Lee, I., and Ng, K. Y. S., Am. Chem. Soc., Div. Fuel Chem., 1988, 33, p. 403.

Lin, C. H., Campbell, K. D., Wang, J. X. and Lunsford, J. H., J. Phys. Chem., 1986, 90, p. 534.

Lin, C. H., Ito, T., Wang, J. X., and Lunsford, J. H., J. Amm. Chem. Soc., 1987, 109, p. 4808.

Lin, C. H., Ito, T., Wang, J. X., and Lunsford, Journal of Catalysis, 1988, 111, p. 302.

Liu, R. S., Iwamoto, M., and Lunsford, J. H., J. Chem. Soc., Chem. Commun., 1982, p. 78.

Liu, H. F., Liu, R. S., Liew, K. Y., Johnson, R. E., and Lunsford, J. H., J. Am. Chem. Soc., 1984, 106, p. 4117.

Lo, M. -Y., Kamat, S. N., and Schrader, G. L., Am. Chem. Soc., Div. Fuel Chem., 1988, 33, p. 378.

Lunsford, J. H., Stud. Surf. Sci. Catal., 1988, 36, p. 343.

Lunsford, J. H., ACS Symp. Ser., 1984, 248, p. 127.

Machida, K., and Enyo, M., J. Chem. Soc., Chem. Commun., 1987, p. 1639.

Maiden, C. J., Stud. Sur. Sci. Catal., 1988, 36, p.1.

Martin, G. A., and Miradatos, C., J. Chem. Soc., Chem. Commun., 1987, p. 1393.

Marshall, G.M., and Shahkar, G., J. Chem. Soc., Far. Tran. 1, 1983, 79, p.1891.

Matsuura, I., Utsumi, Y., Nakai, M., and Doi, T., Chemistry Letters, 1986, p. 1981.

Matsuura, I., Doi, T., and Utsumi, Y., Chemistry Letters, 1987, p. 1473.

Matyi, R.J., Schwartz, L.H., and Butt, J.B., Catal. Rev.-Sci. Eng., 1987, 29(1) p.41.

Mehandru, S. P., Anderson, A. B., and Brazdil, J. F., J. Am. Chem. Soc., 1988, 110, p. 1715.

Meng, H., and Sanger, A. R., Applied Catalysis, 1987, 32, p. 347.

Miradatos, C., and Martin, G. A., Int. Congr. Catal. [Proc.], 9th. 1988, 2, p. II 960.

Miradatos, C., Perrichon, V., Durupty, M. C., and Moral, P., Studies in Surface Science and Catalysis, 1987, 34, p. 183.

Moriyama, T., Takasaki, N., Iwamatsu, E., and Aika, K., Chemistry Letters, 1986, p. 1165.

Nelson. P. F., Lukey, C. A., and Cant, N. W., J. Phys. Chem., 1988, 92, p. 6176.

Otsuka, K., Said, A. A., Jinno, K., and Komatsu, T., Chemistry Letters, 1987, p. 77.

Otsuka, K., Jinno, K., and Morikawa, A., Journal of Catalysis, 1986a, 100, p. 353.

Otsuka, K., and Jinno, K., Inorganica Chimica Acta, 1986, 121, p. 237.

Otsuka, K., and Nakajima, T., J. Chem. Soc., Faraday Trans. 1, 1987, 83, p. 1315.

Otsuka, K., and Nakajima, T., Inorganica Chimica Acta, 1986, 120, L27.

Otsuka, K., Jinno, K., and Morikawa, A., J. Chem. Soc., Chem. Commun., 1986, p. 586.

Otsuka, K., Jinno, K., and Morikawa, A., Chemistry Letters, 1985, p. 499.

Otsuka, K., Liu, Q., Hatano, M., and Morikawa, A., Chemistry Letters, 1986b, p. 467.

Otsuka, K., and Komatsu, T., Chemistry Letters, 1986, p. 1955.

Otsuka, K., Liu, Q., Hatano, M., and Morikawa, A., Chemistry Letters, 1986c, p. 903.

Otsuka, K., Hatano, M., and Komatsu, T., Stud. Surf. Sci. Catal., 1988a, 36, p.

Otsuka, K., Liu, Q., and Morikawas, A., Inorganica Chimica Acta, 1986e, 118, L23.

Otsuka, K., and Komatsu, T., J. Chem. Soc., Chem. Commun., 1987, p. 388.

Otsuka, K., and Hatano, M., Journal of Catalysis, 1987, 108, 252.

Otsuka, K., Komatsu, T., Jinno, K., Uragami, Y., and Morikawa, A., Int. Congr. Catal. [Proc.] 9th 1988b, 2, p. II 915.

Otsuka, K., Sekiyu Gakkaishi, 1987, 30, p. 385.

Paquin, Y., and Forst, W., International J. Chem. Kin., 1973, 5, p.691.

Pitchai, P., and Klier, K., Catal. Rev. Sci. Eng., 1986, 28, p. 13.

Pierrot, A., Tellier, J., and Richard, M., Presentation at IEA Workshop on Enhanced International Collaboration on Chemical Natural Gas Conversion, 1988.

Peri, J. B., Catalysis Science and Technology, 1984, 5, p. 173, Springer Verlag.

Petroleum Gazette, Aust. Inst. of Petrol., 1988, 25(8), p. 17.

Powder Diffraction File, Search Manual, Joint Committee on Powder Diffraction Standards, Pensylvania, USA, 1975.

PreuB, U., and Baerns, M., Chem. Eng. Technol., 1987, 10, p. 297.

Quanzhi, L., and Amenomiya, Y., Applied Catalysis, 1986, 23, p. 173.

Renaud, R., and Leitch, L.C., Can. J. Chem., 1954, 32, p. 545.

Rethwisch, D. G., and Dumesic, J. A., Langmuir, 1986, 2, p. 73.

Roe, G.R., Honours Thesis, 1986, Dept. of Chemistry, University of Tasmania.

Roos, J. A., Bakker, A. G., Bosch, H., van Ommen, J. G., and Roos, J. R. H., Catalysis Today, 1987, 1, p. 133.

Roos, J. A., Korf, S. J., Bakker, A. G., de Bruijn, N. A., and van Ommen, J. G., Stud. Surf. Sci. Catal., 1988, 36, 427.

Scurrell, M. S., and Cooks, M., Stud. Surf. Sci. Catal., 1988, 36, p. 433.

Scurrell, M. S., Applied Cayalysis, 1987, 32, p. 1.

Senkan, S. M., 1987, Patent us 4714796.

Senkan, S. M., Chemical Eng. Prog., 1987, 83, p. 58.

Senkan, S. M., Granada, A., Karra, S. B., Am. Chem. Soc., Div. Fuel Chem., 1988a, 32, p. 299.

Senkan, S. M., Dang, D., Abdelaal, M. K., and Qun, M., Am. Chem. Soc., Div. Fuel Chem., 1988b, 33, p. 421.

Shannon, R.D., and Prewitt, C.T., Acta Cryst., 1969, B25, p. 925.

Shannon, R.D., and Prewitt, C.T., Acta Cryst., 1970, B26, p. 1046.

Shepelev, S. S., and Ione, K. G., Kinetika i Kataliz, 1984, 25, p. 347.

Sinev, M. Yu., Korchak. V. N., and Krylov, Kinetika i Kataliz, 1986, 27, p. 1274.

Sinev, M. Yu., Korchak, V. N., and Krylov, O. V., Int. Congr. Catal. [Proc.], 9th. 1988, 2, p. II 968.

Sinev, M. Yu., Korchak, V. N., and Krylov, O. V., Proc. VI th. Int. Symp. Heterogeneous Catalysis, Sofia, 1987, 1, p. 450,

Skinner, G. B., and Ruehrwein, R. A., J. Phys. Chem., 1959, 63, p. 1736.

Smith, D.J.H., Pet. Tech., 1987, 332, p 10.

Smyrl, N.R., Fuller, E.L., and Powell, G.L., Appl. Spec., 1983, 37, p. 38.

Sofranko, J. A., Leonard, J. J., and Jones, C. A., Journal of Catalysis, 1987, 103, p. 302.

Spencer, N. D., Journal of Catalysis, 1988, 109, p. 187.

Solymosi, F., and Tombascz, I., and Kutsan, G., J. Chem. Soc., Chem. Commun., 1985, 1455.

Tagawa, T., and Imai, H., J. Chem. Soc., Faraday Trans. 1, 1988, 84, p. 923.

Suleimanov, A. I., Ismailov, E. G., Aliev, S. M., and Sokolovskii, V. D., React. Kinet. Catal. Latt., 1987, 1, 34, p. 51.

Tanabe, K., Catalysis Science and Technology, 1981, 2, p. 231, Springer Verlag.

Taylor, H.A., and Flowers, R.G., J. Chem. Physics, 1982, 10, p.58.

Taylor, C. E., Noceti, R. P., and Schehl, R. R., Stud. Surf. Sci. Catal., 1988, 36, p. 491.

Taylor, C. E., and Noceti, R. P., Int. Congr. Catal. [Proc.], 9th. 1988, 2, p. II 990.

Thomas, J. M., Kuan, X., and Stachurski, J., J. Chem. Soc., Chem. Commun., 1988, p. 162.

Top-Jorgensen, Stud. Sur. Sci. Catal, 1988, 36, p. 293.

Tyler, R. J., Presentation to the NERDDC Catalyst R&D Workshop, Melbourne, 1986.

Ueda, W., and Thomas, J., Int. Congr. Catal. [Proc.], 9th. 1988, 2, p. II 960.

Ungar, R. K., Zhang, X., and Lambert, R. M., Applied Catalysis, 1988, 42, L1.

Vinek, H., Latzel, J., Noller, H., and Ebel, M., J. Chem. Soc. Far. Trans. I, 1978, 74, p.2092.

Waddams, A.L., Chemicals from Petroleum: An Introductory Survey, 4th. Edition, John Murray Ltd., London, Chapter 6.

Ward, J. J., and Serrit, A. A., 1987, Patent EP 256857.

Wang, J. X., and Lunsford, J. H., J. Phys. Chem., 1986a, 90, p. 5883.

Wang, J. X., and Lunsford, J. H., J. Phys. Chem., 1986b, 90, p. 3890.

Warnatz, J., Ber. Bunsenges. Phys. Chem., 1983, 87, p. 1008.

Weisz, P.B., Chemtech, 1982, July, p. 424.

Yamagata, N., Tanaka, K., Sasaki, S., and Okazaki, S., Chemistry Letters, 1987, p. 81.

Yang, T.J., and Lunsford, J.H., J. Catal., 1980, 63, p. 505.

Yarlagadda, P. S., Norton, L. A., Hunter, N. R., and Gesser, H.D., Fuel Science and Technology Int'l., 1987, 5(2), p. 169.

Yingli, B., Kaiji, Z., Yutao, J., Chiwen, T., and Xiangguong, Applied Catalysis, 1988, 39, p. 185.

Zhang, H. S., Wang, J. X., Driscoll, D. J., and Lunsford, J. H., Journal of Catalysis, 1988, 112, p. 366.

Zhen, K.J., Khan. M. M., Mak, C. H., Lewis, K. B., and Somarjai, G. A., J. Catal., 1985, 94, p. 501.